Studies on the Health and Bacterial Symbionts of Toheroa (*Paphies ventricosa*)

A thesis

submitted in fulfilment

of the requirements for the degree

of

Doctor of Philosophy in Biological Sciences

at

The University of Waikato

by

Matthew Joseph Bennion

THE UNIVERSITY OF
WAIKATO
Te Whare Wānanga o Waikato

2021

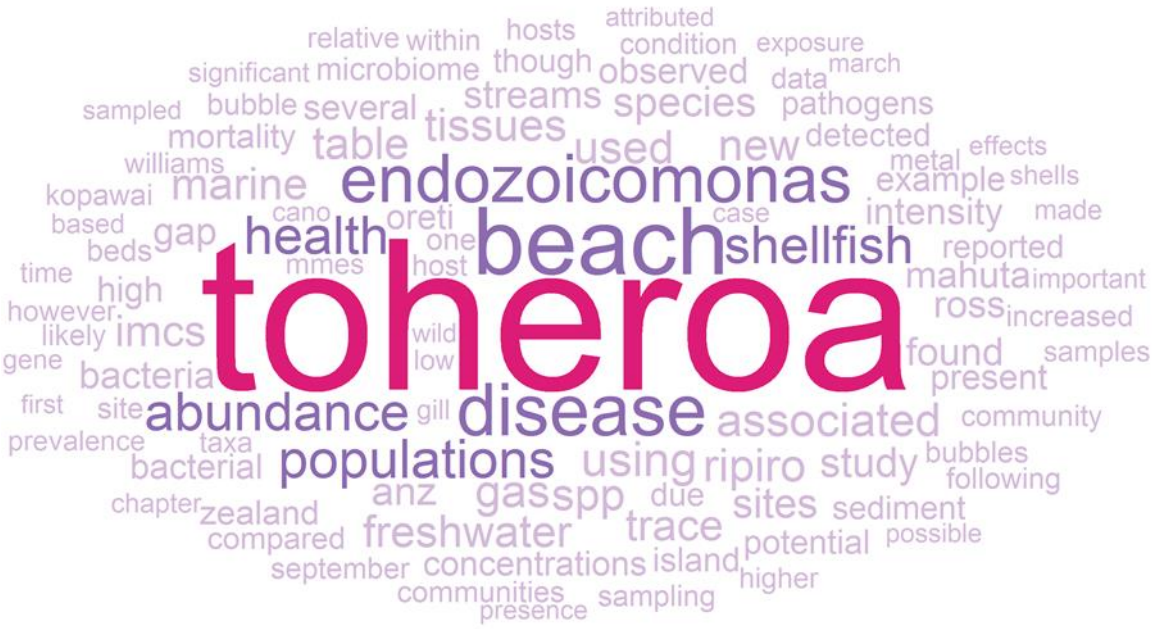

Word cloud constructed from the 100 most frequently used words throughout this thesis document (excluding references, appendices, and captions). Created using the package ‘ggwordcloud’ (Le Pennec and Slowikowski, 2019) in RStudio.

Le Pennec, E., Slowikowski, K. Package ‘ggwordcloud’, A Word Cloud Geom for 'ggplot2', 2019. v0.5.0.

Tēnā koutou katoa

Ko Éire te motu

Ko Néifinn te maunga

Ko Baile an Ghleanna te awa

Ko Bunatrahir te moana

Ko Ó Domhnaill te hapū

Ko Maitiú tōku ingoa

Ar scáth a chéile a mhaireann na daoine

Preface

The main body of this thesis comprises six research chapters. Chapters 3, 4, and 5 of this thesis have been submitted for publication in peer-reviewed journals and are currently under review. Chapter 6 is currently being prepared for publication. The ideas and concepts introduced in this thesis were my own, unless otherwise referenced.

All work was produced under the supervision of Dr Phil Ross at the University of Waikato, Tauranga, Professor Ian R. McDonald at the University of Waikato, Hamilton, and Dr Henry Lane at the National Institute of Water and Atmospheric Research Ltd. (NIWA), Christchurch.

Chapter 3 has been submitted to the Journal of Invertebrate Pathology:
Bennion, M., H., Lane, I., R., McDonald, P., Ross. Histopathology of a Threatened Surf Clam, Toheroa (*Paphies ventricosa*) from Aotearoa New Zealand. *Journal of Invertebrate Pathology.* Under review.

Chapter 4 has been accepted by Diseases of Aquatic Organisms:
Bennion, M., P., Ross, J., Howells, I., R., McDonald, H., Lane. 2021. Characterisation and distribution of the bacterial genus *Endozoicomonas* in a threatened surf clam. *Diseases of Aquatic Organisms*. 146:91-105.

Chapter 5 has been submitted to Marine Biology:
Bennion, M., P., Ross, Lane, H., McDonald, I. The Microbiome of the Toheroa (*Paphies ventricosa*), a Threatened Surf Clam from Aotearoa (New Zealand). Marine Biology. Under review.

Abstract

Disease outbreaks in marine species can have devastating consequences for host populations, host-associated species assemblages, ecosystem functioning, and for human users of these marine resources. At present, the risk factors associated with disease outbreaks, such as warming and pollution, are increasing. Given the increasing risk of disease outbreaks and the role that parasites play in marine ecosystems, there is a vital need to gain knowledge of marine diseases for species conservation, and the monitoring, management, and forecasting of disease. The field of marine disease ecology is growing, but many facets of our understanding remain in their infancy. Faced with a lack of baseline health data, efforts to combat disease outbreak in the ocean are impeded, even though the future of food security hinges on an ability to source food from the ocean. With a shift towards aquaculture, in particular bivalve aquaculture, knowledge of ambient health of wild and farmed species will dictate both yield, and our ability to protect wild stocks.

Disease outbreak poses added risk to species that are already in peril. The toheroa (*Paphies ventricosa*) is a threatened surf clam endemic to Aotearoa (New Zealand). Once bountiful, overharvesting and population collapse put an end to the large-scale fisheries of the early and mid-1900s. The protections enacted on toheroa populations should have ensured their recovery, but recovery has not occurred. Disease has been suggested as one possible explanation. However, without knowledge of disease dynamics in toheroa populations, restorative efforts risk failure, or worse, inflicting further damage. Intracellular microcolonies of bacteria (IMCs) have been linked to numerous shellfish mass mortality events (MMEs) in Aotearoa in recent years, and were first detected in toheroa in 2017. This discovery raised questions regarding the role IMCs might be playing in preventing the recovery of toheroa populations.

To address this uncertainty, this thesis set out to investigate what pathogens and parasites are present in toheroa, and determine what effect they might be having on toheroa health. A histopathology survey was conducted to gather fundamental baseline health information on toheroa populations across their entire distribution. IMCs were found to be the only potential pathogens of note. Histology data coupled with Bayesian models indicated that the probability of higher IMC intensity was associated with decreased toheroa condition. Using PCR, DNA sequencing, and *in situ* hybridisation, IMCs were characterised as bacteria in the genus *Endozoicomonas*. In many marine organisms, *Endozoicomonas* spp. are cosmopolitan members of associated-bacterial communities, often fulfilling biogeochemical cycling functions in host tissues. In toheroa populations, *Endozoicomonas* spp. abundance was found to be seasonal, but site specificity indicated habitat characteristics (specifically, the presence of freshwater outflows) might be a significant driver of their abundance. The bacterial community of toheroa was

subsequently investigated using 16S rRNA gene sequencing, and candidates common to other coastal bivalve molluscs were found to be dominant, including *Spirochaetaceae*, *Mycoplasmataceae*, and *Endozoicomonadaceae* (in order of relative dominance). Freshwater outflows appeared to be such a significant driver of microbiome taxonomic dissimilarity, that specimens collected from sites 1240 km apart hosted more similar bacterial communities than specimens from sites with and without streams on the same beach and within the same region. The key indicator taxa driving microbiome dissimilarity were found to be *Endozoicomonas* spp. and sulfate-reducing bacteria in the phylum Desulfobacterota.

Gas bubbles were also observed on the shells of toheroa at the same time that IMCs were first detected. At that stage, temperature and total dissolved gaseous pressure was thought to contribute to their manifestation. To gain a better understanding of this phenomenon, a spatio-temporal survey was conducted which revealed an association of high gas bubble intensity with the austral-autumn/winter and freshwater outflows. A new hypothesis is therefore presented that links gas bubbles to sulfate-reducing bacteria and hydrogen sulfide (H_2S), a by-product of anaerobic digestion. Given the apparent influence of freshwater on toheroa intrinsic health, the capacity for streams to deliver pollutants to toheroa beds was assessed. Results gained from inductively coupled plasma-mass spectrometry (ICP-MS) suggest that despite the modified nature of adjacent land, streams do not deliver significant loads of bioavailable trace metals to toheroa beds in the intertidal zone. Instead, nutrition in the form of large phytoplankton blooms in autumn/winter is thought to be the primary source of bioavailable trace metals for toheroa.

No observations of significant pathogenesis, associated with *Endozoicomonas* species, were made throughout this research. Furthermore, during the timeframe of this research (apart from intermittent mortality events reported), there is no evidence of an ongoing disease epidemic in toheroa populations. While not providing evidence for the factor preventing the recovery of toheroa, this research does have implications for the ongoing conservation and management of toheroa. It seems reasonable to assume that infectious disease is not a major factor contributing to the limited recovery of toheroa throughout Aotearoa. Instead, associations made between freshwater outflows, nutrition, and detritus indicate that habitat requirements provided by freshwater streams are having significant effects on toheroa health, survival, and homeostasis. Furthermore, evidence presented suggests that the *Endozoicomonas* spp. present in toheroa and other Aotearoa shellfish are likely to be an important endosymbiont. In the future, studies on remaining toheroa populations should prioritise nutritional health. Namely, what role symbionts play in toheroa nutrition, and how niche requirements shape symbiont community composition and function in toheroa tissues. Answers to these questions could profoundly increase the success of toheroa restoration and conservation efforts.

Acknowledgements

Foremost, thank you to my supervisors. Dr Phil Ross, you gave me a chance seven years ago, and again three years ago, both occasions have ultimately shaped this past decade for me, which I am incredibly grateful for. Thank you for your guidance, support, and the opportunity to join the formidable Team Toheroa! Prof Ian McDonald, thank you for igniting my passion for the miniature world, and for all of your time, advice, and encouragement over the last three years. Finally, Dr Henry Lane, I feel incredibly fortunate to have had your unwavering support throughout this process. It is safe to say I would not have gotten far in the aquatic disease world without your wealth of knowledge. Thank you for your kindness and constant cheerleading from start to finish.

Ngā mihi nunui ki ngā tangata whenua o Te Tai Tokerau, Kāpiti-Horowhenua, Tauranga Moana me Murihiku mō te manaaki me āwhina.

I want to acknowledge Roanna Richards-Babbage, John Longmore, Dr Amanda French, Danielle Blackwell, and Sarah Wallace for sharing your expertise with me and giving me your time. A massive thank you to Dr Anjali Pande as well, for your insight at the inception of this project.

To those who, behind the scenes, made sure I was enrolled, paid, and that I was on track to submit, thank you. Especially I want to acknowledge the efforts of Soli Weiss, Gwenda Pennington, Cheryl Ward, and Tanya Mete. I also want to acknowledge the financial support from the University of Waikato, the New Zealand Marine Sciences Society (Student Research Grant), and the Royal Society Te Apārangi (Hutton Fund).

A sincere thank you to the members of Team Toheroa. Jane Cope, you shaped much of this thesis by showing me the ropes on my first day of fieldwork, thank you! Jacinta Forde, I am so grateful to you (and Alana) for the Wellington trips, and all those times you joined me for a Bongo and listened to me rant (Raglan is a highlight too). Lolita Vallyon, thank you for all the fantastic memories from those trips to Baylys Beach (Crow's Nest is a highlight). Vanessa Taikato, look sure there is just not enough space in this thesis for all the things I could thank you for. I truly doubt that I could have done this without you. Thank you for all of the advice, mentoring, talking through ideas/problems, and the lunchtime food critiques. I have loved it all and I would do it all again. I also need to thank so many people at the Coastal Marine Field Station; thank you all so much for the Friday beers, laughter, and support (honourable mentions: Yanika, Holly X2, Mel, Kaeden, Deb, Dave, Alice, Sam, Nikki, Ari, Helen, Roby, & Jacob).

Joanne Howells, your hyping of my research and your excitement for the process was really appreciated, thank you for being such a great friend (and mentor) over the last three years. Special mention: Georgina Flowers, thank you for pointing out the bubbles.

To the Baine & Bennion families, I don't think I would have come to Aotearoa all those years ago if I hadn't had your support. Cathy and Lindsay, thank you for all the weekends you took me and Joe in and made us a part of your family (and for the KoKo trips). Jacqui and Julie, you have both given me so much in the last few years, sincerely thank you. All those times you lent us your home in Raglan afforded me the opportunity to take much-needed breaks.

I also want to thank my more recent extended family too (the McAuley's, the Marinus', and Nancy), for being so good to Joe and me over the last few years.

To my parents, Mary and Pierse and my sister Sarah, I feel so fortunate to have constantly had your support and encouragement throughout this process. Despite being separated by several oceans for the last three years, you all made it seem like you were nearby if I needed you.

Joe, for being a constant source of inspiration and unwavering support, thank you. Coffee mornings over the last three years have been an unanticipated, and joyful, by-product of this PhD and I'm so thankful that I've been able to spend them with you. I think I can officially say that you're my best friend now.

A Note on Site Names

Three sites on Ripiro Beach were continually visited for this research. The first, north of Baylys Beach, was referred to as ‘Island’ throughout this document. This name was used due to the presence of a large boulder (separated them from the cliffs that shadow this site), that resembled an island and made the site easily identifiable. The second, ‘Mahuta Gap’, is a well-known access point to the beach and, as such, the road leading to the beach is named Mahuta Gap Road. The third site has been referred to herein as ‘Kopawai’. Cope (2018) referred to this site as Kopawai also, and the name had been relayed by Barry Searle of Dargaville. A lake not far from the ‘Kopawai’ stream is called ‘Kopaoi’. It is possible this stream has been named Kopaoi previously, however, no information was found regarding a specific name for the stream, so the decision was made to follow the lead of previous work by Cope (2018) and refer to the site as Kopawai throughout this document.

Cope, J., The modification of toheroa habitat by streams on Ripiro Beach. MSc. University of Waikato, Hamilton, New Zealand, 2018, pp. 126.

Glossary

hapū	subtribe
iwi	tribe
kai	food
kai moana	seafood
kaitiaki	guardian
kōrero tuku iho	oral history
kuku	*Perna canaliculus*
mana	prestige, spiritual power
manuhiri	visitor or guest
mātauranga Māori	Māori knowledge
pipi	*Paphies australis*
pōhā	kelp bag
Rakiura	Stewart Island
raranga	weaving
tāngata whenua	local people
te ao Māori	Māori world view
Te Ika-a-Māui	North Island
Te Tai Tokerau	Northland
Te Waipounamu	South Island
Te-Oneroa-a-Tōhē	Ninety Mile Beach
tikanga	custom
tio paruparu	*Ostrea chilensis*
toheroa	*Paphies ventricosa*
tuangi	*Austrovenus stutchburyi*
tuatua	*Paphies subtriangulata*
tukutuku	ornamental latticework (wall panels)
waiata	song
whakataukī	proverb
whanau	extended family
whārenui	meeting house

Table of Contents

List of Figures

List of Tables

Chapter 1
Introduction

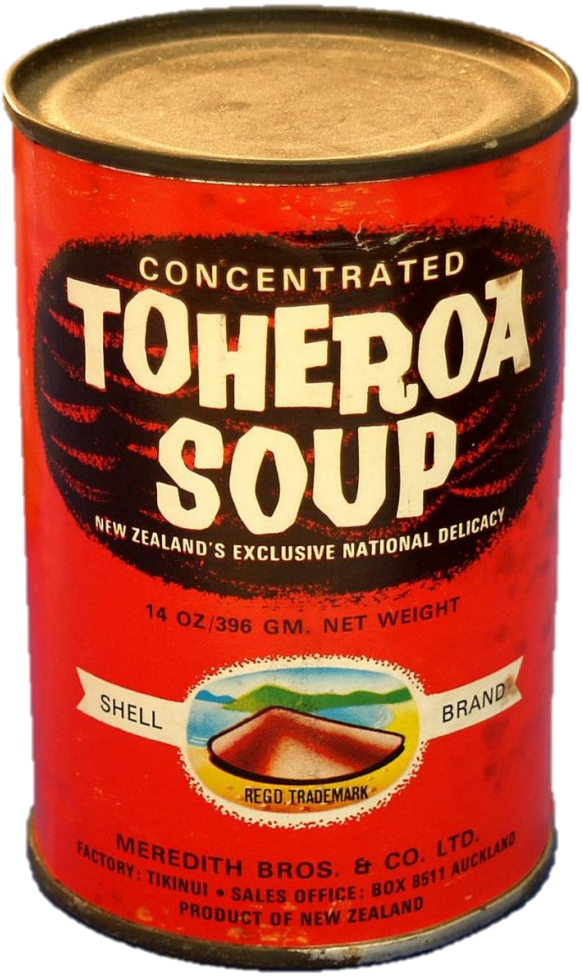

Canned toheroa c.1960s

1.1 Seafood in a Rapidly Changing World

While fisheries management is being used effectively to rebuild some stocks (Hilborn et al., 2020), many others are over-exploited or near-collapse (Pauly and Zeller, 2016; Worm et al., 2009). More than three billion people around the world rely on seafood as their primary source of protein, and a similar number depend on marine and coastal biodiversity for their livelihoods (UN, 2020). Increasingly, seafood is being relied upon to provide a source of nutrition to a rapidly growing human population (Costello et al., 2020). The pressure on many wild stocks and subsequent quotas to manage populations has led to an active shift towards aquaculture (Costello et al., 2020; Willer and Aldridge, 2020). By 2030, farmed seafood produce is expected to account for 60% of global seafood production for direct human consumption (WorldBank, 2013). Seafood already constitutes a significant portion of the diet of many island nations and coastal communities (Cisneros-Montemayor et al., 2016; Guillen et al., 2019), but globally, seafood consumption is predicted to grow in non-coastal areas too (Costello et al., 2020). As Earth's population nears 10 billion people, food stability and security are becoming increasingly important. The State of the World's Fisheries report (FAO, 2016) estimated that bivalve aquaculture accounted for 14-16% of the average per capita animal protein of 1.5 billion people. Moreover, bivalve aquaculture production supports the livelihoods of upwards of 200,000 people in developing nations (FAO, 2018).

Kummu et al. (2016) estimated that 40% of the World's population live within 100 km of the coast. This proportion was found to be relatively stable over time, while the number of people has dramatically increased (Kummu et al., 2016). Proximity to blue spaces, oceans and lakes, has been associated with human well-being (Gascon et al., 2017). The reasons for this are multi-faceted but include the ability to source food locally (Bennett et al., 2018), increased recreation, and interconnectedness with nature (Beaumont et al., 2007). Despite the fact, our reliance on the oceans has never been higher; the ecosystem services we depend on have also never been at greater risk. Dense populations in coastal areas bring a myriad of pressures on coastal and marine ecosystems (Nicholls et al., 2007). For example, over-exploitation of stocks (e.g., various bivalves) (Bhattacharya and Sarkar, 2003), pollution (Lamb et al., 2018; Wilkes et al., 2017), and habitat modification or degradation (e.g., Wilberg et al., 2011). These pressures bring with them a plethora of indirect effects. For example, habitat modification in the form of artificial structures can facilitate the introduction and spread of invasive species (Nyberg and Wallentinus, 2005).

1.1.1 The Future of Seafood Safety and Security

Seafood, harvested or farmed, is predicted to be of vital importance to secure enough food for the Earth's growing human population (Costello et al., 2020). Nevertheless, the safety

standards of seafood produce are continuously tested. Harmful algal blooms (HABs) (Grattan et al., 2016), food fraud (origin and species) (Bennion et al., 2019; Kroetz et al., 2018), pathogens, and pollutants (Liu et al., 2017; Su and Liu, 2007), interrupt supply chains and test industry regulators tasked with upholding food safety standards. Recognising the growing issue of seafood safety, owed to increased consumption and subsequent production, Bank et al. (2020) offered a much-needed definition of seafood safety.

> "*the maintenance and production of healthy marine biota through successful air, land, and water pollution management strategies; effective biohazard and contaminant surveillance of marine fish, shellfish, and sea mammals; algal, gelatinous, and invertebrate resources; and their continually traceable (i.e., origin and species) and proper handling from the sea to the table*".

Several important concepts are covered by this definition, namely disease and pollution mitigation, traceability, and surveillance. Despite the importance of these concepts, it is safe to say that they are not readily applied to all seafood production at present (Pramod et al., 2014; Xiong et al., 2016). This statement applies to some commercial fisheries, where fraud is still prevalent (*c*. 8% of global seafood products are mislabelled) (Luque and Donlan, 2019), and where occasionally unsafe food makes it to market (Cohen et al., 2009; Giusti et al., 2018). But what of non-commercial species? Or those where neither a recreational nor commercial fishery is permitted? Illegally harvested produce or traditional (customary) seafood that is subject to small-scale subsistence harvesting is not subjected to the concepts in the above definition of 'seafood safety'. Of course, illegal harvesting and trading of illicit produce would not be constrained by these concepts (Williams et al., 2020), as by definition they are not compliant with regulatory frameworks. On the other hand, customary fisheries, relied upon by many coastal and Indigenous communities, which are legal and often regulated, would theoretically be covered by this definition of 'seafood safety', but often are not (e.g., high cadmium concentration in traditional food from Torres Strait Island, Australia) (Haswell-Elkins et al., 2007). The distinction being that seafood harvested is often for subsistence rather than for sale, yet this regulatory blind spot has left many small-scale fisheries without continuous monitoring of pathogens (human and animal) (Goyette et al., 2014; Pufall et al., 2012) and pollutants (Belinsky et al., 1996; Burger et al., 2007; Laird and Chan, 2013). The exception to this rule being toxins e.g., tetrodotoxin (TTX) (Harwood et al., 2020) and biotoxin producing harmful algae blooms (HABs) that are in some jurisdictions included in government monitoring programmes at a national level (in Aotearoa New Zealand; mpi.govt.nz).

1.1.2 Seafood and Coastal Indigenous Communities

"Secure access to the ocean and its resources is central for the well-being of coastal communities" (Armitage et al., 2017; Bennett et al., 2018). Access here being defined as the ability to both use and benefit from resources and the marine environment (Bennett et al., 2018). Increasingly, access to marine environments and resources by coastal and Indigenous communities is being reduced. In part due to over-exploitation of resources (Mccarthy et al., 2014) and subsequent restrictions (e.g., marine protected areas: MPAs), environmental conditions and extreme weather (Bennett et al., 2018), disease (Sformo et al., 2017), climate change (geographic range shifts of species) (Weatherdon et al., 2016), and geographical barriers (Wieland et al., 2016). Historically, the oceans have provided a vital source of food for early human settlements, particularly for South Pacific island nations. That being said, reliance on seafood in much of the South Pacific has decreased attributed to several ecological and socio-economic drivers (Lau Islands, Fiji; Turner et al., 2007), such as environmental degradation and new income-generating opportunities. Despite some decreased reliance in parts of the globe, global seafood consumption by Indigenous peoples was recently estimated to be 2.1 million tonnes per annum, based on 1900 coastal Indigenous communities in 87 countries (Cisneros-Montemayor et al., 2016). This estimation represented 27 million people and showed that per capita, seafood consumption is *c*. 15 times higher among Indigenous communities compared to the global average (Cisneros-Montemayor et al., 2016). Evidently, many coastal and Indigenous communities continue to rely on the oceans for food security (e.g., northern Canada; Hoover et al., 2016; Islam and Berkes, 2016) and well-being (Bennett et al., 2018).

Fig. 1.1. A: Archaeological shell midden at Ripiro Beach. B: Mass mortality event of *Dosinia anus* at Waitarere Beach in February 2019. Photograph by J. Howells. C: Toheroa (*P. ventricosa*) at Ripiro Beach. D: Baylys beach at Ripiro Beach, Te Tai Tokerau, Aotearoa (New Zealand).

Ocean resources transcend dietary requirement for many Indigenous and coastal communities. The collection, preparation, and protection of resources can carry cultural significance (Mccarthy et al., 2014; Oleson et al., 2015) or 'non-use' value (Carss et al., 2020). In Aotearoa (New Zealand) for example, kaitiakitanga (guardianship or protection) of the marine environment is both a right and an obligation, which secures natural environments and resources for future generations. The collection of different kai moana (seafood) and the associated cultural practices can also bring with them mana (prestige, spiritual power) to both the kaitiaki (guardians) and the consumers of these marine species. Since the arrival of Māori to Aotearoa (*c*. 1300), coastal communities have sourced kai (food) and other resources from the ocean. Examples of historically important coastal resources for Māori are plentiful but include, pōhā (*Durvillaea* sp.) used as a watertight bag for the transport and preservation of food, and kuku (green-lipped mussel, *Perna canaliculus*) used as a food source (shells also used for raranga: weaving). The significance of ocean resources for Māori can be seen in art

(e.g., tukutuku wall panels), architecture (many wharenui spaces), and archaeological shell middens (Fig. 1.1), and heard in kōrero tuku iho, whakataukī (oral history and proverbs; Wehi et al., 2013), and waiata (songs). Many studies have explored the importance of customary fisheries for tangata whenua (Māori people of respective lands). These studies tend to focus on the impacts of reduced access to ocean resources (Mccarthy et al., 2014) and of fisheries management strategies (policy) for coastal communities (Bodwitch, 2017). More recent explorations have subsequently introduced co-management strategies and concepts aiming to shape marine policy using mātauranga (Indigenous knowledge systems) and te ao Māori lens (the Māori world view) (Maxwell et al., 2020; Reid and Rout, 2020).

Quantifying cultural importance of a resource or an ecosystem service is a difficult, if not impossible task (Carss et al., 2020; Oleson et al., 2015). Cultural value can be personal, perceptive, and locally variable. The ecosystem services valued by Indigenous coastal communities and subsistence fishers are however, under threat. Many threats are localised and extend from ecosystem services to homes and ways of life (e.g., climate change and sea level rise) (Hauer et al., 2020; Weatherdon et al., 2016). Another pressure that does not know boundaries and borders is disease. Disease outbreaks challenge the ecosystem services provided in coastal ecosystems and have the capacity to place pressure on food security, particularly in food-sparse regions (Defeo et al., 2013; Henri et al., 2018; Sformo et al., 2017). Disease could have unforeseen implications for customary practices too. For instance, Mabey et al. (2021) reported a protistan pathogen (*Maullinia* spp.) in three *Durvillaea* spp. in Aotearoa for the first time. The practice of constructing pōhā (bags made from *Durvillaea* sp.) could be impacted if the structural integrity, elasticity, or flexibility of kelp infected with *Maullinia* spp. is compromised (Goecke et al., 2012; Mabey et al., 2021).

1.2 Disease in the Ocean

Until the 1990s, the diversity of microscopic organisms had been significantly underestimated (Ward et al., 1990). This is particularly true for the oceans (Giovannoni et al., 1990), where up to 70% of the total biomass of life is now thought to comprise of single-celled microscopic organisms (Bar-On et al., 2018). Microscopic organisms play an invaluable role in every biome on earth, and beneath its surface (the deep biosphere; Pedersen, 2000). To highlight the important role that microscopic organism assemblages play in various macro- and micro-habitats, a ‘thought experiment’ imagined a world without them; concluding that a world without microbes would be detrimental to all life on Earth (Gilbert and Neufeld, 2014). In the oceans, microbes contribute to every ecosystem process, and facilitate global biogeochemical cycles (Arrigo, 2005; Worden et al., 2015). Of course, they also constitute the microbial assemblages within hosts (Apprill, 2017; Pita et al., 2018), regulating resistance to,

but also contributing to, disease (Egan and Gardiner, 2016). Similarly, parasites can modulate food webs and habitats (reviewed in Lane et al., 2020; Morton et al., 2020), with repercussions for biodiversity and thus, ecosystem functioning at large.

What is a *pathogen*? What constitutes *disease*? As diagnostic methods have become more encompassing and analytical equipment more sensitive, these previously straightforward concepts have been redefined. Pathogen is a context dependent description (Bass et al., 2019). For example, a microbe attributed to disease outbreak in one host, might be a 'normal' or even important constituent of a healthy microbiome of another host e.g., *Endozoicomonas* spp. (Neave et al., 2016). At the same time, some single microbe driven aetiologies may remain dormant within the microbial community of a host, becoming pathogenic opportunistically; this is explained by the epidemiological triad (Fig. 1.2) (Snieszko, 1974). This complicates the definition of 'disease' too. What denotes the onset of disease? The *presence* of a pathogen or parasite? The *presence* of gross signs of illness? Alternatively, at a finer scale, can the shift of a microbiome to a *pathobiome* describe the onset of disease? Described thoroughly by Bass et al. (2019) the pathobiome describes a shift in the microbial community of the host towards a disease-associated microbial community (dysbiosis; Egan and Gardiner, 2016). Typically, this shift results in a less diverse community assemblage, associated with reduced resistance to opportunistic pathogens (Bass et al., 2019; Koskella et al., 2017), although this is not always the case (Meistertzheim et al., 2017; Rubio-Portillo et al., 2018) e.g., sea star wasting disease (Lloyd and Pespeni, 2018). The bacterial (taxonomic) diversity associated with white band and white patch diseases in coralline algae was shown to be similar, and in some cases higher, than in healthy tissue (Meistertzheim et al., 2017). This shift away from single-pathogen aetiology increases the complexity of investigations of disease outbreak, particularly in the oceans, where a dynamic environment and a medium for vector-free horizontal transmission of microbes already paints a complicated picture (McCallum et al., 2004). However, the many synergistic factors, which co-exist and contribute to disease outbreak, warrant a more holistic approach. A single-pathogen approach will never be able to address comprehensively, the complex aetiology of disease outbreak in the ocean.

Disease outbreak in the ocean appears to be on the rise too (Harvell, 2019; Harvell et al., 2002; Harvell et al., 2004; Ward and Lafferty, 2004), and in some taxa more than others (Tracy et al., 2019). As mentioned, the aetiology of disease outbreak is complicated and multifactorial. Thus, explaining the reasons for this rise are equally complex. Climate change (Burge and Hershberger, 2020; Harvell et al., 2002), pollutants (Bojko et al., 2020; Lamb et al., 2018), habitat degradation (Diggles, 2013; Pollock et al., 2014), and increased shipping traffic (invasions; Lohan et al., 2020) can be associated with this rise, but each factor is only a piece of a given aetiological puzzle. For example, changes in water temperature associated with a changing climate will undoubtedly have a profound impact on certain disease

aetiologies (Burge et al., 2014; Burge and Hershberger, 2020), as evidenced by experimental scenario testing, for example, *Mytilus edulis* (Mackenzie et al., 2014). However, remediating effects could likely be felt elsewhere, in different hosts, under new circumstances. Cold water diseases could be mediated by increased water temperatures, for example viral haemorrhagic septicaemia virus and *Flavobacterium psychrophilum* (Bacteroidetes) which both have the capacity to cause disease in fish in temperatures below 12°C (Bricknell et al., 2021, and references therein).

Disease is the greatest limitation to global aquaculture production (Stentiford et al., 2012; Stentiford et al., 2017). Significant work is being conducted at regional, national, and global scales to mitigate disease, usually targeting single emerging pathogens. At a regional scale, central and regional government agencies and marinas make efforts to reduce biosecurity risks associated with recreational and commercial activities. National reference laboratories strive to identify and prepare for emerging risks and globally the World Organisation for Animal Health (OIE) maintains a list of notifiable diseases (OIE, 2021). Most of the effort currently placed on disease characterisation and management has been for aquaculture (Groner et al., 2016). This is probably due to economic incentive but could also be attributed to the complexity of managing disease in the ocean. Though difficult, it is not impossible, and several 'success' stories illustrate this (see Groner et al., 2016). For example, efforts in Chesapeake Bay, Virginia (promotion of resistant populations) reduced the impact of *Haplosporidium nelsoni* (MSX) in *Crassostrea virginica* (Carnegie and Burreson, 2011) and Culver and Kuris (2000) present a case of eradication of a marine pathogen via selective culling. Additionally, Ben-Horin et al. (2016) provide another case for selective culling, showing that fishing of diseased red abalone (*H. rufescens*) could increase yield and promote conservation goals. Although the development of disease through complex and synergistic aetiology renders understanding the underlying mechanisms behind disease difficult, mitigation does not necessarily echo this complexity. Lamb et al. (2018) showed how marine plastic debris was associated to coral disease. Similarly, microplastic debris been pitted as a potential vector for *Vibrio* spp. transmission (Frère et al., 2018; Kirstein et al., 2016). Pollock et al. (2014) showed how coral disease was associated to sedimentation via dredging and Lamb et al. (2017) showed that seagrass beds remediated pathogen loads in coastal habitats. The intricate mechanisms at the microbial scale in these cases are likely complex. However, straightforward management such as, reducing marine plastic pollution, better management of sedimentation, and restoration seagrass habitats, would likely modulate pathogen-associated pressure in these cases.

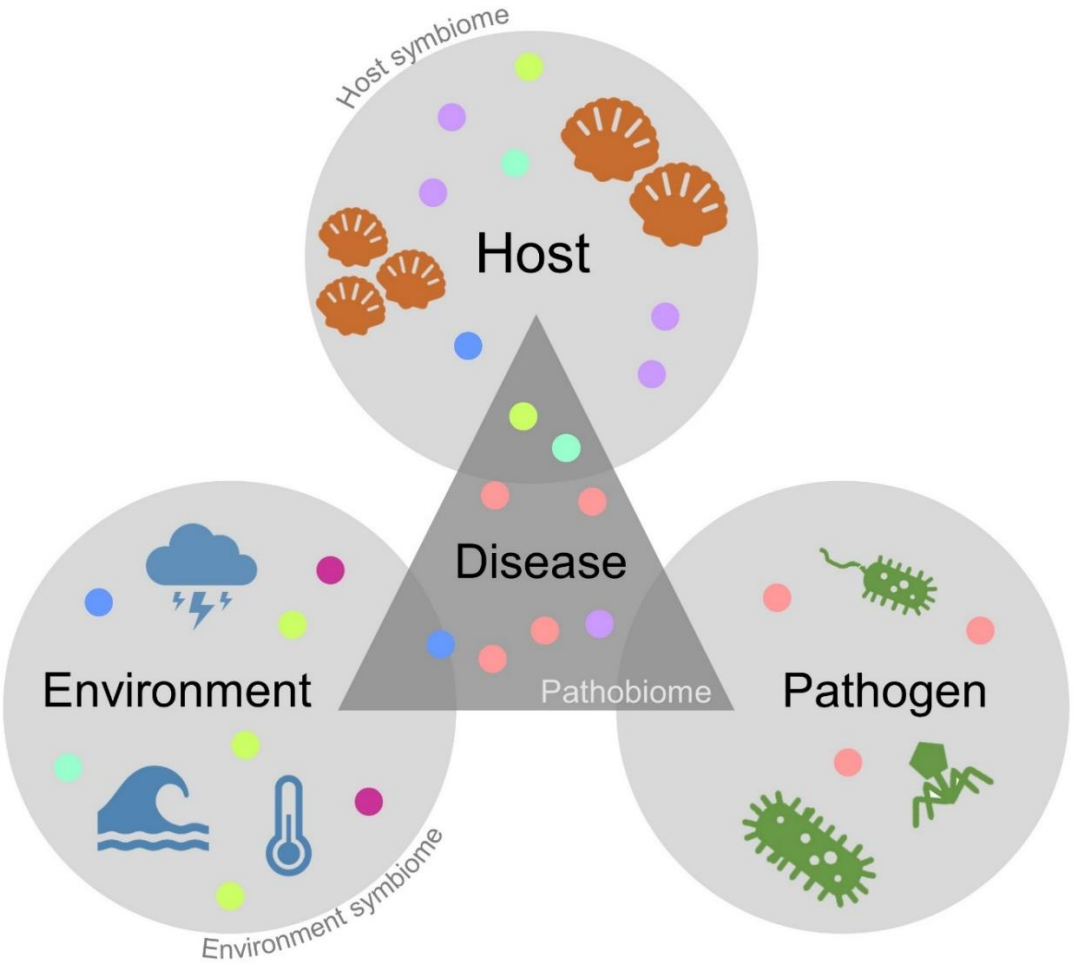

Fig. 1.2. The epidemiological triad as described by Snieszko (1974). Updated to include models described by Bass et al. (2019), including the concept of environmental and host symbiomes, and the transition to the pathobiome or 'diseased state'. Coloured circles represent constituents of respective microbial communities. Pyramid represents the disease epidemiological triad; spheres depict respective symbiomes with distinct microbial communities.

1.2.1 Important Diseases of Marine Molluscs

The prevention, control, and where possible, eradication of animal diseases is wholly reliant on a comprehensive understanding of said diseases and their distribution. FAO (2016) now list 104 mollusc species under production in an aquaculture setting. Despite this growth, disease is still recognised as the greatest limitation to the prosperity and success of this industry (Rowley et al., 2014; Stentiford et al., 2012). With annual losses attributed to disease exceeding US$6 billion (Stentiford et al., 2012; WorldBank, 2014) across the industry. Of all pathogens in marine molluscs, it is said that none has been more destructive to the farming sector than *Perkinsus* (Villalba et al., 2004). Though Carella and Sirri (2017) posit that, due to a lack of specific chemotherapies, viruses are probably the most destructive disease-causing agents in aquaculture of fish and shellfish. Similarly, losses in farmed crustaceans are mainly

associated with viral pathogens (Stentiford et al., 2012). Shellfish do not have an adaptive immune system; thus, vaccines are not a viable option (Guo and Ford, 2016; Lane et al., 2020). *Perkinsus* spp. (protozoa) can cause lethal effects, but also sub-lethal effects, that can cause energy fluxes leading to slower growth and poor condition of hosts (Dittman et al., 2001). Furthermore, these sub-lethal effects can weaken hosts rendering them more susceptible to other opportunistic pathogens or adverse environmental conditions (Villalba et al., 2004). A wide array of *Perkinsus* spp. infect an even wider array of host shellfish. Owed to its vast geographic and host distribution, and its destructive capacity, a wealth of studies has been published on its aetiology, *c.* 25 papers a year since 1980 (Scopus search for '*Perkinsus*').

Vibrio spp. have been attributed to mortality in numerous commercially important shellfish, resulting in significant economic losses (Travers et al., 2015). Importantly, the danger that some *Vibrio* spp. pose to consumers of infected shellfish has raised their notoriety (at least 12 *Vibrio* spp. cause infections in humans) (Baker-Austin et al., 2018), compared to other non-zoonotic pathogens. An opportunistic bacterium, *Vibrio* spp. has been implicated in 'summer mortality syndrome', a phenomenon widely observed in Pacific oysters (Lacoste et al., 2001; Wendling and Wegner, 2013). In *Crassostrea gigas*, both spawning investment and temperature were found to have an additive effect on mortality in those infected with *Vibrio* spp. (Wendling and Wegner, 2013). This case highlights the complexity of disease forensics, as additive effects directly challenge the simple notion of 'pathogen plus host equals disease'. When microbial communities, pollutants, and other environmental pressures are added to the mix, elucidating causes, and predicting outcomes becomes incredibly challenging. In oysters, *Bonamia* (Phylum: Haplosporidia) can cause lethal effects. In the northern hemisphere, *Bonamia ostreae* is more often reported, for example in the United States (east and west coasts; Friedman and Perkins, 1994), northwest Europe (Sas et al., 2020), and in *Ostrea edulis* imports to China from the United States (Feng et al., 2013). In Aotearoa (New Zealand), *Bonamia exitosa* is more commonly reported (Hine et al., 2001) and in Australia, *Bonamia roughleyi* (previously *Mikrocytos roughleyi*) (Carnegie et al., 2014) has long been detected in oyster hosts. However, *B. ostreae* was recently reported for the first time in tio paruparu (Bluff oyster; *Ostrea chilensis*) (Lane et al., 2016). A range of additive effects or 'risk factors' have been associated with infection prevalence and mortality for these aforementioned diseases, which are host, pathogen, and geographically dissimilar. Water temperature, density, and several other intrinsic and extrinsic factors are commonly associated with *Bonamia*–linked mortality in oysters (Table 1.1).

Mentioned diseases of marine molluscs caused by *Vibrio, Bonamia*, and *Perkinsus* spp. are, relatively speaking, straightforward to detect in hosts both by traditional histopathology and by PCR (polymerase chain reaction). A case where the same diagnostic ease was not encountered was in the case of withering syndrome in abalone (Harvell, 2019).

In the mid-1980s researchers recorded Black abalone (*Haliotis cracherodii*) disappearing from their study plots in the Californian intertidal (Haaker et al., 1992). At first, mass die-offs were attributed to an El Niño southern oscillation event, but continued, and spreading mass mortalities suggested an infectious agent was likely present (Lafferty and Kuris, 1993). It was not until nearly 20 years after the first signs of disease, and observed mass mortalities, that researchers linked withering syndrome to an intracellular bacterium *Candidatus* Xenohaliotis californiensis or Withering Syndrome *Rickettsia*-Like Organism (WS-RLO) (Friedman et al., 2000). Following correct identification of the agent responsible for over 20 years of rolling mass mortality events, the pathogen was traced across the globe after a series of first reports of new hosts and new geographic ranges (Fig. 1.3 & Appendix, Table A.1). The spread was subsequently attributed to abalone farms, both in the transport of live animals (Crosson et al., 2014) and the discharge from said aquaculture facilities (Lafferty and Ben-Horin, 2013). Complicated diagnostics stemmed from the limited immune response recorded in hosts infected with what was then dubbed a 'Rickettsiales-like prokaryote' (RLP), although infection intensity was later associated with gross signs of illness (Moore et al., 2000). This trait is shared among many other shellfish spp. that have been identified as hosts of *Rickettsia*-like organisms (RLOs) (Howells et al., 2021) (Table A.1). To-date, RLOs have been recorded all over the world, in clams, oysters, scallops, cockles, and mussels (Fig. 1.3, Table A.1).

Often, RLOs are detected during routine histopathology surveys (Table, A.1). For this reason, and due to the general lack of an inflammatory response (Cano et al., 2020), many remain uncharacterised. This makes comparisons challenging, because without identification of the agent, inferences about effects at a host or population level are diminished. To shed light on this uncertainty, an active move away from the use of the term '*Rickettsia*-like organism' has been suggested (Cano et al., 2018). 'RLO' is a nomenclature placeholder, and as Cano et al. (2018) show, the term can be misleading, and agents are often not bacteria in the genus *Rickettsia*. 'Intracellular microcolonies of bacteria' or 'IMCs' is a more accurate representation of observed inclusions (Cano et al., 2020). Importantly this term calls attention to the fact that the bacteria in question remains uncharacterised. IMCs are often observed during routine histology (Table A.1), but the lack of specific molecular tools and focused studies means their characterisation is an issue. Furthermore, where IMCs are detected, an absence of host response or pathomorphological changes in hosts i.e., tissue necrosis or immune response, reduces the perceived necessity of investigation. That being said, withering syndrome in abalone (Crosson et al., 2014) and mass mortality events reported in several shellfish spp. associated with IMCs (Table A.1; Cano et al., 2020; Cano et al., 2018) underscore the threat they could pose to hosts and therefore, warrant the effort of formal characterisation.

1.2.2 Mass Mortality Events (MMEs)

Mass mortalities of shellfish are a natural phenomenon (Turra et al., 2016) (Fig. 1.1). Superficially, causes can be broken down to intrinsic and extrinsic factors (Table 1.1), though several factors acting concurrently (cumulative stressors) are usually in play (Barbosa Solomieu et al., 2015; Cabanellas-Reboredo et al., 2019; Turra et al., 2016). For example, Cabanellas-Reboredo et al. (2019) link temperature (>13.5 °C) and salinity (36.5–39.7 psu) to mass mortalities of pen shell *Pinna nobilis* populations infected with the likely culprit; *Haplosporidium pinnae*. Garrabou et al. (2019) and Oliver et al. (2017) attribute MMEs in *C. gigas* & abalone spp. to heatwaves, but while high temperatures may result in thermal stress, it is likely that many 'extrinsic factors' are instead additive stressors, increasing host susceptibility to opportunistic pathogens (Harvell et al., 2019). Determining whether MMEs are increasing in the oceans encounters the same problems as trying to determine whether disease outbreaks are increasing (Harvell et al., 2002; Tracy et al., 2019). Specifically, baselines (empirical population data) of shellfish health and MMEs do not exist for many species. To plug this knowledge gap going forward, efforts are being made to record mortality events. For example, in the Mediterranean, MME-T-MEDNet has been set up to collate public observations and make the data readily available (Garrabou et al., 2019). Shellfish MMEs can result in losses for commercial farmers (Barbosa Solomieu et al., 2015) and fishers e.g., *Haliotis* spp. (Rogers-Bennett et al., 2019), but the impacts are especially felt by subsistence fishers and small-scale fisheries in coastal communities (Defeo et al., 2013; Turra et al., 2016). Unfortunately, populations that are relied upon by subsistence and small-scale fishers often do not receive the same monitoring effort than their commercial counterparts (Denadai, 2015; Turra et al., 2016). *"Generally, the degree to which parasites and diseases of aquatic animals have been studied reflect the commercial importance of the host concerned and the severity of infection"* (Lane et al., 2020). As already mentioned, MMEs do occur naturally and do modulate populations. Where their occurrence should raise concern, is where said MMEs begin to track to new populations and (or) when MMEs are sustained or where human activity can be linked to onset. For example, withering syndrome, which tracked the west coast of North America (Crosson et al., 2014 and references therein), as did the eerily similar and arguably more devastating sea star wasting disease (Harvell et al., 2019). The causative agent(s) of sea star wasting disease are still under investigation, but recent research points towards a complex aetiology caused by microbial organic matter remineralisation in the animal-water interface (see Aquino et al., 2021 for details). For comparison, some population densities of abalone were found to have reduced by 99% (*H. cracherodii*) following the onset of the epidemic (Moore et al., 2000; Crosson et al., 2014). In the case of sea star wasting disease, some populations have diminished by between 80-100% across a *c*. 3000 km range

(Harvell et al., 2019) from Mexico to Alaska. Mortality has been linked to the combined effects of marine heatwaves and a disease epidemic (Harvell et al., 2019). With an estimated 5.75 billion sunflower stars (*Pycnopodia helianthoides*) perishing between 2013 and 2020. This has even led to the listing of sunflower stars as critically endangered by the International Union for Conservation of Nature (IUCN) (Hakai, 2020).

1.2.3 Shellfish Disease in Aotearoa (New Zealand)

In terms of disease outbreaks, marine invertebrates in Aotearoa have fared largely unscathed by the pathogens that have wreaked havoc on counterparts in North America (Harvell et al., 2019), Europe (Travers et al., 2015), and Asia (Thitamadee et al., 2016). A significant contributing factor being the relative isolation of Aotearoa, and biosecurity regulations that have been introduced to reduce invasion risk (e.g., Biosecurity Act 1993). These restrictions have been heightened due to the COVID-19 pandemic (Lane et al., 2020). For example, withering syndrome, caused by WS-RLO has not yet made its way to Aotearoa, where Pāua (Māori name for several abalone spp.) would be at considerable risk (Castinel et al., 2014). In recent history, the preparedness of Aotearoa for an ocean outbreak was tested when *B. ostreae* was detected in Bluff oysters (*O. chilensis*) for the first time (prevalence = 40.3%, n = 60) (Lane et al., 2016). The Bluff oyster fishery in Aotearoa is estimated to be worth NZ$20-25 million per annum, providing direct employment (*c.* 250 jobs) to Southland and the Bluff region (Grey, 2017). Following detection, the decision was made to attempt to eradicate *B. ostreae* from Aotearoa by depopulating oyster farms, along with the implementation of controlled areas limiting the movement of some bivalve species within the controlled areas (Ross et al., 2017). These measures appeared to have been successful (Grey, 2017), but signalled the end of the Bluff oyster aquaculture industry in Aotearoa (Lane et al., 2020). The Bluff oyster case provides a rare example where a marine disease outbreak was successfully controlled in the ocean. This case should serve as a warning. Future outbreaks could be a lot harder to control (particularly where the aetiological agent is difficult to discern) and it should bolster the rationale for increased surveillance, and pre-emptive mitigation (Groner et al., 2016).

A report published by the Cawthron Institute in 2014 identified several diseases that pose a risk to shellfish aquaculture in Aotearoa (Castinel et al., 2014). The focus of the report was farmed species, however, disease in the ocean does not respect ‘borders’ between wild and farmed populations (Behringer et al., 2020). Many of the risks identified transcend the farming sector, a point that the authors acknowledge (Castinel et al., 2014). Although the report focuses on diseases and pathogens that could negatively affect the farming of green-lipped mussels (*P. canaliculus*), Pacific oysters (*C. gigas*), and flat oysters (*O. chilensis*), many of

the diseases could also affect many other commercially important seafood from Aotearoa. The report details risk from 28 organisms which pose a potential threat, 11 of which have already been detected in Aotearoa, highlighting the ever-present risk of disease emergence. The two main pathogens that are identified are ostreid herpesvirus-type 1 microvar (OsHV-1) and *Marteilia refringens* (Castinel et al., 2014). Both OsHV-1 (oysters) and *M. refringens* (oysters and mussels) have been associated with large-scale mortalities worldwide (Burge et al., 2006; Kerr et al., 2018). In 2009, OsHV-1 infected oyster farms in northern Aotearoa reported 5-60% mortality in adults and up to 100% losses of spat (Bingham et al., 2013; Lane et al., 2020). In France, 80-100% losses of Pacific oysters in 2008 was attributed to OsHV-1 (Segarra et al., 2010). Furthermore, declines of *O. edulis* attributed to *M. refringens* (Arzul et al., 2011) shows the irreparable damage that disease can do to wild populations, fisheries and the aquaculture sector (see Murray et al., 2012 for a Scotland based risk assessment). The case for increased monitoring of wild and farmed populations, increased biosecurity efforts and careful management of the movement of live shellfish in Aotearoa is clear.

1.3 Toheroa: Iconic, Endemic, and Threatened

The toheroa (*Paphies ventricosa*) is a large (100-150 mm in length) surf clam from the genus *Paphies,* which is endemic to Aotearoa (Fig. 1.1). They are present in large numbers on only a handful of high-energy surf beaches, primarily the west coast of Te Ika-a-Māui (North Island) and south coast of Te Waipounamu (South Island). Populations are generally intertidal, but there are reports of sub-tidal populations (see Ross et al., 2018a). Toheroa are an iconic species and are taonga (treasured; highly prized) kai moana for many Māori (particularly in Tai Tokerau, Kāpiti-Horowhenua, and Murihiku). Their historical importance in the diet of pre-European Māori is evident from archaeological examination of shell middens (Cassie, 1955; Rapson, 1952). The remaining toheroa populations are geographically disjoined (Fig. 1.4), which may be the result of translocations by pre-European Māori, conducted to establish and/or replenish populations isolated from seeding populations (Ross et al., 2018b; V. Taikato, pers. comm.). Genetic separation between northern and southern populations, as well as low genetic diversity in southernmost populations, supports this concept. Historical translocations of marine flora and fauna have been identified globally e.g., *O. edulis* (Bromley et al., 2016) conducted for similar reasons, and in Aotearoa, toheroa are by no means the only example of historical translocations by Māori e.g., the coastal herb *Arthropodium cirratum* (Shepherd et al., 2018).

An intensive commercial fishery and an even more extensive and less regulated recreational fishery ensured a short lifespan of the toheroa fisheries of the early 20th century. Diminishing populations led to a closure of the various regional fisheries (1969 – 1980) and

the introduction of a customary permit system to regulate the collection of toheroa, the same system that exists today. The fate of the toheroa fishery echoes a similar tale of the orange roughy (*Hoplostethus atlanticus*), where unsustainable harvesting led to a collapse of stocks in the 1990s, which have yet to recover to pre-fishery abundances (Clark, 2001). The separation between these two cases is that commercial fisheries still exist for orange roughy, which continue to inhibit their recovery, despite some recovery in selected stocks (Kloser et al., 2015). In contrast, the commercial and recreational fisheries for toheroa have been closed for more than 40 years, and despite this high level of protection, toheroa populations have not recovered to abundances recorded in the early 1900s.

1.3.1 The Toheroa Fishery

See Fig. 1.5 for an overview of the toheroa fishery from 1890 to the present day.

At the beginning of the 20th century, toheroa were incredibly abundant on only a handful of beaches (Ross et al., 2018a). Oreti Beach and Te Waewae Bay in the south of the Te Waipounamu (South Island) (Akroyd et al., 2002; Greenway, 1969; Heasman et al., 2012; Ross et al., 2018a) (Fig. 1.4). In the Te Ika-a-Māui (North Island), major toheroa populations were present along the Kāpiti-Horowhenua coast and from Muriwai (Auckland's west coast) to Te-Oneroa-a-Tōhē (Ninety Mile Beach) (Akroyd et al., 2002; Greenway, 1969; Heasman et al., 2012; Ross et al., 2018a) (Fig. 1.1 and 1.4).

The first toheroa cannery opened on Ripiro Beach in the late 1890s (Stace, 1991), soon after, five commercial factories were opened along the western coastline of the Northland region (Redfearn, 1974; Ross et al., 2018a; Stace, 1991). However, the impact of the recreational fishery cannot be overlooked (Ross et al., 2018a). The decline of toheroa was acknowledged in 1932, when the first restrictions on the amateur fishery were introduced (Williams et al., 2013b). Yet even with these initial protections in place, over one weekend in 1966, close to 1,000,000 toheroa were harvested by 50,000 people in 12,000 vehicles on Ripiro Beach (Murton, 2006). Restrictions on the harvest of toheroa came in waves, which were regionally specific (Fig. 1.5). The commercial fishery ceased in 1969, and in 1993, after one final 'open day', the recreational harvest was closed entirely, cemented in legislation by the Fisheries (Amateur Fishing) Regulations 2013 (SR 2013/482).

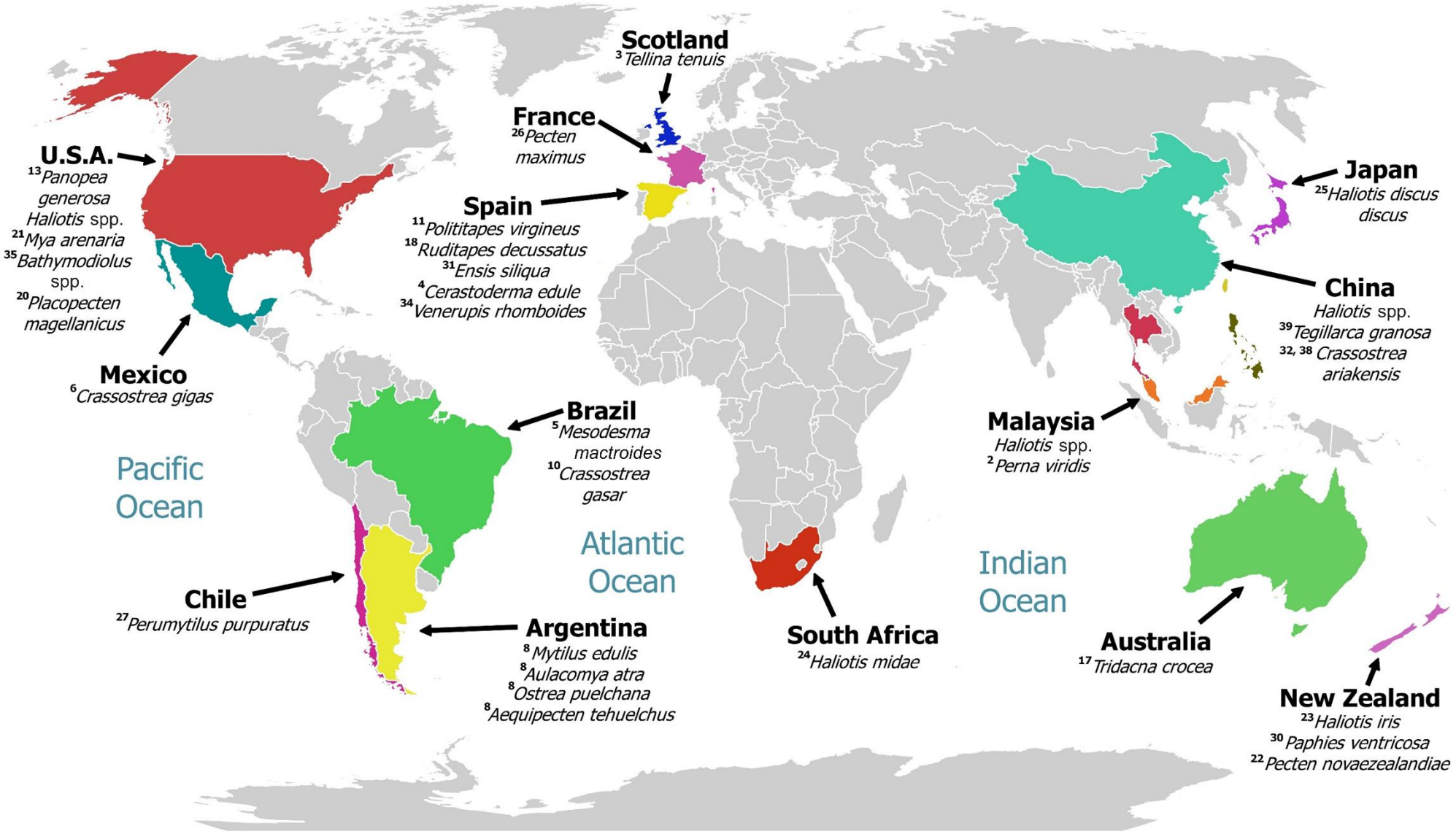

Fig. 1.3. Geographic distribution of intracellular microcolonies (IMCs) in a selection of host species. Hosts have been identified from North and South America, to Europe, Asia, and the South Pacific. Numbers beside species names correspond to 'ID' in Table A.1. Produced using Quantum GIS (QGIS v3.2.3). Spatial data obtained from DIVA-GIS.

Table 1.1. Intrinsic and extrinsic factors associated with shellfish mass mortality events (mostly in the wild). Factor(s) responsible for mortality is given, as well as, examples and associated risk factors of respective mortality events. See Soon and Ransangan (2019) for a dedicated review of extrinsic factors.

	Agent/variable	Location	Year(s)	Species	Associated risk factor(s)	Reference
Intrinsic						
Bacteria	WS-RLO†	Mainly NW USA	1980-90s	Abalone spp.	Temperature	Friedman et al. (1997); Moore et al. (2000)
	Vibrio spp.	Brittany, France; Spain	1990s; 2001-2002	*C. gigas*	Temperature	Lacoste et al. (2001); Gómez-León et al. (2005)
	Endozoicomonas spp.	United Kingdom, Aotearoa (New Zealand)	2017; 2010s	*P. maximus;* Mollusc spp.	Temperature; seasonality	Cano et al. (2018); Howells et al. (2021)
Viral	Ostreid herpesvirus-1 (OsHV-1)	Australia, Aotearoa New Zealand, S Korea	2010; 2011	*C. gigas*	Temperature, interactions with other pathogens; size/age	Hwang et al. (2013); Jenkins et al. (2013); Renault et al. (2012); de Kantzow et al. (2017); Alfaro et al. (2019)
Fungi	*Chaetothyriales*	Fiji Basin	2005	*Bathymodiolus brevior*	Elevated temperature	Van Dover et al. (2007)
Protists	*Bonamia ostreae*	Netherlands	1980s-2000s	*O. edulis*	Population density, temperature, gametogenesis, age, food availability, salinity	Engelsma et al. (2010)
	Perkinsus olseni	NW Spain	1990s	*Tapes decussatus*	Age/size, temperature	Villalba et al. (2005)
	Perkinsus marinus	Virginia, USA	1950s	Oyster spp.	Seasonality	Andrews and Hewatt (1957)
Extrinsic						
Hydrology	Big and small wave action	NW England; SE Brazil	2000s; 2007/08	*Cerastoderma edule; Tivela mactroides*	Strong hydrodynamic forces; low wave-energy events	Burdon et al. (2014); Turra et al. (2016)
Sedimentation	Dredging	USA	1970; various	*C. virginica*; Oyster spp.	4-5 months post dredging*; Ex situ*	Rose (1973); Wilber and Clarke (2001)
Low salinity	High rainfall/flooding	NJ, USA	2011	*C. virginica*	Tropical storm, hurricane	Munroe et al. (2013)
High water temperature	Heatwaves	NW Mediterranean; Australia	2003; 2015/16	Mollusc spp.; *C. gigas* & abalone spp.	Thermal/metabolic stress, potentially disease	Garrabou et al. (2009); Oliver et al. (2017)
Anoxia	Eutrophication	N France	1980s	*C. edule*	Depletion of dissolved oxygen	Desprez et al. (1992); Rybarczyk et al. (1996)
Algal blooms	Various spp.; *Phaeocystis globosa*	Various; SW Netherlands	Various; 2001	Various; *Mytilus edulis*	Smothering & age; sedimentation & anoxia	Shumway (1990); Peperzak and Poelman (2008)
Pollution	Industrial related pollutants in water and sediment	Argentina	1996	*Corbicula fluminea*	Various (incl. PCBs, PAHs and trace elements)	Cataldo et al. (2001)*

†*C.* X. californiensis; **Ex situ* observations using field samples (wild specimens and contaminated water)

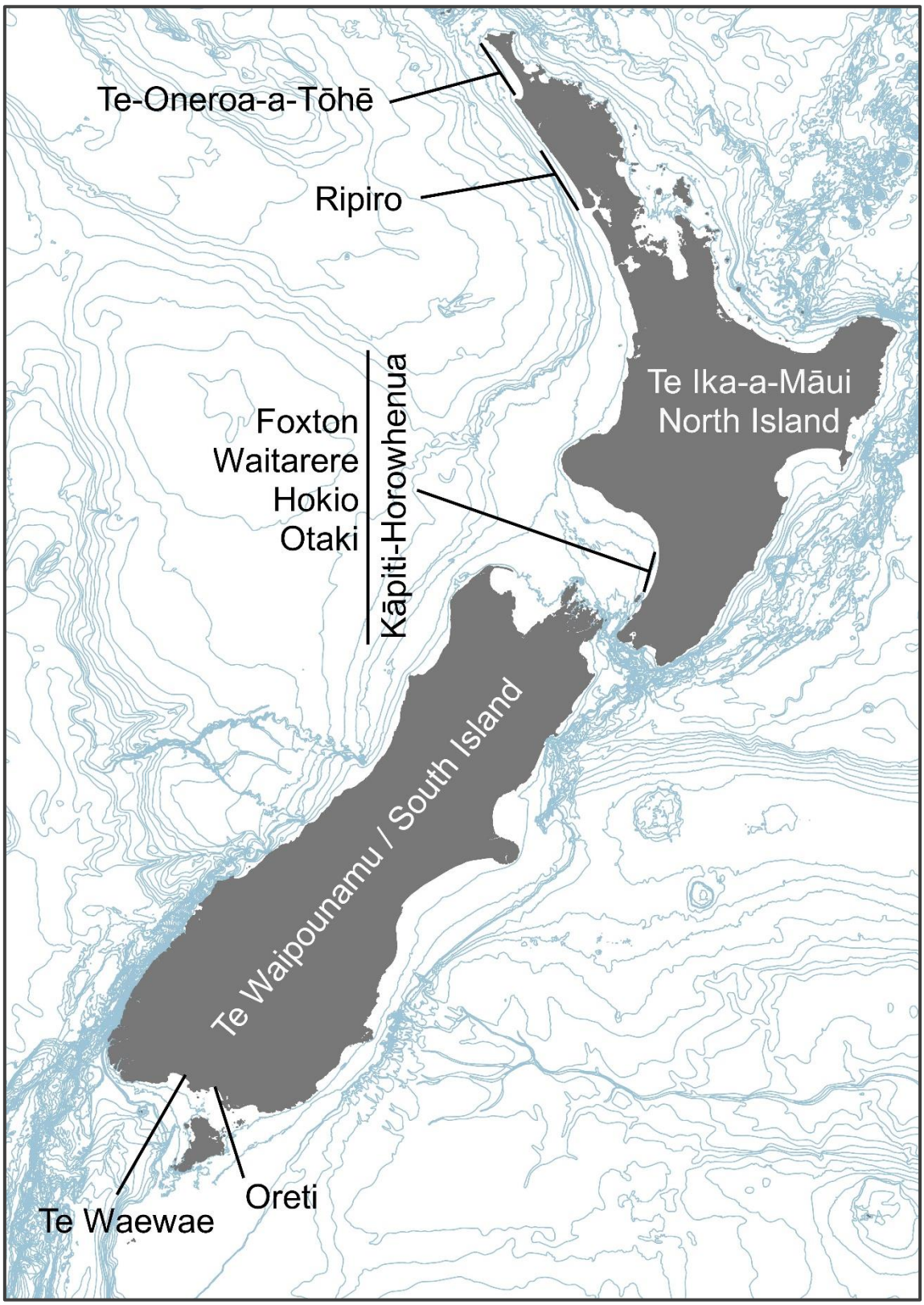

Fig. 1.4. The major remaining toheroa populations around Aotearoa (New Zealand). Information obtained from Ross et al. (2018a) and references therein. Bathymetric lines are in 100 m depth intervals. Bathymetry data obtained from NIWA (www.niwa.co.nz). Spatial data obtained from DIVA-GIS. Produced using Quantum GIS (QGIS v3.2.3). CRS: WGS 84 (EPSG: 4326).

1.3.2 The Recovery of Toheroa (or lack thereof)

The toheroa recreational and commercial fishery was closed with the expectation that populations would recover. However, population surveys have shown that recovery has not taken place at the pace or scale expected following closure of the fisheries (Beentjes, 2010a; Beentjes, 2010b; Berkenbusch, 2015; Williams et al., 2013a). Aside from reviews speculating at possible factors preventing the recovery of populations (Ross et al., 2018a; Williams et al., 2013b) tailored studies focusing on said factors are rare. Recruitment has received attention in recent years, with focus placed on southernmost populations (Fig. 1.4) (Gadomski, 2017). Furthermore, Ross et al. (2018b) investigated how historical translocations by Māori may have altered population structures, but also may explain why some populations are not being naturally reseeded, as the distance to parent populations is too great to support reseeding. Public perceptions surrounding northern populations and predation via South Island pied oystercatchers (*Haematopus finschi*), led to studies of predation pressure to elucidate impact. Findings by Vallyon (2020) however, suggest that while oystercatchers might place localised pressure on selected sub-populations, pressure is spatio-temporally specific and not at a scale which could be attributed to recovery prevention. One potential factor which has been placed under recent spotlight is changing land use inland of beaches (e.g., exotic pine forest plantation, cattle pasture, and human settlement), and subsequent knock-on effects for toheroa habitats (Cope, 2018; Smith, 2013; Williams et al., 2013b).

Surveys of toheroa populations in Te Tai Tokerau (Akroyd et al., 2002; Rapson, 1954; Redfearn, 1974) and Murihiku (Southland) (Beentjes, 2010b) have confirmed local ecological knowledge suggesting the toheroa tend to be found at higher densities where freshwater streams flow onto the beach, than at areas without a stream. In Te Tai Tokerau (Northland), links have been made to pine (*Pinus radiata*) plantations that consume freshwater/groundwater thereby reducing the volume of freshwater reaching toheroa habitats (Williams et al., 2013b). The authors combed historical maps to identify streams that were no longer present on Ripiro Beach. The findings of Williams et al. (2013b) coupled with personal observations, are shown in Fig. 1.6. Evidently, some streams that once flowed onto the beach are no longer present. At Ninety Mile Beach, Williams et al. (2013b) estimated that this stream reduction is even greater with *c*. 53 fewer freshwater streams present compared to the 1950s. Without understanding why streams are important for toheroa life histories, these assessments are incomplete. Cope (2018) attempted to close this knowledge gap by investigating what role the streams played in habitat modification. Focus was placed on temperature, salinity, sedimentology, and topography (Cope, 2018). Findings suggested that the toheroa-stream relationship is likely driven by the modification of intertidal sediments and beach

profile rather than the presence of freshwater itself. Furthermore, reduced desiccation risk due to closer proximity to the water table and modified topography, which could aggregate spat and juvenile toheroa were suggested as additional contributing factors (Cope, 2018). Williams et al. (2013b) mentioned water quality as a potential recovery prevention factor, echoed by Ross et al. (2018a). Reports of inland pollution and poor water quality resulting in toheroa mortality have been reported in the past. For example, agrichemicals used to control black beetle (*Heteronychus arator*) in pine plantations were reportedly linked to mortalities in the 1970s (Smith, 2013). Reduced populations have also been linked to poor stream water quality in Mitimiti, again linked to plantation forestry (Smith, 2013). Many of these connections, like so many other aspects of the toheroa recovery puzzle, have not been formally investigated. Regardless, it appears that freshwater streams influence habitats and toheroa health in certain locations and populations, respectively.

Arguably, the most fundamental and persistent knowledge gaps are of toheroa health. Mass mortality events of toheroa have been reported in 1888, 1900, 1917, 1932, 1938, 1956–1959, 1970–1971, 1991, 1993, 1994, 2001, 2013 (Cassie, 1955; Hine and Wesney, 1997; Rapson, 1954; Ross et al., 2018a; Williams et al., 2013b), and 2019 (P. Ross, pers. comm.). Hine and Wesney (1997) linked the mortalities in 1991, 1993, and 1994 at unspecified locations to virus-like particles, but no follow-up study was conducted. In 2017, following observations of gross ill health in Ripiro Beach populations, Ross et al. (2018c) reported RLOs (IMCs) and gas bubble disease in toheroa (Fig. 1.3 and Table A.1). IMCs have a large host range and have been linked to mass mortality events in the past. Consequently, there is a clear necessity to investigate whether IMCs and gas bubble disease are either causal, or contributing factors, preventing the expected recovery of toheroa.

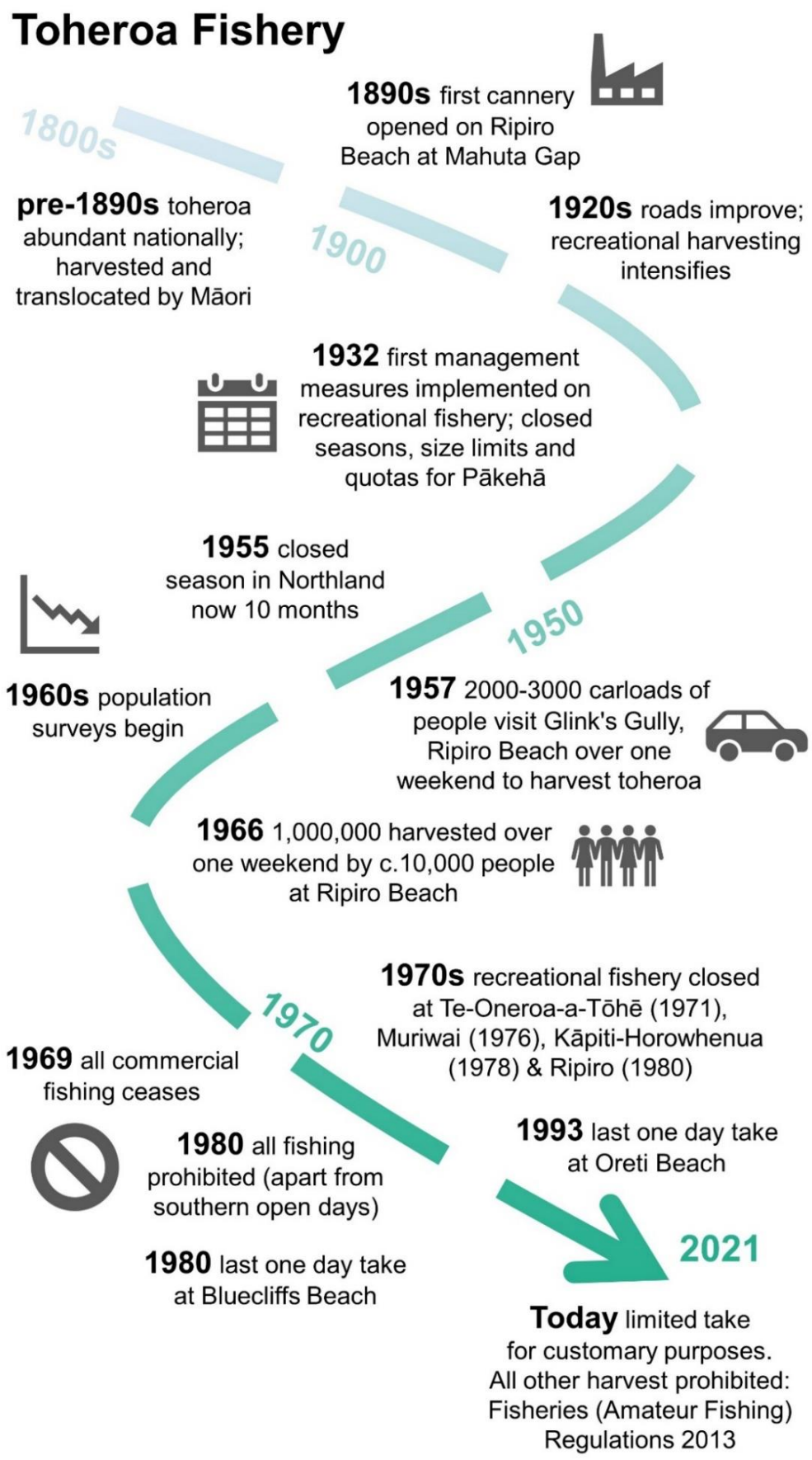

Fig. 1.5. Infographic timeline of toheroa fishery from the 1800s to 2021. Information and dates obtained from (Ross et al., 2018a) and (Williams et al., 2013b) and references therein. Only selected timestamps are shown.

1.4 Disease and Conservation

Disease can impede management and conservation goals of native species (Raymundo et al., 2020; Sas et al., 2020). Managing diseases in the ocean is a complex task (Altizer et al., 2013; Ben-Horin et al., 2016; McCallum et al., 2003; McCallum et al., 2004) and management tools that are applicable terrestrially, are not always directly transferrable to the marine environment (McCallum et al., 2004). Foremost, the ability to manage disease in the marine environment depends on adequate surveillance (Groner et al., 2016), and diagnostics (Carnegie et al., 2016; Lane et al., 2020). In terms of mitigation, often the approach is to target environmental disturbances (where possible), cull/selectively fish, or establish protected areas (Raymundo et al., 2020). Unlike in controlled farm settings, management focused on the parasite or pathogen is typically not a viable option. This is due to the vector-free transmission provided by the medium of seawater (McCallum et al., 2004). Though exceptions to this rule exist, for example Ben-Horin et al. (2016) showed that targeted fishing of diseased abalone (*Haliotis rufescens*) could promote yield and reduce disease prevalence while stock densities were maintained or improved.

The majority of marine disease studies, from a conservation perspective, have been carried out on coral reef ecosystems (Lamb et al., 2014; Lamb and Willis, 2011; Raymundo et al., 2020; Raymundo et al., 2018). Ecosystem services driven by 3-dimensional biogenic habitats like corals (Boström et al., 2011; Woodhead et al., 2019) and their associated biota, justify this attention. Losses of coral reef ecosystems (and other keystone species) owed to disease have profound repercussions for entire tropical ecosystems, where biodiversity loss and reduced functional diversity often follow (Harvell and Lamb, 2020). Unsurprisingly the etiology of coral disease manifestation is complex and difficult to unpick (see 'moving target hypothesis'; Sutherland et al., 2016). Nevertheless, efforts to reduce disease manifestation have proved successful (Groner et al., 2016; Raymundo et al., 2020), demonstrating that disease mitigation efforts can be fruitful, even when aetiologies are not fully understood.

Marine protected areas for conservation often focus on over-exploitation. Usually striving to reduce, or eliminate (marine reserves), direct harvesting pressure (Gaines et al., 2010). However, secondary effects of protected areas in terms of disease are less understood. Lamb et al. (2016) found that marine protected areas alleviated coral disease under acute and chronic environmental disturbances. Importantly the authors highlight that spatially fixed marine protected areas are likely substantially less effective at disease mitigation for mobile biota than for sedentary counterparts. Coupled with shortcomings of fixed marine protected areas and range shifts linked to climate change (Hannah et al., 2007), a static approach to MPAs focused on target species may have more success mitigating disease than those spatially locked.

Shellfish restoration projects (e.g., Essex Native Oyster Restoration Initiative, UK and Revive our Gulf, Aotearoa) have seen a dramatic upsurge in recent years (Pogoda et al., 2020; zu Ermgassen et al., 2020). With native oyster reefs being the focus of many projects. Like coral reefs, shellfish reefs provide a 3-dimensional biogenic habitat, delivering an array of ecosystem services (Grabowski et al., 2012). Many of these projects face regionally specific hurdles, mainly attributed to habitat degradation and disease (Carnegie and Burreson, 2011; Pogoda et al., 2020; Sas et al., 2020). Disease was recently reviewed as a limiting factor to restoration success, demonstrated by the effect of *B. ostreae* in European populations of *O. edulis* (Sas et al., 2020). Importantly, the authors mention that with significant 'unknowns' remaining regarding the risk factors which aggravate bonamiosis in *O. edulis*, a precautionary approach should be taken when introducing naïve oysters to areas where oysters are not currently present. Unassisted re-emergence of native oysters (*O. edulis*) in Belfast Lough, Northern Ireland has recently been reported, following 100 years of local extinction (Smyth et al., 2021). Under the same pretext, perhaps the toheroa simply requires more time. That being said, the authors note that dredging in the port, may have altered hydrodynamics in a manner that could have contributed to this re-emergence.

A comparison can be drawn between toheroa and native oyster restoration projects, particularly in respect to the impact diseases have (various oyster spp.), or might be having (toheroa) on the recovery of native populations (e.g., bonamiosis in the case of oysters,Holbrook et al., 2021). The poor recovery of toheroa populations remains a mystery and no single factor stands out as a likely cause. Disease has been mentioned by previous reviews (Ross et al., 2018a; Williams et al., 2013b) but no formal investigations of toheroa health exist. Furthermore, Ross et al. (2018c) reported IMCs and a mysterious affliction (gas bubble disease) in toheroa for the first time, justifying investigatory work. Like the native oyster reef projects, the conservation and restoration of toheroa is potentially hampered, if not at least reduced, without a working knowledge of the role that disease is currently playing in toheroa populations. For example, what role might disease be playing in the food web encompassing toheroa or what impact could parasites/pathogens be having on recruitment (Wahle et al., 2009) and therefore, the accuracy of population surveys/stock assessments? (Hoenig et al., 2017). IMCs have been dismissed in the past due to their apparent benign presence (without immune response) in hosts (Cano et al., 2020, and references therein). Though as history shows, this is not always the case (Table, A1) and exceptions to the rule exist (Crosson et al., 2014; Moore et al., 2000). It could be that disease currently plays a minor role in the ongoing recovery of toheroa. If only to rule out disease as an opponent to management and conservation goals, systematic investigatory effort is required to provide empirical data of toheroa health.

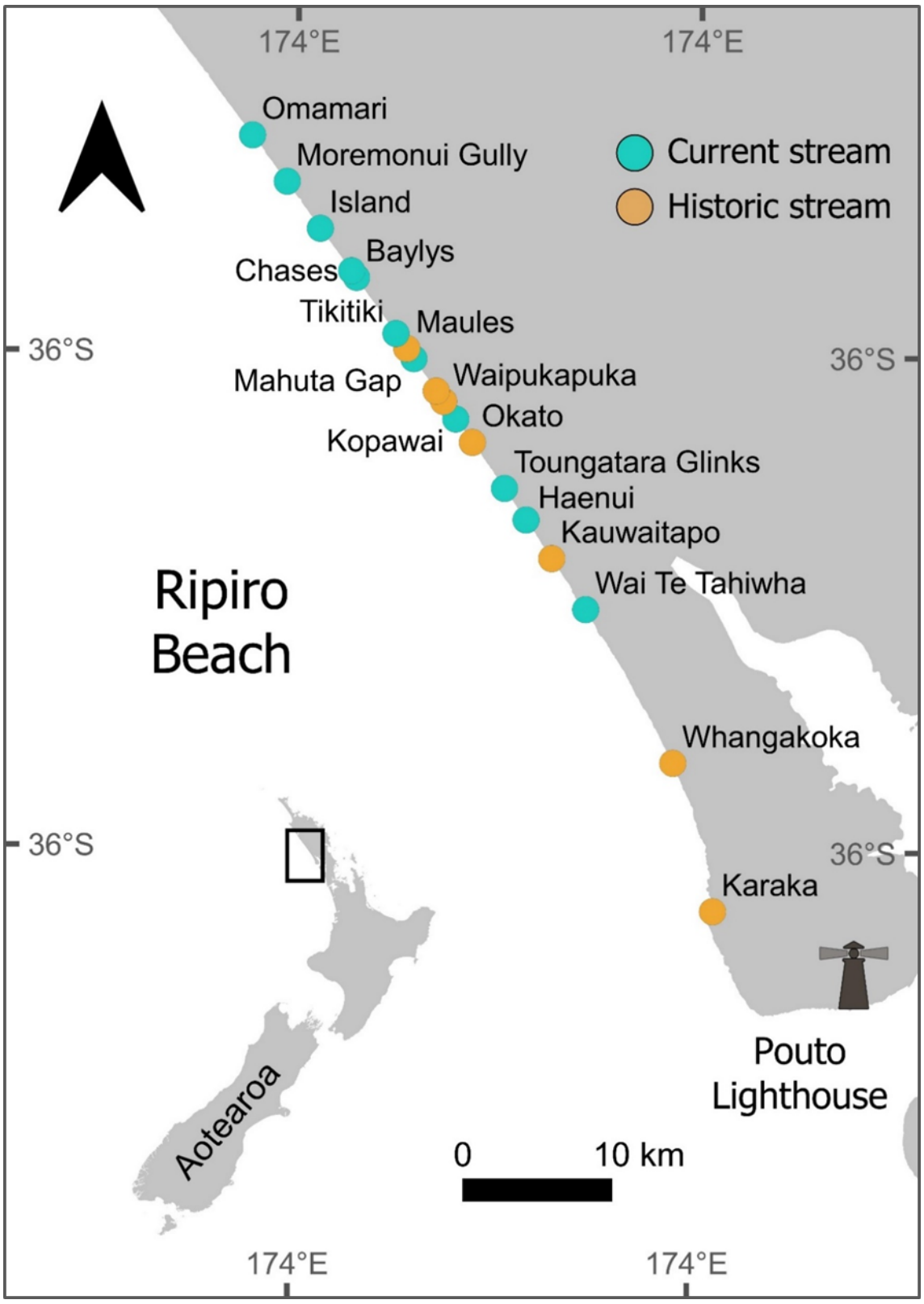

Fig. 1.6. Current and historical (pre 1950s) stream locations on Ripiro Beach, Te Tai Tokerau. Stream locations and names derived from multiple sources, including Cope (2018), Williams et al. (2013b), Barry Searle, Dargaville (J. Forde, pers. comm.), personal observations and GoogleEarth. Spatial data obtained from DIVA-GIS. CRS: WGS 84 (EPSG: 4326). Note: some of these 'streams' are ephemeral, the flow at Island for example, is variable in its volume and presence.

1.5 Current State of Knowledge

There is no baseline of data for toheroa health. When *Rickettsia*-like organisms and gas bubble disease were reported in 2018 (Ross et al., 2018c), little data of toheroa intrinsic health was available to investigators to advise response. Additionally, due to these knowledge gaps, the scale at which disease might be contributing to the limited recovery of toheroa can only be speculated on at present. Assessments of remaining toheroa populations (Berkenbusch, 2015; Williams et al., 2013a) have not considered disease, despite its importance for stock assessments (Hoenig et al., 2017; Lane et al., 2020). With little capacity in this area, considering disease in toheroa population assessments has not been possible. Furthermore, routine surveillance of toheroa populations is likely to inform the direction of future research. In this sense, disease-related mortality could be included into population assessments (if applicable) and conservation efforts of remaining wild populations could incorporate disease mitigation strategies into management plans (also, if applicable). Finally, research on toheroa aquaculture is currently underway, if aquaculture for conservation or commercial enterprise begins, its success will hinge on a working knowledge of toheroa health.

1.6 Overview of this Thesis

Recognising the significant gaps that exist in our knowledge of toheroa health, this thesis primarily attempts to provide an overarching snapshot of toheroa health from remaining major populations in Aotearoa New Zealand (Fig. 1.4). To achieve this, several diagnostic tools were used, and six exploratory studies were conducted.

In **Chapter 2**, I shine a light on the capacity gaps within the marine disease sphere in Aotearoa. This first section focuses on what appears to be an upsurge in the occurrence of MMEs in Aotearoa and their association to *Endozoicomonas* spp., and subsequently makes the case for increased surveillance of wild shellfish, particularly of those that do not comprise a commercial fishery. In **Chapter 3**, I attempt to close some of the knowledge gaps in this area with respect to toheroa, where key baseline health information is obtained using traditional pathology methods. This data is combined with computational modelling to draw attention to the persistent relevance and value of histology in aquatic pathology. In **Chapter 4**, I use molecular pathology techniques to characterise the bacteria referred to as a '*Rickettsia*-like organism' by Ross et al. (2018c) and seasonal infection patterns are investigated to determine what pressure this potential pathogen might placing on remaining toheroa populations. In **Chapter 5,** I examine the importance of freshwater streams for toheroa life histories, with reference to the capacity of freshwater streams to modulate the toheroa microbiome. Following *in situ* observations, and findings from Chapters 3 & 4, questions arose regarding the

potential for streams to deliver pollutants to toheroa beds in the intertidal. To explore these questions, in **Chapter 6**, I conduct a preliminary study to examine trace metal concentrations in toheroa tissues. In **Chapter 7**, I examine the pathogenesis of 'gas bubble disease' often observed in toheroa and a new manifestation pathway hypothesis is presented, providing a unique paradigm in shellfish health globally.

Finally, in **Chapter 8**, my general discussion, I consider the role of symbionts in toheroa and other Aotearoa shellfish. I also discuss persistent knowledge gaps and importantly, current limitations in our ability to respond to diseases in marine organisms.

1.7 References

Akroyd, J. A. M., et al., 2002. Abundance, distribution, and size structure of toheroa (*Paphies ventricosa*) at Ripiro Beach, Dargaville, Northland, New Zealand. New Zealand Journal of Marine and Freshwater Research. 36**,** 547-553.

Alfaro, A. C., et al., 2019. The complex interactions of Ostreid herpesvirus 1, *Vibrio* bacteria, environment and host factors in mass mortality outbreaks of *Crassostrea gigas*. Reviews in Aquaculture. 11**,** 1148-1168.

Altizer, S., et al., 2013. Climate Change and Infectious Diseases: From Evidence to a Predictive Framework. Science. 341**,** 514-519.

Andrews, J. D., Hewatt, W. G., 1957. Oyster Mortality Studies in Virginia. II. The Fungus Disease Caused by *Dermocystidium marinum* in Oysters of Chesapeake Bay. Ecological Monographs. 27**,** 1-25.

Apprill, A., 2017. Marine Animal Microbiomes: Toward Understanding Host–Microbiome Interactions in a Changing Ocean. Frontiers in Marine Science. 4**,** 222.

Aquino, C. A., et al., 2021. Evidence That Microorganisms at the Animal-Water Interface Drive Sea Star Wasting Disease. Frontiers in Microbiology. 11, 610009.

Armitage, A., et al., 2017. Governing the Coastal Commons Communities, Resilience and Transformation. Routledge, London, UK.

Arrigo, K. R., 2005. Marine microorganisms and global nutrient cycles. Nature. 437**,** 349-355.

Arzul, I., et al., 2011. Can the protozoan parasite *Bonamia ostreae* infect larvae of flat oysters *Ostrea edulis*? Veterinary Parasitology. 179**,** 69-76.

Baker-Austin, C., et al., 2018. *Vibrio* spp. infections. Nature Reviews Disease Primers. 4**,** 1-9.

Bank, M. S., et al., 2020. Seafood Safety Revisited: Response to Comment on "Defining Seafood Safety in the Anthropocene". Environmental Science & Technology. 54**,** 12805-12806.

Bar-On, Y. M., et al., 2018. The biomass distribution on Earth. Proceedings of the National Academy of Sciences. 115**,** 6506–6511.

Barbosa Solomieu, V., et al., 2015. Mass mortality in bivalves and the intricate case of the Pacific oyster, *Crassostrea gigas*. Journal of Invertebrate Pathology. 131**,** 2-10.

Bass, D., et al., 2019. The Pathobiome in Animal and Plant Diseases. Trends in Ecology & Evolution. 34**,** 996-1008.

Beaumont, N. J., et al., 2007. Identification, definition and quantification of goods and services provided by marine biodiversity: Implications for the ecosystem approach. Marine Pollution Bulletin. 54**,** 253-265.

Beentjes, M. P., 2010a. Toheroa survey of Bluecliffs Beach, 2009, and review of historical surveys. New Zealand Fisheries Assessment Report 2010/7. 42.

Beentjes, M. P., 2010b. Toheroa survey of Oreti Beach, 2009, and review of historical surveys. New Zealand Fisheries Assessment Report 2010/6. 40.

Behringer, D. C., et al., Disease in fisheries and aquaculture. In: D. Behringer, et al., Eds., Marine Disease Ecology. Oxford University Press, Oxford, 2020.

Belinsky, D. L., et al., 1996. Composition of Fish Consumed by the James Bay Cree. Journal of Food Composition and Analysis. 9**,** 148-162.

Ben-Horin, T., et al., 2016. Fishing diseased abalone to promote yield and conservation. Philosophical Transactions of the Royal Society B: Biological Sciences. 371**,** 20150211.

Bennett, N. J., et al., 2018. Coastal and Indigenous community access to marine resources and the ocean: A policy imperative for Canada. Marine Policy. 87**,** 186-193.

Bennion, M., et al., 2019. Trace element fingerprinting of blue mussel (*Mytilus edulis*) shells and soft tissues successfully reveals harvesting locations. Science of The Total Environment. 685**,** 50-58.

Berkenbusch, K., Distribution and abundance of toheroa in Southland, 2013–14. New Zealand Fisheries Assessment Report 2015/17, 2015, pp. 41.

Bhattacharya, A., Sarkar, S. K., 2003. Impact of Overexploitation of Shellfish: Northeastern Coast of India. AMBIO: A Journal of the Human Environment. 32**,** 70-75.

Bingham, P., et al., 2013. Investigation into the first diagnosis of ostreid herpesvirus type 1 in Pacific oysters. Surveillance. 40**,** 20-24.

Bodwitch, H., 2017. Challenges for New Zealand's individual transferable quota system: Processor consolidation, fisher exclusion, & Māori quota rights. Marine Policy. 80**,** 88-95.

Bojko, J., et al., Pollution can drive marine diseases. In: D. Behringer, et al., Eds., Marine Disease Ecology. Oxford University Press, Oxford, 2020.

Boström, C., et al., 2011. Seascape ecology of coastal biogenic habitats advances, gaps, and challenges. Marine Ecology Progress Series. 427**,** 191-218.

Bricknell, I. R., et al., 2021. Resilience of cold water aquaculture: a review of likely scenarios as climate changes in the Gulf of Maine. Reviews in Aquaculture. 13**,** 460-503.

Bromley, C., et al., 2016. Bad moves: Pros and cons of moving oysters – A case study of global translocations of *Ostrea edulis* Linnaeus, 1758 (Mollusca: Bivalvia). Ocean & Coastal Management. 122**,** 103-115.

Burdon, D., et al., 2014. Mass mortalities in bivalve populations: A review of the edible cockle *Cerastoderma edule* (L.). Estuarine, Coastal and Shelf Science. 150**,** 271-280.

Burge, C. A., et al., Climate Change Influences on Marine Infectious Diseases: Implications for Management and Society. In: C. A. Carlson, S. J. Giovannoni, Eds., Annual Review of Marine Science, Vol 6, 2014, pp. 249-277.

Burge, C. A., et al., 2006. Mortality and herpesvirus infections of the Pacific oyster *Crassostrea gigas* in Tomales Bay, California, USA. Diseases of Aquatic Organisms. 72**,** 31-43.

Burge, C. A., Hershberger, P. K., Climate change can drive marine diseases. In: D. Behringer, et al., Eds., Marine Disease Ecology. Oxford University Press, Oxford, 2020.

Burger, J., et al., 2007. Mercury levels and potential risk from subsistence foods from the Aleutians. Science of The Total Environment. 384**,** 93-105.

Cabanellas-Reboredo, M., et al., 2019. Tracking a mass mortality outbreak of pen shell *Pinna nobilis* populations: A collaborative effort of scientists and citizens. Scientific Reports. 9**,** 13355.

Cano, I., et al., 2020. Cosmopolitan Distribution of *Endozoicomonas*-Like Organisms and Other Intracellular Microcolonies of Bacteria Causing Infection in Marine Mollusks. Frontiers in Microbiology. 11**,** 2778.

Cano, I., et al., 2018. Molecular Characterization of an *Endozoicomonas*-Like Organism Causing Infection in the King Scallop (*Pecten maximus* L.). Applied and Environmental Microbiology. 84**,** e00952-17.

Carella, F., Sirri, R., 2017. Editorial: Fish and Shellfish Pathology. Frontiers in Marine Science. 4**,** 3.

Carnegie, R. B., et al., 2016. Managing marine mollusc diseases in the context of regional and international commerce: policy issues and emerging concerns. Philosophical Transactions of the Royal Society B: Biological Sciences. 371**,** 20150215.

Carnegie, R. B., Burreson, E. M., 2011. Declining impact of an introduced pathogen: *Haplosporidium nelsoni* in the oyster *Crassostrea virginica* in Chesapeake Bay. Marine Ecology Progress Series. 432**,** 1-15.

Carss, D. N., et al., 2020. Ecosystem services provided by a non-cultured shellfish species: The common cockle *Cerastoderma edule*. Marine Environmental Research. 158**,** 104931.

Cassie, R. M., 1955. Population Studies on the Toheroa, *Amphidesma ventricosum* Gray (Eulamellibranchiata). Marine and Freshwater Research. 6**,** 348-391.

Castinel, A., et al., Review of disease risks for New Zealand shellfish aquaculture: Perspectives for management. Cawthron Report 2297. Prepared for Ministry for Business, Innovation and Employment. Cawthron Institute, Nelson, NZ, 2014, pp. 31.

Cataldo, D., et al., 2001. Environmental toxicity assessment in the Paraná river delta (Argentina): simultaneous evaluation of selected pollutants and mortality rates of *Corbicula fluminea* (Bivalvia) early juveniles. Environmental Pollution. 112**,** 379-389.

Cisneros-Montemayor, A. M., et al., 2016. A Global Estimate of Seafood Consumption by Coastal Indigenous Peoples. PLOS ONE. 11**,** e0166681.

Clark, M., 2001. Are deepwater fisheries sustainable? — the example of orange roughy (*Hoplostethus atlanticus*) in New Zealand. Fisheries Research. 51**,** 123-135.

Cohen, N. J., et al., 2009. Public health response to puffer fish (Tetrodotoxin) poisoning from mislabeled product. Journal of Food Protection. 72**,** 810-817.

Cope, J., The modification of toheroa habitat by streams on Ripiro Beach. MSc. University of Waikato, Hamilton, New Zealand, 2018, pp. 126.

Costello, C., et al., 2020. The future of food from the sea. Nature. 588**,** 95-100.

Crosson, L. M., et al., 2014. Abalone withering syndrome: distribution, impacts, current diagnostic methods and new findings. Diseases of Aquatic Organisms. 108**,** 261-270.

Culver, C. S., Kuris, A. M., 2000. The Apparent Eradication of a Locally Established Introduced Marine Pest. Biological Invasions. 2**,** 245-253.

de Kantzow, M. C., et al., 2017. Risk factors for mortality during the first occurrence of Pacific Oyster Mortality Syndrome due to Ostreid herpesvirus – 1 in Tasmania, 2016. Aquaculture. 468**,** 328-336.

Defeo, O., et al., 2013. Impacts of Climate Variability on Latin American Small-scale Fisheries. Ecology and Society. 18**,** 30.

Denadai, M. R., 2015. Harvesting the Beach Clam *Tivela mactroides*: Short- and Long-Term Dynamics. Marine and Coastal Fisheries: Dynamics, Management, and Ecosystem Science. 7**,** 103-115.

Desprez, M., et al., 1992. Biological impact of eutrophication in the bay of Somme and the induction and impact of anoxia. Netherlands Journal of Sea Research. 30**,** 149-159.

Diggles, B. K., 2013. Historical epidemiology indicates water quality decline drives loss of oyster (*Saccostrea glomerata*) reefs in Moreton Bay, Australia. New Zealand Journal of Marine and Freshwater Research. 47**,** 561-581.

Dittman, D. E., et al., 2001. Effects of *Perkinsus marinus* on reproduction and condition of the eastern oyster, *Crassostrea virginica*, depend on timing. Journal of Shellfish Research. 20**,** 1025-1034.

Egan, S., Gardiner, M., 2016. Microbial Dysbiosis: Rethinking Disease in Marine Ecosystems. Frontiers in Microbiology. 7**,** 991-991.

Engelsma, M. Y., et al., 2010. Epidemiology of *Bonamia ostreae* infecting European flat oysters *Ostrea edulis* from Lake Grevelingen, The Netherlands. Marine Ecology Progress Series. 409**,** 131-142.

FAO, The State of World Fisheries and Aquaculture 2016. Contributing to food security and nutrition for all. Food and Agriculture Organization of the United Nations, Rome, 2016, pp. 200.

FAO, The State of World Fisheries and Aquaculture 2018 - Meeting the sustainable development goals. Food and Agriculture Organization of the United Nations, Rome, 2018, pp. 211.

Feng, C., et al., 2013. Detection and characterization of *Bonamia ostreae* in *Ostrea edulis* imported to China. Diseases of Aquatic Organisms. 106**,** 85-91.

Frère, L., et al., 2018. Microplastic bacterial communities in the Bay of Brest: Influence of polymer type and size. Environmental Pollution. 242**,** 614-625.

Friedman, C. S., et al., 2000. '*Candidatus* Xenohaliotis californiensis', a newly described pathogen of abalone, *Haliotis* spp., along the west coast of North America. International Journal of Systematic and Evolutionary Microbiology. 50**,** 847-855.

Friedman, C. S., Perkins, F. O., 1994. Range extension of *Bonamia ostreae* to Maine, U.S.A. Journal of Invertebrate Pathology. 64**,** 179-181.

Friedman, C. S., et al., 1997. Withering syndrome of the black abalone, *Haliotis cracherodii* (Leach): Water temperature, food availability, and parasites as possible causes. Journal of Shellfish Research. 16**,** 403-411.

Gadomski, K., Reproduction and larval ecology of the toheroa, *Paphies ventricosa*, from Oreti Beach, Southland, New Zealand. PhD. University of Otago, 2017, pp. 155.

Gaines, S. D., et al., 2010. Designing marine reserve networks for both conservation and fisheries management. Proceedings of the National Academy of Sciences. 107**,** 18286-18293.

Garrabou, J., et al., 2009. Mass mortality in Northwestern Mediterranean rocky benthic communities: effects of the 2003 heat wave. Global Change Biology. 15**,** 1090-1103.

Garrabou, J., et al., 2019. Collaborative Database to Track Mass Mortality Events in the Mediterranean Sea. Frontiers in Marine Science. 6**,** 707.

Gascon, M., et al., 2017. Outdoor blue spaces, human health and well-being: A systematic review of quantitative studies. International Journal of Hygiene and Environmental Health. 220**,** 1207-1221.

Gilbert, J. A., Neufeld, J. D., 2014. Life in a World without Microbes. PLOS Biology. 12**,** e1002020.

Giovannoni, S. J., et al., 1990. Genetic diversity in Sargasso Sea bacterioplankton. Nature. 345**,** 60-63.

Giusti, A., et al., 2018. Emerging risks in the European seafood chain: Molecular identification of toxic *Lagocephalus* spp. in fresh and processed products. Food Control. 91**,** 311-320.

Goecke, F., et al., 2012. A Novel Phytomyxean Parasite Associated with Galls on the Bull-Kelp *Durvillaea antarctica* (Chamisso) Hariot. PLOS ONE. 7**,** e45358.

Gómez-León, J., et al., 2005. Isolation of *Vibrio alginolyticus* and *Vibrio splendidus* from aquacultured carpet shell clam (*Ruditapes decussatus*) larvae associated with mass mortalities. Applied and Environmental Microbiology. 71**,** 98-104.

Goyette, S., et al., 2014. Seroprevalence of parasitic zoonoses and their relationship with social factors among the Canadian Inuit in Arctic regions. Diagnostic Microbiology and Infectious Disease. 78**,** 404-10.

Grabowski, J. H., et al., 2012. Economic Valuation of Ecosystem Services Provided by Oyster Reefs. BioScience. 62**,** 900-909.

Grattan, L. M., et al., 2016. Harmful algal blooms and public health. Harmful Algae. 57**,** 2-8.

Greenway, J. P. C., 1969. Population surveys of toheroa (Mollusca: Eulamellffiranchiata) on Northland Beaches, 1962–67. New Zealand Journal of Marine and Freshwater Research. 3**,** 318-338.

Grey, J., Bluff oysters look to be clear from parasite. NZ Herald, 2017. Access date: Dec 2020. https://www.nzherald.co.nz/business/bluff-oysters-look-to-be-clear-from-parasite/UP7VWHK3V7I52BW6TI5HRX4AGI/.

Groner, M. L., et al., 2016. Managing marine disease emergencies in an era of rapid change. Philosophical Transactions of the Royal Society B-Biological Sciences. 371**,** 20150364.

Guillen, J., et al., 2019. Global seafood consumption footprint. Ambio. 48**,** 111-122.

Guo, X., Ford, S. E., 2016. Infectious diseases of marine molluscs and host responses as revealed by genomic tools. Philosophical Transactions of the Royal Society B: Biological Sciences. 371**,** 20150206.

Haaker, P. L., et al., Mass mortality and withering syndrome in black abalone, *Haliotis cracherodii*, in California. In: S. A. Shepherd, et al., Eds., Abalone of the world: biology, fisheries, and culture. Proc 1st Int Symp Abalone. University Press, Cambridge, 1992, pp. 214-224.

Hakai, Sunflower Stars Now Critically Endangered. Hakai Institute, British Columbia, Canada, 2020. Access date: Dec 2020. https://www.hakaimagazine.com/videos-visuals/sunflower-sea-stars-now-critically-endangered/.

Hannah, L., et al., 2007. Protected area needs in a changing climate. Frontiers in Ecology and the Environment. 5**,** 131-138.

Harvell, C. D., 2019. Ocean outbreak: confronting the rising tide of marine disease. University of California Press, Oakland (CA).

Harvell, C. D., Lamb, B. J., Disease outbreaks can threaten marine biodiversity. In: R. B. Silliman, D. K. Lafferty, Eds., Marine Disease Ecology. Oxford University Press, Oxford, United Kingdom, 2020, pp. 18.

Harvell, C. D., et al., 2002. Climate Warming and Disease Risks for Terrestrial and Marine Biota. Science. 296**,** 2158-2162.

Harvell, C. D., et al., 2019. Disease epidemic and a marine heat wave are associated with the continental-scale collapse of a pivotal predator (*Pycnopodia helianthoides*). Science Advances. 5**,** eaau7042.

Harvell, D., et al., 2004. The rising tide of ocean diseases: unsolved problems and research priorities. Frontiers in Ecology and the Environment. 2**,** 375-382.

Harwood, T., et al., Tetrodotoxin in non-commercial New Zealand bivalve shellfish. New Zealand Food Safety Technical Paper No: 2020/17. Ministry for Primary Industries, Wellington, NZ, 2020, pp. 18.

Haswell-Elkins, M., et al., 2007. Exploring potential dietary contributions including traditional seafood and other determinants of urinary cadmium levels among indigenous women of a Torres Strait Island (Australia). Journal of Exposure Science and Environmental Epidemiology. 17**,** 298-306.

Hauer, M. E., et al., 2020. Sea-level rise and human migration. Nature Reviews Earth & Environment. 1**,** 28-39.

Heasman, K., et al., Factors affecting populations of Toheroa (*Paphies ventricosa*): a literature review. Manaaki Taha Moana Research Report No. 10. 2012, pp. 29.

Henri, D. A., et al., 2018. Using Inuit traditional ecological knowledge for detecting and monitoring avian cholera among Common Eiders in the eastern Canadian Arctic. Ecology and Society. 23**,** 22.

Hilborn, R., et al., 2020. Effective fisheries management instrumental in improving fish stock status. Proceedings of the National Academy of Sciences. 117**,** 2218-2224.

Hine, P. M., et al., 2001. *Bonamia exitiosus* n.sp. (Haplosporidia) infecting flat oysters *Ostrea chilensis* in New Zealand. Diseases of Aquatic Organisms. 47**,** 63-72.

Hine, P. M., Wesney, B., 1997. Virus-like particles associated with cytopathology in the digestive gland epithelium of scallops *Pecten novaezelandiae* and toheroa *Paphies ventricosum*. Diseases of Aquatic Organisms. 29**,** 197-204.

Hoenig, J. M., et al., 2017. Impact of disease on the survival of three commercially fished species. Ecological Applications. 27**,** 2116-2127.

Holbrook, Z., et al., 2021. What do the terms resistance, tolerance, and resilience mean in the case of *Ostrea edulis* infected by the haplosporidian parasite *Bonamia ostreae*. Journal of Invertebrate Pathology. 182**,** 107579.

Hoover, C., et al., 2016. The Continued Importance of Hunting for Future Inuit Food Security. Solutions. 6**,** 40-50.

Howells, J., et al., 2021. Intracellular bacteria in New Zealand shellfish are identified as *Endozoicomonas* species. Diseases of Aquatic Organisms. 143**,** 27-37.

Hwang, J. Y., et al., 2013. Ostreid herpesvirus 1 infection in farmed Pacific oyster larvae *Crassostrea gigas* (Thunberg) in Korea. Journal of Fish Diseases. 36**,** 969-972.

Islam, D., Berkes, F., 2016. Indigenous peoples' fisheries and food security: a case from northern Canada. Food Security. 8**,** 815-826.

Jenkins, C., et al., 2013. Identification and characterisation of an ostreid herpesvirus-1 microvariant (OsHV-1 µ-var) in *Crassostrea gigas* (Pacific oysters) in Australia. Diseases of Aquatic Organisms. 105**,** 109-126.

Kerr, R., et al., 2018. *Marteilia refringens* and *Marteilia pararefringens* sp. nov. are distinct parasites of bivalves and have different European distributions. Parasitology. 145**,** 1483-1492.

Kirstein, I. V., et al., 2016. Dangerous hitchhikers? Evidence for potentially pathogenic *Vibrio* spp. on microplastic particles. Marine Environmental Research. 120**,** 1-8.

Kloser, R. J., et al., 2015. Indicators of recovery for orange roughy (*Hoplostethus atlanticus*) in eastern Australian waters fished from 1987. Fisheries Research. 167**,** 225-235.

Koskella, B., et al., 2017. A signature of tree health? Shifts in the microbiome and the ecological drivers of horse chestnut bleeding canker disease. New Phytologist. 215**,** 737-746.

Kroetz, K., et al., Examining Seafood Fraud Through the Lens of Production and Trade: How Much Mislabeled Seafood Do Consumers Buy? Resources for the Future, Washington DC, 2018, pp. 24.

Kummu, M., et al., 2016. Over the hills and further away from coast: global geospatial patterns of human and environment over the 20th–21st centuries. Environmental Research Letters. 11**,** 034010.

Lacoste, A., et al., 2001. A *Vibrio splendidus* strain is associated with summer mortality of juvenile oysters *Crassostrea gigas* in the Bay of Morlaix (North Brittany, France). Diseases of Aquatic Organisms. 46**,** 139-145.

Lafferty, K., Ben-Horin, T., 2013. Abalone farm discharges the withering syndrome pathogen into the wild. Frontiers in Microbiology. 4**,** 373.

Lafferty, K. D., Kuris, A. M., 1993. Mass mortality of abalone *Haliotis cracherodii* on the California Channel Islands: tests of epidemiological hypotheses Marine Ecology Progress Series. 96**,** 239-248.

Laird, B. D., Chan, H. M., 2013. Bioaccessibility of metals in fish, shellfish, wild game, and seaweed harvested in British Columbia, Canada. Food and Chemical Toxicology. 58**,** 381-387.

Lamb, J. B., et al., 2014. Scuba diving damage and intensity of tourist activities increases coral disease prevalence. Biological Conservation. 178**,** 88-96.

Lamb, J. B., et al., 2017. Seagrass ecosystems reduce exposure to bacterial pathogens of humans, fishes, and invertebrates. Science. 355**,** 731-733.

Lamb, J. B., et al., 2016. Reserves as tools for alleviating impacts of marine disease. Philosophical Transactions of the Royal Society B: Biological Sciences. 371**,** 20150210.

Lamb, J. B., Willis, B. L., 2011. Using coral disease prevalence to assess the effects of concentrating tourism activities on offshore reefs in a tropical marine park. Conservation Biology. 25**,** 1044-1052.

Lamb, J. B., et al., 2018. Plastic waste associated with disease on coral reefs. Science. 359**,** 460-462.

Lane, H. S., et al., 2020. Aquatic disease in New Zealand: synthesis and future directions. New Zealand Journal of Marine and Freshwater Research. 1-42.

Lane, H. S., et al., 2016. *Bonamia ostreae* in the New Zealand oyster *Ostrea chilensis*: a new host and geographic record for this haplosporidian parasite. Diseases of Aquatic Organisms. 118**,** 55-63.

Liu, J., et al., 2017. Bioaccumulation of heavy metals and health risk assessment in three benthic bivalves along the coast of Laizhou Bay, China. Marine Pollution Bulletin. 117**,** 98-110.

Lloyd, M. M., Pespeni, M. H., 2018. Microbiome shifts with onset and progression of Sea Star Wasting Disease revealed through time course sampling. Scientific Reports. 8**,** 16476.

Lohan, K. M. P., et al., Invasions can drive marine disease dynamics. In: D. Behringer, et al., Eds., Marine Disease Ecology. Oxford University Press, Oxford, 2020.

Luque, G. M., Donlan, C. J., 2019. The characterization of seafood mislabeling: A global meta-analysis. Biological Conservation. 236**,** 556-570.

Mabey, A. L., et al., 2021. Pathogen inferred to have dispersed thousands of kilometres at sea, infecting multiple keystone kelp species. Marine Biology. 168**,** 47.

Mackenzie, C. L., et al., 2014. Future Oceanic Warming and Acidification Alter Immune Response and Disease Status in a Commercial Shellfish Species, *Mytilus edulis* L. PLOS ONE. 9**,** e99712.

Maxwell, K., et al., 2020. He waka eke noa/we are all in the same boat: A framework for co-governance from aotearoa New Zealand. Marine Policy. 121**,** 104213.

McCallum, H., et al., 2003. Rates of spread of marine pathogens. Ecology Letters. 6**,** 1062-1067.

McCallum, H. I., et al., 2004. Does terrestrial epidemiology apply to marine systems? Trends in Ecology & Evolution. 19**,** 585-591.

Mccarthy, A., et al., 2014. Local people see and care most? Severe depletion of inshore fisheries and its consequences for Māori communities in New Zealand. Aquatic Conservation: Marine and Freshwater Ecosystems. 24**,** 369-390.

Meistertzheim, A.-L., et al., 2017. Pathobiomes Differ between Two Diseases Affecting Reef Building Coralline Algae. Frontiers in Microbiology. 8**,** 1686-1686.

Moore, J. D., et al., 2000. Withering syndrome in farmed red abalone *Haliotis rufescens*: Thermal induction and association with a gastrointestinal *Rickettsiales*-like prokaryote. Journal of Aquatic Animal Health. 12**,** 26-34.

Morton, J. P., et al., Disease can shape marine ecosystems. In: D. Behringer, et al., Eds., Marine Disease Ecology. Oxford University Press, Oxford, 2020.

Munroe, D., et al., 2013. Oyster mortality in Delaware Bay: Impacts and recovery from Hurricane Irene and Tropical Storm Lee. Estuarine, Coastal and Shelf Science. 135**,** 209-219.

Murray, A. G., et al., 2012. A review of the risk posed to Scottish mollusc aquaculture from *Bonamia*, *Marteilia* and oyster herpesvirus. Aquaculture. 370-371**,** 7-13.

Murton, B., 2006. 'Toheroa Wars': Cultural politics and everyday resistance on a northern New Zealand beach. New Zealand Geographer. 62**,** 25-38.

Neave, M. J., et al., 2016. Diversity and function of prevalent symbiotic marine bacteria in the genus *Endozoicomonas*. Applied Microbiology and Biotechnology. 100**,** 8315-8324.

Nicholls, R. J., et al., Coastal systems and low-lying areas. In: M. L. Parry, et al., Eds., Climate Change 2007: Impacts, Adaptation and Vulnerability. Contribution of Working Group II to the Fourth Assessment Report of the Intergovernmental Panel on Climate Change. Cambridge University Press, Cambridge, 2007, pp. 315-356.

Nyberg, C. D., Wallentinus, I., 2005. Can species traits be used to predict marine macroalgal introductions? Biological Invasions. 7**,** 265-279.

OIE, Information on aquatic and terrestrial animal diseases. World Organisation for Animal Health, 2021. Access date: Dec 2020. https://www.oie.int/en/what-we-do/animal-health-and-welfare/animal-diseases/.

Oleson, K. L. L., et al., 2015. Cultural bequest values for ecosystem service flows among indigenous fishers: A discrete choice experiment validated with mixed methods. Ecological Economics. 114**,** 104-116.

Oliver, E. C. J., et al., 2017. The unprecedented 2015/16 Tasman Sea marine heatwave. Nature Communications. 8**,** 16101.

Pauly, D., Zeller, D., 2016. Catch reconstructions reveal that global marine fisheries catches are higher than reported and declining. Nature Communications. 7**,** 10244.

Pedersen, K., 2000. Exploration of deep intraterrestrial microbial life: current perspectives. FEMS Microbiology Letters. 185**,** 9-16.

Peperzak, L., Poelman, M., 2008. Mass mussel mortality in The Netherlands after a bloom of *Phaeocystis globosa* (prymnesiophyceae). Journal of Sea Research. 60**,** 220-222.

Pita, L., et al., 2018. The sponge holobiont in a changing ocean: from microbes to ecosystems. Microbiome. 6**,** 1-18.

Pogoda, B., et al., 2020. Site selection for biogenic reef restoration in offshore environments: The Natura 2000 area Borkum Reef Ground as a case study for native oyster restoration. Aquatic Conservation: Marine and Freshwater Ecosystems. 30**,** 2163-2179.

Pollock, F. J., et al., 2014. Sediment and Turbidity Associated with Offshore Dredging Increase Coral Disease Prevalence on Nearby Reefs. PLOS ONE. 9**,** e102498.

Pramod, G., et al., 2014. Estimates of illegal and unreported fish in seafood imports to the USA. Marine Policy. 48**,** 102-113.

Pufall, E. L., et al., 2012. Prevalence of zoonotic anisakid nematodes in Inuit-harvested fish and mammals from the eastern Canadian Arctic. Foodborne Pathogens and Disease. 9**,** 1002-1009.

Rapson, A. M., 1952. The Toheroa, *Amphidesma ventricosum* Gray (Eulamellibranchiata), Development and Growth. Australian Journal of Marine and Freshwater Research. 3**,** 170-198.

Rapson, A. M., 1954. Feeding and Control of Toheroa (*Amphidesma ventricosum* Gray) (Eulamellibranchiata) Populations in New Zealand. Australian Journal of Marine and Freshwater Research. 5**,** 486-512.

Raymundo, L. J., et al., Disease ecology in marine conservation and management. In: D. Behringer, et al., Eds., Marine Disease Ecology. Oxford University Press, Oxford, 2020.

Raymundo, L. J., et al., 2018. Adding insult to injury: Ship groundings are associated with coral disease in a pristine reef. PLOS ONE. 13**,** e0202939.

Redfearn, P., 1974. Biology and distribution of the toheroa, *Paphies* (Mesodesma) *ventricosa* (Gray). Fisheries Research Bulletin No. 11. New Zealand Ministry of Agriculture and Fisheries. 51.

Reid, J., Rout, M., 2020. The implementation of ecosystem-based management in New Zealand – A Māori perspective. Marine Policy. 117**,** 103889.

Renault, T., et al., 2012. Analysis of Clinical Ostreid Herpesvirus 1 (*Malacoherpesviridae*) Specimens by Sequencing Amplified Fragments from Three Virus Genome Areas. Journal of Virology. 86**,** 5942-5947.

Rogers-Bennett, L., et al., 2019. Using Density-Based Fishery Management Strategies to Respond to Mass Mortality Events. Journal of Shellfish Research. 38**,** 485-495.

Rose, C. D., 1973. Mortality of market-sized oysters (*Crassostrea virginica*) in the vicinity of a dredging operation. Chesapeake Science. 14**,** 135-138.

Ross, P. M., et al., 2018a. The biology, ecology and history of toheroa (*Paphies ventricosa*): a review of scientific, local and customary knowledge. New Zealand Journal of Marine and Freshwater Research. 52**,** 196-231.

Ross, P. M., et al., *Bonamia* Response 2015: Report from the Technical Advisory Group on Resilience Breeding in Flat Oysters. Ministry for Primary Industries, Wellington, 2017, pp. 16.

Ross, P. M., et al., 2018b. Historical translocations by Māori may explain the distribution and genetic structure of a threatened surf clam in Aotearoa (New Zealand). Scientific Reports. 8**,** 17241.

Ross, P. M., et al., 2018c. First detection of gas bubble disease and *Rickettsia*-like organisms in *Paphies ventricosa*, a New Zealand surf clam. Journal of Fish Diseases. 41**,** 187-190.

Rowley, A. F., et al., 2014. The potential impact of climate change on the infectious diseases of commercially important shellfish populations in the Irish Sea-a review. Ices Journal of Marine Science. 71**,** 741-759.

Rubio-Portillo, E., et al., 2018. Biogeographic Differences in the Microbiome and Pathobiome of the Coral *Cladocora caespitosa* in the Western Mediterranean Sea. Frontiers in Microbiology. 9**,** 22.

Rybarczyk, H., et al., 1996. Eutro-phication in the Baie de Somme: consequences and impacts on the benthic population. Oceanologica Acta. 19**,** 131–140.

Sas, H., et al., 2020. *Bonamia* infection in native oysters (*Ostrea edulis*) in relation to European restoration projects. Aquatic Conservation: Marine and Freshwater Ecosystems. 30**,** 2150-2162.

Segarra, A., et al., 2010. Detection and description of a particular Ostreid herpesvirus 1 genotype associated with massive mortality outbreaks of Pacific oysters, *Crassostrea gigas*, in France in 2008. Virus Research. 153**,** 92-99.

Sformo, T. L., et al., 2017. Observations and first reports of saprolegniosis in Aanaakłiq, broad whitefish (*Coregonus nasus*), from the Colville River near Nuiqsut, Alaska. Polar Science. 14**,** 78-82.

Shepherd, L. D., et al., 2018. Genetic structuring of the coastal herb *Arthropodium cirratum* (*Asparagaceae*) is shaped by low gene flow, hybridization and prehistoric translocation. PLOS ONE. 13**,** e0204943.

Shumway, S. E., 1990. A Review of the Effects of Algal Blooms on Shellfish and Aquaculture. Journal of the World Aquaculture Society. 21**,** 65-104.

Smith, S., Factors influencing the abundance of Toheroa (*Paphies ventricosa*) on Northland beaches: Perspectives from the beach. In: J. Williams, et al., Eds., Review of factors affecting the abundance of toheroa (*Paphies ventricosa*). New Zealand Aquatic Environment and Biodiversity Report No. 114, 2013, pp. 76.

Smyth, D., et al., 2021. “Good news everyone”, the natives have returned: Assemblages of European flat oysters make a reappearance in Belfast Lough after a century of absence. Regional Studies in Marine Science. 41**,** 101585.

Snieszko, S. F., 1974. The effects of environmental stress on outbreaks of infectious diseases of fishes. Journal of Fish Biology. 6**,** 197-208.

Soon, T. K., Ransangan, J., 2019. Extrinsic Factors and Marine Bivalve Mass Mortalities: An Overview. Journal of Shellfish Research. 38**,** 223-232.

Stace, G., The elusive toheroa. New Zealand Geographic Magazine, Vol. 9, 1991.

Stentiford, G. D., et al., 2012. Disease will limit future food supply from the global crustacean fishery and aquaculture sectors. Journal of Invertebrate Pathology. 110**,** 141-157.

Stentiford, G. D., et al., 2017. New Paradigms to Help Solve the Global Aquaculture Disease Crisis. PLOS Pathogens. 13**,** e1006160.

Su, Y.-C., Liu, C., 2007. *Vibrio parahaemolyticus*: A concern of seafood safety. Food Microbiology. 24**,** 549-558.

Sutherland, K. P., et al., 2016. Shifting white pox aetiologies affecting *Acropora palmata* in the Florida Keys, 1994-2014. Philosophical Transactions of the Royal Society B: Biological Sciences. 371**,** 20150205.

Thitamadee, S., et al., 2016. Review of current disease threats for cultivated penaeid shrimp in Asia. Aquaculture. 452**,** 69-87.

Tracy, A. M., et al., 2019. Increases and decreases in marine disease reports in an era of global change. Proceedings of the Royal Society B: Biological Sciences. 286**,** 20191718.

Travers, M. A., et al., 2015. Bacterial diseases in marine bivalves. Journal of Invertebrate Pathology. 131**,** 11-31.

Turner, R. A., et al., 2007. Declining reliance on marine resources in remote South Pacific societies: ecological versus socio-economic drivers. Coral Reefs. 26**,** 997-1008.

Turra, A., et al., 2016. Frequency, Magnitude, and Possible Causes of Stranding and Mass-Mortality Events of the Beach Clam *Tivela mactroides* (Bivalvia: Veneridae). PLOS ONE. 11**,** e0146323.

UN, United Nations, Conserve and sustainably use the oceans, seas and marine resources. California, USA, 2020. Access date: Nov 2020. https://www.isglobal.org/en/-/sdg-14-conserve-and-sustainably-use-the-oceans-seas-and-marine-resources-for-sustainable-development.

Vallyon, L.-M. D., Birds vs. Clams: Assessing the impacts of South Island pied oystercatcher predation on Toheroa at Ripiro Beach, New Zealand. MSc. University of Waikato, 2020, pp. 115.

Van Dover, C. L., et al., 2007. A fungal epizootic in mussels at a deep-sea hydrothermal vent. Marine Ecology. 28**,** 54-62.

Villalba, A., et al., 2005. Study of perkinsosis in the carpet shell clam *Tapes decussatus* in Galicia (NW Spain). II. Temporal pattern of disease dynamics and association with clam mortality. Diseases of Aquatic Organisms. 65**,** 257-267.

Villalba, A., et al., 2004. *Perkinsosis* in molluscs: A review. Aquatic Living Resources. 17**,** 411-432.

Wahle, R. A., et al., 2009. Distinguishing disease impacts from larval supply effects in a lobster fishery collapse. Marine Ecology Progress Series. 376**,** 185-192.

Ward, D. M., et al., 1990. 16S rRNA sequences reveal numerous uncultured microorganisms in a natural community. Nature. 345**,** 63-65.

Ward, J. R., Lafferty, K. D., 2004. The elusive baseline of marine disease: Are diseases in ocean ecosystems increasing? PLOS Biology. 2**,** 542-547.

Weatherdon, L. V., et al., 2016. Projected Scenarios for Coastal First Nations' Fisheries Catch Potential under Climate Change: Management Challenges and Opportunities. PLOS ONE. 11**,** e0145285.

Wehi, P., et al., 2013. Marine resources in Māori oral tradition: He kai moana, he kai mā te hinengaro. Journal of Marine and Island Cultures. 2**,** 59-68.

Wendling, C. C., Wegner, K. M., 2013. Relative contribution of reproductive investment, thermal stress and *Vibrio* infection to summer mortality phenomena in Pacific oysters. Aquaculture. 412**,** 88-96.

Wieland, R., et al., 2016. Debunking trickle-down ecosystem services: The fallacy of omnipotent, homogeneous beneficiaries. Ecological Economics. 121**,** 175-180.

Wilber, D. H., Clarke, D. G., 2001. Biological Effects of Suspended Sediments: A Review of Suspended Sediment Impacts on Fish and Shellfish with Relation to Dredging Activities in Estuaries. North American Journal of Fisheries Management. 21**,** 855-875.

Wilberg, M. J., et al., 2011. Overfishing, disease, habitat loss, and potential extirpation of oysters in upper Chesapeake Bay. Marine Ecology Progress Series. 436**,** 131-144.

Wilkes, R., et al., 2017. Intertidal seagrass in Ireland: Pressures, WFD status and an assessment of trace element contamination in intertidal habitats using *Zostera noltei*. Ecological Indicators. 82**,** 117-130.

Willer, D. F., Aldridge, D. C., 2020. Sustainable bivalve farming can deliver food security in the tropics. Nature Food. 1**,** 384-388.

Williams, J., et al., Distribution and abundance of toheroa (*Paphies ventricosa*) and tuatua (*P. subtriangulata*) at Ninety Mile Beach in 2010 and Dargaville Beach in 2011. Ministry of Primary Industries, Wellington, 2013a, pp. 52.

Williams, J. R., et al., Review of factors affecting the abundance of toheroa (*Paphies ventricosa*). New Zealand Aquatic Environment and Biodiversity Report No. 114, 2013b, pp. 76.

Williams, M., et al., 2020. Illegal, unreported, and unregulated fishing: A risk scoring method for prioritizing inspection of fish imported to Australia for zoonotic parasites. Journal of Biosafety and Biosecurity. 2**,** 81-90.

Woodhead, A. J., et al., 2019. Coral reef ecosystem services in the Anthropocene. Functional Ecology. 33**,** 1023-1034.

Worden, A. Z., et al., 2015. Rethinking the marine carbon cycle: Factoring in the multifarious lifestyles of microbes. Science. 347**,** 1257594.

WorldBank, FISH TO 2030 Prospects for Fisheries and Aquaculture. The World Bank, Washington DC, 2013, pp. 81.

WorldBank, Reducing disease risks in aquaculture. World Bank, Washington, DC, 2014, pp. 214.

Worm, B., et al., 2009. Rebuilding Global Fisheries. Science. 325**,** 578-585.

Xiong, X., et al., 2016. The uncertainty of seafood labeling in China: A case study on Cod, Salmon and Tuna. Marine Policy. 68**,** 123-135.

zu Ermgassen, P. S. E., et al., 2020. Forty questions of importance to the policy and practice of native oyster reef restoration in Europe. Aquatic Conservation: Marine and Freshwater Ecosystems. 30**,** 2038-2049.

Chapter 2
Wild Shellfish Health in Aotearoa (New Zealand): A Case for Increased Surveillance

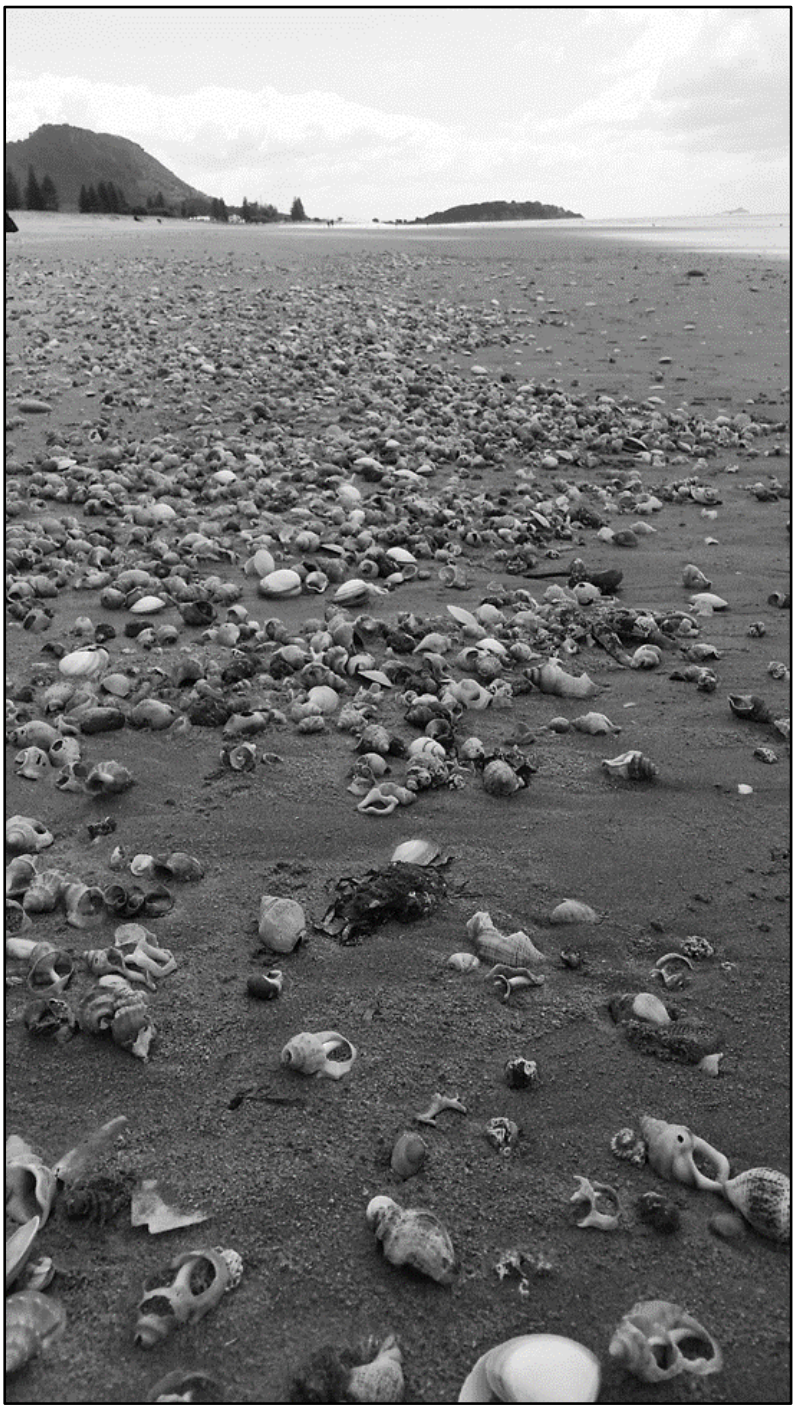

Shellfish mass mortality
October 2019
Mount Maunganui

2.1 Abstract

While the main constraint to aquaculture is recognised as disease, and a large research focus has been placed on mitigation and control to protect stocks, the same effort has not been extended to protecting wild populations. Wild shellfish populations are therefore (for the most part), without a 'baseline' with which to compare against sudden mass mortality events (MMEs) and 'unhealthy' individuals. The absence of a significant economic incentive may explain some of this disparity; however, the importance of many shellfish species to coastal communities and Indigenous people around the world cannot be overstated and warrants greater attention. Outbreaks of disease in the oceans are increasing in frequency. Climate change, pollution, biofouling, and human-facilitated transport of vector and reservoir species to new ecological niches, are cited as some of the factors contributing to this rise. Here, I discuss the pressures many coastal shellfish populations face in a disease context, with a focus on the current shellfish mortality landscape in Aotearoa (New Zealand). This case emphasises the need for surveillance of wild shellfish health and the repercussions of disease outbreaks on receiving communities that place intrinsic value in the seafood available on their doorstep.

2.2 Introduction

The impact of emerging pathogens on receiving habitats, ecosystems, and communities are far-reaching. Shellfish play an invaluable role in coastal environments (Dairain et al., 2019; Rullens et al., 2019). As filter feeders, many are capable of filtering vast quantities of water (some oysters species can filter *c.* 200 litres per day) and infaunal species, like clams, are important bioturbators (Meysman et al., 2016), performing a critical role in nutrient cycling (Dairain et al., 2019). Humans depend on the ocean and its flora and fauna for a vast array of goods and services too (Carss et al., 2020; Rullens et al., 2019; Smale et al., 2019). Employment and economics of many rural coastal regions centred on shellfish are calculable, though the value placed on many shellfish species by Indigenous (Cisneros-Montemayor et al., 2016), rural, and (or) isolated communities is much more challenging to quantify. Particularly 'non-use' value i.e., value not related to consumption (Carss et al., 2020). For hundreds of years, the oceans have provided a reliable (and seemingly infinite) source of protein for humans, which was often a deciding factor for early human settlements. The importance of seafood, namely shellfish, throughout human history is still evident today, illustrated by the presence art, sculptures, landmarks, and spiritual buildings, celebrating the cultural heritage of shellfish harvesting/gathering (van der Schatte Olivier et al., 2018). This historical importance is also evidenced by middens; archaeological shell mounds (Codding et al., 2014; Gillies et al., 2018) and the presence of shell fragments in burial tombs, ringforts,

and monasteries e.g., the common cockle *Cerastoderma edule* in Ireland (Carss et al., 2020). For example, middens in the Greater Hauraki region of Aotearoa (New Zealand), settled originally by Māori (*c*. 1300), indicate a reliance on three shellfish taxa, though study sites in this area show records for 147 shellfish taxa (Smith, 2013). Middens pinpoint historical settlements and provide an insight into ancient human diet compositions and the ecological history of shellfish during this time (Codding et al., 2014; Gillies et al., 2018; Szabó and Amesbury, 2011). Many of these settlements have today lost their connection to their original purpose of settlement, the reasons for this are site-specific but some common themes include overexploitation, pollution, disease, and subsequent t decline of key shellfish taxa (e.g., Chesapeake Bay, USA, Schulte, 2017).

The ocean is a microbial frontier (Harvell and Lamb, 2020). A millilitre of seawater can contain on average 10^7 of viruses (Wommack and Colwell, 2000) and close to the same number of bacteria (Jacquet et al., 2010). Despite microscopic organisms accounting for *c.* 60 % of biomass within the oceans (Bar-On et al., 2018), we know very little about species assemblages and are only beginning to understand the role they can play in crucial biological processes (Amin et al., 2012; Azam and Malfatti, 2007). Microscopic organisms play vital roles in the ocean, including nutrient cycling, structuring communities, and of course health and disease. Compared to the presumed overall biomass (Bar-On et al., 2018), relatively few microscopic organisms are pathogenic (Belkin and Colwell, 2006). Nevertheless, the incidence of disease outbreak in the oceans appears to be on the rise (Harvell et al., 1999; Lafferty et al., 2004; Maynard et al., 2015), though our knowledge of disease in marine systems is in its infancy, so even establishing the scale of this rise, is not without its complications (Ward and Lafferty, 2004). Anthropogenic-driven rapid change in the oceans is influencing disease emergence. Oceanic thermal fluctuations (Ben-Horin et al., 2013; Szekeres et al., 2016), plastic pollution (Frère et al., 2018; Kirstein et al., 2016; Lamb et al., 2018), and habitat degradation (Diggles, 2013; Pollock et al., 2014) have been directly associated with disease emergence in marine biota. Increased movement of humans and goods around the world has led to the passive transport of many disease-causing and parasitic organisms to new habitats and hosts. In the ocean, biofouling, and the shipment of microbes within ballast water of large vessels have been identified as major pathways for new and emerging pathogens (Drake et al., 2007; Hayes et al., 2019; Sardain et al., 2019). At the same time, climate change and pollution permit range expansion of pathogens e.g., *Perkinsus marinus* and MSX, *Haplosporidium nelsoni* in the United States (Burge et al., 2014), and simultaneously reduce the resilience of host species, leading to disease (Maynard et al., 2015). Conversely, pathogen fitness can too be modulated by a rapidly changing environment, reducing disease burden on hosts (Harvell et al., 2002). For example, bacterial cold-water disease in fish (BCWD), caused

by *Flavobacterium* sp. is generally associated with polar latitudes, what influence will oceanic warming have for this 'cold water' disease?

Establishing the pathogen(s) responsible for the onset of disease can be a slow, laborious task, as is determining the many factors that might be contributing to the pathogenicity of any given pathogen (Lafferty and Hofmann, 2016; Sutherland et al., 2016). This is evidenced by white pox disease (WPX) in corals, where Sutherland et al. (2016) propose the moving target hypotheses to describe the complex aetiology of WPX. The investigation of abalone withering-syndrome also highlights this issue with respect to disease in the oceans. Researchers originally linked abalone mortality to a coccidian parasite (Apicomplexa) (Friedman et al., 1995), but soon after, found it was not associated with withering syndrome (Friedman et al., 1993). Originally dismissed as a possible aetiological agent of withering syndrome, in 1995, Gardner and co-authors (Gardner et al., 1995) showed an association between Rickettsiales-like prokaryotes and withering syndrome (Moore et al., 2000). Withering-syndrome *Rickettsia*-like organism (WS-RLO) was finally proved the aetiological agent behind mortalities, almost 20 years after the first observed mortalities, when targeted laboratory experiments successfully fulfilled Koch's postulates (Friedman et al., 2002). This case is one of countless, which highlight our lack of knowledge of microbes and emerging pathogens in the oceans, and our limited grasp of host biology in the oceans compared to terrestrial pathology. Characterising diseases in the oceans is not a simple task, many different microbes or environmental factors may be working concurrently leading to disease, in this sense establishing cause and effect is extremely challenging. This renders not only identifying the aetiological agent(s) difficult, but also limits our ability to respond to disease outbreaks (Sutherland et al., 2016). Contributors to disease outbreak may be multifactorial and without knowledge of what underpins interactions therein, any response is, at least in part, uninformed. Groner et al. (2016) recognise that management of diseases in the oceans is not a straightforward task but mention that the need to move from reactive management towards one based in proactive or pre-emptive framework. Pre-emptive measures do exist, in the form of operational research to identify and understand emerging issues and biosecurity specific legislation that drives preventative measures (Carnegie et al., 2016; Lafferty and Hofmann, 2016). Essentially, proactive management tools are available, and many are in play, but an absence of basic knowledge of microbial and host biology in most cases, limits their effectiveness at present.

In the present study, I discuss the risk emerging pathogens pose to wild shellfish populations at a time of rapid change and prevalent burdens in coastal environments. Importantly, I highlight how this risk extends ecological boundaries, posing knock-on negative impacts on communities that rely on the ability to source seafood from their

locale for economic, recreational, and customary purposes. Using Aotearoa and the recent apparent upsurge in the frequency of shellfish mass mortality events (MMEs) associated with a potentially emerging bacterial pathogen; I consider how a lack of baseline health information impedes management of treasured species.

2.3 Consequences of Disease Outbreaks

A summary of the ecological, social, and economic services provided by wild shellfish populations are provided in Table 2.1. The consequences of MMEs are complex. In the same way marine heatwaves pose a threat to the provision of many services from the oceans (Smale et al., 2019), the occurrence of unexpected shellfish MMEs and parasitism has the potential to reduce service provision gained from shellfish (Table 2.1). Many marine mollusc populations fluctuate naturally (Barber et al., 2019). Mortalities can occur due to storms (Eggleston and Hickman, 1972), but also potentially as a natural method of population regulation e.g., sea star wasting disease (Lafferty, 2017). Unprecedented and anthropogenic-driven MMEs, however, pose a significant threat to the provision of services briefly outlined in Table 2.1. These services can be ecological and environmental or socio-economic. The customary, cultural, and ritual services provided by shellfish, in the form of a traditional diet, subsistence fishery or customary practices, can also be reduced when shellfish populations are impacted (Gillies et al., 2018; Mccarthy et al., 2014; Ross et al., 2018a).

It is challenging to quantify the consequences of shellfish MMEs (which threaten a certain species or stock) to rural regions that depend on the availability shellfish in their locale. Disease outbreaks in highly valued species, however, provide an insight into the substantial impacts that can be felt by receiving communities. In Chesapeake Bay, USA, the combination of *Perkinsus* and MSX resulted in mortalities upwards of 90% in stocks in the Virginia oyster fishery, with profound implications for receiving communities, which led to increased shell planting efforts and federal economic subsidies in the 1960s, and ultimately contributed to the collapse of the fishery (Schulte, 2017). Similarly, in the Foveaux Strait, Aotearoa pre-epizootic (Bonamiosis) in 1985, 23 vessels were operating in the Bluff oyster (*Ostrea chilensis*) fishery (Fu, 2013). Post-epizootic, stocks had declined to *c.* 9% their pre-epizootic abundance, and after a closure of the fishery from 1993 to 1996, 11 vessels remained active in the fishery (Fu, 2013).

Table 2.1 A summary of services provided by stable shellfish populations in near-shore ecosystems.

	How service is delivered	Where service is gained
Ecological and environmental		
Ecological	• Some coastal shellfish spp. are reef builders, creating a 3-dimensional habitat for a vast number of associated biota (Dame, 2016). • As benthic detritivores, many filter-feeding bivalves play a crucial role in marine food webs, facilitating bottom-up energy transfer (Rullens et al., 2019). • Infaunal species are significant bioturbators, critical for nutrient cycling and oxygenation (Carss et al., 2020; Dairain et al., 2019).	Overall ecosystem health
Environment	• Filter feeders are capable of remediating pollutants and pathogens (Ma et al., 2017; Rullens et al., 2019) from the water column, some of which pose a threat to other marine species, as well as, humans (Burge et al., 2016). • As reef builders, bioturbators, and filter feeders, the cumulative effects of shellfish on receiving habitats are dynamic and profound, encouraging diverse assemblages, delivering knock-on benefits for surrounding environments.	Overall ecosystem health, human health
Anthropologic and socio-economic		
Customary purposes	• Many Indigenous people use shellfish for a variety of customary and spiritual practices. • In Aotearoa, being able to collect shellfish carries mana (respect) for iwi and hapū and this means you can provide for your whanau (family) and manuhiri (guests). • Certain species or a variety of different shellfish may constitute a traditional diet of a town, nation, community, or Indigenous people. • For instance, in Aotearoa, toheroa (*P. ventricosa*) and several other mollusc species, such as Pāua (*Haliotis* spp.), pipi (*P. australis*), and tuangi (*Austrovenus stutchburyi*) have been harvested and managed by Māori for several hundred years, evidenced by kōrero tuku iho (oral history), whakataukī (proverbs) (Wehi et al., 2013; Whaanga et al., 2018), and archaeological shell middens.	Cultural, spiritual, social, wellbeing
Commercial fisheries	• Many wild shellfish populations are exploited globally, creating and maintaining jobs in harvesting, processing, and distribution (particularly in rural regions) (Schulte, 2017). • Although farmed produce has overtaken wild caught fisheries in terms of production tonnage, FAO (FAO, 2018) report the global production of wild caught marine molluscs was 6,325,516 tonnes in 2017.	Economic, employment
Recreational fisheries	• Much more challenging to quantify, the economic and social value of recreational fisheries for wild shellfish is also significant e.g., *C. edule* in the northeast Atlantic (Carss et al., 2020). • Recreational fisheries (together with commercial fisheries) form the basis of many seafood and shellfish focused festivals throughout the world (van der Schatte Olivier et al., 2018), which bring with them, socio-economic benefits in the hospitality sector for host towns and cities.	Social, economic
Well-being & health	• Sourcing food in respective locales can provide benefits through contact and connection with nature, via the ‘blue space’ effect (Foley and Kistemann, 2015). • Additionally, marine molluscs as a source of animal protein have been highlighted as ‘healthy’ source of several important nutrients (Venugopal and Gopakumar, 2017).	Human health

2.4 Risk factors

2.4.1 Pollution

In 2018, a landmark study was published in *Science* describing the interaction between marine plastic debris and disease in corals (Lamb et al., 2018). This study provides the basis for future work in this field and highlights significant 'unknowns' surrounding the indirect effects of plastic pollution on disease in the oceans (Bidegain and Paul-Pont, 2018). Microplastic pollution has recently been uncovered as a potential facilitator of disease in the ocean too (Audrézet et al., 2021), reportedly as a vector of pathogens e.g., *Vibrio* spp. (Frère et al., 2018; Kirstein et al., 2016). Sewage pollution can directly influence the microbial communities in receiving habitats, posing risk to both humans and marine life (Lamb et al., 2017). Elevated trace metals can also influence pathogenicity and virulence of pathogenic organisms, for example cadmium (Paul-Pont et al., 2010). Other pollutants can also affect disease by modulating host health via immune and endocrine systems (e.g., Cu, Pipe and Coles, 1995) or influencing the pathogenicity or virulence of microbes (Sures, 2008). Non-infectious disease can also pose a serious risk to marine life. The effects of organohalogens (e.g., PAHs, PBDEs, PCBs) and organotin compounds (TBT) on marine species is well documented, particularly in large marine mammals (Jepson et al., 2003), though their impact on marine molluscs is also well understood (Jones and Ross, 2018; McDowell et al., 1999; Morley, 2010). For example, imposex induced by TBT-based antifouling paint, can reduce the reproductive potential of afflicted gastropod populations (e.g., muricid dogwhelk *Haustrum scobina*), threatening recruitment (Jones and Ross, 2018, and references therein).

Pathogen run-off from terrestrial landscapes into the oceans or *pollutagens*, pose a risk to a variety of marine biota, most famously *Toxoplasma gondii* a protozoan parasite associated with domestic cats and sea otters (Burgess Tristan et al., 2018) cetaceans and pinnipeds (Dubey et al., 2003; Roberts et al., 2020). Similarly, emerging viruses in crustacean aquaculture (WSSV, TSV, and IMNV) with sources unknown have been postulated as potential spill over pathogens, deriving from terrestrial insect viruses from co-habitation ponds (Walker and Winton, 2010). These trans-boundary pathogens raise important questions of the microbial risks associated with large-scale habitat degradation such as, deforestation (Morris et al., 2016) and melting permafrost (Carlson et al., 2018; Houwenhuyse et al., 2018). What these significant geomorphological changes mean for disease outbreak in the oceans is as-of-yet unbeknown, but the risk of pollutagens from land-based sources via run-off is a concerning potential.

2.4.2 Habitat Degradation

Habitat degradation takes many forms in coastal environments. From intermittent bouts of anthropogenic influence, such as, sedimentation from dredging. To chronic degradation from large-scale coastal redevelopment. Sediment plumes caused by dredging activity have been associated with coral disease, where heavily impacted corals (by sedimentation) were two-fold more likely to succumb to disease (white syndromes) in some areas of western Australia (Pollock et al., 2014). Elsewhere in Australia, the loss of oyster reefs (*Saccostrea glomerata*) has also been associated with declined water quality (Diggles, 2013). By 2030 it is estimated that 27% of the world's population will live <100 km of the coast (*c.* 2.2 billion people) (Kummu et al., 2016), which will undoubtedly increase burdens in coastal environments. Hard manmade substrates such as ports and seawalls facilitate the establishment of non-native species, giving them a competitive advantage over native species (Foster et al., 2016). Moreover, invasive species can act as vectors and reservoirs of new or emerging pathogens (Bax et al., 2003), facilitating transmission to species that have not yet naturally developed resilience (e.g., tunicates, Costello et al., 2021).

2.4.3 Climate Change

Marine heatwaves are increasing in frequency (Oliver et al., 2018). These heatwaves are having profound impact on many biogenic habitats throughout the globe (Smale et al., 2019), causing kelp dieback and coral bleaching events when they strike. Heatwaves have also been associated with MMEs of marine molluscs, for example, farmed oysters (*Crassostrea gigas*) and wild blacklip abalone (*Haliotis rubra*) in Australia in 2016 (Oliver et al., 2017) and farmed oysters (also *C. gigas*) in Ireland (Prado-Alvarez et al., 2016). Aside from mean temperature rise, fluctuating temperatures can increase susceptibility to disease, via modulation of inflicting pathogens (Ben-Horin et al., 2013; Szekeres et al., 2016). Temperature-related impacts on receiving near-shore shellfish populations go beyond direct temperature-associated stress. Heat stress can cause mortality (Oliver et al., 2017), but recent heatwaves have resulted in range shifts of wild molluscs (Sanford et al., 2019) and regime shifts at impacted sites in heatwave prone regions (Wernberg et al., 2016). Similarly, secondary impacts include the promotion of toxic algae blooms (Harvell et al., 1999), and pathogen range shifts too (Harvell et al., 2002). This has led to the expansion of pathogen ranges to new ecological niches at the same time, expanding host range as well as geographical distribution of potential pathogens, for example, the oyster parasite *Haplosporidium nelsoni* (MSX) which is tracking poleward on the Atlantic coast of the USA (Burge et al., 2014; Ford et al., 2018).

Disease outbreaks have been associated with marine heatwaves (Green et al., 2019; Oliver et al., 2017), as rapid increase in temperatures tip the balance in favour of microbes by elevating the pathogenicity and (or) virulence of pathogens which favour higher temperatures. For example, *Perkinsus marinus* epizootics during summer months, in both wild and farmed *C. virginica* (Burreson and Ragone Calvo, 1996). Alternatively, these extreme environmental conditions could increase host susceptibility to disease. A similar case is raised by (Hooper et al., 2019), where severe infection of *Endozoicomonas* sp. persisted seasonally (Cano et al., 2018), indicating that reported mass mortalities of king scallops (*Pecten maximus*) were likely a result of reduced host resilience, succumbing to opportunistic pathogens. A changing climate is predicted to increase the incidence of extreme whether events in the near future (Burge et al., 2014; Green et al., 2019). The impacts of these extreme whether events will be intensified in coastal environments where near shore geomorphology contribute to wave-action and sedimentation, with repercussions for shellfish (Quiah et al., 2020). Additionally, the effect of ocean acidification is predicted to be profound, in a disease context (Burge et al., 2014). The consequences of a rapidly changing environment for diseases in marine shellfish requires further study, though experimental work (Mackenzie et al., 2014; Zha et al., 2017) and projections (Green et al., 2019), highlight the risk emerging pathogens might play in coming years. The opposite must be considered too, that is, the possible mitigating effects oceanic warming and low-pH might have on pathogenesis (via reduced pathogen fitness) in certain habitats (Olsen et al., 2015), and the repercussions for population dynamics therein (Harvell et al., 2002).

2.5 *Shellfish Mass Mortalities in Aotearoa: A Case for Increased Surveillance*

In Aotearoa, kai moana (seafood) is a staple of the diet for both Māori (Indigenous people of Aotearoa) and pākehā (New Zealanders of European decent). Alike many marine mollusc species aforementioned, those residing wild in the coastal waters of Aotearoa are too subject to a wide array of anthropogenic pressures. Resistance to the ongoing threat posed by invasive species and emerging pathogens remains a high priority for government agencies and stakeholders (Georgiades et al., 2020; MPI, 2016), to protect the unique flora and fauna residing within Aotearoa and immediately offshore. Biosecurity efforts also include maintaining regular reporting and database management to enable the identification of emerging pathogens and quantification of associated risk for industry and the environment. Despite many preventative measures and monitoring protocols in place (MPI, 2016), the risk of introductions (pathogenic and otherwise) remains high. This is especially true for the marine environment where numerous

pathways exist, many of which are challenging to manage, such as, biofouling on ships and marine debris (Hayes et al., 2019). The present case places a spotlight on certain limitations within the shellfish health sphere. Principally, how reactive approaches have introduced knowledge gaps that could be closed with systematic health screening of wild populations, and empowerment of communities to enhance passive surveillance.

2.5.1 Customary Fishing in Aotearoa

Sourcing food from the oceans has been an integral part of the human history of Aotearoa (Mccarthy et al., 2014; Whaanga et al., 2018). Archaeological shell middens dotted around the coast pinpoint areas where historical harvesting and shucking of shellfish took place. Similar to seafaring Indigenous peoples from other corners of the globe, seafood constituted a substantial portion of pre-European Māori diet. Today, many Māori continue to source food from the ocean (Mccarthy et al., 2014) (Table 2.1). A case that emphasises the importance of shellfish harvesting is that of the toheroa (*Paphies ventricosa*) (Fig. 2.1). Harvested for hundreds of years, the toheroa is a large and iconic surf clam, endemic to Aotearoa. Commercial fishing and intensive recreational harvesting in the 1900s led to a collapse of stocks, and subsequent closure of the fisheries (Miskelly, 2016; Ross et al., 2018a). Despite the last open season having been in 1993, toheroa have never been declared a fully protected species. Now managed by the Fisheries (Kai moana Customary Fishing) Regulations 1998, the collection of toheroa is under a permit system for customary purposes. The overexploitation, collapse and closure of the fishery has had a lasting effect on many coastal communities, who place intrinsic value in toheroa. Nearly 70 years since the first protective measures were placed on toheroa, populations have not recovered (Ross et al., 2018a; Williams et al., 2013). Although, the issue remains within the national psyche, periodically gaining the attention of national media (Harvie, 2017). This case places emphasis on just one of the treasured kai moana unique to Aotearoa, though there are many others.

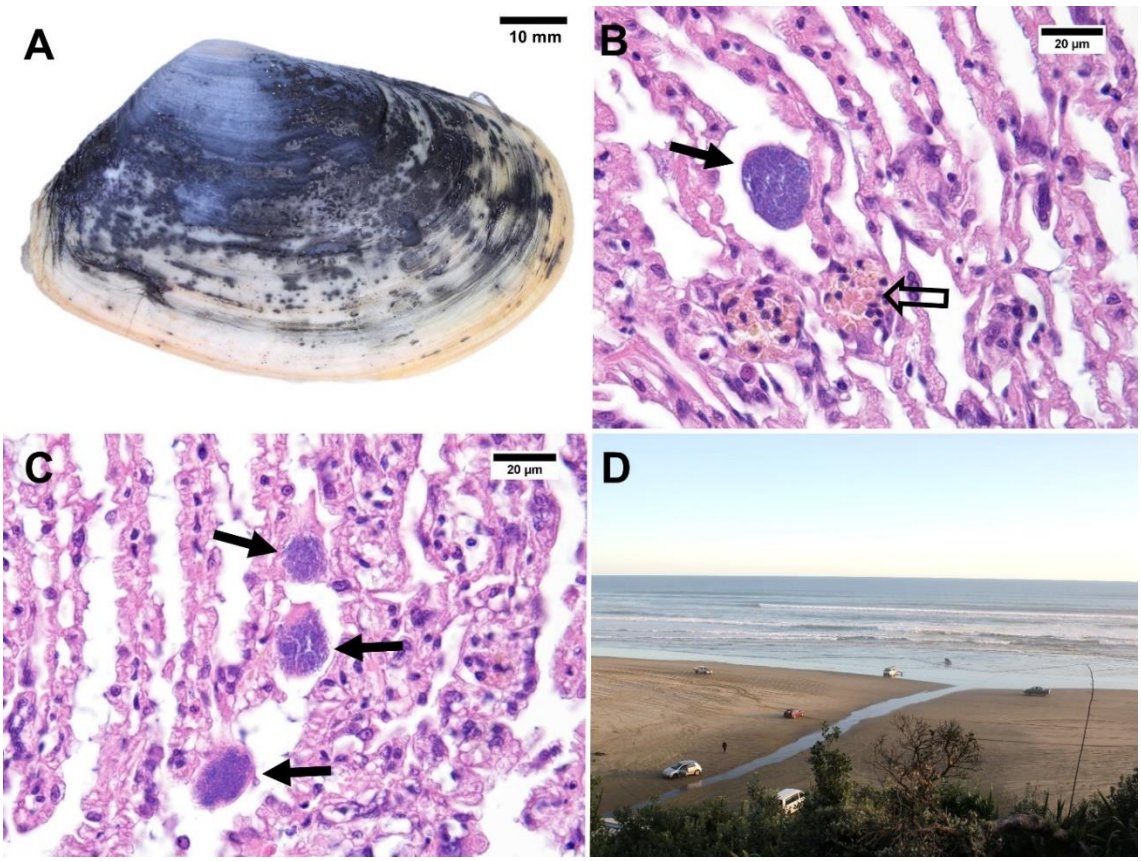

Fig. 2.1. A: *P. ventricosa* (toheroa) a large surf clam endemic to Aotearoa (New Zealand). B & C: Histological tissue sections (H&E stained) of toheroa gills (Olympus BX51 at x100 magnification, under oil). Filled arrows indicate cells infected with intracellular microcolonies of bacteria, hollow arrow denotes lipofuscin pigmented cells. D: A freshwater stream at Ripiro Beach, the characteristic habitat of toheroa. Toheroa are generally found in high-density beds either side of freshwater streams (in the lower intertidal) on high-energy surf beaches.

2.5.2 Recent Series of Mass Mortality Events

Between 2012 and 2018, investigators at the Animal Health Laboratory (Biosecurity New Zealand) noted an increase in the regularity of MMEs around Aotearoa (Fig. 2.2). Most of these mortality events were brought to the attention of investigators by members of the public, who had recognised an abnormal morality or the abundance of 'sick' individuals and dialled the Ministry for Primary Industries biosecurity hotline (0800 80 99 66) to report the observation (Fig. 2.3, tile 1). Some of these MMEs raised a substantial amount of public concern and garnered media attention (Herald, 2018). Initially, no direct causal factor behind observable mortality was evident. MMEs were occurring in a variety of shellfish species, though surf clams of the *Paphies* genus dominated the mortality landscape (Fig. 2.2). In a search for a cause, freshwater smothering, sedimentation, and pollution were considered as potential contributing factors. A tentative link was subsequently made between temperature and MMEs, with seven MMEs recorded in spring, seven in autumn, only one in winter, but 16 in the summers between 2012 and 2018 (Biosecurity New Zealand, unpublished data).

Following post-mortem assessment of sick and deceased individuals from MMEs via histopathology, no aetiological agents behind mortality were immediately obvious to investigators. *Rickettsia*-like organisms were identified as a potential pathogen in 2017 following the extensive mortality events at Waihi Beach, Bay of Plenty of pipi (*P. australis*) and tuatua (*P. subtriangulata*) (Fig. 2.2). The presence of basophilic inclusions (cells infected with intracellular bacteria) was detected in the gills and digestive glands of many moribund individuals (Fig. 2.1 & Fig. 2.3, tile 2). The term *'Rickettsia*-like organism' or 'RLO' has long been used as a broad term to describe unidentified intracellular bacteria (Fournier and Raoult, 2009). RLOs are gram-negative, obligate intracellular bacteria that divide by binary fission (Fournier and Raoult, 2009). In marine molluscs, RLOs have been detected globally, with an extensive host range, including finfish, molluscs, and crustaceans (Gollas-Galvan et al., 2014). They have been associated with mortality in several species and regions (Friedman and Crosson, 2012), but most famously in abalone, where mortality has resulted in widespread declines in some species (principally black abalone, *Haliotis cracherodii*) caused by withering syndrome-RLO (Friedman and Crosson, 2012; Wetchateng et al., 2010). After this link was established, work began to characterise the bacteria in question. Identification of infiltrating pathogens is a critical first step to understand the role disease might be playing in any mortality event. Gene sequencing (16S rRNA) subsequently revealed the intracellular bacteria to be *Endozoicomonas* spp., rather than Rickettsiales (Howells et al., 2021) (Fig. 2.3, tile 3).

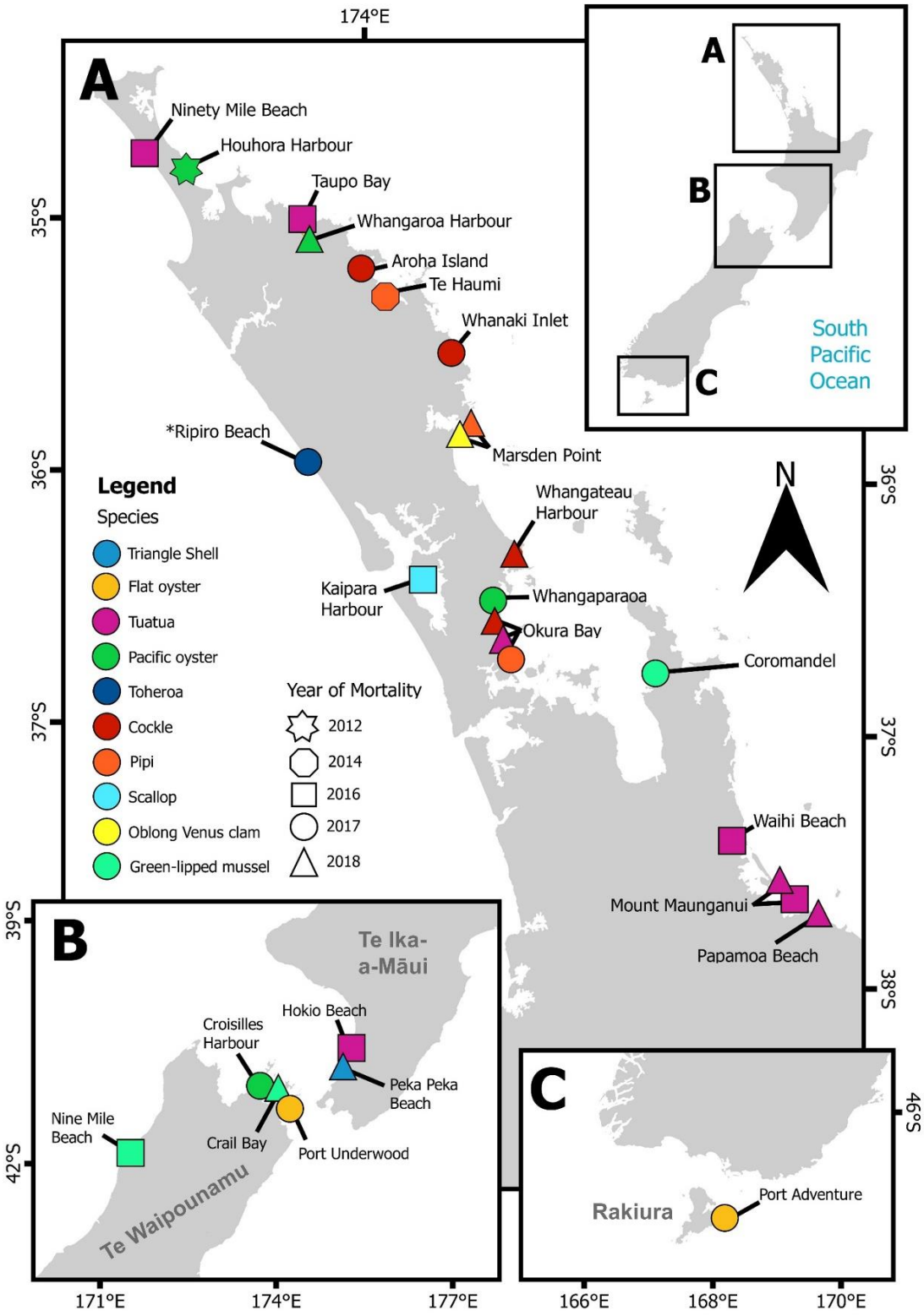

Fig. 2.2. Locations of shellfish MMEs in Aotearoa between 2012 and 2018. Data obtained from Ministry for Primary Industries (Biosecurity New Zealand). Triangle shell: *Crassula aequilatera*, Flat oyster: *Ostrea chilensis*, Tuatua: *Paphies subtriangulata*, Pacific oyster: *Crassostrea gigas*, Toheroa: *Paphies ventricosa*, Cockle: *Austrovenus stutchburyi*, Pipi: *Paphies australis*, New Zealand scallop: *Pecten novaezelandiae*, Oblong Venus clam: *Venerupis largillierti*, Green-lipped mussel: *Perna canaliculus*. Produced using Quantum GIS (QGIS v3.2.3). Spatial layers obtained from DIVA-GIS. CRS: WGS 84 (EPSG: 4326).

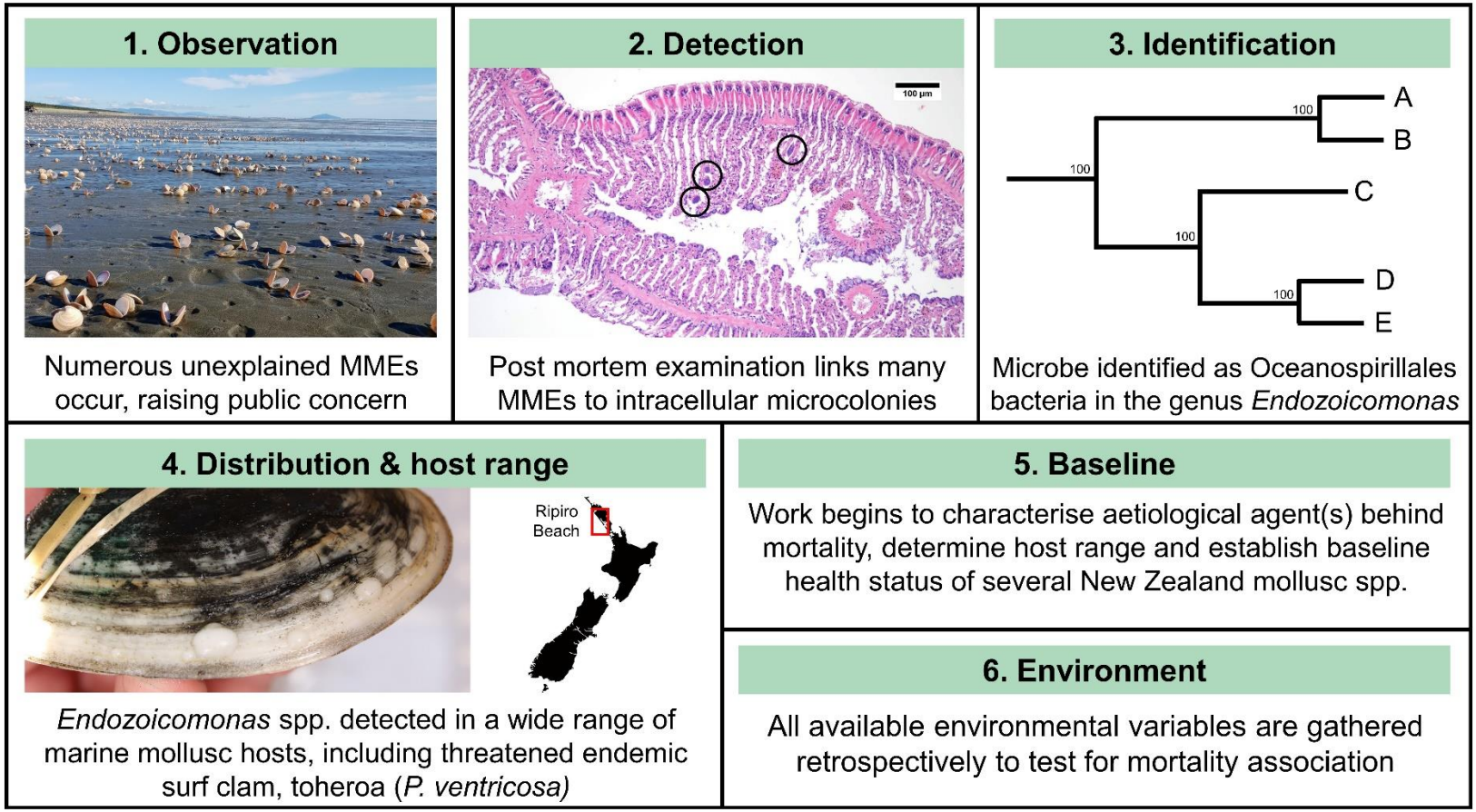

Fig. 2.3. Reconstruction of key events from the Aotearoa (New Zealand) shellfish mortality case. Photograph 1: Mass mortality event of *Dosinia anus* at Waitarere Beach in April 2019 (Photograph: J. Howells). Photograph 2: Histological tissue section of toheroa (*P. ventricosa*) gills (H&E stained) under light microscopy (Olympus BX51 at x20 magnification). Circles indicate cells infected with intracellular microcolonies of bacteria (IMCs). Photograph 3 (Tile 4): Toheroa collected from Ripiro Beach, Te Tai Tokerau following the detection of non-infectious gas bubble disease (Ross et al., 2018b), intracellular microcolonies of bacteria were subsequently detected via histopathology.

2.5.3 Potential Pathogen Identified: Endozoicomonas spp.

Coincidently, as investigators in Aotearoa determined the correct identity of the intracellular bacteria, as *Endozoicomonas* spp. rather than *Rickettsia*-like, a mortality event of king scallops (*P. maximus*) from Lyme Bay in the United Kingdom was linked to the presence of *Endozoicomonas* spp. (Cano et al., 2018). Cano and co-authors refer to the use of '*Rickettsia*-like organism' as a general term to describe any unidentified intracellular bacterium as 'potentially misleading', illustrated by not only their study, but also now by the case presented herein. Since the description of the genus *Endozoicomonas* in 2007, the number of publications and submissions of *Endozoicomonas* nucleotide data to NCBI's GenBank database has grown rapidly (Neave et al., 2016). A search in the Scopus database for '*Endozoicomonas*' returned 101 published articles (as of Sept 2020). An upward trend is also detected when the published manuscripts featuring '*Endozoicomonas'* are considered as a proportion of all manuscripts published over the same time-frame (Fig. 2.4). Detections of *Endozoicomonas* bacteria have been in a variety of hosts from diverse taxa, though most detections to-date have been within coral microbiomes, detections have been made in sponges, molluscs and fishes too, with a seemingly global distribution (Neave et al., 2016). The geographic distribution of the *Endozoicomonas* genus is shown here using occurrence data obtained from the Geographic Biodiversity Information Facility or 'GBIF', a search for '*Endozoicomonas*' returned 10,292 georeferenced occurrence records, from every ocean/continent on earth (Fig. 2.4). The functional role of *Endozoicomonas* bacteria in marine hosts has been examined (reviewed by Neave et al., 2016) (see Fig. 2.5). Although a variety of roles are suggested, health and disease seem to be a common theme in fish (Katharios et al., 2015; Mendoza et al., 2013), molluscs (Cano et al., 2018; Hooper et al., 2019), and some corals (Neave et al., 2016) (Fig. 2.5). The role these microbes play in the shellfish mortality landscape in Aotearoa is currently unknown, but their pathogenic potential in marine organisms is reputed, justifying further exploration.

2.5.4 Host Range, Distribution, and Research Priorities

The link between MMEs of various shellfish and intracellular bacteria was originally made due to the detection of bacterial infections in several different species collected during investigatory responses. Since then, *Endozoicomonas* bacteria have been detected in the gills and digestive glands of *Dosinia anus*, *P. ventricosa*, *P. subtriangulata*, *P. donacina*, *P. australis*, *Pecten novaezelandiae, Perna canaliculus*, and *Austrovenus stutchburyi*, with qPCR prevalence between 95-100% (Howells et al., 2021) (Fig. 2.3, tile 4). Furthermore, a tentative link has been made between shellfish submitted during a 'mortality' event, 'healthy' shellfish, and *Endozoicomonas* spp. gene copies.

With generally higher *Endozoicomonas* spp. gene copies recorded in mortality specimens than apparently healthy specimens (Howells et al., 2021), suggesting opportunistic propensity. The geographic distribution of MMEs reported between 2012 and 2018 fall along a large longitudinal range, from the top of the North Island of Aotearoa (Ninety-mile Beach/Te-Oneroa-a-Tōhē) to Rakiura (Stewart Island) (Fig. 2.2). Work has begun to develop an understanding of the seasonal infection patterns of *Endozoicomonas* bacteria and other parasites and pathogens in a handful of mollusc species particularly implicated in mortality events. This is under the aim of developing an understanding of ambient condition or baseline health information; a difficult task in dynamic systems (Groner et al., 2016; Ward and Lafferty, 2004) (Fig 4, tile 5). Furthermore, following recognition of the regularity of these MMEs, efforts are being made determine environmental conditions prior to MMEs, retrospectively, to gain an insight into the potential contribution the environment (air and sea surface temperature, rainfall, wave height, and wind speed). Retrospective data collection can be used to guide future research, but it will not provide informative results with which to manage response.

Speciating the potential aetiological agent in question is also a significant priority. As Cano et al. (2018) show, genome of the *Endozoicomonas* sp. isolated from king scallops in their study was much smaller than other symbiotic *Endozoicomonas* spp. (4.83 Mb cf. 6.83 Mb, respectively) (Neave et al., 2014). Cano and co-authors go on to postulate that a smaller genome could be a result of a loss of regulatory genes, which could increase pathogen virulence. Therefore, speciating the aetiological agent holds important knock-on implications for gaining an understanding of pathogen distribution and transmission dynamics. Investigatory work based on the MMEs described herein is ongoing. Establishing the cause of observable MMEs remains a high priority. Although significant progress has been made since 2017, it remains unknown whether the intracellular bacterium detected then, contribute to pathogenesis. Moreover, without population estimates and long-term empirical data it is not possible to determine whether the MMEs here are microorganism-related or a result of rapid environmental change. Importantly, it is still unknown whether observed MMEs are a natural phenomenon that in fact, requires no action.

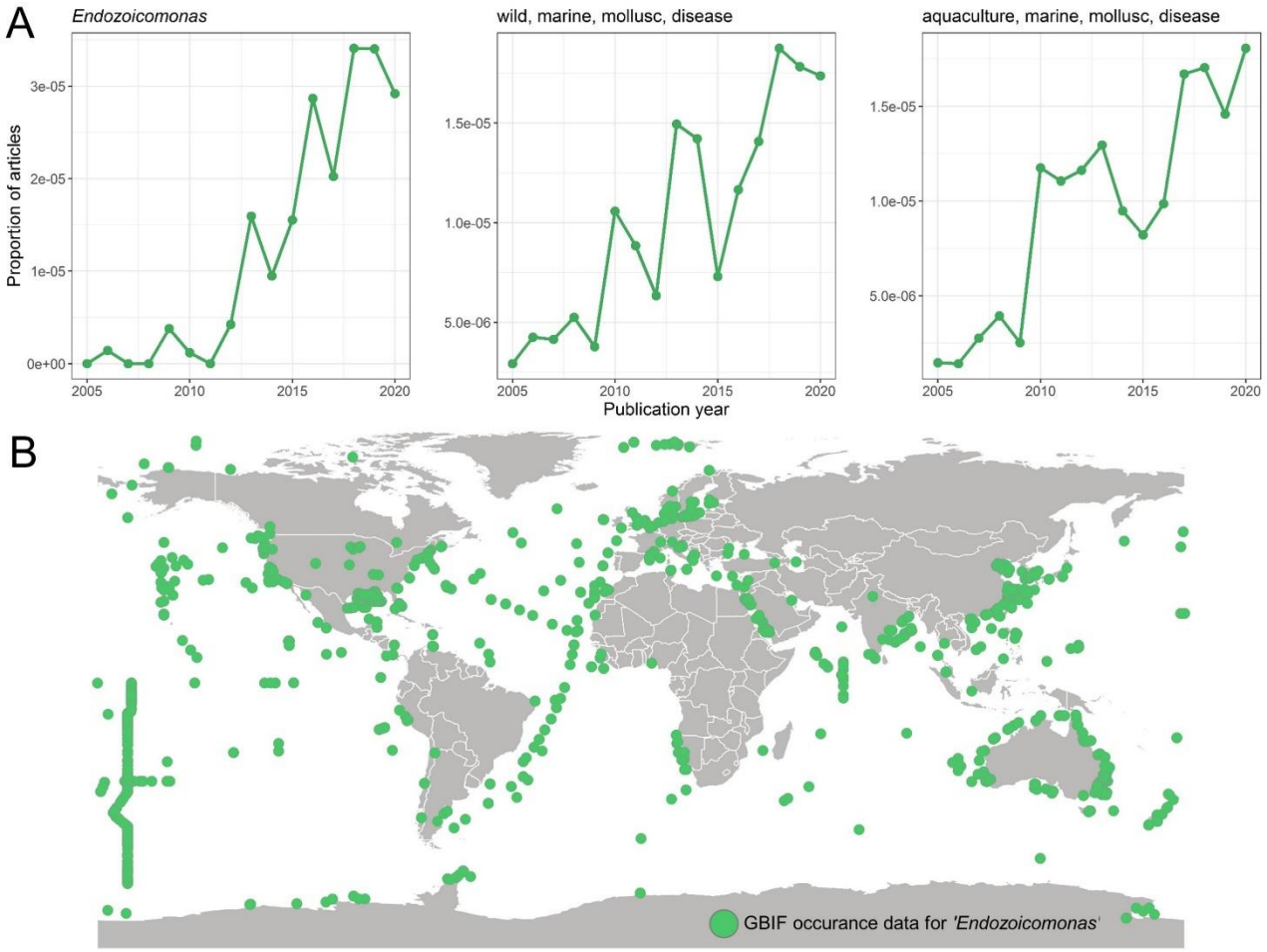

Fig. 2.4. A: Proportion of published articles in the Europe PubMed database featuring the keywords above, normalised against total publications within the same period (2005-2020). Figure produced in RStudio (Team, 2013) using 'ggplot2' (Wickham, 2009) and 'europepmc' (Jahn, 2020) packages. Figures indicate an upward trend since 2005 of published articles featuring '*Endozoicomonas'* and articles encompassing mollusc disease, both wild and cultured. Search conducted in Aug 2020. B: Occurrence data for the bacterial genus *Endozoicomonas* in the Global Biodiversity Information Facility (GBIF) database. A search for '*Endozoicomonas*' returned 10,292 georeferenced records, between 2007 and 2017 (GBIF, 2020). Spatial layers obtained from DIVA-GIS, map produced using QGIS v.3.8 Zanzibar.

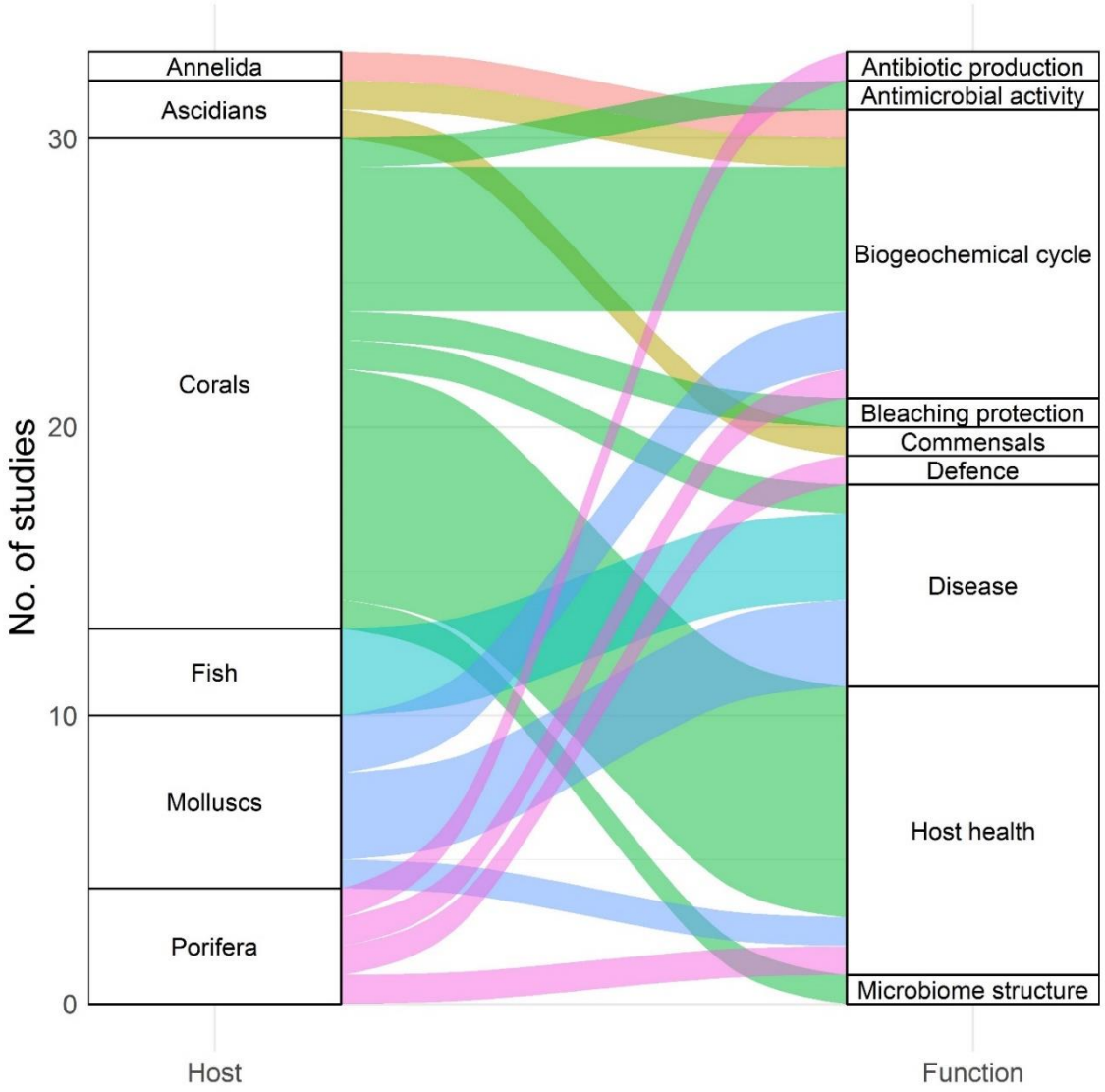

Fig. 2.5. Alluvial plot showing the number of studies that have associated the bacterial genus *Endozoicomonas* to different functions in hosts. Note: most studies have thus far focused on coral hosts. Figure adapted from (Neave et al., 2016), and updated (as of Nov 2020). Produced in RStudio using the ggalluvial package (Brunson, 2020). Studies were grouped into 'host health' if vague mentions were made of *Endozoicomonas* spp. importance in host-associated bacterial communities e.g., 'microbiome structuring'. See Table B.1 for details of studies used to produce this figure.

2.6 Discussion

Globally, the annual consumption of seafood by coastal Indigenous communities has been estimated to be 2.1 million tonnes (Cisneros-Montemayor et al., 2016). Moreover, Cisneros-Montemayor and co-authors estimate that on average consumption of seafood by Indigenous communities is 15 times that of non-indigenous populations. At the same time, seafood consumption is growing worldwide, doubling between 1960 and 2014 (FAO, 2016; Guillen et al., 2019). Outbreaks of disease in the oceans are predicted to rise too (Maynard et al., 2015). Anthropogenic pollution and climate change are cited as some of the major contributors to this rise, and already disease is considered

the greatest limiting factor to aquaculture (Rowley et al., 2014; Stentiford et al., 2012). Lately the threat posed by disease to wild populations is being increasingly recognised too, evidenced by an upsurge in research encompassing disease in wild molluscs (Fig. 2.4). Anthropogenic stressors are tipping the balance in favour of opportunistic pathogenic microbes, the repercussions of which are recognised for commercial seafood industries (Rowley et al., 2014; Stentiford et al., 2012). At the same time, the consequences for rural and Indigenous communities can be profound too, particularly for subsistence fisheries e.g., saprolegniosis in Aanaakłiq, broad whitefish (*Coregonus nasus*) in Alaska (Sformo et al., 2017).

2.6.1 Where does the Aotearoa Case Fit in a Global Context?

This case, although specific to Aotearoa is not inherently unique to Aotearoa. Seafood provision is fundamental to the day-to-day lives of many coastal communities globally (Cisneros-Montemayor et al., 2016; FAO, 2018). Despite this, fundamental knowledge of the health status of many harvested marine mollusc species is underdeveloped. Though this is not the rule and exceptions exist, namely for Chesapeake Bay oysters (reviewed in Schulte, 2017), which should be used as reference models. It is hoped that the case here illustrates some of the services provided by coastal shellfish species, outside of their well-recognised ecological and commercial value, placing a spotlight on customary and health-associated benefits provided by stable shellfish populations (Table 2.1). These benefits are complex to quantify, as they can be subjective, personal, and differ regionally. However, services provisioned in these ways are increasingly being recognised in studies, bills, and fisheries assessments. In a disease context, these services underscore the need for regular health screening of wild shellfish populations, including those that do not constitute a profitable commercial or recreational fishery. At the same time, the frequency of unexplained shellfish MMEs occurring around the Aotearoa coastline (Fig. 2.2) has placed a magnifying glass over current management and response protocols (Howells et al., 2021). This is not a phenomenon unique to Aotearoa, where shellfish MMEs have been tentatively linked to a variety of environmental factors (e.g., salinity and temperature) around the globe (see Table 1, Chapter 1). Groner et al. (2016) remark on the limitations of current management of disease in marine species, showing that reactive responses at present restrict the effectiveness of management post-outbreak, reducing our ability to mitigate contributing factors where possible. The present case provides a real-world example of this limitation as to-date, response to the recent series of mollusc MMEs in Aotearoa has been grounded in an investigatory capacity, due to a lack of baseline data.

Table 2.2. Resources and online databases focused (or encompassing data) on marine organism health. The table below includes a variety of schemes that place focus in different aspects of marine organism health from genomic epidemiology and diagnoses to data sharing and outreach.

Name	Type	Purpose	Link
EURL for Mollusc Diseases	Reference/ educational material	The European Union Reference Laboratory for Mollusc Diseases (Ifremer) hosts tutorials for the detection, identification, and surveillance of OIE notifiable diseases	https://www.eurl-mollusc.eu/
The Mass Mortality Events Database (MME-T-MEDNet)	Data repository	A collaborative database, with the goal of assembling and standardizing data of MMEs within the Mediterranean	http://cormednet.medrecover.org/mme/public/home_mass_mortality
Fisheries and Oceans Canada	Reference/ educational material	Fisheries and Oceans Canada maintain a reference site for parasites and pathogens in commercially important fish and molluscs in Canadian waters	http://www.dfo-mpo.gc.ca/index-eng.htm
AquaPathogen X	Data repository	A template database for recording information on individual isolates of aquatic pathogens, data can then be viewed and queried	http://wfrc.usgs.gov
Bio-atlas	Virtual histological slide box	Set up primarily to store and share scanned Zebrafish (*Danio rerio*) histology slides, Bio-atlas offers a repository for scanned histological sections	http://bio-atlas.psu.edu/zf/progress.php
Microreact	Genomic data	Microreact encourages users to upload, visualise and explore genomic epidemiological data	https://microreact.org/showcase
Ocean Biogeographic Information System (OBIS)	Occurrence/ spatial data repository	Serving as a repository for ocean biogeographic data, OBIS encourages users to share geospatial data	https://obis.org/
Global Biodiversity Information Facility (GBIF)	Occurrence/ spatial data repository	Similar to OBIS, the Global Biodiversity Information Facility acts as a repository for geospatial data from any taxa	https://www.gbif.org/en/
CoralWatch	Citizen science initiative	CoralWatch combines global coral health monitoring and public outreach to both educate and encourage awareness, while gathering data of coral health	https://coralwatch.org/
Coral Health and Monitoring Programme (NOAA)	Data repository	CHAMPs is a repository administrated by NOAA, for researchers and members of the public to deposit, share and download coral health and monitoring data	https://www.coral.noaa.gov/
Beneficial Microorganisms for Marine Organisms (BMMO)	Network	A network of research groups collecting and collating data of beneficial marine microorganisms to aid the management and manipulation of marine microbiomes	http://bmmo.microbe.net/

2.6.2 What are the Repercussions for Management?

Now, more than four years since the first associations of mortality with an intracellular bacteria, it is still unclear whether *Endozoicomonas* spp. impacts host health, causes mortality or, whether it is in fact an important constituent of the bacterial community of Aotearoa shellfish. As reported for *Mytilus edulis* from New Jersey, USA (Schill et al., 2017). Similarly, Dubé et al. (2019) found that an OTU classified to the family *Endozoicimonaceae* was highly represented in the microbial community in several black-lip pearl oyster *Pinctada margaritfera* tissues, but that interestingly, the gonad microbiome was dominated by this OTU (43.3%). Note: the family "*Endozoicimonaceae"* is not widely accepted (Neave et al., 2016; Shiu and Tang, 2019). Although significant progress has been made, fundamental 'unknowns' such as these remain, primarily attributed to a lack of understanding of ambient conditions prior to the current on-going investigation. Work is beginning in this area, but a surveillance programme akin to The Mussel Watch Project (Goldberg et al., 1978) requires development in an Aotearoa context. Garrabou et al. (2019) provide a case for a database to track MMEs in the Mediterranean Sea. While MME data is collected by the Ministry for Primary Industries in Aotearoa (Fig. 2.2), a database like MME-T-MEDNet (Table 2.2) would also strengthen investigatory work into the causes of MMEs, or at least standardise data collection and dissemination. Evident from this case, there is a need for basic reference material of wild shellfish health in Aotearoa. The mortalities observed between 2012 and 2018 (Fig. 2.2) were not owed to an on-going epidemic (Lane et al., 2020), but instead intermittent bouts of substantial losses (the extent of which is also unknown). These should serve as a warning and be used to highlight the preparedness of managers to respond to future mortality events. At this stage, these intermittent 'warnings' should be used to trigger proactive action, rather than waiting for an epizootic episode and implementing a reactive response. Lessons learned internationally should serve as a warning too, sea star wasting disease (Montecino-Latorre et al., 2016) and abalone withering syndrome (Crosson et al., 2014) illustrate how quickly diseases can spread in the oceans and how important data, pre-epizootic episode is, when unexpected MMEs occur.

There has been an apparent increase in submissions of dying/deceased shellfish specimens and reports from the public of shellfish MMEs in Aotearoa (Howells et al., 2021; Lane et al., 2020). The majority of the MMEs in Fig. 2.2 were first detected by local communities (reported via the Ministry for Primary Industries biosecurity hotline). However, not all of these mortalities were formally investigated by authorities. Although this presents a limitation in terms of the usefulness of the MME occurrence data collected (as aetiological agents cannot be retroactively identified), the public in this case demonstrated the role citizen science can play in the surveillance of remote, coastal environments. Local communities, kaitiaki (guardians), tangata whenua (people of

respective lands), and regional councils are the usual first responders to mortality events. Enabling local communities to best respond to future MMEs should therefore, become a priority. Outreach programmes (e.g., community science projects) offer the opportunity to educate, gather data and create a dialogue between communities and authorities (Table 2.2). Many examples of successful community science programmes coupled with public data repositories exist for a variety of fields e.g., seagrass mapping (SeagrassSpotter, Jones et al., 2018) and invasive species monitoring ('Is it Alien to you? Share it!!!', Giovos et al., 2019), but similar programmes within the 'marine organism health' sphere are comparably scarce. Furthermore, a 'common web portal' for shellfish in Aotearoa, akin to the one suggested for cockles (*C. edule*) by Mahony et al. (2020), could provide both a data repository (standardising data collection and retention) and facilitate knowledge transmission between managers, stakeholders, and tangata whenua.

In short systematic surveillance and monitoring of the health of wild shellfish is needed (Howells et al., 2021; Lane et al., 2020). Several modelling, diagnostic, and immunological approaches could all provide much greater insight into the role disease plays in MMEs. These include the '*omics approaches'* (genomics, transcriptomics, proteomics, and metabolomics) (Nguyen et al., 2019) and predictive dispersal models of pathogens (Foreman et al., 2015). Many tools exist which can be applied within investigations to gather greater insight of host-pathogen-environment dynamics in the oceans. The effectiveness of these tools is reduced, however, in the absence of detailed information of population health prior to disease outbreak. Additionally, evidenced by the present case, when so many unknowns are present, it is also unclear whether these approaches are even necessary. For example, whether mortality is even the result of an aetiological agent or an as-yet-unknown environmental trigger (extrinsic factor).

2.6.3 Recommendations to Increase Disease Response Capacity

1. **Increased surveillance** of healthy populations, and the environmental parameters that influence said populations, is necessary, not only to allow for rapid detection of new and emerging pathogens, but also to provide a baseline of ambient health of wild shellfish populations.
2. The creation of baselines is redundant if data are not gathered in a standardised manner. This is especially important for capture-all techniques. For example, often researchers use visual scales (Low, Moderate, and High) to grade pathological features while conducting routine histology. The production of a set of **best-practice guidelines for Aotearoa shellfish**

health studies could standardise the approach of both researchers and investigators.

3 To maximise the role coastal communities can play in the monitoring of marine organism health, greater emphasis should be placed on education and outreach initiatives in this area (marine organism health), to **equip and encourage local communities to identify and respond to abnormal mortality events** (see Table 2.2, CoralWatch for an example of a community focused project in this field).

2.7 References

Amin, S. A., et al., 2012. Interactions between diatoms and bacteria. Microbiology and molecular biology reviews : MMBR. 76**,** 667-684.

Audrézet, F., et al., 2021. Biosecurity implications of drifting marine plastic debris: Current knowledge and future research. Marine Pollution Bulletin. 162**,** 111835.

Azam, F., Malfatti, F., 2007. Microbial structuring of marine ecosystems. Nature Reviews Microbiology. 5**,** 782.

Bar-On, Y. M., et al., 2018. The biomass distribution on Earth. Proceedings of the National Academy of Sciences. 115**,** 6506–6511.

Barber, J. S., et al., 2019. Intertidal clams exhibit population synchrony across spatial and temporal scales. Limnology and Oceanography. 64**,** S284-S300.

Bax, N., et al., 2003. Marine invasive alien species: a threat to global biodiversity. Marine Policy. 27**,** 313-323.

Belkin, S., Colwell, R. R., 2006. Oceans and health: pathogens in the marine environment. Springer.

Ben-Horin, T., et al., 2013. Variable intertidal temperature explains why disease endangers black abalone. Ecology. 94**,** 161-168.

Bidegain, G., Paul-Pont, I., 2018. Commentary: Plastic waste associated with disease on coral reefs. Frontiers in Marine Science. 5**,** 237.

Brunson, J., ggalluvial: Alluvial Plots in 'ggplot2'. R package version 0.11. 3. 2020.

Burge, C. A., et al., 2016. The Use of Filter-feeders to Manage Disease in a Changing World. Integrative and Comparative Biology. 56**,** 573-587.

Burge, C. A., et al., Climate Change Influences on Marine Infectious Diseases: Implications for Management and Society. In: C. A. Carlson, S. J. Giovannoni, Eds.), Annual Review of Marine Science, Vol 6, 2014, pp. 249-277.

Burgess Tristan, L., et al., 2018. Defining the risk landscape in the context of pathogen pollution: *Toxoplasma gondii* in sea otters along the Pacific Rim. Royal Society Open Science. 5**,** 171178.

Burreson, E. M., Ragone Calvo, L. M., 1996. Epizootiology of *Perkinsus marinus* disease of oysters in Chesapeake Bay, with emphasis on data since 1985. Journal of Shellfish Research. 15**,** 17-34.

Cano, I., et al., 2018. Molecular Characterization of an *Endozoicomonas*-Like Organism Causing Infection in the King Scallop (*Pecten maximus* L.). Applied and Environmental Microbiology. 84**,** e00952-17.

Carlson, C. J., et al., 2018. Spores and soil from six sides: interdisciplinarity and the environmental biology of anthrax (*Bacillus anthracis*). Biological Reviews. 93**,** 1813-1831.

Carnegie, R. B., et al., 2016. Managing marine mollusc diseases in the context of regional and international commerce: policy issues and emerging concerns. Philosophical Transactions of the Royal Society B: Biological Sciences. 371**,** 20150215.

Carss, D. N., et al., 2020. Ecosystem services provided by a non-cultured shellfish species: The common cockle *Cerastoderma edule*. Marine Environmental Research. 158**,** 104931.

Cisneros-Montemayor, A. M., et al., 2016. A Global Estimate of Seafood Consumption by Coastal Indigenous Peoples. PLOS ONE. 11**,** e0166681.

Codding, B. F., et al., 2014. Global Patterns in the Exploitation of Shellfish. The Journal of Island and Coastal Archaeology. 9**,** 145-149.

Costello, K. E., et al., 2021. The role of invasive tunicates as reservoirs of molluscan pathogens. Biological Invasions. 23**,** 641-655.

Crosson, L. M., et al., 2014. Abalone withering syndrome: distribution, impacts, current diagnostic methods and new findings. Diseases of Aquatic Organisms. 108**,** 261-270.

Dairain, A., et al., 2019. Influence of parasitism on bioturbation: from host to ecosystem functioning. Marine Ecology Progress Series. 619**,** 201-214.

Dame, R., 2016. Ecology of Marine Bivalves: An Ecosystem Approach. CRC Press, Boca Raton.

Diggles, B. K., 2013. Historical epidemiology indicates water quality decline drives loss of oyster (*Saccostrea glomerata*) reefs in Moreton Bay, Australia. New Zealand Journal of Marine and Freshwater Research. 47**,** 561-581.

Drake, L. A., et al., 2007. Potential microbial bioinvasions via ships' ballast water, sediment, and biofilm. Marine Pollution Bulletin. 55**,** 333-341.

Dubé, C. E., et al., 2019. Microbiome of the Black-Lipped Pearl Oyster *Pinctada margaritifera*, a Multi-Tissue Description With Functional Profiling. Frontiers in Microbiology. 10**,** 1548.

Dubey, J. P., et al., 2003. *Toxoplasma gondii*, *Neospora caninum*, *Sarcocystis neurona,* and *Sarcocystis canis*-like infections in marine mammals. Veterinary Parasitology. 116**,** 275-296.

Eggleston, D., Hickman, R. W., 1972. Mass stranding of molluscs at Te Waewae bay, southland, New Zealand New Zealand Journal of Marine and Freshwater Research. 6**,** 379-382.

FAO, The State of World Fisheries and Aquaculture 2016. Contributing to food security and nutrition for all. Food and Agriculture Organization of the United Nations, Rome, 2016, pp. 200.

FAO, The State of World Fisheries and Aquaculture 2018 - Meeting the sustainable development goals. Food and Agriculture Organization of the United Nations, Rome, 2018, pp. 211.

Foley, R., Kistemann, T., 2015. Blue space geographies: Enabling health in place. Health & Place. 35**,** 157-165.

Ford, S. E., et al., 2018. Investigating The Life Cycle of *Haplosporidium Nelsoni* (MSX): A Review. Journal of Shellfish Research. 37**,** 679-693.

Foreman, M. G. G., et al., 2015. Modelling Infectious Hematopoietic Necrosis Virus Dispersion from Marine Salmon Farms in the Discovery Islands, British Columbia, Canada. PLOS ONE. 10**,** e0130951.

Foster, V., et al., 2016. Identifying the physical features of marina infrastructure associated with the presence of non-native species in the UK. Marine Biology. 163**,** 173.

Fournier, P.-E., Raoult, D., 2009. Current Knowledge on Phylogeny and Taxonomy of *Rickettsia* spp. Annals of the New York Academy of Sciences. 1166**,** 1-11.

Frère, L., et al., 2018. Microplastic bacterial communities in the Bay of Brest: Influence of polymer type and size. Environmental Pollution. 242**,** 614-625.

Friedman, C., et al., 1993. Transmissibility of a coccidian parasite of abalone, *Haliotis* spp. Journal of Shellfish Research. 12**,** 201-205.

Friedman, C. S., et al., 2002. Transmission of withering syndrome in black abalone, *Haliotis cracherodii* leach. Journal of Shellfish Research. 21**,** 817-824.

Friedman, C. S., Crosson, L. M., 2012. Putative Phage Hyperparasite in the Rickettsial Pathogen of Abalone, "*Candidatus* Xenohaliotis californiensis". Microbial Ecology. 64**,** 1064-1072.

Friedman, C. S., et al., 1995. *Pseudoklossia haliotis* sp. n. (Apicomplexa) from the Kidney of California Abalone, *Haliotis* spp. (Mollusca). Journal of Invertebrate Pathology. 66**,** 33-38.

Fu, D., An updated stock assessment for Foveaux Strait dredge oysters (*Ostrea chilensis*) for the 2012 fishing year Ministry of Primary Industries, Wellington, 2013, pp. 57.

Gardner, G. R., et al., 1995. Association of Prokaryotes with Symptomatic Appearance of Withering Syndrome in Black Abalone *Haliotis cracherodii*. Journal of Invertebrate Pathology. 66**,** 111-120.

Garrabou, J., et al., 2019. Collaborative Database to Track Mass Mortality Events in the Mediterranean Sea. Frontiers in Marine Science. 6**,** 707.

GBIF, GBIF Occurrence Download 2020. Access date: July 2020. https://doi.org/10.15468/dl.bwnttk.

Georgiades, E., et al., 2020. Regulating Vessel Biofouling to Support New Zealand's Marine Biosecurity System – A Blue Print for Evidence-Based Decision Making. Frontiers in Marine Science. 7**,** 390.

Gillies, C. L., et al., 2018. Australian shellfish ecosystems: Past distribution, current status and future direction. PLOS ONE. 13**,** e0190914.

Giovos, I., et al., 2019. Citizen-science for monitoring marine invasions and stimulating public engagement: a case project from the eastern Mediterranean. Biological Invasions. 21**,** 3707-3721.

Goldberg, E. D., et al., 1978. The Mussel Watch. Environmental Conservation. 5**,** 101-125.

Gollas-Galvan, T., et al., 2014. *Rickettsia*-like organisms from cultured aquatic organisms, with emphasis on necrotizing hepatopancreatitis bacterium affecting penaeid shrimp: an overview on an emergent concern. Reviews in Aquaculture. 6**,** 256-269.

Green, T. J., et al., 2019. Simulated Marine Heat Wave Alters Abundance and Structure of *Vibrio* Populations Associated with the Pacific Oyster Resulting in a Mass Mortality Event. Microbial Ecology. 77**,** 736-747.

Groner, M. L., et al., 2016. Managing marine disease emergencies in an era of rapid change. Philosophical Transactions of the Royal Society B-Biological Sciences. 371**,** 20150364.

Guillen, J., et al., 2019. Global seafood consumption footprint. Ambio. 48**,** 111-122.

Harvell, C. D., et al., 1999. Review: Marine ecology - Emerging marine diseases - Climate links and anthropogenic factors. Science. 285**,** 1505-1510.

Harvell, C. D., Lamb, B. J., Disease outbreaks can threaten marine biodiversity. In: R. B. Silliman, D. K. Lafferty, Eds., Marine Disease Ecology. Oxford University Press, Oxford, United Kingdom, 2020, pp. 18.

Harvell, C. D., et al., 2002. Climate Warming and Disease Risks for Terrestrial and Marine Biota. Science. 296**,** 2158-2162.

Harvie, W., Decades of fishing bans have not rescued seafood delicacy toheroa. 2020. Stuff NZ, 2017. Access date: Sept 2020. https://www.stuff.co.nz/environment/110671140/decades-of-fishing-bans-have-not-rescued-seafood-delicacy-toheroa.

Hayes, K. R., et al., 2019. The Assessment and Management of Marine Pest Risks Posed by Shipping: The Australian and New Zealand Experience. Frontiers in Marine Science. 6**,** 489.

Herald, New Zealand Herald: MPI tests link shellfish deaths to emerging RLO pathogens. 2018. Access date: June 2019. https://www.nzherald.co.nz/nz/news/article.cfm?c_id=1&objectid=11923877.

Hooper, P. M., et al., 2019. Shedding and survival of an intracellular pathogenic *Endozoicomonas*-like organism infecting king scallop *Pecten maximus*. Diseases of Aquatic Organisms. 134**,** 167-173.

Houwenhuyse, S., et al., 2018. Back to the future in a petri dish: Origin and impact of resurrected microbes in natural populations. Evolutionary Applications. 11**,** 29-41.

Howells, J., et al., 2021. Intracellular bacteria in New Zealand shellfish are identified as *Endozoicomonas* species. Diseases of Aquatic Organisms. 143**,** 27-37.

Jacquet, S., et al., 2010. Viruses in aquatic ecosystems: important advancements of the last 20 years and prospects for the future in the field of microbial oceanography and limnology. Advances in Oceanography and Limnology. 1**,** 97-141.

Jahn, N., europepmc: R Interface to the Europe PubMed Central RESTful Web Service. 2020.

Jepson, P. D., et al., 2003. Gas-bubble lesions in stranded cetaceans - Was sonar responsible for a spate of whale deaths after an Atlantic military exercise? Nature. 425**,** 575-576.

Jones, B. L., et al., 2018. Crowdsourcing conservation: The role of citizen science in securing a future for seagrass. Marine Pollution Bulletin. 134**,** 210-215.

Jones, M. R. L., Ross, P. M., 2018. Recovery of the New Zealand muricid dogwhelk *Haustrum scobina* from TBT-induced imposex. Marine Pollution Bulletin. 126**,** 396-401.

Katharios, P., et al., 2015. Environmental marine pathogen isolation using mesocosm culture of sharpsnout seabream: striking genomic and morphological features of novel *Endozoicomonas* sp. Scientific Reports. 5**,** 17609.

Kirstein, I. V., et al., 2016. Dangerous hitchhikers? Evidence for potentially pathogenic *Vibrio* spp. on microplastic particles. Marine Environmental Research. 120**,** 1-8.

Kummu, M., et al., 2016. Over the hills and further away from coast: global geospatial patterns of human and environment over the 20th–21st centuries. Environmental Research Letters. 11**,** 034010.

Lafferty, K. D., 2017. Marine infectious disease ecology. Annual Review of Ecology, Evolution, and Systematics. 48**,** 473-496.

Lafferty, K. D., Hofmann, E. E., 2016. Marine disease impacts, diagnosis, forecasting, management and policy. Philosophical Transactions of the Royal Society B: Biological Sciences. 371**,** 20150200.

Lafferty, K. D., et al., 2004. Are Diseases Increasing in the Ocean? Annual Review of Ecology, Evolution, and Systematics. 35**,** 31-54.

Lamb, J. B., et al., 2017. Seagrass ecosystems reduce exposure to bacterial pathogens of humans, fishes, and invertebrates. Science. 355**,** 731-733.

Lamb, J. B., et al., 2018. Plastic waste associated with disease on coral reefs. Science. 359**,** 460-462.

Lane, H. S., et al., 2020. Aquatic disease in New Zealand: synthesis and future directions. New Zealand Journal of Marine and Freshwater Research. 1-42.

Ma, X., et al., 2017. The biofilteration ability of oysters (*Crassostrea gigas*) to reduce *Aeromonas salmonicida* in salmon culture. Applied Microbiology and Biotechnology. 101**,** 5869-5880.

Mackenzie, C. L., et al., 2014. Future Oceanic Warming and Acidification Alter Immune Response and Disease Status in a Commercial Shellfish Species, *Mytilus edulis* L. PLOS ONE. 9**,** e99712.

Mahony, K. E., et al., 2020. Mobilisation of data to stakeholder communities. Bridging the research-practice gap using a commercial shellfish species model. PLOS ONE. 15**,** e0238446.

Maynard, J., et al., 2015. Projections of climate conditions that increase coral disease susceptibility and pathogen abundance and virulence. Nature Climate Change. 5**,** 688.

Mccarthy, A., et al., 2014. Local people see and care most? Severe depletion of inshore fisheries and its consequences for Māori communities in New Zealand. Aquatic Conservation: Marine and Freshwater Ecosystems. 24**,** 369-390.

McDowell, J. E., et al., 1999. The effects of lipophilic organic contaminants on reproductive physiology and disease processes in marine bivalve molluscs. Limnology and Oceanography. 44**,** 903-909.

Mendoza, M., et al., 2013. A novel agent (*Endozoicomonas elysicola*) responsible for epitheliocystis in cobia *Rachycentrum canadum* larvae. Diseases of Aquatic Organisms. 106**,** 31-37.

Miskelly, C. M., 2016. Legal protection of New Zealand's indigenous aquatic fauna – an historical review. Tuhinga. 27**,** 81-115.

Montecino-Latorre, D., et al., 2016. Devastating Transboundary Impacts of Sea Star Wasting Disease on Subtidal Asteroids. PLOS ONE. 11**,** e0163190.

Moore, J. D., et al., 2000. Withering syndrome in farmed red abalone *Haliotis rufescens*: Thermal induction and association with a gastrointestinal *Rickettsiales*-like prokaryote. Journal of Aquatic Animal Health. 12**,** 26-34.

Morley, N. J., 2010. Interactive effects of infectious diseases and pollution in aquatic molluscs. Aquatic Toxicology. 96**,** 27-36.

Morris, A. L., et al., 2016. Deforestation-driven food-web collapse linked to emerging tropical infectious disease, *Mycobacterium ulcerans*. Science Advances. 2**,** e1600387.

MPI, Biosecurity 2025 Direction Statement for New Zealand's Biosecurity System. Ministry for Primary Industries, Wellington, New Zealand, 2016, pp. 30.

Neave, M. J., et al., 2016. Diversity and function of prevalent symbiotic marine bacteria in the genus *Endozoicomonas*. Applied Microbiology and Biotechnology. 100**,** 8315-8324.

Neave, M. J., et al., 2014. Whole-genome sequences of three symbiotic *endozoicomonas* strains. Genome Announcements. 2**,** e00802-14.

Nguyen, T. V., et al., 2019. Omics approaches to investigate host–pathogen interactions in mass mortality outbreaks of *Crassostrea gigas*. Reviews in Aquaculture. 11**,** 1308-1324.

Oliver, E. C. J., et al., 2017. The unprecedented 2015/16 Tasman Sea marine heatwave. Nature Communications. 8**,** 16101.

Oliver, E. C. J., et al., 2018. Longer and more frequent marine heatwaves over the past century. Nature Communications. 9**,** 1324.

Olsen, Y. S., et al., 2015. Warming Reduces Pathogen Pressure on a Climate-Vulnerable Seagrass Species. Estuaries and Coasts. 38**,** 659-667.

Paul-Pont, I., et al., 2010. Interactive effects of metal contamination and pathogenic organisms on the marine bivalve *Cerastoderma edule*. Marine Pollution Bulletin. 60**,** 515-525.

Pipe, R. K., Coles, J. A., 1995. Environmental contaminants influencing immunefunction in marine bivalve molluscs. Fish & Shellfish Immunology. 5**,** 581-595.

Pollock, F. J., et al., 2014. Sediment and Turbidity Associated with Offshore Dredging Increase Coral Disease Prevalence on Nearby Reefs. PLOS ONE. 9**,** e102498.

Prado-Alvarez, M., et al., 2016. Occurrence of OsHV-1 in *Crassostrea gigas* Cultured in Ireland during an Exceptionally Warm Summer. Selection of Less Susceptible Oysters. Frontiers in Physiology. 7, 492.

Quiah, J., et al., The Impact of Excess Sediment on Bivalve Aquaculture. NC State Extension Publications, 2020. Access date: Novemeber 2021. https://content.ces.ncsu.edu/the-impact-of-excess-sediment-on-bivalve-aquaculture#section_heading_15196.

Roberts, J. O., et al., 2020. The effects of *Toxoplasma gondii* on New Zealand wildlife: implications for conservation and management. Pacific Conservation Biology. 27, 208-220.

Ross, P. M., et al., 2018a. The biology, ecology and history of toheroa (*Paphies ventricosa*): a review of scientific, local and customary knowledge. New Zealand Journal of Marine and Freshwater Research. 52**,** 196-231.

Ross, P. M., et al., 2018b. First detection of gas bubble disease and *Rickettsia*-like organisms in *Paphies ventricosa*, a New Zealand surf clam. Journal of Fish Diseases. 41**,** 187-190.

Rowley, A. F., et al., 2014. The potential impact of climate change on the infectious diseases of commercially important shellfish populations in the Irish Sea-a review. Ices Journal of Marine Science. 71**,** 741-759.

Rullens, V., et al., 2019. Ecological Mechanisms Underpinning Ecosystem Service Bundles in Marine Environments – A Case Study for Shellfish. Frontiers in Marine Science. 6**,** 409.

Sanford, E., et al., 2019. Widespread shifts in the coastal biota of northern California during the 2014–2016 marine heatwaves. Scientific Reports. 9**,** 4216.

Sardain, A., et al., 2019. Global forecasts of shipping traffic and biological invasions to 2050. Nature Sustainability. 2**,** 274-282.

Schill, W. B., et al., 2017. *Endozoicomonas* Dominates the Gill and Intestinal Content Microbiomes of *Mytilus edulis* from Barnegat Bay, New Jersey. Journal of Shellfish Research. 36**,** 391-401.

Schulte, D. M., 2017. History of the Virginia Oyster Fishery, Chesapeake Bay, USA. Frontiers in Marine Science. 4**,** 127.

Sformo, T. L., et al., 2017. Observations and first reports of saprolegniosis in Aanaakłiq, broad whitefish (*Coregonus nasus*), from the Colville River near Nuiqsut, Alaska. Polar Science. 14**,** 78-82.

Shiu, J.-H., Tang, S.-L., The Bacteria *Endozoicomonas*: Community Dynamics, Diversity, Genomes, and Potential Impacts on Corals. In: Z. Li, Ed., Symbiotic Microbiomes of Coral Reefs Sponges and Corals. Springer Netherlands, Dordrecht, 2019, pp. 55-67.

Smale, D. A., et al., 2019. Marine heatwaves threaten global biodiversity and the provision of ecosystem services. Nature Climate Change. 9**,** 306-312.

Smith, I., 2013. Pre-European Maori exploitation of marine resources in two New Zealand case study areas: species range and temporal change. Journal of the Royal Society of New Zealand. 43**,** 1-37.

Stentiford, G. D., et al., 2012. Disease will limit future food supply from the global crustacean fishery and aquaculture sectors. Journal of Invertebrate Pathology. 110**,** 141-157.

Sures, B., 2008. Environmental Parasitology. Interactions between parasites and pollutants in the aquatic environment. Parasite. 15**,** 434-438.

Sutherland, K. P., et al., 2016. Shifting white pox aetiologies affecting *Acropora palmata* in the Florida Keys, 1994– 2014. Philosophical Transactions of the Royal Society B: Biological Sciences. 371**,** 20150205.

Szabó, K., Amesbury, J. R., 2011. Molluscs in a world of islands: The use of shellfish as a food resource in the tropical island Asia-Pacific region. Quaternary International. 239**,** 8-18.

Szekeres, P., et al., 2016. On the neglected cold side of climate change and what it means to fish. Climate Research. 69**,** 239-245.

Team, R. C., R: A language and environment for statistical computing. R Foundation for Statistical Computing, Vienna, Austria, 2013.

van der Schatte Olivier, A., et al., 2018. A global review of the ecosystem services provided by bivalve aquaculture. Reviews in Aquaculture. 12**,** 3-25.

Venugopal, V., Gopakumar, K., 2017. Shellfish: Nutritive Value, Health Benefits, and Consumer Safety. Comprehensive Reviews in Food Science and Food Safety. 16**,** 1219-1242.

Walker, P. J., Winton, J. R., 2010. Emerging viral diseases of fish and shrimp. Veterinary research. 41**,** 51.

Ward, J. R., Lafferty, K. D., 2004. The elusive baseline of marine disease: Are diseases in ocean ecosystems increasing? PLOS Biology. 2**,** 542-547.

Wehi, P., et al., 2013. Marine resources in Māori oral tradition: He kai moana, he kai mā te hinengaro. Journal of Marine and Island Cultures. 2**,** 59-68.

Wernberg, T., et al., 2016. Climate-driven regime shift of a temperate marine ecosystem. Science. 353**,** 169.

Wetchateng, T., et al., 2010. Withering syndrome in the abalone *Haliotis diversicolor supertexta*. Diseases of Aquatic Organisms. 90**,** 69-76.

Whaanga, H., et al., 2018. Māori oral traditions record and convey indigenous knowledge of marine and freshwater resources. New Zealand Journal of Marine and Freshwater Research. 52**,** 487-496.

Wickham, H., 2009. ggplot2: Elegant Graphics for Data Analysis. Springer, New York.

Williams, J. R., et al., Review of factors affecting the abundance of toheroa (*Paphies ventricosa*). New Zealand Aquatic Environment and Biodiversity Report No. 114, 2013, pp. 76.

Wommack, K. E., Colwell, R. R., 2000. Virioplankton: viruses in aquatic ecosystems. Microbiology and molecular biology reviews : MMBR. 64**,** 69-114.

Zha, S., et al., 2017. Laboratory simulation reveals significant impacts of ocean acidification on microbial community composition and host-pathogen interactions between the blood clam and *Vibrio harveyi*. Fish & Shellfish Immunology. 71**,** 393-398.

Chapter 3
Histopathology of a Threatened Surf Clam, Toheroa (*Paphies ventricosa*) from Aotearoa (New Zealand)

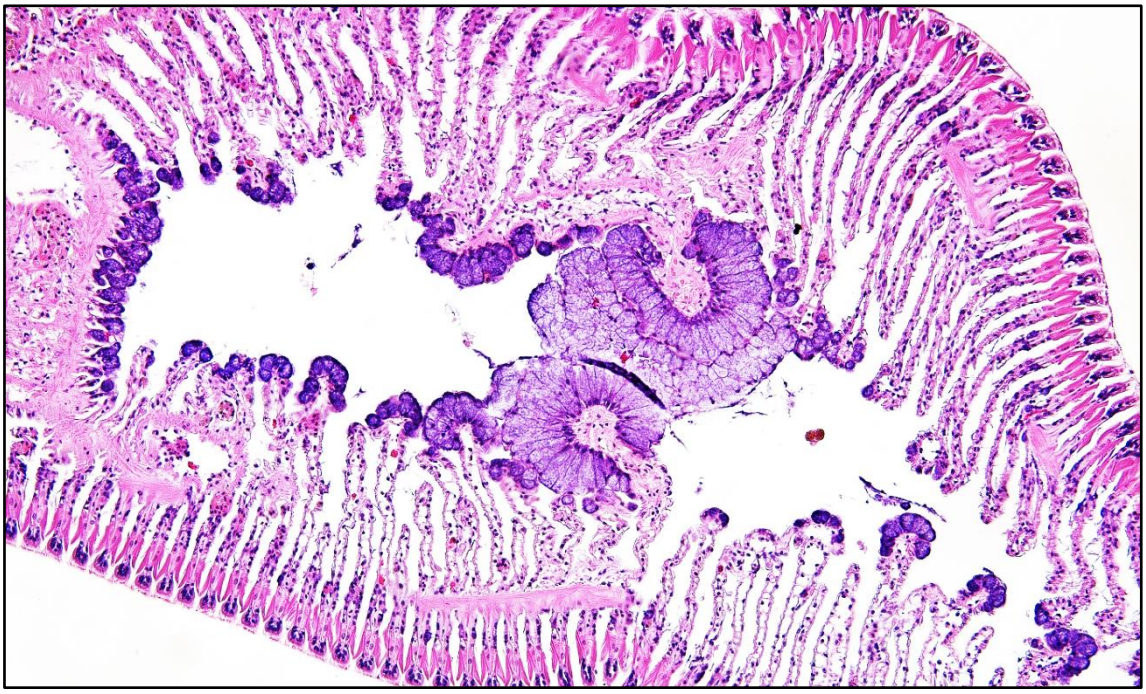

Toheroa gill tissue section

3.1 Abstract

The toheroa (*Paphies ventricosa*) is endemic to Aotearoa (New Zealand). Following decades of overfishing in the 1900s, commercial and recreational fishing of toheroa is now prohibited. For unknown reasons, protective measures in place for over 40 years have not ensured the recovery of toheroa populations. For the first time, a systematic pathology survey was undertaken to provide a baseline of toheroa health in remaining major populations (four beaches, *n* = 238 toheroa). Using histopathology, parasites and pathologies (including sex, gonad development and other pathomorphological features) in a range of tissues are assessed and quantified spatio-temporally. Particular focus is placed on intracellular microcolonies of bacteria (IMCs), where 89/238 toheroa were positive for inclusions. The lowest IMC prevalence was recorded from toheroa gathered from Oreti Beach, South Island (1/40). Bayesian ordinal logistic regression is used to model IMC infection and several facets of toheroa health. Model outputs show poor condition to be the most important predictor of high IMC intensity in toheroa tissues. The precarious state of many toheroa populations around Aotearoa should warrant greater attention from scientists, conservationists, and regulators. It is hoped that this study will provide some insight into the current health status of a treasured and iconic constituent of several expansive (>60 km long) surf beaches in Aotearoa.

3.2 Introduction

Disease in the ocean is increasingly a focus of researchers, stakeholders, and government bodies (Behringer et al., 2020; Lafferty, 2017), with most attention given to commercially fished or farmed species (Behringer et al., 2020; Stentiford et al., 2017), given their commercial value. Exceptions exist, namely corals (Lamb et al., 2018; Pollock et al., 2014), sea stars (Harvell et al., 2019; Lloyd and Pespeni, 2018), and megafauna (VanWormer et al., 2019) where disease has been studied from a conservation perspective. Unsurprisingly, focus tends to be placed on wild species when there is considerable commercial benefit, either direct (fisheries) or indirect (e.g., ecotourism), or when species are the targets for monitoring programmes (e.g., biomonitoring and toxicological pathology). In comparison, wild species with little commercial value are understudied. This is especially true for shellfish and likely even more so for protected species, where recreational harvesting is prohibited or restricted, thus limiting sample collection for study. In the wild, marine diseases are challenging to detect and manage (Lafferty, 2017) and even more difficult to eradicate (Culver and Kuris, 2000). Only regular and robust surveillance of populations can ensure detection of pathogens with enough time to implement tailored mitigation measures (Groner et al., 2016).

Routine surveys offer an opportunity to identify and respond to new and emerging pathogens before the manifestation of disease and (or) gross signs of illness take place (Cremonte et al., 2005; Lohrmann et al., 2019). Although this is the ideal scenario, it is not always realistic for wild shellfish populations as the scale of these investigations are generally too large to be conducted on a meaningfully regular basis. Exceptions do exist for example, various bivalve spp. in Ireland (Mahoney et al., 2021; Lynch et al., 2021). Instead, current management strategies for many wild shellfish populations globally, are centred on response to abnormal levels of mortality or tip-offs from members of the public following an observation of sick or moribund animals (Lane et al., 2020). This approach limits the scope of many response measures (Groner et al., 2016).

Typically, disease prevention at a national or regional scale is the goal of nations or states. Biosecurity mitigation and management protocols, both pre- and post- borders, are employed by many nations to reduce the spread of invasive species and potentially emerging pathogens (Carnegie et al., 2016; Lafferty and Hofmann, 2016). Although the importance of these strategies cannot be overstated, particularly in the South Pacific (Hayes et al., 2019; Hewitt et al., 2004), invasive species and new pathogens remain a threat, and do occasionally disperse and establish in new regions and hosts (e.g., Bingham et al., 2013; Lane et al., 2016; Mabey et al., 2021). The emergence of disease continues to plague the aquaculture industry and wild fisheries, with periodic detection of pathogens in new hosts around the world. For example, the recent discovery of *Bonamia ostreae* in the New Zealand flat oyster, *Ostrea chilensis* (Lane et al., 2016) and the on-going incidence of Quahog Parasite Unknown (QPX) on east coast of North America (Smolowitz, 2018). Additionally, following extensive oyster mortalities in 2008 (Segarra et al., 2010) ostreid herpesvirus type 1 microvariant (OsHV-1 µVar) was infamously detected in France, and later detected in Aotearoa (Bingham et al., 2013). These cases emphasize the persistent need to monitor wild fisheries and aquaculture sites for emerging pathogens. Aquaculture-associated practices (i.e., translocating and outplanting) have been associated with the spread of novel pathogens to previously unaffected areas and wild populations for instance, the viral pathogen *Piscine orthoreovirus*-1 in salmon (Mordecai et al., 2021). Examples exist for shellfish too, like the case of *Xenohaliotis californiensis* in abalone spp. from the United States (Friedman and Finley, 2003) and OsHV-1 in *Crassostrea gigas* from Aotearoa (Bingham et al., 2013).

Histopathology surveys of commercially exploited and threatened shellfish are periodically published in international peer-reviewed journals e.g., for the wedge clam, *Donax trunculus* in Italy (Carella et al., 2019), razor clams, *Ensis* spp. in Spain (Darriba et al., 2010; Ruiz et al., 2013), Chilean mussel, *Mytilus chilensis* in Chile (Lohrmann et al., 2019), tiger prawn, *Penaeus semisulcatus* and Jinga shrimp, *Metapenaeus affinis* in

Kuwait (Stentiford et al., 2014), and common cockle, *Cerastoderma edule* in Ireland (Mahony et al., 2021). Routine haematoxylin and eosin staining allows for an explorative examination of shellfish health, where pathogens and non-infectious pathology can be detected. Furthermore, open-source packages produced for R and Python make the use of complex models more accessible to investigative pathologists. For instance, several studies within the field of aquatic pathology have shown how investigators can apply histological observations and computational modelling to examine co-infection, immune response, reproductive development, and sex determination, extending the utility of histological observations (Bignell et al., 2011; Downes et al., 2018; Farley et al., 2013; Parker et al., 2018).

Regular histopathological surveys are beneficial to understanding the composition of pathogens and parasites present in commercially fished and protected wild populations (Cremonte et al., 2005; Darriba et al., 2010; Lohrmann et al., 2019). At no time is this need more evident, than when disease outbreaks strike or when mass mortality events (MMEs) occur in the absence of apparent extrinsic/environmental risk factors (Soon and Ransangan, 2019) - the lack of baseline disease data has the potential to make subsequent disease investigations more challenging.

In Aotearoa, wild kai moana (seafood) is a staple component of the diets of Māori (Indigenous people of Aotearoa) and Pākehā (New Zealanders of European decent). Māori hold many kai moana species in high regard, with a large surf clam, the toheroa (*Paphies ventricosa*) being one of the most revered in certain regions (Tai Tokerau, Kāpiti-Horowhenua, and Murihiku). Toheroa populations have been protected since the 1970s (Miskelly, 2016) but for unknown reasons have failed to recover to their pre-exploitation abundances (Ross et al., 2018a; Williams et al., 2013). Illegal harvesting, land use change, and vehicles on beaches, have been discussed as possible explanations. Disease has also been suggested as possibly playing a part in the continued decline of the toheroa, although this is yet to be determined (Ross et al., 2018a; Ross et al., 2018b).

Intracellular microcolonies (IMCs) of bacteria have been detected worldwide in a large number of hosts (Cano et al., 2020), including fish e.g., Chinook salmon, *Oncorhynchus tshawytscha* in New Zealand (Brosnahan et al., 2017) and lump fish, *Cyclopterus lumpus* L. in Ireland (Marcos-Lopez et al., 2017), molluscs e.g., king scallops, *Pecten maximus* in the UK (Cano et al., 2018), geoducks, *Panopea generosa* in the United States (Dorfmeier et al., 2015), flat oysters, *Ostrea edulis* in Italy (Tinelli et al., 2020) and Jinjiang oysters, *Crassostrea rivularis* in China (Zhang et al., 2017), and numerous crustacean hosts (Gollas-Galvan et al., 2014). In 2017, Ross et al. (2018b) detected IMCs in toheroa populations for the first time (labelled at the time as ‘RLOs’ or *Rickettsia*-like organisms). Since then, studies in Aotearoa have linked mortality events

to the presence of IMCs (Howells et al., 2021). Elsewhere, IMCs have also been associated with host mortality (Cano et al., 2020; Carvalho et al., 2013; Zhu et al., 2012), though most famously in the case of *X. californiensis* causing abalone mass mortalities (Crosson and Friedman, 2018; Moore et al., 2000).

Considering the absence of baseline data concerning the health status toheroa in Aotearoa, a histopathology survey of major remaining populations was conducted with a focus on IMCs. Additionally, IMC infection models were constructed to assess the potential impact of IMCs on host populations, and to investigate the potential role of IMCs in shellfish MMEs in Aotearoa New Zealand.

3.3 Methods

3.3.1 Site Description and Specimen Collection

Specimens for histological assessment were collected from four locations around Aotearoa New Zealand (Fig. 3.1 & Table 3.1), Te-Oneroa-a-Tōhē/Ninety Mile Beach (*n* = 15) in November 2019, Ripiro Beach (*n* = 180) March 2019 to January 2020 (every second month), Foxton (*n* = 3) in March 2019, and Oreti Beach (*n* = 40) in February 2019. Three sites were sampled at Ripiro Beach (Ripiro Waka te Haua), Island, Mahuta Gap, and Kopawai. Toheroa tend to aggregate in dense beds in the intertidal near freshwater outflows (Redfearn, 1974). The three sites sampled on Ripiro Beach were selected based on the presence of freshwater streams and dense beds of adult toheroa. Extensive pine forestry (*Pinus radiata*) is the dominant land use adjacent to Te-Oneroa-a-Tōhē, whereas the land adjacent to Ripiro and Foxton Beaches is primarily used for cattle pasture. The backdrop to Oreti Beach is a mixture of pasture farmland and forest (native and plantation).

Typically, specimens of adult size (>45 mm) were sampled for histology (Table 3.1 & Appendix C, Fig. C.1). Specimens were hand-dug transported to the laboratory on ice, and held in chilled, UV treated seawater (maximum 12 hours) prior to processing to encourage the flushing of sand and improve quality of sections for histology. Specimens were dissected 24 hours (maximum) after sampling. Toheroa were gathered under Special Permit No. 706 and 706-2 issued by Fisheries New Zealand.

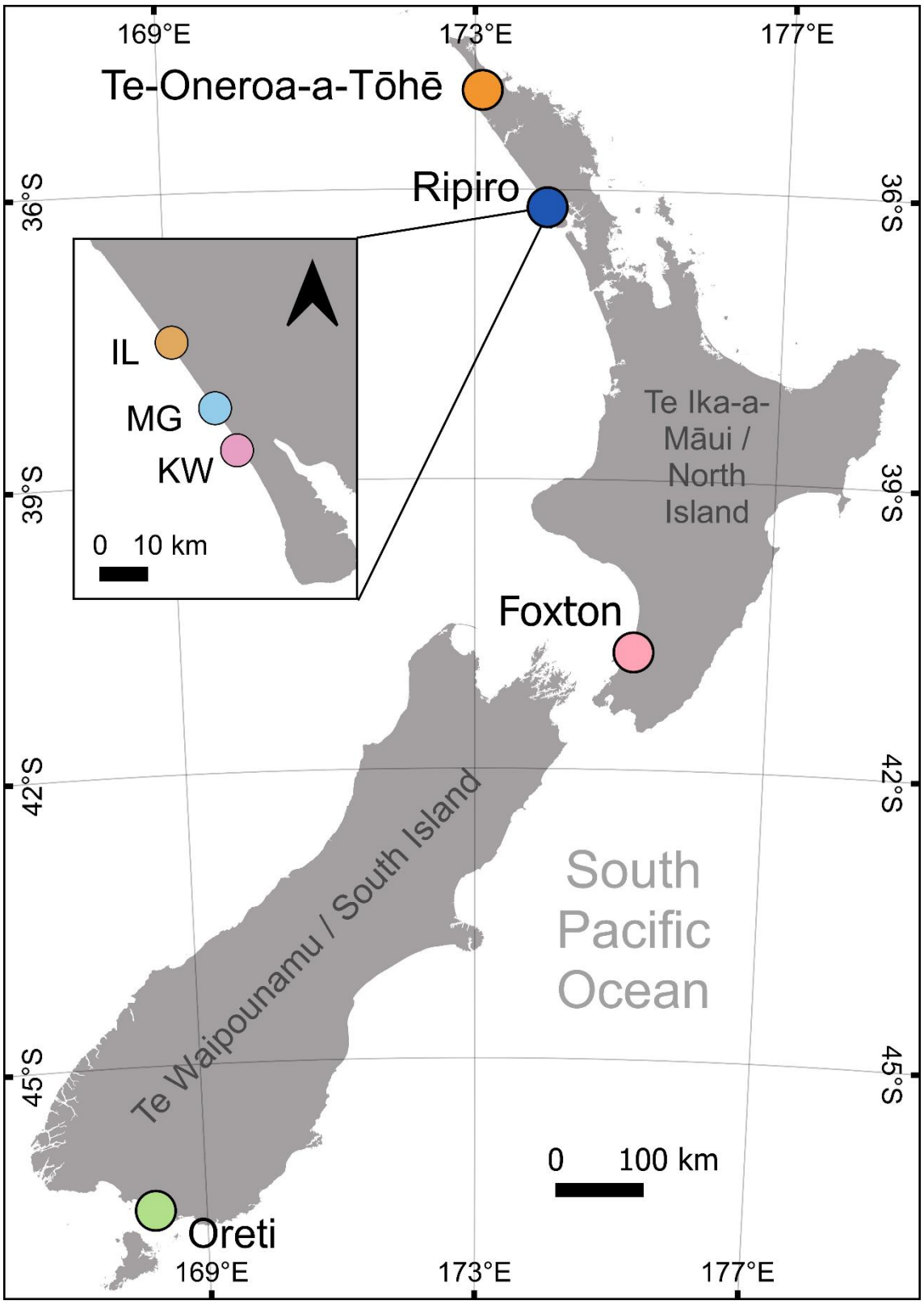

Fig. 3.1. Map of Aotearoa (New Zealand) showing the four beaches sampled in this study, Te-Oneroa-a-Tōhē/Ninety Mile Beach, Ripiro Beach, Foxton, and Oreti Beach. Three sites on Ripiro Beach were sampled every second month from March 2019 to January 2020, pictured in inset (IL: Island, MG: Mahuta Gap, and KW: Kopawai). Spatial data obtained from Diva-GIS. CRS: WGS 84 (EPSG: 4326).

3.3.2 Condition and Gross Pathology

Using the condition index described by Herrmann et al. (2009) and Gadomski and Lamare (2015), condition was estimated using total mass (including shells) and soft tissue mass (blotted dry) using the following formula,

$$\text{Condition index (\%)} = \left(\frac{M_s}{M_s - M_t}\right) \times 100$$

where M_s is the soft tissue mass (g) and M_t is the total mass (g, shell included). The condition index was applied to all specimens from all sampled locations.

Gross pathology was assessed at three stages. In the field, initial gross signs of illness were recorded (gas bubbles), foremost the presence of shell abnormalities (damage, discoloration, and malformation) were recorded at this time. Immediately prior to dissecting specimens, gross pathology (coloration & tissue damage) was assessed again and once more when valves had been opened. Key attributes that were assessed were coloration, responsiveness, and soft tissue damage and/or malformation.

3.3.3 Histopathology

Toheroa were measured (posterior to anterior shell length, mm) and weighed (total mass and soft tissue mass, g). Using a razor blade, a cross section was obtained and placed into 10% Formalin (4% formaldehyde/seawater solution for a maximum of 48 hours) for histology. Following fixing, cut sections were trimmed and placed into tissue cassettes in 70% ethanol (EtOH) until further processing. Samples were transported to SVS Laboratories Ltd. Hamilton, NZ for embedding, sectioning, and staining with haematoxylin and eosin.

Histology slides were examined using an Olympus BX53 compound light microscope and photographed using an Olympus DP27 at x20, x40, and x100 magnification (under oil). All tissues were examined for abnormalities and the presence of any parasites and pathology. Sex and gametogenic stage were recorded using slides produced by Gadomski and Lamare (2015) for reference. Female oocytes were measured (n = 10 for each specimen, averaged over the longest two-axes, d_1 and d_2) and oocyte density per mm^2 was estimated (Gadomski, 2017) using ImageJ v1.44. The IMCs, lipofuscin, mucous cell hyperplasia, thinning of digestive tubules, and gill ciliates were all graded on a five-step scale. The abundance of IMCs and gill ciliates was graded as follows, None = 0, Low = 1-10, Medium = 11-20, High = 21-30, Severe = >31. Mucous cell hyperplasia and lipofuscin (i.e., spent haemocyte accumulations containing lipofuscin-like pigment) were visually graded as follows, None [0] = tissue not visibly

affected, Low [1] = <10% tissue affected, Medium [2] = 10-30% tissue affected, High [3] = 30-70% tissue affected, and Severe [4] = >70% tissue affected. Thinning off digestive tubule walls was assessed using the following semi-quantitative scale: None [0] = normal wall thickness in most tubules, Low [1] = average thickness less than usual, Medium [2] = wall thickness one-half as thick as usual, High [3] = most walls atrophied/extremely thin, Severe [4] = walls extremely thin, all or nearly all affected (Kim et al., 2006).

The number of diatoms present in each specimen was not quantified, but specimens that presented with extremely high numbers of diatoms in excreta, or within digestive tubules, were noted with a comment. This was then recorded as 'prevalence', though this does not suggest other specimens did not contain diatoms, instead this is to represent specimens featuring extremely high numbers of diatoms.

3.3.4 Environmental Variables

The intensity of IMCs was modelled using several health observations including, reproductive development, lipofuscin, mucous cell hyperplasia, gill ciliates, and condition. The aim was to investigate possible interactive effects and establish whether aforementioned characteristics can predict IMC infection intensity outcome in toheroa tissues. Bayesian ordinal logistic regression models were constructed using the 'brms' package in R (Bürkner, 2017; Bürkner and Vuorre, 2019). Only data obtained for Ripiro Beach specimens (n = 180) was included in models. In total, nine models were created using a combination of factors to determine the best fitting model. The ninth, a null model, was created using the intercept only. Month was included in all models (except the null) as a group-level effect to account for between month random effects. Weakly informative priors were used, Normal(0, 2) on the intercept, Normal(0, 0.1) on the fixed factor 'condition', Normal(0, 0.5) for all other fixed-level effects, and Cauchy(0, 5) for group-level effects (sd). Model performance was assessed using several diagnostic tools including trace and density plots (Bürkner, 2017). Model fit was assessed via posterior predictive checks. Models were compared using the 'loo' package (Vehtari et al., 2018) and based on performance (epld and looic), the best-fitting model was selected.

To compare oocyte density over time at Ripiro Beach, a one-way ANOVA test was used followed by Tukey's test (p-adj for multiple comparisons). A map of specimen sampling locations and sites was produced using Quantum GIS (v.3.8.1). Boxplots, stacked bars, and ridgeline plots were produced in R using the packages 'ggplot2' (Wickham, 2009) and 'ggridges' (Wilke, 2020).

3.3.5 Model Construction and Data Analysis

IMC intensity was modelled using several intrinsic health observations including, reproductive development, lipofuscin pigmentation, mucous cell hyperplasia, gill ciliates, and condition. The aim was to investigate possible co-infection effects and establish whether aforementioned intrinsic characteristics can predict IMC infection intensity outcome in toheroa tissues. Bayesian ordinal logistic regression models were constructed using the 'brms' package in RStudio (Bürkner, 2017; Bürkner and Vuorre, 2019). Only data obtained for Ripiro Beach specimens (n = 180) was included in models. In total, nine models were created using a combination of aforementioned factors, to determine the best fitting model. The ninth, a null model, was created using the intercept only. Month was included in all models (except the null) as a group-level effect to account for between month random effects. Weakly informative priors were used, Normal(0, 2) on the intercept, Normal(0, 0.1) on the fixed factor 'condition', Normal(0, 0.5) for all other fixed-level effects, and Cauchy(0, 5) for group-level effects (sd). Model performance was assessed using several diagnostic tools including trace and density plots (Bürkner, 2017). Model fit was assessed via posterior predictive checks. Models were compared using the 'loo' package (Vehtari et al., 2018) and based on performance (epld and looic), the best-fitting model was selected.

To compare oocyte density over time at Ripiro Beach, a one-way ANOVA test was used followed by Tukey's test (p-adj for multiple comparisons). A map of specimen sampling locations and sites was produced using Quantum GIS (v.3.8.1). Boxplots, stacked bars, and ridgeline plots were produced in RStudio using ggplot2 (Wickham, 2009) and ggridges (Wilke, 2020).

3.4 Results

3.4.1 Macroscopic Observations & Gross Pathology

3.4.1.1 Shell Abnormalities

Gas bubbles were detected on the shells of toheroa during every sampling expedition to Ripiro Beach (Table 3.2 & Fig. 3.2, A). Specimens gathered at Mahuta Gap (Fig. 3.1) consistently had the highest prevalence of gas bubbles under the periostracum on the shells (Fig. C.2). Gas bubbles were only present for a short time after sampling. Ripiro Beach specimens were the only cohort examined for gross pathology *in situ*. Several specimens showed signs of shell abnormality (Table 3.2), ruled to be attributed to damage incurred over animal's life history.

3.4.1.2 Tissues

No significant gross pathology of the soft tissues was observed. A small number of individuals from Oreti Beach (15%, *n* = 40) and Foxton (33%, *n* = 3) presented a pale/yellow colour (likely attributed to haemolymph expulsion). Some toheroa presented a vibrant pink coloration in several tissues (Table 3.2 & Fig. 3.2, B), primarily in the posterior and anterior adductor muscles and the mantle. One of the three specimens sampled from Foxton and 13% (*n* = 15) of specimens collected from Te-Oneroa-a-Tōhē, were found to have considerable damage to the foot that could be attributed to predation activity (either avian or crustacean) (Table 3.2).

Table 3.1. Location and specimen collection related information. Air temperature was gathered on-site for each Ripiro Beach sampling session. Sea surface temperature (SST) and chlorophyll-*a* were obtained via MODIS-aqua satellite data (see methods). Mean mass and length ± standard error. CI: condition index, mean (%) ± 95% confidence interval.

Location	**Date**	***n***	**Air Temp °C**	**SST °C**	**Chl-*a* (mg m^{-3})**	**Mean length (mm) (±SE)**	**Mean mass (g) (±SE)**	**Condition index (%) (±CI)**
Oreti Beach	Feb-19	40	-	16.0	1.47	113.42 (1.4)	251.05 (12.4)	36.96 (2.7)
Foxton Beach	Mar-19	3	-	18.8	0.47	93.00 (13.0)	122.00 (43.2)	35.34 (18.8)
Te-Oneroa-a-Tōhē	Nov-19	15	-	16.9	0.96	69.93 (2.6)	49.27 (4.3)	51.31 (6.5)
Ripiro Beach	Mar-19	30	25	21.0	0.40	80.93 (1.7)	78.53 (5.1)	39.52 (2.5)
	May-19	30	18	18.2	0.70	80.80 (1.8)	88.23 (5.5)	38.69 (2.6)
	Jul-19	30	9	15.3	0.79	77.73 (1.6)	69.17 (4.6)	55.93 (4.9)
	Sep-19	30	13	14.9	0.89	80.90 (1.9)	78.87 (5.5)	59.35 (3.3)
	Nov-19	30	17	17.7	1.10	74.23 (2.6)	64.67 (5.8)	53.12 (5.1)
	Jan-20	30	20	20.0	0.25	58.67 (1.9)	31.2 (3.5)	51.41 (3.1)

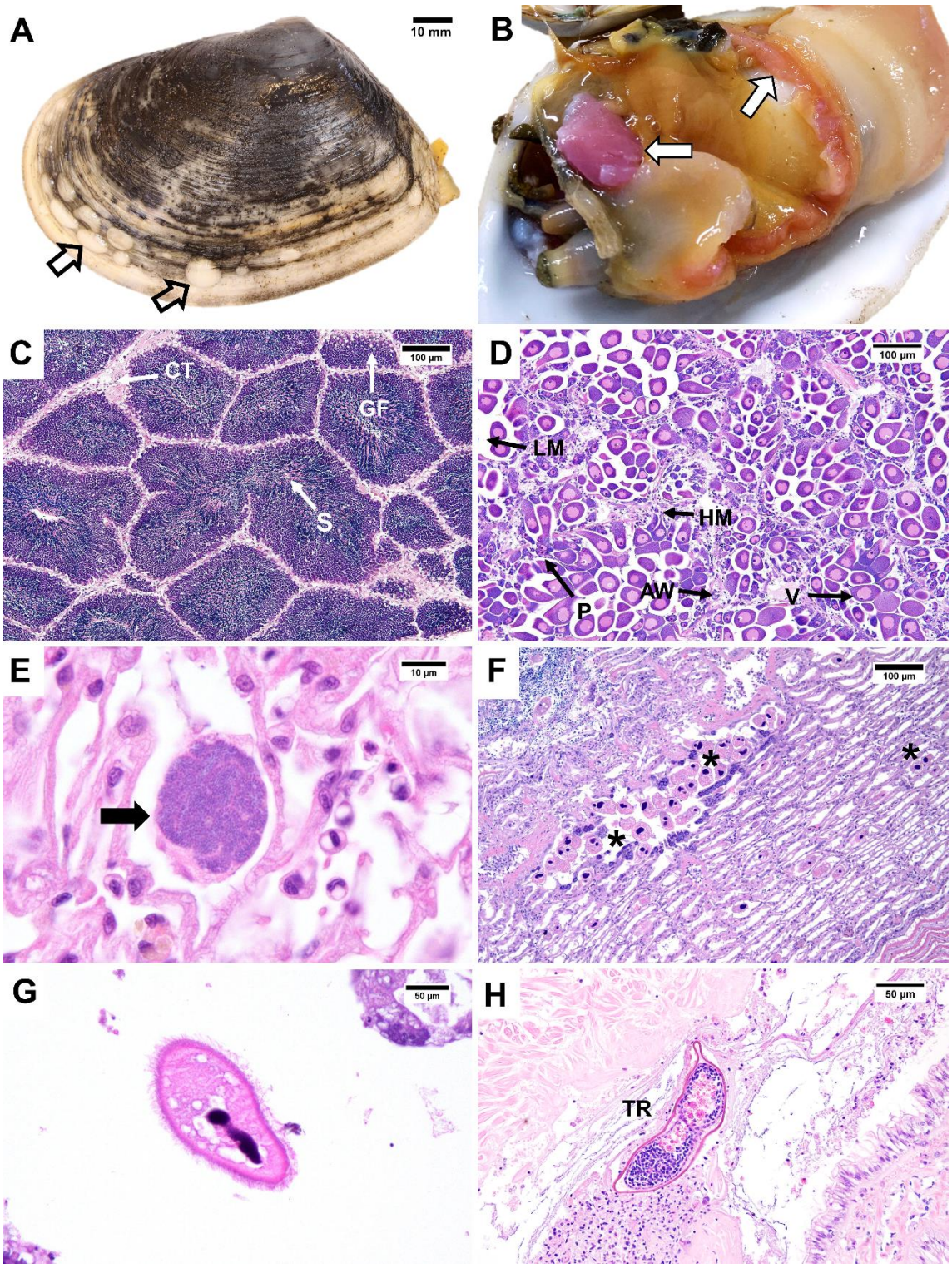

Fig. 3.2. A: Toheroa with large gas bubbles present under the periostracum (hollow arrows). B: Toheroa presenting pink flesh (arrows) in the mantle and posterior adductor muscle. C: Male gonads, CT = connective tissue, S = spermatozoa, GF = gonad follicle. D: Female gonads, AW = alveoli wall, HM = haemocytes, LM = lumen, P = pre-vitellogenic oocyte, V = vitellogenic oocyte. E: Intracellular microcolonies or IMCs in the gill (filled arrow). F: Gill lattice with high intensity gill ciliate infiltration (asterisk). G: *Frontonia*-like ciliate. H: Putative digenean trematode (TR) in the infrabranchial chamber.

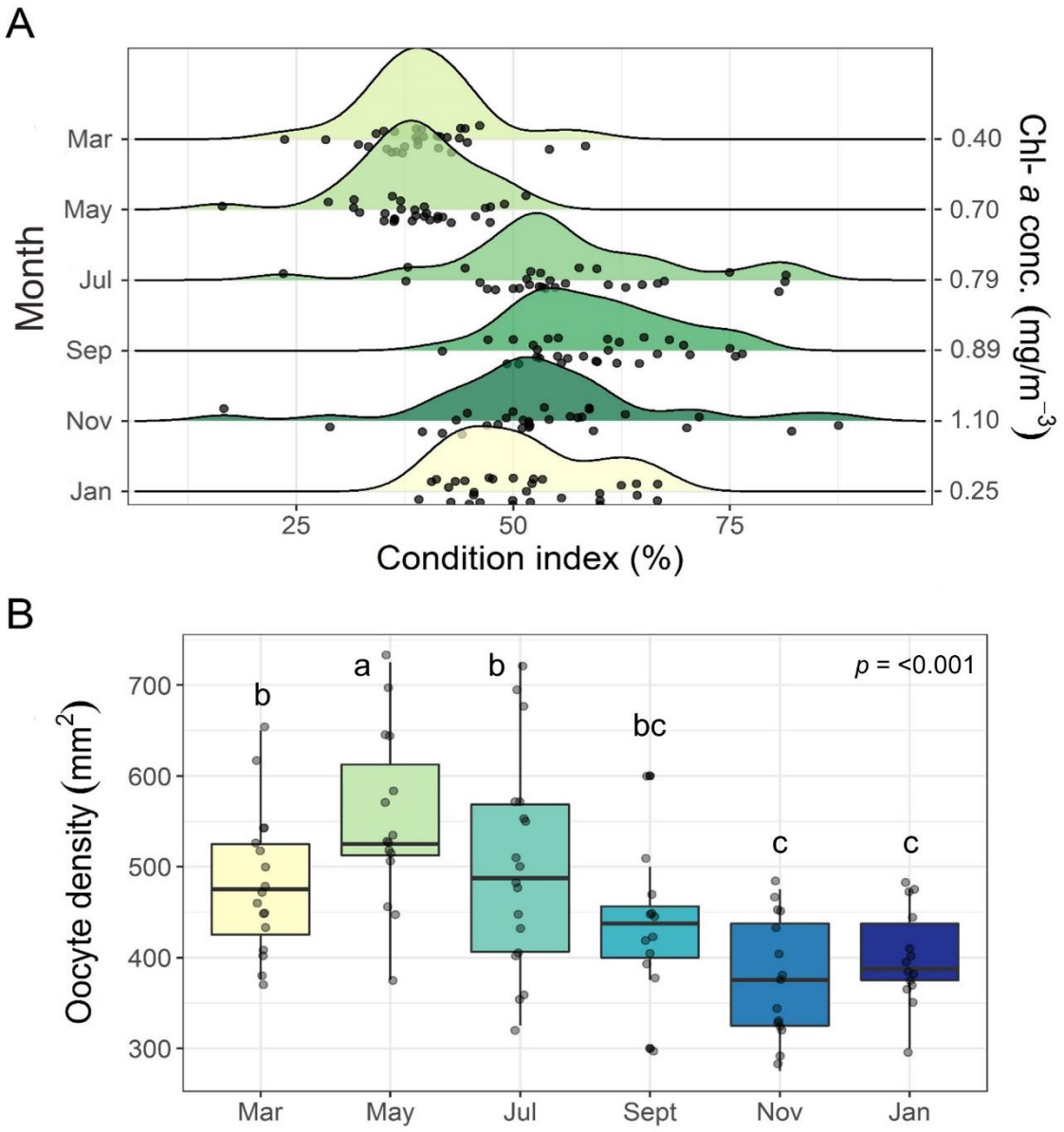

Fig. 3.3. A: Ridgeline plot showing the condition index score calculated for individual toheroa specimens gathered during each sampling occasion at Ripiro Beach (n = 30, for each month). Average monthly chlorophyll-*a* concentrations estimated from a composite of daily images (obtained by the MODIS-aqua programme) are shown for each sampled month (secondary y-axis). B: Boxplot showing the average oocyte density (per mm^2) in female toheroa (sites pooled) from Ripiro Beach sampled between March 2019 and January 2020. For boxes that do not share the same letter, corresponding means are significantly different (Tukey's test, cut-off p = <0.05). Lateral line: median, box: interquartile range, line: min/max.

3.4.1.3 Condition

Although specimens were not strictly graded during collection, there are clear differences in the length and mass of specimens from different geographic regions (Table 3.1 and Fig C.1). The toheroa from Oreti Beach were substantially larger (length and mass) than those gathered from northern beaches. For example, the mean mass (g) of Oreti specimens was 251.05 (±SE 12.4) compared to 68.44 (±SE 2.5) for all Ripiro Beach specimens. Condition scores for Ripiro Beach varied seasonally (Fig. 3, A). Condition was lowest in May-19 (mean = 38.69, 95% CI = 2.6), and highest in Sept-19 (mean = 59.35, 95% CI = 3.3).

3.4.2 Reproductive Health

Photomicrographs of male and female gonads are presented in Fig. 3.2 (C and D). Proportionally, similar numbers of male and female toheroa (and no hermaphroditic individuals) were recorded at Ripiro Beach throughout this study (Fig 3.4, B). The proportion of toheroa in each gametogenic stage differed between sexes and over time (Fig. 3.4, A & C). The number of males presenting in the 'ripe' stage of gametogenesis peaked in March and declined to a minimum in January when over 30% (*n* = 16) of specimens were either in the early active or partially spawned/spent gametogenic stage. There was little change in gametogenic phases of female toheroa between Mar-19 and Jul-19 (Fig. 3.4, C). In September, many more specimens were found to be ripe (58%, *n* = 12), with 33% (*n* = 12) in the late active phase. Similarly, in November 47% (*n* = 15) of females were in the ripe phase and (40% *n* = 15) were classed as late active. In January, 64% were found to be in the late active phase, with 14% (*n* = 14) of individuals classed as ripe (Fig. 3.4, C).

Average oocyte diameter for specimens from Ripiro Beach gathered seasonally are displayed using a ridgeline plot (Fig. 3.4, D). Oocyte diameter was largest in March (mean = 40.84 µm, ±SE = 0.4), and smallest in July (mean = 33.74 µm, ±SE = 0.5). Following the July sampled specimens, average oocyte diameter begins to steadily increase again, finally rising to 39.71 µm (±SE = 0.4) in January. Oocyte density also varied over sampling dates (F = 8.72, df = 5, p = <0.001) (Fig. 3.3, B). Density was highest in May (mean = 547.92, ±SE = 21.2) and lowest in November (mean = 376.67, ±SE = 17.0) (p = <0.001), though slightly higher again in January the following year (mean = 400, ±SE = 13.4).

3.4.3 Pathogens, Parasites, and Symbionts

3.4.3.1 Bacteria

Intracellular microcolonies were only detected in one specimen from Oreti (3%, *n* = 40), and Foxton (33%, *n* = 3) beaches. Whereas 13% (*n* = 15) of specimens gathered at Te-Oneroa-a-Tōhē were positive for IMCs. Prevalence was considerably higher at Ripiro Beach (*n* = 30 for each sampling occasion), with a range of 23% to 77% in Jan-20 and Mar-19, respectively (Table 3.2). Intensity of IMCs in toheroa from Ripiro Beach is shown in Fig. 3.5, A. For most of the sampled dates, intensity of IMCs is between [0-3] or 'None' to 'Medium'. Several High intensity infections occurred in March (7%), May (7%), July (10%), September (7%), and January (3%). Only two Severe cases were ever detected, one in May (3%) and another in September (3%). Regardless of sampling period or site, IMCs were only observed in the gills of toheroa specimens (Fig. 3.2, E). The IMCs generally measured ~20-25 µm along the longest-axis. No association between any inflammatory response and IMC presence was made.

3.4.3.2 Protozoa

Protozoan gill ciliates were detected in many specimens, but mainly those gathered from Ripiro Beach (Fig. 3.2, F). In Te-Oneroa-a-Tōhē specimens, 33% (*n* = 15) presented gill ciliates. No gill ciliates were detected in any specimens from Foxton and Oreti beach (Table 3.2). Gill ciliates were consistently detected in Ripiro Beach specimens, and most of this prevalence is owed to the Mahuta Gap site, where gill ciliates were present in 88% of specimens sampled (*n* = 60) between Mar-19 and Jan-20. Intensity of gill ciliate infiltration varied over sampling dates (Fig. 3.5, B). Considering the High and Severe scores [3 & 4], there appears to be some slight seasonal variation at Ripiro Beach (*n* = 30 for each sampling occasion), where 23% and 27% of specimens were given a gill ciliate intensity score of severe in March and May, respectively, versus the following two sampling dates July (severe = 10%) and September (severe = 0%). Upper intensity (High and Severe) then picks up again in November (20%) and decreases again in January (0%) (Fig. 3.5, B). In some cases, evidence of irritation (increased abundance of mucous cells) and/or disruption of the gill lattice appeared to be associated with large quantities of gill ciliates (Fig. 3.2, F). On two instances (in September and November 2019), *Frontonia*-like ciliates (distinguishable by shape and size) were detected in toheroa specimens (Table 3.2, Fig. 3.2, G).

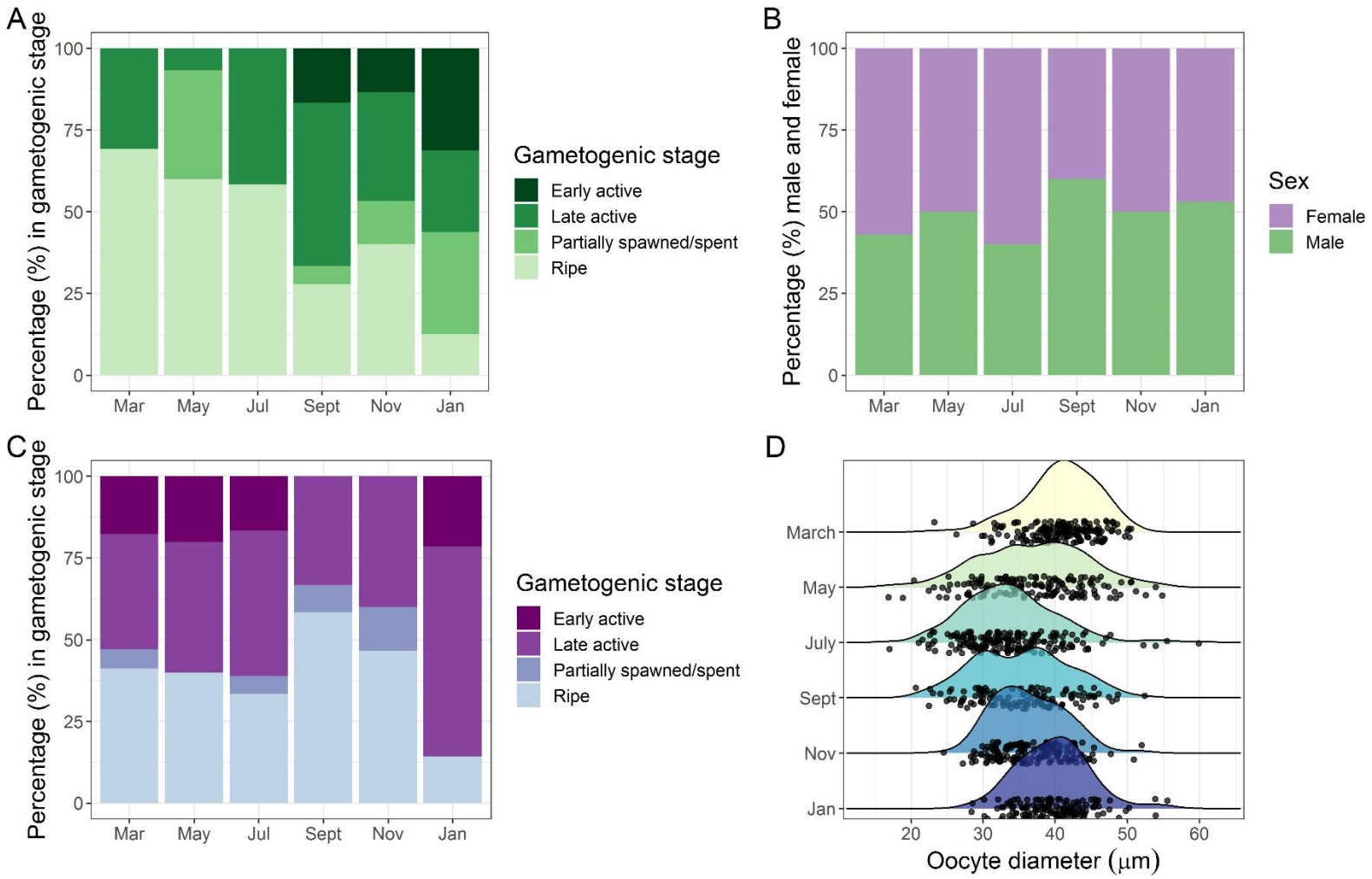

Fig. 3.4. Sex and reproduction statistics of toheroa gathered from Ripiro Beach. A (Male) and C (Female): Stacked bar plots showing the proportion of individuals in each gametogenic stage at the time of specimen collection. B: Percentage of individuals that were male/female over each sampling occasion. D: Ridgeline plot showing oocyte diameter (μm) over a bi-monthly period from Mar-19 to Jan-20. Dots represent mean oocyte diameter (*n* = 150-180 measured oocytes for each month), ridges illustrate the distribution of data for each month.

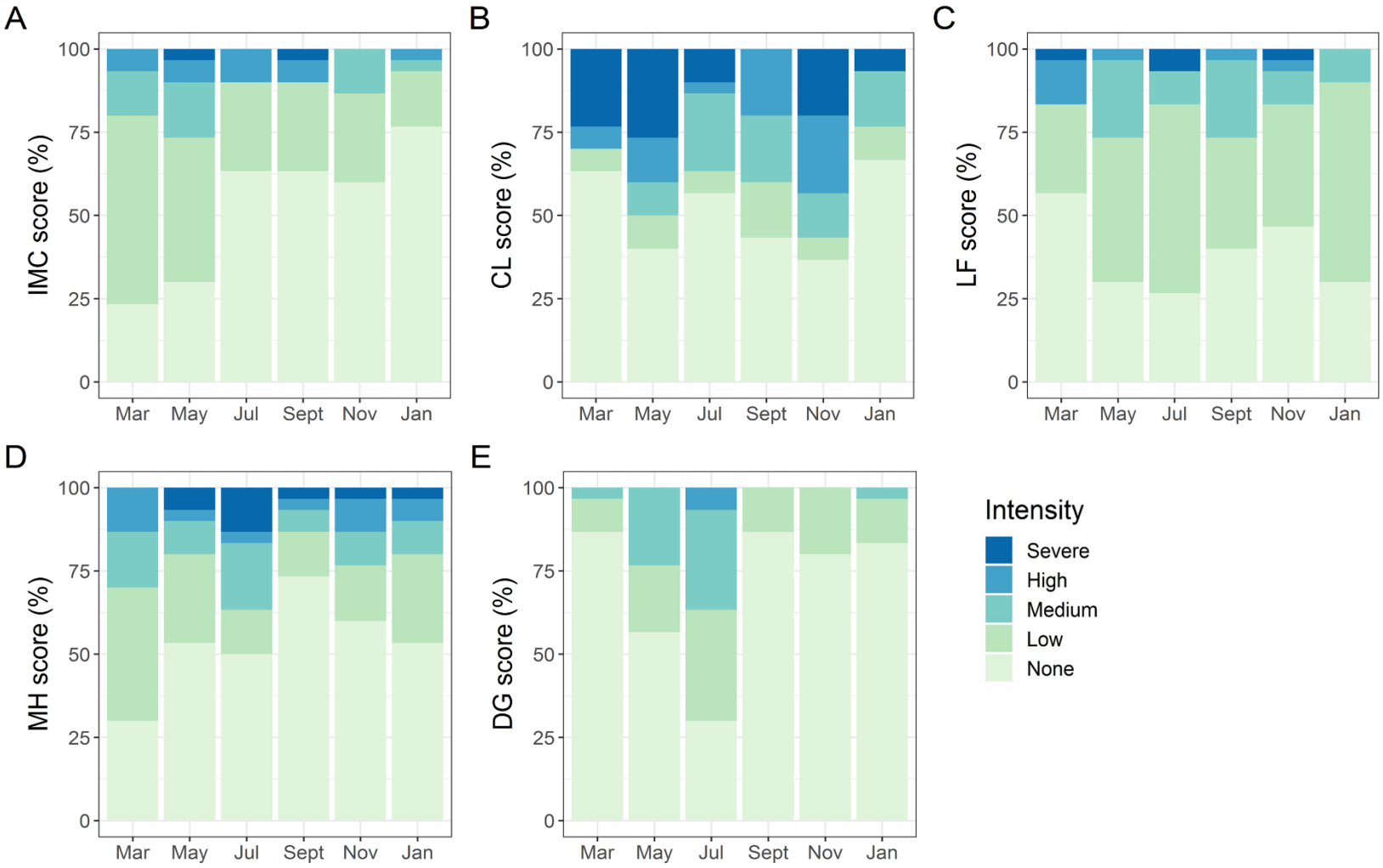

Fig. 3.5. Stacked bars showing the proportion (%) of specimens which scored None, Low, Medium, High, or Severe of respective intensity of parasites or pathomorphological features (intensity levels described in text). A: Intracellular microcolonies of bacteria (IMC), B: Gill ciliates (CL), C: Lipofuscin (LF), D: Mucous cell hyperplasia (MH), and E: Thinning of digestive tubules (DG). Each bar constructed from examination of *n* = 30 toheroa. Specimens gathered at Ripiro Beach between March 2019 and January 2020.

3.4.3.3 Helminths Parasites

The detection of parasitic worms was somewhat rare in all the specimens examined in this study. One specimen from Te-Oneroa-a-Tōhē and one specimen from Ripiro Beach (July-19) were found to host unidentified nematodes (Table 3.2). On four occasions, specimens from Ripiro Beach were found to be hosting putative Digenean trematodes within their respective body cavities (Fig. 3.2, H), two in May, one in July and another in September 2019 (Table 3.2). One specimen from Oreti Beach presented with sporocysts of a Digenean trematode (Fig. 3.6, A).

3.4.3.4 Fungi

Fungal hyphae and spores (fruiting bodies) were present in on the surface of the periostracum (mantle edge) of several toheroa specimens (Table 3.2 & Fig. 3.6, B). Similar fungal structures have previously been observed on the mantle/periostracum of members of the *Paphies* genus nearby, in northern Aotearoa (J. Howells, personal communication).

3.4.4 Pathomorphological Features

3.4.4.1 Lipofuscin

In a large number of toheroa specimens examined, lipofuscin (brown/yellow pigment) within accumulations of spent haemocytes was observed (Fig. 3.6, C). Primarily, observations were made in the gills (often in the haemal sinuses) and less frequently in the digestive gland. The prevalence and intensity of lipofuscin varied depending on site and sampling date (Table 3.2). The highest prevalence and intensity of lipofuscin was found to be from the Oreti Beach specimens (88%, n = 40). No lipofuscin was detected in the Foxton specimens (n = 3), and 27% (n = 15) of Te-Oneroa-a-Tōhē specimens were positive for lipofuscin. There was some slight variation in the prevalence of lipofuscin in the Ripiro Beach specimens (range = 43-73%, n = 30 for each sampling occasion) over time. Additionally, in terms of intensity, there was also some seasonal variation in the Ripiro Beach specimens (Fig. 3.5, C). Many specimens that were positive for lipofuscin in tissues were graded as Low and Medium (Fig. 3.5, C). The highest percentage of specimens that were graded as High [3] were sampled in March (13%, n = 30), and the greatest proportion of specimens graded as Severe were sampled in July (7%, n = 30).

3.4.4.2 Mucous Cell Hyperplasia

Large basophilic hyperplasic mucous cells were detected in a large proportion of specimens (mainly in the gill channels and on the labial palps) regardless of site and sampling date (range = 27-100%) (Fig. 3.6, D). Where extensive mucous cell (goblet) hyperplasia was observed in toheroa specimens, large quantities of mucus was often observed in close association (Fig. 3.6, E). All three specimens from Foxton were positive for mucous cell hyperplasia (100%), though the next highest prevalence was in specimens from Oreti Beach (98%, *n* = 40). From Te-Oneroa-a-Tōhē, 33% (*n* = 15) of specimens were positive for mucous cell hyperplasia. Considering the seasonal sampling effort at Ripiro Beach (Table 3.2, *n* = 30 for each sampling occasion), prevalence was highest in March (70%) and lowest in September (27%). In terms of intensity (Fig. 3.5, D), the highest proportion of specimens graded as High were sampled in March (13%) followed closely by November (10%), but the highest proportion graded as Severe were those sampled in July (13%).

3.4.4.3 Thinning of Digestive Tubules

Thinning of tubule walls (Fig. 3.6, F) was observed in 48% (*n* = 40) of Oreti Beach specimens, 67% (2 of 3) of Foxton specimens and 67% (*n* = 15) of Te-Oneroa-a-Tōhē specimens. In Ripiro Beach individuals (Table 3.2), thinning of digestive tubule walls was prevalent in 20% or less of specimens from March, September, November, and January (*n* = 30 for each sampling occasion at Ripiro Beach). Thinning tubule walls was prevalent in 43% of May specimens and 70% of specimens from July. In most of the cases where specimens were exhibited thinning of digestive tubules, the ‘severity’ of thinning was graded at a Low or Medium level. No specimens were graded as Severe and only 7% of specimens from the July sampling effort were graded as High. None of the specimens gathered in September and November were graded above Low for tubule wall thinning (Fig. 3.5, E).

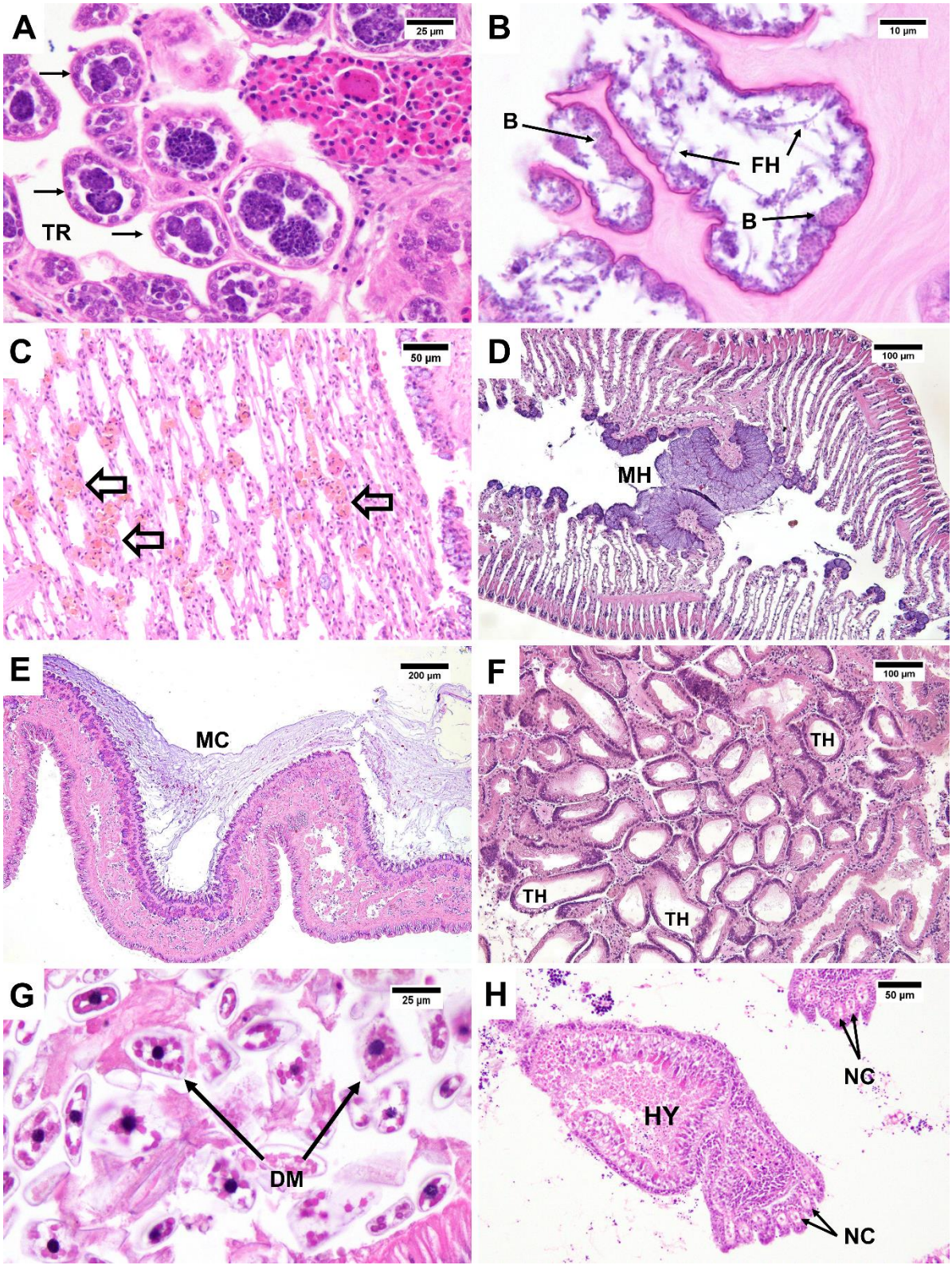

Fig. 3.6. A: Sporocyst of Digenean trematode (arrows). B: Putative fungal hyphae (FH) and fruiting bodies (B) on the surface of the periostracum/mantle edge. C: Lipofuscin (brown/yellow pigment) within spent haemocyte accumulations (hollow arrows) in the gill lattice. D: Gill water channel with large basophilic-stained mucous cell hyperplasia (MH). E: Labial palp and large amounts of mucus (MC) from secretory cells (basophilic). F: Thinning of the digestive tubule walls (TH). G: Diatoms (*Attheya*-like) in the gut lumen (DM and thin arrows). H: Nematocysts (NC) within a hydroid (HY) (Cnidarian) in the suprabranchial chamber.

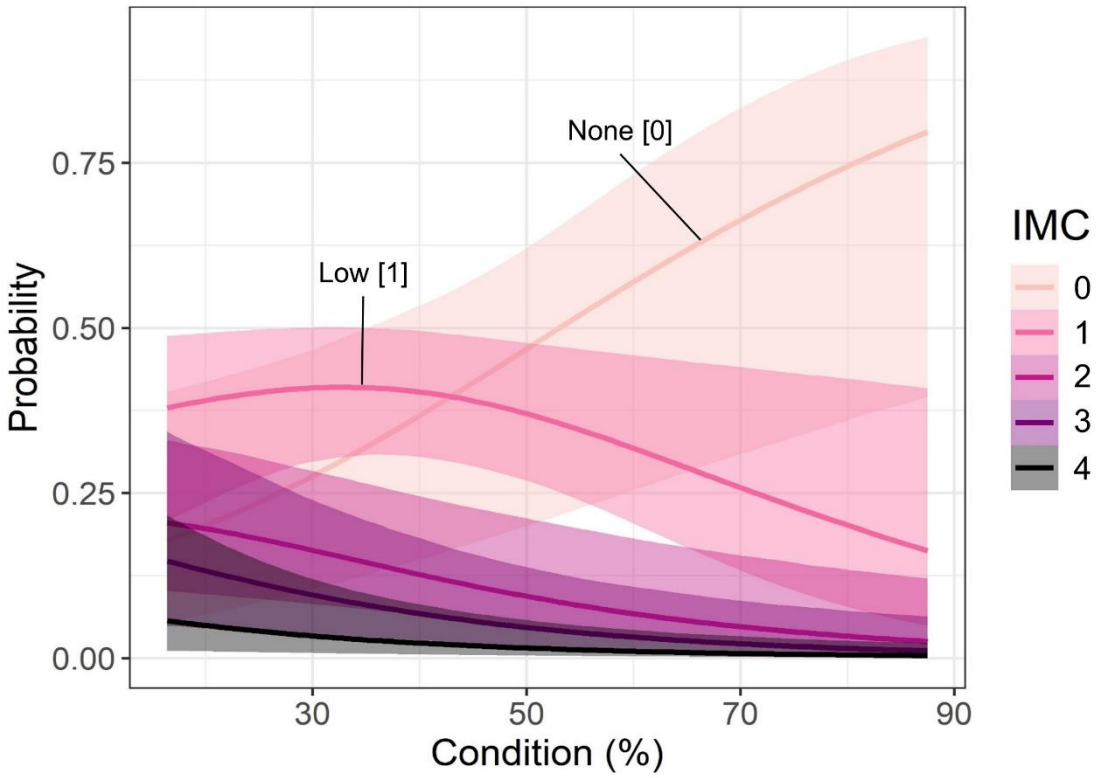

Fig. 3.7. Marginal effects from the best performing model (Model 3) showing the posterior mean estimates of the probability of IMC infection intensity against toheroa condition (%). Shaded area = 95% confidence interval. IMC intensity levels: None [0], Low [1], Medium [2], High [3], Severe [4].

Table 3.2. Prevalence of parasites and other histological and gross pathology in toheroa. Figures are in percentage (%) prevalence for each respective sampling session/location as a proportion of *n*. For graded pathomorphological features (e.g., mucous cell hyperplasia), prevalence is shown as the pooled proportion above a grade of zero (None). Te-Oneroa-a-Tōhē: Ninety Mile Beach.

Site	**Oreti Beach**	**Foxton Beach**	**Te-Oneroa-a-Tōhē**	**Ripiro Beach**					
Date	Feb-19	Mar-19	Nov-19	Mar-19	May-19	Jul-19	Sep-19	Nov-19	Jan-20
n	40	3	15	30	30	30	30	30	30
Histology (%)									
Pathogens and parasites									
Intracellular microcolonies	3	33	13	77	70	37	37	40	23
Unidentified gill ciliates	0	0	33	37	60	43	57	63	33
Frontonia-like ciliate	0	0	0	0	0	0	3	3	0
Nematodes	0	0	7	0	0	0	0	3	0
Putative Digenean trematodes	3	0	0	0	6	3	3	0	0
Fungal hyphae	0	0	0	0	6	3	9	0	6
Hydroids (larvae)	0	0	13	0	3	10	0	0	0
Pathomorphological features									
Lipofuscin	88	0	27	43	70	73	60	53	70
Mucous cell hyperplasia	98	100	33	70	47	50	27	40	47
Thinning of digestive tubules	48	67	67	13	43	70	13	20	17
Diatoms (very high abundance)	0	0	0	0	17	0	3	0	3
Gross pathology (%)									
Shell abnormality	3	0	0	7	0	0	0	0	0
Gas bubbles on shell	-	-	-	30	43	43	50	27	3
Foot malformation	0	33	13	0	0	0	0	0	0
Pale/yellow flesh	15	33	0	0	0	0	0	0	0
Pink flesh	0	0	0	3	3	0	3	0	0

3.4.5 Other Conditions

Large quantities of diatoms were observed in histological sections from several specimens (Fig. 3.6, G). Diatoms were detected primarily in the rectum (excreta) and within digestive tubules. Diatoms were visible in greater abundance in specimens gathered from Ripiro Beach in May (Table 2), relative to specimens gathered at other sites and dates. In some specimens, larval stage hydroids were detected, usually in the infra- or supra-branchial chambers (Fig. 3.6, H). Hydroid larvae were observed in 13% (*n* = 15) of specimens collected from Te-Oneroa-a-Tōhē. The only other times they were detected via histology was in one specimen from Ripiro Beach in May and three in July (Table 3.2).

3.4.6 IMC Infection Model

Based on the epld and looic, the models performed differently depending on the parameters included (Table 3.3). The model with the highest looic (i.e., lowest ranking) was the 'null' model (looic = 406), in contrast the best performing model was Model 3 (looic = 389.5). The worst performing model, after the null model, was the model containing lipofuscin, mucous cell hyperplasia and gill ciliates (looic = 395.2). Indicating that these parameters have little effect on IMC intensity outcome. The next worst performing model was Model 4 (looic = 393). The best performing models after Model 3, were Models 2 and 7 (looic = 389.6), which both contained condition and a combination of other factors (i.e., lipofuscin, condition, ciliates, condition, and sex and gametogenic stage). This indicates that the addition of some parameters (i.e., condition) increases the predictive accuracy over others and that all other parameters used herein contributed little additive effect when combined with condition. Examination of parameter estimates for the best performing model (Model 3) revealed condition is the most important predictive parameter. Only the 95% probability interval for condition is below zero, indicating a negative interaction with IMC intensity. Compared to sites, which contained zero in estimated confidence intervals (Table 3.4). For condition, the odds ratio (OR) estimate is 0.96, suggesting that there is a 4% decrease in the odds of a higher IMC infection intensity level for every unit increase of toheroa condition. Marginal effects are displayed in Fig. 3.7. Probability estimates show how decreasing condition raises the probability of an IMC infection level increase, though the probability of an infection level 'Low' remains below 0.25. Trace plots and posterior predictive checks suggested good model performance and fit (Fig. C.3 & C.4).

Table 3.3. Model comparisons for gill histopathology scores for IMCs: intracellular microcolonies based on the leave-one-out information criterion (looic) and epld from the 'brms' and 'loo' packages (Bürkner, 2017; Vehtari et al., 2018) in RStudio. MH: mucous cell hyperplasia, LF: lipofuscin pigmented cells, CI: condition index, GamSt: gametogenesis stage.

Model	**Model formula**	**epld**	**looic**	**Δlooic[a]**
Model 1	Site + LF + MH + Ciliate + (1|gr(Month))[b]	-197.6	395.2	5.7
Model 2	Site + LF + CI + Ciliate + (1|gr(Month))	-194.8	389.6	0.1
Model 3	Site + CI + (1|gr(Month))	-194.7	389.5	0
Model 4	Site + CI + Ciliate + (1|gr(Month))	-196.5	393	3.5
Model 5	Site + Sex + GamSt + (1|gr(Month))	-196.5	392.9	3.4
Model 6	Site + CI*GamSt + (1|gr(Month))	-195.9	391.8	2.3
Model 7	Site + CI + Sex*GamSt + (1|gr(Month))	-194.8	389.6	0.1
Model 8	Site + LF + MH + CI + Sex + GamSt + (1|gr(Month))	-195.4	390.8	1.3
Null	Intercept only	-203	406	16.5

[a]Δlooic: looic of given model – looic of best performing model
[b]Month included in all models (except null) as a group-level (random) effect

Table 3.4. Parameter estimates and odd ratios (OR) from the posterior distribution of the best performing model (Model 3).

	Parameter estimates				**Odds ratio**		
	Mean	SE	2.5%	97.5%	OR	2.5%	97.5%
Mahuta Gap	-0.23	0.29	-0.79	0.34	0.80	0.45	1.40
Kopawai	-0.13	0.29	-0.69	0.43	0.88	0.50	1.54
Condition	-0.04	0.02	-0.07	-0.01	0.96	0.93	0.99

3.5 Discussion

This study represents the most comprehensive assessment of toheroa health across their entire ecological range, providing a baseline for future studies on this treasured, but threatened species. Foremost, the most frequently observed potential pathogens were intracellular microcolonies of bacteria or IMCs in the gills. Intracellular microcolonies, referred to as RLOs by Ross et al. (2018b), have been associated with mortality events of several shellfish in Aotearoa (Howells et al., 2021; Howells et al., 2019). In this study, their intensity was consistently low. It must be noted that this could be due to survivor bias. Prevalence data indicates a possible spatial effect in terms of bacterial inclusions, as only 3% (n = 40) of Oreti specimens were positive for IMCs, whereas even within the lowest prevalence occasion at Ripiro Beach (Jan-20), 30% (n = 30) of specimens were positive for IMCs. Relatively few parasites were detected in toheroa tissues, for instance, only seven of 238 animals (2.5%) were positive for helminth parasites. The prevalence and intensity of gill ciliates varied considerably but was consistently high at Mahuta Gap (Fig. C.2). Protozoan ciliates are often associated with flowing water (Foissner and Berger, 1996), additionally toheroa beds are typically congregated in close proximity to freshwater outflows (Cope, 2018; Ross et al., 2018a; Williams et al., 2013). Noted during field visits, the stream at Mahuta Gap was at a relatively constant flow level compared to Kopawai and Island (the freshwater stream at Island was typically dry during site visits). Gill ciliate prevalence was highest at Ripiro Beach from May to November (i.e., austral winter/spring). This could be explained by higher rainfall during this period that would increase freshwater input into streams flowing onto the beach.

Gas bubbles on toheroa shells from Ripiro Beach was first reported by Ross et al. (2018b). The authors postulated that high temperatures during summer months might result in supersaturated total dissolved oxygen within the shell cavity, resulting in gas bubbles similar to those in other shellfish, finfish, and crustacea (Espmark et al., 2010; Malouf et al., 1972). The results of this study indicate a reversed seasonal pattern (Table 3.2). The highest prevalence of gas bubbles was in September compared to warmer months like March and January. Like the detection of gill ciliates, much of this prevalence is owed to specimens gathered at the sub-site Mahuta Gap (Fig. C.2). The only obvious environmental variable distinguishing these relatively close sub-sites from each other is a consistently flowing stream at Mahuta Gap. It is therefore suggested that another mechanism (possibly linked to freshwater outflow) might driving gas bubble manifestation on toheroa shells, in place of temperature alone. Another intriguing observation that remains unexplained is the presentation of pink flesh in some specimens (Fig. 3.2, B). The proportion of toheroa presenting pink flesh was 3/238 herein, a ratio of 79:1, extremely close to the personal communication evidence of 80:1

reported by (Ross et al., 2018a). Considering no signs of ill health were linked to this coloration, it appears to be of little consequence for affected individuals.

Hyperplasic mucous cells as morphological response/association to polluted sediment (Gardner and Yevich, 1988) and prokaryotic inclusions (Villalba et al., 1993) have previously been observed in marine organisms. The models used here indicated little association between IMCs (i.e., prokaryotic inclusions) and mucous cell hyperplasia (Table 3.3). Bower and Blackbourn (2003) note that mucous cells in geoducks (*P. generosa*), like to those reported herein (Fig. 6, E), assist in feeding by entrapping food items (in mucus) which are then carried to the labial palps by ciliary action. While this is likely the case for toheroa too, observations of site-specific variation in the prevalence and intensity of mucous cell hyperplasia suggests another factor may be encouraging their proliferation. At Oreti Beach, the prevalence of mucous cell hyperplasia was 98% (n = 40), much higher than elsewhere. All specimens were collected from high-energy surf beaches, though Oreti Beach being the southernmost collection site (below 45°S, Fig. 3.1) typically experiences harsher weather conditions compared to the beaches sampled in northern Aotearoa. Furthermore, the large size of Oreti Beach specimens (mean length = 113.42, ± SE = 1.4), suggests longer life histories and thus longer exposure periods to chronic irritation (sand and grit) which could give rise to excess mucus production/goblet cell hyperplasia in response. Therefore, hyperplasia of secretory cells and excess mucus production as a response to chronic irritation may explain the site-specific difference detected here (Table 3.2). It should be noted, that what has been referred to as ‘mucous cell hyperplasia’ herein, may not be hyperplasia per se, rather it could be a normal response to increased food availability to aid food particle entrapment (by subsequent mucus production). Mucus is also the first line of defence for many marine invertebrates (Allam and Pales Espinosa, 2016; Shnit-Orland and Kushmaro, 2009), entrapping and sloughing pathogens and providing a source of innate immunity in a given host’s holobiont. Consequently, mucus production in toheroa as a defensive mechanism to pathogen challenge is another possible explanation for extensive mucous cell hyperplasia in some toheroa.

Lipofuscin is a common waste product (haemocytic and lysosomal) in bivalves characterised by yellow/brown pigmented granules. When attributed to lysosomal digestion i.e., tissue turnover, it is often associated with aging and/or ‘wear and tear’ (Lohrmann et al., 2019; Terman and Brunk, 2004). For this reason, it is sometimes used as a proxy for age determination of crustacea (Ju et al., 1999; O'Donovan and Tully, 1996), where age determination is challenging. Lipofuscin was often observed in the gills and to a lesser extent, the digestive gland of toheroa specimens. Lipofuscin (within spent haemocyte accumulations) was not visually linked to any other patho-morphological or immunological features. We suggest that the increased abundance of lipofuscin in

southern specimens, which were much larger in size (Fig. C.1) is simply attributed to longer life histories (aging) and subsequently increased tissue turnover.

Bivalve-inhabiting hydroids have previously been detected in mollusc hosts, namely *Eugymnanthea inquilina* (Piraino et al., 1994), and *Eutima japonica*, the latter of which has been associated with mortality in the Japanese scallop *Mizuhopecten yessoensis* (Baba et al., 2007). Considering the detection of hydroids was consistently within body cavities (supra- and infra-branchial chambers) of toheroa individuals, their presence appears to be of little consequence for toheroa hosts.

Mean condition was highest in September, coinciding with the second highest concentration of chlorophyll-*a* of all the sampled dates at Ripiro Beach. Comparing condition to chlorophyll-*a* concentration (Fig. 3, A), it would appear some relationship exists, though condition was still elevated in Jan-20, despite the low mean monthly chlorophyll-*a* concentration estimated (0.249 mg m^{-3}). A positive association would be expected as chlorophyll-*a* concentration would generally correspond to availability of suspended organic matter. During the May sampling expedition in 2019 to Ripiro Beach, an elevated presence of phytoplankton was observed in the surf and swash zone (spume), as well as dense mats of decaying microalgae biomass coating the intertidal (diatoms subsequently noted in the histology, see Table 2). The 'spume', a result of increased wave action and phytoplankton detritus on high-energy surf beaches, is a common occurrence on surf beaches on the western coast of Aotearoa (reviewed in Campbell, 1996). These autumn blooms have been associated with toheroa health in the past, where Cassie (1955) noted that dense phytoplankton blooms were commonplace on beaches where toheroa were abundant. The hypothesis was drawn that toheroa relied on these seasonal blooms to obtain sufficient nutrients (Cassie, 1955; Williams et al., 2013). Previously, it has been suggested that toheroa condition improves significantly after autumn rains commence, coinciding with these phytoplankton blooms (Williams et al., 2013). Rapson (1954) found that the most abundant diatoms in the water at Ripiro Beach in May were *Attheya armata* (previously *Chaetoceros armatum*) (Guiry and Guiry, 2020; Odebrecht et al., 2014), accounting for 96% of the phytoplankton taxa present (Williams et al., 2013). Perhaps unsurprisingly, diatoms were detected in high abundance in the digestive organs of specimens gathered during this time in the present study (Ripiro Beach, May-19, Fig. 3.6, G). Although difficult to discern from histology, the most abundant diatom present resembles *Attheya armata* (Fig. 3.6, G) consistent with observations made by Rapson (1954). Prevalence of digestive tubule thinning (which could be attributed to digestive phases or atrophy) fluctuated in specimens from Ripiro Beach, with highest prevalence in July (70%, n = 30) and the lowest in September and March (13%, n = 30). It was thought that the phytoplankton blooms observed in autumn months (July & May) would mitigate thinning of digestive tubules. Though considering

the highest mean oocyte density estimated in this study was in May. It is possible that this disparity between food availability and condition in specimens from May and July could be explained by the reproductive cycle of toheroa, given the energy demands of reproduction.

Previous examinations of the reproductive cycle in northern toheroa populations describe that, whilst they continuously spawn and possess no resting phase, there are two or three main spawning events either side of the austral-summer (Redfearn, 1974; Smith, 2003). This was confirmed by Gadomski and Lamare (2015) for southern toheroa populations. Oocyte size was greatest here in March (mean = 40.84 µm), closely followed by January (mean = 39.71 µm). Gadomski and Lamare (2015) reported the highest mean oocyte diameter in January and February. Furthermore, in the present study, the highest proportion of male specimens in the ripe gametogenic stage was in March, and for females, the highest proportion in the ripe stage was in September, closely followed by November (Fig. 3.4, A & C). These observations for Ripiro Beach toheroa are also in close agreement with the findings of Gadomski and Lamare (2015) and Smith (2003). Inferences of spawning events are challenging due to the bi-monthly sampling strategy used here. However, the high proportion of ripe males in March, and the high proportion of ripe females in September and November, suggests two main spawning events. One in late summer/autumn (March) and another in late spring/early summer (November). This is not mirrored by oocyte diameter frequencies (Fig. 3.4, D) and oocyte density estimates (Fig. 3.3, B), where a reduction in oocyte diameter and density after March and May (possible spawning event) is not complimented by an increase in oocyte density and diameter in early summer (mixture of rounded and angular oocytes). This suggests that this spawning event (late summer/autumn) is probably minor compared to the early summer spawning event, supported by reproductive stages (Fig. 3.3, A & C), and that continuous spawning is likely taking place, with the absence of a significant resting period, in agreement with previous observations of toheroa reproduction.

To maximise the potential of histopathology data collected herein, ordinal logistic regression models were constructed to in a bid to predict IMC infection intensity based on several factors of toheroa health. Models showed condition to be the greatest predictor of IMC infection out of all the parameters assessed. Increasing condition raised the probability of an IMC infection intensity level of ‘None’ (Fig. 3.7). Sex, gametogenic stage, lipofuscin, and mucous cell hyperplasia did not add significant information for model predictive success, suggesting little association of these factors with IMC infection intensity. Furthermore, an interaction between reproductive stages and condition did not improve model performance (Table 3.3), indicating little interactive effect. This indicates that reduced condition (regardless of reproduction) increases the probability of a higher

infection intensity, or alternatively, that increased infection intensity could contribute to decreased toheroa condition (Fig. 3.7). Without further investigation, it is not clear whether this association is due to direct infection effects i.e., IMC infection reducing condition, or if instead, reduced host fitness (condition) increases host susceptibility to opportunistic bacteria. As no immune response was associated with IMCs (typical for IMCs in molluscs; Cano et al., 2020), it is possible that they do not have a measurable negative effect on toheroa health. These IMCs present in Aotearoa shellfish have recently been identified as *Endozoicomonas* spp. (Bennion et al., in press; Howells et al., 2021), a symbiont of many marine invertebrates (Neave et al., 2016). Consequently, treating IMCs in toheroa tissues as endosymbionts, rather than pathogens, may be more appropriate (Dorfmeier et al., 2015; Lohrmann et al., 2019), until their niche within marine mollusc hosts in Aotearoa New Zealand is resolved.

The prevalence of IMCs in this study was quite high (sometimes >70%), though intensity was typically graded as 'Low'. Considering the first detection of IMCs in toheroa in 2017 (Ross et al., 2018b) and the association of a large number of shellfish mortalities in Aotearoa with IMCs (Howells et al., 2019), baseline assessments of healthy specimens such as this one provide a valuable reference for investigators attempting to establish causes of mortality. Furthermore, the reasons for the limited recovery of toheroa populations, despite many years of protection (Miskelly, 2016), remain a mystery (Ross et al., 2018a; Williams et al., 2013). This study has provided a benchmark with which to measure toheroa health status against in the future, by recording as many pathomorphological and health related features by histology as feasibly possible. The only potential disease-causing agent detected in all remaining major toheroa populations were IMCs (Table 3.2). Although not apparent in this study, their potential to cause mortality cannot currently be ruled out, and the link made between IMC intensity and toheroa condition points to potential interactive effects (Fig. 3.7). Given their detection in apparently healthy toheroa at relatively high intensity, however, and the absence of evidence of an ongoing epidemic in toheroa populations, it is unlikely they are a barrier to toheroa recovery at a national level.

3.6 Conclusion

No obvious aetiological agent or parasitic organism was detected that could be a barrier to toheroa recovery across their entire ecological range. Although this could be due to survivorship bias. The detection of IMCs in all toheroa populations and their recent association with mass mortality events of other shellfish in Aotearoa (Howells et al., 2021) raises questions of their niche within shellfish hosts. Furthermore, the association between reduced condition and IMC infection intensity warrants further exploration of health related impacts of IMCs and (or) their opportunistic pathogen potential. This could

be achieved by experimental study of IMCs in Aotearoa shellfish hosts under risk factor challenge (e.g., salinity or temperature). Similar *ex situ* approaches could be taken to elucidate the causes (pathomorphological features) and affects (parasites & pathogens) of a variety of other health features in toheroa hosts for example, mucous cell hyperplasia, helminths, and fungal infections.

This study marks the most comprehensive health assessment of toheroa to-date, but studies like this have yet to be carried out for many other Aotearoa shellfish species. Histopathology surveys of other shellfish endemic to Aotearoa New Zealand (e.g., *Paphies* clams) would yield equally important baselines for future health assessments/investigations of mortality events. Finally, this study demonstrates how ordinal logistic regression models can be used to maximise the value of some types of histopathological data (e.g., intensity scale), increasing its utility in an investigatory and exploratory capacity.

3.7 References

Allam, B., Pales Espinosa, E., 2016. Bivalve immunity and response to infections: Are we looking at the right place? Fish & Shellfish Immunology. 53**,** 4-12.

Baba, K., et al., 2007. Occurrence and detrimental effects of the bivalve-inhabiting hydroid *Eutima japonica* on juveniles of the Japanese scallop *Mizuhopecten yessoensis* in Funka Bay, Japan: relationship to juvenile massive mortality in 2003. Marine Biology. 151**,** 1977-1987.

Behringer, D. C., et al., Disease in fisheries and aquaculture. In: D. Behringer, et al., Eds., Marine Disease Ecology. Oxford University Press, Oxford, 2020.

Bennion, M., et al., in press. Characterisation and distribution of the bacterial genus *Endozoicomonas* in a threatened surf clam. Diseases of Aquatic Organisms.

Bignell, J. P., et al., 2011. Histopathology of mussels (*Mytilus* sp.) from the Tamar estuary, UK. Marine Environmental Research. 72**,** 25-32.

Bingham, P., et al., 2013. Investigation into the first diagnosis of ostreid herpesvirus type 1 in Pacific oysters. Surveillance. 40**,** 20-24.

Bower, S. M., Blackbourn, J., Geoduck clam (*Panopea generosa*): Anatomy, Histology, Development, Pathology, Parasites and Symbionts: Normal Histology - Digestive System. Vol. 2020. Fisheries and Oceans Canada, Government of Canada, 2003.

Brosnahan, C. L., et al., 2017. First report of a *rickettsia*-like organism from farmed Chinook salmon, *Oncorhynchus tshawytscha* (Walbaum), in New Zealand. New Zealand Journal of Marine and Freshwater Research. 51**,** 356-369.

Bürkner, P.-C., 2017. brms: An R Package for Bayesian Multilevel Models Using Stan. Journal of Statistical Software. 80**,** 1-28.

Bürkner, P.-C., Vuorre, M., 2019. Ordinal Regression Models in Psychology: A Tutorial. Advances in Methods and Practices in Psychological Science. 2**,** 77-101.

Campbell, E. E., 1996. The global distribution of surf diatom accumulations. Revista Chilena de Historia Natural. 69**,** 495-501.

Cano, I., et al., 2020. Cosmopolitan Distribution of *Endozoicomonas*-Like Organisms and Other Intracellular Microcolonies of Bacteria Causing Infection in Marine Mollusks. Frontiers in Microbiology. 11**,** 2778.

Cano, I., et al., 2018. Molecular Characterization of an *Endozoicomonas*-Like Organism Causing Infection in the King Scallop (*Pecten maximus* L.). Applied and Environmental Microbiology. 84**,** e00952-17.

Carella, F., et al., 2019. Baseline pathological data of the wedge clam *Donax trunculus* from the Tyrrhenian Sea (Mediterranean Basin). Diseases of Aquatic Organisms. 133**,** 107-118.

Carnegie, R. B., et al., 2016. Managing marine mollusc diseases in the context of regional and international commerce: policy issues and emerging concerns. Philosophical Transactions of the Royal Society B: Biological Sciences. 371**,** 20150215.

Carvalho, Y. B. M., et al., 2013. *Rickettsia*-Associated Mortality of the Yellow Clam *Mesodesma mactroides* (Bivalvia: Mesodesmatidae) in Southern Brazil. Malacologia. 56**,** 301-307.

Cassie, R. M., 1955. Population Studies on the Toheroa, *Amphidesma ventricosum* Gray (Eulamellibranchiata). Australian Journal of Marine and Freshwater Research. 6**,** 348-391.

Cope, J., The modification of toheroa habitat by streams on Ripiro Beach. MSc. University of Waikato, Hamilton, New Zealand, 2018, pp. 126.

Cremonte, F., et al., 2005. A histopathological survey of some commercially exploited bivalve molluscs in northern Patagonia, Argentina. Aquaculture. 249**,** 23-33.

Crosson, L. M., Friedman, C. S., 2018. Withering syndrome susceptibility of northeastern Pacific abalones: A complex relationship with phylogeny and thermal experience. Journal of Invertebrate Pathology. 151**,** 91-101.

Culver, C. S., Kuris, A. M., 2000. The Apparent Eradication of a Locally Established Introduced Marine Pest. Biological Invasions. 2**,** 245-253.

Darriba, S., et al., 2010. Histological survey of symbionts and other conditions in razor clam *Ensis arcuatus* (Jeffreys, 1865) (Pharidae) of the coast of Galicia (NW Spain). Journal of Invertebrate Pathology. 104**,** 23-30.

Dorfmeier, E. M., et al., 2015. Temporal and Spatial Variability of Native Geoduck (*Panopea generosa*) Endosymbionts in the Pacific Northwest. Journal of Shellfish Research. 34**,** 81-90.

Downes, J. K., et al., 2018. Investigation of co-infections with pathogens associated with gill disease in Atlantic salmon during an amoebic gill disease outbreak. Journal of Fish Diseases. 41**,** 1217-1227.

Espmark, A. M., et al., 2010. Development of gas bubble disease in juvenile Atlantic salmon exposed to water supersaturated with oxygen. Aquaculture. 306**,** 198-204.

Farley, J. H., et al., 2013. Reproductive Dynamics and Potential Annual Fecundity of South Pacific Albacore Tuna (*Thunnus alalunga*). PLOS ONE. 8**,** e60577.

Foissner, W., Berger, H., 1996. A user-friendly guide to the ciliates (Protozoa, Ciliophora) commonly used by hydrobiologists as bioindicators in rivers, lakes, and waste waters, with notes on their ecology. Freshwater Biology. 35**,** 375-482.

Friedman, C. S., Finley, C. A., 2003. Anthropogenic introduction of the etiological agent of withering syndrome into northern California abalone populations via conservation efforts. Canadian Journal of Fisheries and Aquatic Sciences. 60**,** 1424-1431.

Gadomski, K., Reproduction and larval ecology of the toheroa, *Paphies ventricosa*, from Oreti Beach, Southland, New Zealand. PhD. University of Otago, 2017, pp. 155.

Gadomski, K., Lamare, M., 2015. Spatial variation in reproduction in southern populations of the New Zealand bivalve *Paphies ventricosa* (Veneroida: Mesodesmatidae). Invertebrate Reproduction & Development. 59**,** 81-95.

Gardner, G. R., Yevich, P. P., 1988. Comparative histopathological effects of chemically contaminated sediment on marine organisms. Marine Environmental Research. 24**,** 311-316.

Gollas-Galvan, T., et al., 2014. *Rickettsia*-like organisms from cultured aquatic organisms, with emphasis on necrotizing hepatopancreatitis bacterium affecting penaeid shrimp: an overview on an emergent concern. Reviews in Aquaculture. 6**,** 256-269.

Groner, M. L., et al., 2016. Managing marine disease emergencies in an era of rapid change. Philosophical Transactions of the Royal Society B-Biological Sciences. 371**,** 20150364.

Guiry, M., Guiry, G., Algaebase. Worldwide electronic publication. National University of Ireland Galway, 2020. Access date: May 2020. https://www.algaebase.org/.

Harvell, C. D., et al., 2019. Disease epidemic and a marine heat wave are associated with the continental-scale collapse of a pivotal predator (*Pycnopodia helianthoides*). Science Advances. 5**,** eaau7042.

Hayes, K. R., et al., 2019. The Assessment and Management of Marine Pest Risks Posed by Shipping: The Australian and New Zealand Experience. Frontiers in Marine Science. 6**,** 489.

Herrmann, M., et al., 2009. Reproductive cycle and gonad development of the Northern Argentinean *Mesodesma mactroides* (Bivalvia: Mesodesmatidae). Helgoland Marine Research. 63**,** 207.

Hewitt, C. L., et al., 2004. New Zealand marine biosecurity: Delivering outcomes in a fluid environment. New Zealand Journal of Marine and Freshwater Research. 38**,** 429-438.

Howells, J., et al., 2021. Intracellular bacteria in New Zealand shellfish are identified as *Endozoicomonas* species. Diseases of Aquatic Organisms. 143**,** 27-37.

Howells, J., et al., Investigation of *Rickettsia*-like organisms in New Zealand wild shellfish. Biosecurity New Zealand, Ministry for Primary Industries, Wellington, NZ, 2019, pp. 58.

Ju, S.-J., et al., 1999. Use of extractable lipofuscin for age determination of blue crab *Callinectes sapidus*. Marine Ecology Progress Series. 185**,** 171-179.

Kim, Y., et al., Histopathology analysis. Histological techniques for marine bivalve molluscs: Update. NOAA Technical Memorandum NOS NCCOS 26. United States National Ocean Service, Silver Spring, Maryland, 2006, pp. 64.

Lafferty, K. D., 2017. Marine infectious disease ecology. Annual Review of Ecology, Evolution, and Systematics. 48**,** 473-496.

Lafferty, K. D., Hofmann, E. E., 2016. Marine disease impacts, diagnosis, forecasting, management and policy. Philosophical Transactions of the Royal Society B: Biological Sciences. 371**,** 20150200.

Lamb, J. B., et al., 2018. Plastic waste associated with disease on coral reefs. Science. 359**,** 460-462.

Lane, H. S., et al., 2020. Aquatic disease in New Zealand: synthesis and future directions. New Zealand Journal of Marine and Freshwater Research. 1-42.

Lane, H. S., et al., 2016. *Bonamia ostreae* in the New Zealand oyster *Ostrea chilensis*: a new host and geographic record for this haplosporidian parasite. Diseases of Aquatic Organisms. 118**,** 55-63.

Lloyd, M. M., Pespeni, M. H., 2018. Microbiome shifts with onset and progression of Sea Star Wasting Disease revealed through time course sampling. Scientific Reports. 8**,** 16476.

Lohrmann, K. B., et al., 2019. Histopathological assessment of the health status of *Mytilus chilensis* (Hupé 1854) in southern Chile. Aquaculture. 503**,** 40-50.

Mabey, A. L., et al., 2021. Pathogen inferred to have dispersed thousands of kilometres at sea, infecting multiple keystone kelp species. Marine Biology. 168**,** 47.

Mahony, K. E., et al., 2021. Latitudinal influence on gametogenesis and host–parasite ecology in a marine bivalve model. Ecology and Evolution. 11**,** 7029–7041.

Malouf, R., et al., 1972. Occurrence of Gas-Bubble Disease in Three Species of Bivalve Molluscs. Canadian Journal of Fisheries and Aquatic Sciences. 29**,** 588-589.

Marcos-Lopez, M., et al., 2017. *Piscirickettsia salmonis* infection in cultured lumpfish (*Cyclopterus lumpus* L.). Journal of Fish Diseases. 40**,** 1625-1634.

Miskelly, C. M., 2016. Legal protection of New Zealand's indigenous aquatic fauna – an historical review. Tuhinga. 27**,** 81-115.

Moore, J. D., et al., 2000. Withering syndrome in farmed red abalone *Haliotis rufescens*: Thermal induction and association with a gastrointestinal *Rickettsiales*-like prokaryote. Journal of Aquatic Animal Health. 12**,** 26-34.

Mordecai, G. J., et al., 2021. Aquaculture mediates global transmission of a viral pathogen to wild salmon. Science Advances. 7**,** eabe2592.

Neave, M. J., et al., 2016. Diversity and function of prevalent symbiotic marine bacteria in the genus *Endozoicomonas*. Applied Microbiology and Biotechnology. 100**,** 8315-8324.

O'Donovan, V., Tully, O., 1996. Lipofuscin (age pigment) as an index of crustacean age: correlation with age, temperature and body size in cultured juvenile *Homarus gammarus* L. Journal of Experimental Marine Biology and Ecology. 207**,** 1-14.

Odebrecht, C., et al., 2014. Surf zone diatoms: A review of the drivers, patterns and role in sandy beaches food chains. Estuarine, Coastal and Shelf Science. 150**,** 24-35.

Parker, L. M., et al., 2018. Ocean acidification but not warming alters sex determination in the Sydney rock oyster, *Saccostrea glomerata*. Proceedings of the Royal Society B: Biological Sciences. 285**,** 20172869.

Piraino, S., et al., 1994. Ecology of the bivalve-inhabiting hydroid *Eugymnanthea inquilina* in the coastal sounds of Taranto (Ionian Sea, SE Italy). Marine Biology. 118**,** 695-703.

Pollock, F. J., et al., 2014. Sediment and Turbidity Associated with Offshore Dredging Increase Coral Disease Prevalence on Nearby Reefs. PLOS ONE. 9**,** e102498.

Rapson, A. M., 1954. Feeding and Control of Toheroa (*Amphidesma ventricosum* Gray) (Eulamellibranchiata) Populations in New Zealand. Australian Journal of Marine and Freshwater Research. 5**,** 486-512.

Redfearn, P., 1974. Biology and distribution of the toheroa, *Paphies* (Mesodesma) *ventricosa* (Gray). Fisheries Research Bulletin No. 11. New Zealand Ministry of Agriculture and Fisheries. 51.

Ross, P. M., et al., 2018a. The biology, ecology and history of toheroa (*Paphies ventricosa*): a review of scientific, local and customary knowledge. New Zealand Journal of Marine and Freshwater Research. 52**,** 196-231.

Ross, P. M., et al., 2018b. First detection of gas bubble disease and *Rickettsia*-like organisms in *Paphies ventricosa*, a New Zealand surf clam. Journal of Fish Diseases. 41**,** 187-190.

Ruiz, M., et al., 2013. Histological survey of symbionts and other conditions of pod razor clam *Ensis siliqua* (Linnaeus, 1758) in Galicia (NW Spain). Journal of Invertebrate Pathology. 112**,** 74-82.

Segarra, A., et al., 2010. Detection and description of a particular Ostreid herpesvirus 1 genotype associated with massive mortality outbreaks of Pacific oysters, *Crassostrea gigas*, in France in 2008. Virus Research. 153**,** 92-99.

Shnit-Orland, M., Kushmaro, A., 2009. Coral mucus-associated bacteria: a possible first line of defense. FEMS Microbiology Ecology. 67**,** 371-380.

Smith, S., The reproduction and recruitment of toheroa (*Paphies ventricosa*). MSc. University of Auckland, Auckland, 2003.

Smolowitz, R., 2018. A Review of QPX Disease In The northern quahog (= Hard Clam) *Mercenaria mercenaria*. Journal of Shellfish Research. 37**,** 807-819.

Soon, T. K., Ransangan, J., 2019. Extrinsic Factors and Marine Bivalve Mass Mortalities: An Overview. Journal of Shellfish Research. 38**,** 223-232.

Stentiford, G. D., et al., 2014. Histopathological survey of potential biomarkers for the assessment of contaminant related biological effects in species of fish and

shellfish collected from Kuwait Bay, Arabian Gulf. Marine Environmental Research. 98**,** 60-67.

Stentiford, G. D., et al., 2017. New Paradigms to Help Solve the Global Aquaculture Disease Crisis. PLOS Pathogens. 13**,** e1006160.

Terman, A., Brunk, U. T., 2004. Lipofuscin. The International Journal of Biochemistry & Cell Biology. 36**,** 1400-1404.

Tinelli, A., et al., 2020. Histological features of *Rickettsia*-like organisms in the European flat oyster (*Ostrea edulis* L.). Environmental Science and Pollution Research. 27**,** 882-889.

VanWormer, E., et al., 2019. Viral emergence in marine mammals in the North Pacific may be linked to Arctic sea ice reduction. Scientific Reports. 9**,** 15569.

Vehtari, A., et al., 2018. loo: Efficient leave-one-out cross-validation and WAIC for Bayesian models. R package version. 2**,** 1003.

Villalba, A., et al., 1993. Occurrence of Multiple Hyperplastic Growths on the Gills of Pacific Oyster, *Crassostrea gigas*, and Their Relationship with Associated Pathologic Conditions. Journal of Invertebrate Pathology. 61**,** 296-302.

Wickham, H., 2009. ggplot2: Elegant Graphics for Data Analysis. Springer, New York.

Wilke, C. O., 2020. ggridges: Ridgeline Plots in 'ggplot2'. R package version 0.5.3.

Williams, J. R., et al., Review of factors affecting the abundance of toheroa (*Paphies ventricosa*). New Zealand Aquatic Environment and Biodiversity Report No. 114, 2013, pp. 76.

Zhang, Y., et al., 2017. Identification of *Rickettsia*-Like Organism (RLO) in the Oyster *Crassostrea rivularis* Gould. Annals of Clinical Cytology and Pathology. 3**,** 1056.

Zhu, Z. W., et al., 2012. *Rickettsia*-like organism infection associated with mass mortalities of blood clam, *Tegillarca granosa*, in the Yueqing Bay in China. Acta Oceanologica Sinica. 31**,** 106-115.

Chapter 4
Characterisation and Distribution of the Bacterial Genus *Endozoicomonas* in a Threatened Surf Clam

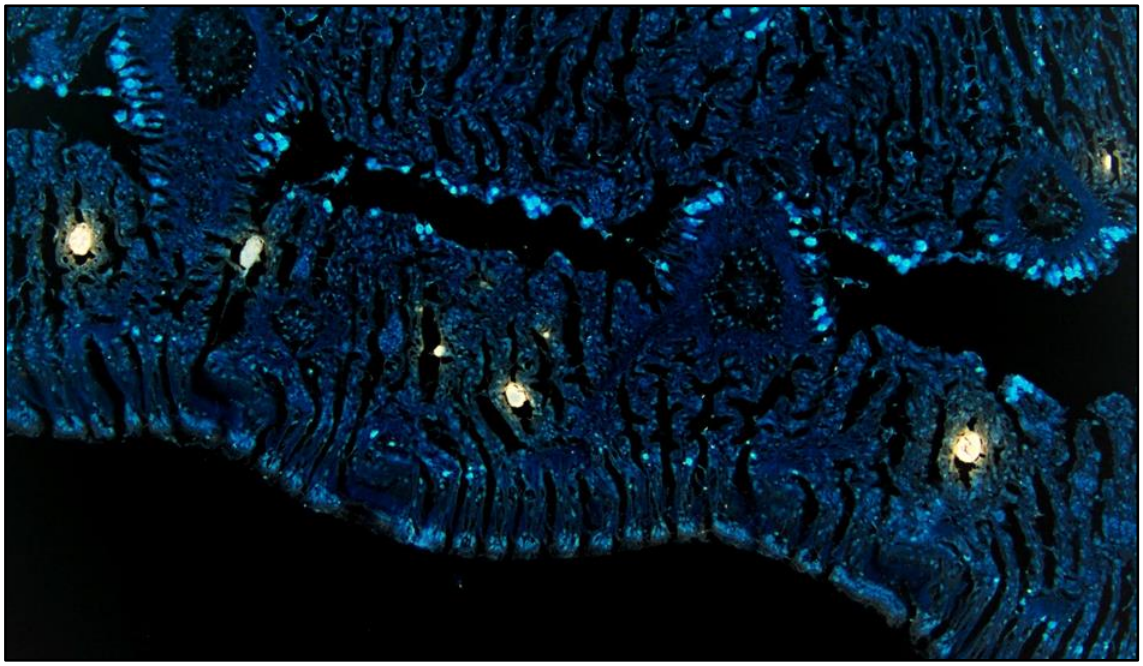

In situ hybridization of *Endozoicomonas* 16S rRNA gene
Toheroa gill tissue

4.1 Abstract

The toheroa is a large Aotearoa (New Zealand) endemic surf clam of cultural importance to many Māori, the indigenous people of Aotearoa. Extensive commercial and recreational harvesting in the 20th century dramatically reduced populations, leading to the collapse and closure of the fishery. Despite being protected for >40 years, toheroa have inexplicably failed to recover. In 2017, intracellular microcolonies (IMCs) of bacteria were detected in 'sick' toheroa in northern Aotearoa. Numerous mass mortality events (MMEs) have recently been recorded in Aotearoa shellfish, with many events linked by the presence of IMCs resembling *Rickettsia*-like organisms (RLOs). While similar IMCs have been implicated in MMEs in surf clams elsewhere, the impact of these IMCs on the health or recovery of toheroa is unknown.

A critical first step towards understanding the significance of a pathogen in a host population is pathogen identification and characterisation. To begin this process, I examined 16S rRNA gene sequences of the putative IMCs from four toheroa populations that identified (97% homology) to *Endozoicomonas* spp. sequences held in the NCBI database. Phylogenetic analysis identified closely related *Endozoicomonas* strains from each of the sampled locations and *in situ* hybridization, using 16S rRNA gene probes confirmed the presence of the sequenced IMC gene in the gill and digestive gland tissues of toheroa. Quantitative PCR revealed site-specific and seasonal abundance patterns of *Endozoicomonas* spp. in toheroa populations. Although implicated in disease outbreaks elsewhere, the role of *Endozoicomonas* spp. within the Aotearoa shellfish mortality landscape remains uncertain.

4.2 Introduction

Paphies ventricosa (Māori: toheroa) is a surf clam endemic to the west and south coasts of Aotearoa. For Māori (Indigenous people of Aotearoa) in these regions (Te Tai Tokerau, Kāpiti-Horowhenua, and Murihiku), toheroa were once a staple food source and remain a species of cultural significance. At the beginning of the 1900s, a significant commercial and recreational fishery for toheroa began. The commercial fishery peaked in the early 1940s with nearly 80 tonnes of toheroa canned per annum from west coast Northland beaches (Redfearn, 1974; Williams et al., 2013b). The recreational fishery was probably larger and less managed, with anecdotal reports of up to 1,000,000 toheroa being harvested from one beach over a single weekend (Murton, 2006 and references therein). Following the collapse of toheroa populations (Ross et al., 2018a; Williams et al., 2013b), the fishery was closed (apart from a permitted customary fishery), with the last recreational open day at Oreti Beach, Southland in 1993 (McKinnon and Olsen, 1994). Although protection measures have been in place for several decades to aid their

restoration (Miskelly, 2016), populations have inexplicably failed to recover from the overexploitation of the early 20th century (Ross et al., 2018a; Williams et al., 2013b).

The list of factors possibly responsible for the continued demise of toheroa is long and includes continued harvesting (both legal and illegal), adjacent land use and its effect on habitat quality, recruitment limitation, vehicle impacts (many of the toheroa beaches are state highways), toxic algae blooms, climate change, food availability and disease (Ross et al., 2018a and references therein; Williams et al., 2013b). Although a definitive explanation for the diminished state of toheroa populations remains elusive, a recent surge in recorded shellfish mass-mortality events (MMEs) in northern Aotearoa linked to intracellular microcolonies (IMCs) of bacteria justifies a closer look at the role of disease in influencing the population dynamics and health of toheroa. (Howells et al., 2021).

Several well-studied pathogens of marine molluscs have been reported in Aotearoa, including *Perkinsus osleni* (Hine and Diggles, 2002a), *Bonamia* spp. (Lane et al., 2016) and ostreid herpesvirus 1 (OsHV-1) (Bingham et al., 2013). However, many pathogens that could impact wild and farmed mollusc populations, have not yet been reported in Aotearoa e.g., *Marteilia* spp. (Castinel et al., 2014). Until recently, the only published material of disease in toheroa was a single report of 'virus-like particles' associated with mortality events at an unspecified location in 1991, 1993, and 1994 (Hine and Wesney, 1997). No follow-up study was conducted. Instead, recent studies have focused on intracellular microcolonies of bacteria (IMCs) (Cano et al., 2020; Howells et al., 2021; Ross et al., 2018b).

IMCs are commonly referred to as *Rickettsia*-like organisms or 'RLOs', which are simply nomenclature placeholders until more data becomes available on their identification (Fournier and Raoult, 2009). As shown by Cano et al. (2018), the use of this term is not entirely accurate, where RLOs observed via histology (H&E stained) in *Pecten maximus* from Lyme Bay, United Kingdom were instead found to be attributed to *Endozoicomonas* species. Nevertheless, the use of the term RLO is commonplace in aquatic pathology, where microcolonies of bacteria dubbed 'RLOs' have been detected in many molluscs (Gollas-Galvan et al., 2014; Sun and Wu, 2004), finfish (Marcos-Lopez et al., 2017; Rozas and Enriquez, 2014), and crustaceans (Gollas-Galvan et al., 2014; Thrupp et al., 2016). Often their detection is a secondary observation made during routine histopathology surveys of farmed or wild harvest species (da Silva et al., 2015; Dorfmeier et al., 2015; Lohrmann et al., 2019). A relatively small number of dedicated studies on RLOs exist (e.g. Cano et al., 2018; Darriba et al., 2012), possibly attributed to the often-benign effects associated with RLOs (i.e., the absence of immunological responses) (Carballal et al., 2001) and asymptomatic hosts (Horwitz et al., 2016). Conversely, *Candidatus* Xenohaliotis californiensis, the bacteria attributed to withering syndrome in abalone (Di et al., 2016; Friedman et al., 2000; Moore et al., 2000), which

is responsible for massive losses of both wild and farmed abalone (Moore et al., 2002), has received considerable research effort. Hooper et al. (2019) present another case where IMCs have received dedicated study, with examination of the survival of *Endozoicomonas* spp. outside of the host *P. maximus*.

Some studies that mention IMCs do not attribute inclusions to major pathomorphological impacts in hosts (Carballal et al., 2001; Horwitz et al., 2016). On the other hand, hypertrophy of cells and lysis is commonly reported (Ceuta and Boehs, 2012; Hine and Diggles, 2002b; Tinelli et al., 2020; Villalba et al., 1999), typically in the gill and digestive gland epithelia of hosts. On occasion, IMCs have been associated with MMEs or population decline (Cano et al., 2020), for instance in abalone (Crosson et al., 2014; Moore et al., 2000), king scallops (Cano et al., 2018; Le Gall et al., 1988), oysters (Wu et al., 2005), and several clam species (Norton et al., 1993; Villalba et al., 1999; Zhu et al., 2012). In cases where mortality has been associated with IMCs, drivers of pathogenesis are often considered (Wu et al., 2005; Zhu et al., 2012) but are rarely examined experimentally (excl. withering syndrome in abalone, Ben-Horin et al., 2013).

Routine histopathology seasonal surveys of important bivalves have observed seasonal infection patterns of IMCs (Ceuta and Boehs, 2012; Dorfmeier et al., 2015). Again, due to the typically benign prognoses made in association with IMCs, investigatory pathology tends to stop here, without characterising the aetiological agent in question (e.g., electron microscopy or PCR) (Travers et al., 2015). Therefore, terms like ‘RLO’ or ‘*Rickettsia*-like’ persist in the literature, despite the influence some IMCs appear to have on host populations (Cano et al., 2020). The characterisation of a pathogen is a critical first step towards understanding its impact (Cano et al., 2018; Friedman et al., 2000; Hewson et al., 2014). Without correct diagnosis, linking mortalities to environmental drivers and establishing trends is reductive, illustrated currently by the perplexing case of sea star wasting disease (Hewson et al., 2014). In the case of withering syndrome in abalone, IMCs were at first dismissed as benign (as they often are) delaying a correct diagnosis for almost 10 years following the first observations of mortalities in the late 1980s (Friedman et al., 2000; Gardner et al., 1995), at which point the disease outbreak had caused catastrophic losses of wild populations, particularly black abalone (*Haliotis cracherodii*).

The IMCs in toheroa tissues reported on by Ross et al. (2018b) were subsequently identified as *Endozoicomonas* spp. by Howells et al. (2021). Howells et al. (2021) found little genetic variation between strains derived from the same host species. Furthermore, *Endozoicomonas* DNA sequences isolated from several clam species in Aotearoa (*P. ventricosa*, *Paphies australis*, *Paphies subtriangulata*, *Paphies donacina*, and *Dosinia anus*) were 100% identical (Howells et al., 2021; Howells et al., 2019), and were 95-97% similar to *Endozoicomonas* sp. strain S-B4-1U (NCBI accession no.

KX611231.1). Cano et al. (2020) reported on *Endozoicomonas* spp. in toheroa and other marine molluscs. An operational taxonomic unit (OTU) taxonomically assigned to the *Endozoicomonas* genus was found to be present in toheroa at low abundance. The same OTU was found in high abundance in *Mizuhopecten yessoensis* from Japan. Furthermore, reference was made to an OTU present in toheroa, which was found to be closely related (94.5%, NCBI accession no. U77480.1) to a sulfur-oxidising endosymbiont found in tubeworms (*Ridgeia piscesae*) (Cano et al., 2020). This opens an intriguing avenue for exploration of the microbiota associated with toheroa.

It is possible that like many cases globally, the IMCs recorded in toheroa are benign, or at least are benign under certain environmental conditions. Nevertheless, the limited recovery of toheroa to-date is puzzling to researchers and fisheries managers. If only to eliminate disease as a factor contributing to their failed recovery, an in-depth investigation of the IMCs first detected by Ross et al. (2018b) is necessary. Consequently, in this study I investigate and characterise the IMCs present in toheroa using molecular tools and histopathology. Additionally, seasonal abundance patterns of *Endozoicomonas* spp. are examined at Ripiro Beach, the largest remaining toheroa population in northern Aotearoa.

4.3 Methods

4.3.1 Site Description and Sample Collection

Toheroa were sampled from four locations across the entire latitudinal distribution of the species (Fig. 4.1): Ninety Mile Beach (Te-Oneroa-a-Tōhē) and Ripiro Beach on the west coast of northern Aotearoa; Foxton Beach in the Kāpiti-Horowhenua region; and Oreti Beach on the south coast of the South Island. Bi-monthly sampling was conducted at three sites at Ripiro Beach (Island, Kopawai, and Mahuta Gap; n = 180) between March 2019 and January 2020 (these are the same specimens as those in Chapter 3). Single collections were made from Ninety Mile Beach (n = 15), Foxton (n = 3) and Oreti Beach (n = 40) with the timing of these being opportunistic (Table 4.1). All sampling locations are typical habitats favoured by toheroa: long, wide and mostly high-energy surf beaches (Fig. 4.1) (Williams et al., 2013; Ross et al., 2017). At Ripiro Beach, the three sites used represent different habitat types. At Mahuta Gap and Kopawai, freshwater streams flow onto the beach and over toheroa beds. At Island, no freshwater stream is present, at times, an overland ephemeral flow is present but the toheroa bed at this site is typically outside of the transient flow path.

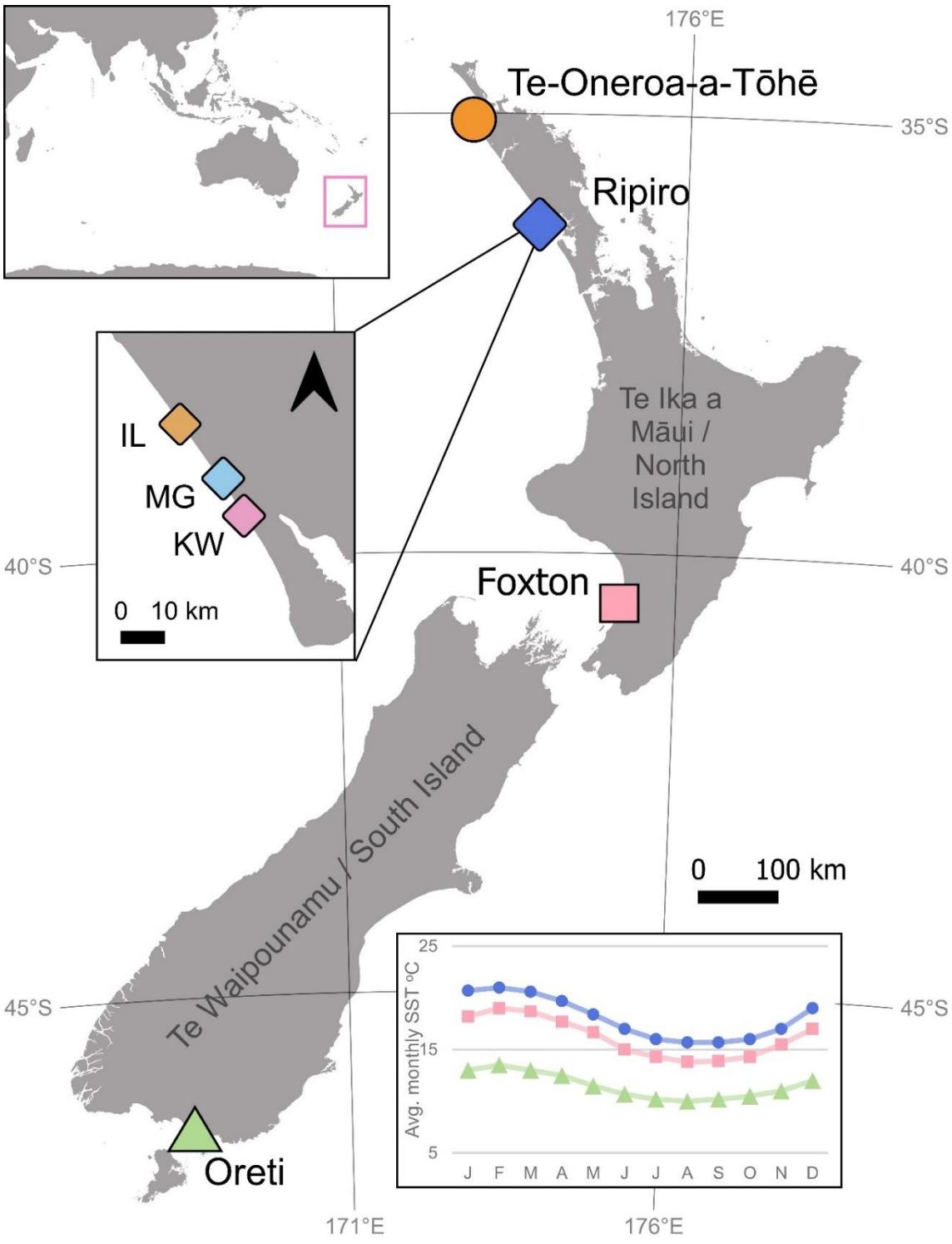

Fig. 4.1. Sampling locations in the North and South Islands of Aotearoa (New Zealand). Insert: sea surface temperature obtained from www.seatemperature.org. Average temperatures given close to respective sampling regions, Te-Oneroa-a-Tōhē, Ripiro, Foxton and Oreti beaches (line colour corresponds to respective sites). IL: Island, MG: Mahuta Gap, KW: Kopawai. Produced using Quantum GIS v3.8 Zanzibar. Spatial data obtained from DIVA-GIS. CRS: WGS 84 (EPSG: 4326).

Toheroa were hand dug, generally specimens >45 mm in length were sampled, though grading was not strict. Toheroa are protected, and their collection is restricted under Fisheries Regulations 2013 (SR 2013/482 r25). Specimens were subsequently gathered under special permit issued by Fisheries New Zealand (Special Permit no.706-2). To investigate what impact population density might have on IMC intensity, random quadrats (0.25 m^2) were hand dug (~15 cm in depth) at three sites at Ripiro Beach (Island, Mahuta Gap, and Kopawai) in November 2019 to estimate density per m^2 in toheroa beds. In total, 14 quadrats were excavated. Following specimen collection, tissue samples (gills and digestive gland) were stored in 70% EtOH until DNA extraction. The remaining tissue was placed in 10% formalin for histology (see below).

4.3.2 Histology

To examine toheroa tissues for the presence of IMCs, all specimens were fixed in 10% formalin (formaldehyde/seawater solution) for a maximum of 48 hours. Specimens were trimmed (cross-section) encompassing all major organs (with particular care to capture gill and digestive gland tissues) and placed in histological tissue cassettes and stored in 70% EtOH. Fixed and trimmed tissue sections in tissue cassettes were ethanol treated, set in paraffin wax, and stained using haematoxylin and eosin (H&E) at SVS Laboratories Ltd., Hamilton. Stained histological tissue sections were viewed using an Olympus BX53 light microscope. Each sample was examined for the presence of IMCs, any other pathological abnormalities, and inflammation.

4.3.3 DNA Extraction and Quantitative PCR

Gill (20 mg) and digestive gland tissues (5 mg) were combined and macerated using a scalpel and placed into 1.5 ml microcentrifuge tubes (n = 237). Tissue digest buffer (180 µl) and digest enzyme (20 µl proteinase K) were added to each tissue containing tube and lysed overnight at 56 °C on a heat-shaking platform. DNA extraction was carried out using the QIAamp® DNA Mini Kit (Qiagen, Valencia, CA, USA), following manufacturer's instructions. The presence of amplifiable DNA within the extract was confirmed by using an 18S rRNA internal control (Life Technologies Ribosomal 18S rRNA Endogenous Control).

Quantitative PCR (qPCR) was used to examine the prevalence and intensity of *Endozoicomonas* spp. in toheroa (n = 237). Using a CFX Real-Time thermal cycler (Bio-Rad), a forward primer NZELO-F (5'-AAGGAACACCAGTGGCGAA-3') was paired with the reverse primer NZELO-R (5'-TAGTAGACATCGTTTACGGCGT-3') with an internal probe NZELO-Pr (5'-56-FAM-TCAGCGTCAGTGTCAGACCAGAGTGT-3BHQ_1-3') to amplify 118 bp region of the *Endozoicomonas* spp. 16S rRNA gene (Howells et al., 2021).

The PCR mix consisted of the following per reaction: 6.5 µl ultrapure H_2O, 10 µl PerfeCTa qPCR ToughMix, 0.6 µl NZELO-F (300 nM), 0.6 µl NZELO-R (300 nM), 0.3 µl of NZELO-Pr (150 nM) and 2 µl DNA template (*c.* 130 ng μl^{-1}). The reaction was incubated at 95°C for 2 minutes, the reaction then went through 40 cycles of a denature step at 95°C for 5 seconds, and an annealing and extension step at 66°C for 5 seconds. Positive controls were used based on *Endozoicomonas elysicola* (NR_041264), gBlock® gene fragment. Three positive controls were used ($1x10^{-4}$, $1x10^{-5}$, and $1x10^{-6}$ ng μl^{-1}) in duplicate. The 16S rRNA gene copy number for each sample was determined by means of a standard curve, constructed using the positive controls (see Appendix D, Figs. D.2 & D.3).

4.3.4 DNA Sequencing and Nucleotide Data Processing

Using conventional PCR, primer pairs ECF ('5-AACTGGGCAGCTAGAGTGCGG-3') and ECR ('5-GTCACCGGCAGTCTCCCCAGA-3') amplified a 528 bp fragment of the 16S rRNA gene (Mendoza et al., 2017). For each reaction, the PCR mix consisted of the following: 12.5 µl Kapa 2G Fast Ready Mix, 9.5 µl ultrapure H_2O, 1 µl ECF (400 nM), 1 µl ECR (400 nM), and 1 µl DNA template (*c.* 130 ng μl^{-1}). The reaction was incubated at 95 °C for 2 minutes, then went through 35 cycles of a denature step at 95 °C for 10 seconds, an annealing step at 60°C for 10 seconds, and an extension step at 72 °C for 1 second (Howells et al., 2021). All PCR runs included a negative and positive control. All amplified PCR products were gel-cut and purified using a Zymoclean™ Gel DNA Recovery Kit, following the manufacturer's instructions (Zymo Research, Irvine, CA, USA) and then quantified using a Qubit Fluorometer (Life Technologies, Auckland). The purified PCR products were sequenced in the forward and reverse direction at the Waikato DNA Sequencing Facility. Aligned sequences were trimmed and manually checked to identify any errors in base pair calling using Geneious v.9 (Kearse et al., 2012), resulting in a sequence of *c.* 500 bp. Consensus sequences were compared to published sequences using the National Centre for BioTechnology Information (NCBI) nucleotide BLAST tool (Johnson et al., 2008).

Sequences of the 16S rRNA gene of *Endozoicomonas* spp. from Ninety-Mile Beach (*n* = 3), Ripiro Beach (*n* = 11), Foxton (*n* = 1), and Oreti Beach (*n* = 4) toheroa specimens were used to create phylogenetic trees. The relationship of these Aotearoa *Endozoicomonas* spp. was compared to published *Endozoicomonas* spp. sequences and other aquatic bacteria. All nucleotide sequences were imported into Geneious v.9 (Kearse et al., 2012) aligned using default parameters (global alignment 70% similarity), and a neighbour-joining tree was constructed using the Jukes-Cantor substitution matrix with 100,000 bootstrapped replicates. Sequences have been deposited in the GenBank database. Accession numbers: MZ540688 and MZ540689.

4.3.5 In situ *Hybridization*

In situ hybridization (ISH) was used to confirm inclusions observed using histology were *Endozoicomonas* species. Dioxigenin (DIG)-labelled ISH probe was prepared using the DIG PCR probe synthesis kit (Roche Diagnostics). DIG-labelled PCR products were generated using ECF ('5-AACTGGGCAGCTAGAGTGCGG-3') and ECR ('5-GTCACCGGCAGTCTCCCCAGA-3') primers following manufacturer's protocol. Tissue sections were processed for ISH as previously described (Bueno et al., 2017; Howells et al., 2021). Tissues were considered *Endozoicomonas* spp. positive if dark blue precipitates were observed using an Olympus BX53 light microscope. ISH was carried out on specimens (n = 5) collected from various toheroa populations (Oreti Beach, Foxton Beach and Ripiro Beach). Specimens chosen were first confirmed IMC-positive by histology before attempting ISH. Negative controls prepared alongside IMC-positive samples worked as expected.

4.3.6 Data Analyses and Visualisation

To examine the degree in which *Endozoicomonas* spp. abundance varied over space and time, Kruskal-Wallis tests were used on 16S rRNA gene copy data derived by qPCR. If Kruskal-Wallis tests indicated a statistically significant difference (95% confidence) between groups (sampled sites or months), Dunn tests were used to investigate where these differences lay. To avoid committing Type I Error, p-values were adjusted using Bonferroni's correction, accounting for multiple comparisons. All statistical analyses were carried out in RStudio (R Core Team, 2013) and data visualisation was achieved using ggplot2 (Wickham, 2009). Kruskal-Wallis and Dunn tests were carried out using the 'Dunn test' package (Dinno, 2015; Dinno and Dinno, 2017) in RStudio. A map of sampling locations (Fig. 4.1) was produced using Quantum GIS v3.8 Zanzibar with spatial data from DIVA-GIS (diva-gis.org).

4.4 Results

4.4.1 Histology and In situ *Hybridization*

Histological examination of toheroa tissues revealed spatial and temporal differences in IMC prevalence. IMCs were typically detected in the gills (Fig. 4.2), and only occasionally in the digestive gland. Morphologically, inclusions did not vary substantially in shape and size, typically measuring 20-25 µm along the longest axis. At Ripiro Beach, IMC prevalence was highest in March 2019 (77%) and lowest in January 2020 (33%). Prevalence was 3% at Oreti Beach (February 2019), 33% at Foxton (March 2019), and 13% at Ninety Mile Beach (Nov 2019). Haemocyte and lipofuscin

accumulations (Fig. 4.2, B) were routinely observed in toheroa tissues, but no direct link to IMCs was made.

ISH labelling of bacterial inclusions in the gills and digestive gland confirmed the presence of *Endozoicomonas* in toheroa tissues. Dark blue staining of inclusions in the gills and digestive glands confirmed the inclusions observed via histology were *Endozoicomonas* spp., validating the use of the target 16S rRNA gene described above. Most of the ISH labelling was observed in the gills (Fig. 4.2, C-E & Fig. D.1), although to a much lesser degree, dark blue ISH positive intracellular microcolonies of bacteria were observed in the digestive gland (Fig. 4.2, F).

4.4.2 Distribution and Phylogeny of Endozoicomonas *Species*

Phylogenetic analysis of the 16S rRNA gene sequences from this study, and including several similar intracellular and marine bacteria, showed the toheroa IMC to be a member of the *Gammaproteobacteria* subgroup of the *Proteobacteria*, showing closest similarity to *Endozoicomonas* spp. isolated from marine organisms (Fig. 4.3).

Sequences obtained from the North Island (Ninety Mile, Ripiro, and Foxton Beach) were 100% similar, and sequences obtained from Oreti Beach were 100% similar. When these sequences were compared, they were found to be closely related (99.2% identity). The North Island sequence (Toheroa-North) was found to be identical (100% identity) to a sequence previously reported in several clam spp. from Aotearoa (Howells et al., 2021). Both sequences were also closely related to the sequence previously reported in *Pecten novaezelandiae*, New Zealand scallop (97.1% similar, Fig. 4.4). The Oreti Beach sequence was more closely related to a sequence reported by Howells et al. (2021) from *Perna canaliculus*, green-lipped mussels (94.2%) than the North Island sequence (93.6%) (Fig. 4.4 & Table 4.2). When the sequences were compared to internationally published sequences, both were found to be closely related to *Endozoicomonas elysicola* (NCBI accession no. NR_041264.1), with 97.5% identity.

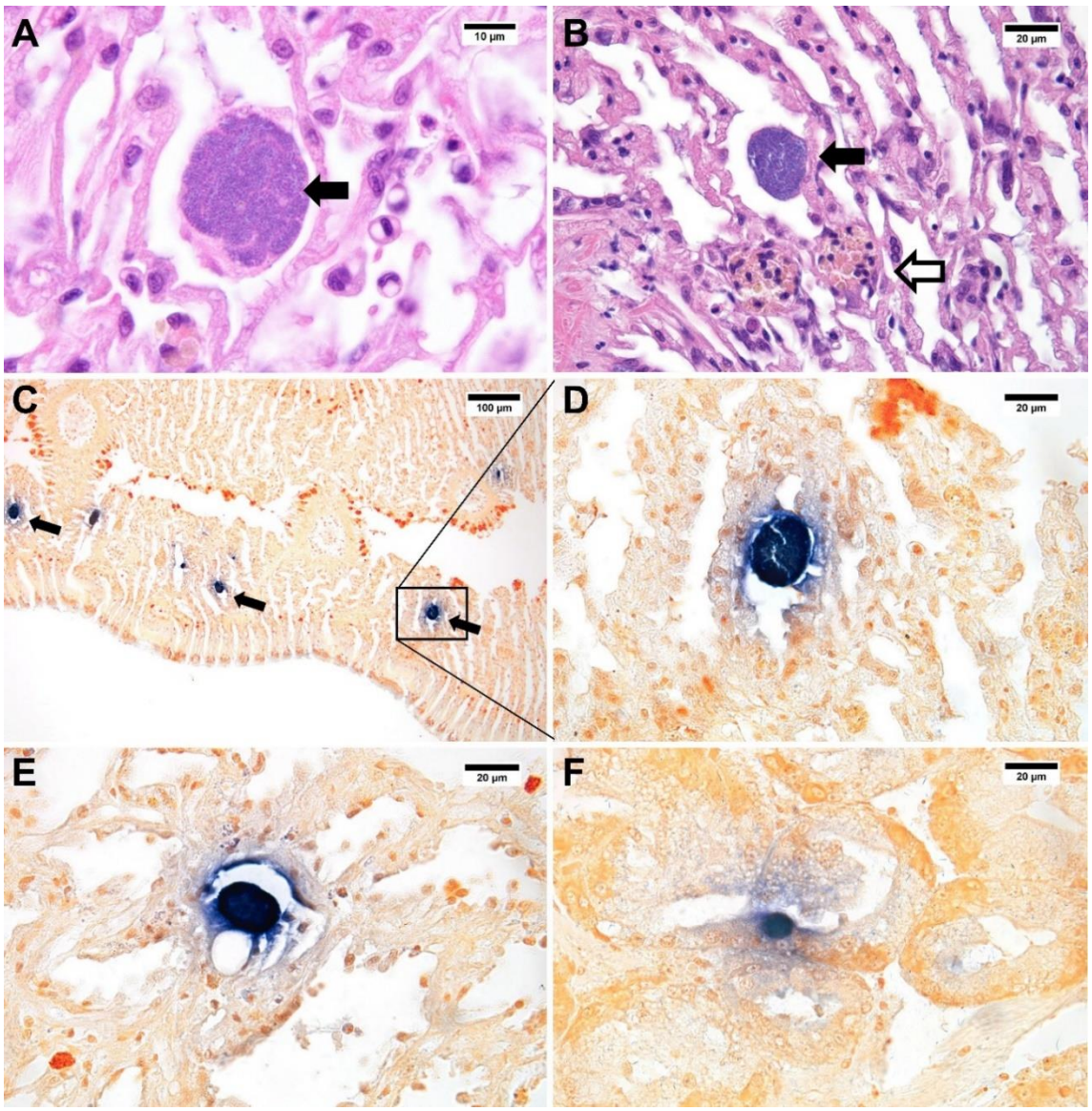

Fig. 4.2. Photomicrographs of toheroa (*P. ventricosa*) tissues. A and B: H&E-stained tissue sections of toheroa gills showing the presence of intracellular microcolonies of bacteria (filled arrows) and lipofuscin pigmented cells (hollow arrows) at x100 under oil. C, D, and E: *In situ* hybridization using *Endozoicomonas* spp. specific probe in the gills of toheroa (x20 and x100 under oil). Dark blue stain indicates a positive reaction with *Endozoicomonas* spp. genetic material. F) *In situ* hybridization in the digestive gland with a dark blue inclusion indicating the presence of *Endozoicomonas* spp. genetic material (x100, under oil). H&E and ISH stained tissue sections viewed using an Olympus BX53 and photographed using an Olympus DP27.

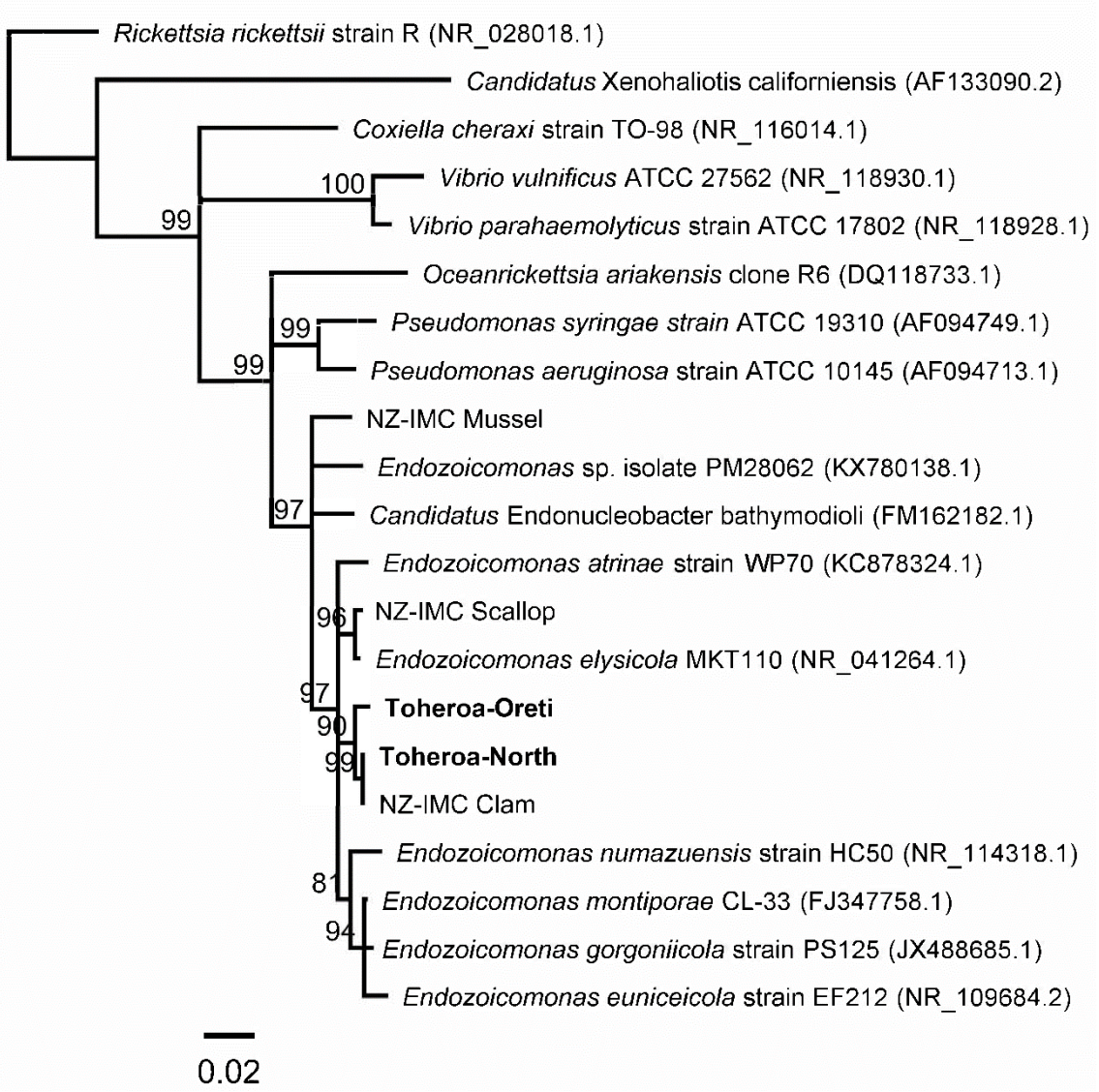

Fig. 4.3. Phylogenetic tree showing genetic relatedness of amplified 16S rRNA gene sequences isolated from toheroa (*P. ventricosa*) from four locations (Fig. 4.1) in Aotearoa (bold font), to other marine bacteria from around the world. Branches labelled with consensus support (%) based on 100,000 bootstrapped replicates and NCBI accession numbers.

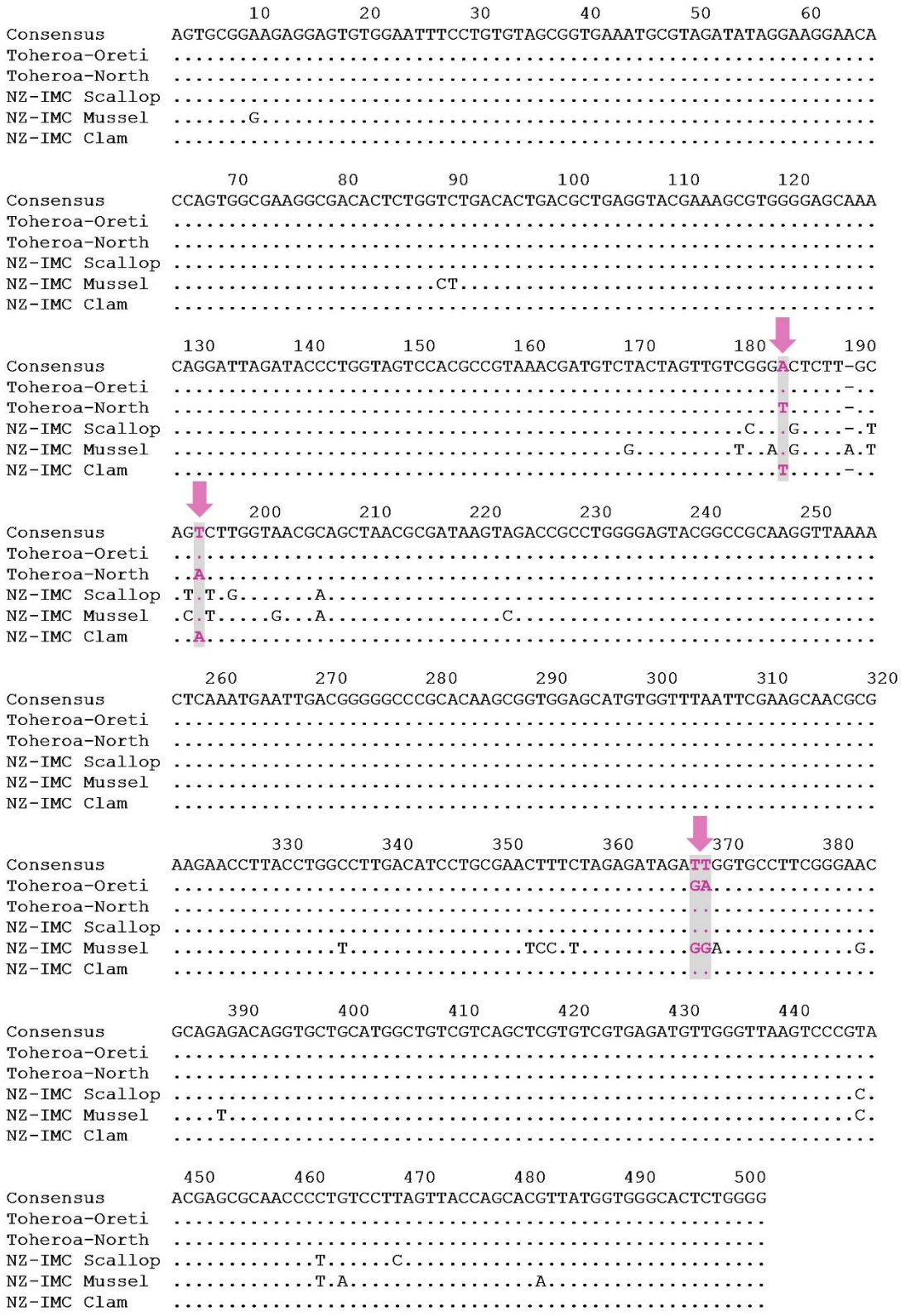

Fig. 4.4. *Endozoicomonas* spp. 16s rRNA gene alignment. Sequences (500 bp) derived from toheroa tissues are shown, Toheroa-North (Ninety Mile, Ripiro, and Foxton) and Toheroa-Oreti (Toheroa sampled from Oreti Beach). Sequences from Howells et al. (2021) are also shown. NZ-IMC Clam (*A. stutchburyi, P. australis, P. subtriangulata, P. donacina, D. anus*), NZ-IMC Scallop (*P. novaezelandiae*), and NZ-IMC Mussel (*P. canaliculus*). Key differences/similarities between sequences are marked with an arrow.

Table 4.1. Summary table showing the sites which were sampled for toheroa, the month and the number of specimens gathered, *n*. Prevalence of IMCs determined by histology and prevalence of *Endozoicomonas* spp. determined by qPCR is shown. IL: Island, MG: Mahuta Gap, KW: Kopawai.

Location	Sites	Date	*n*	Sea temp. (°C)	Air temp. (°C)	Prevalence (%) histology	Prevalence (%) qPCR
Ninety Mile	-	Nov-19	15	17[a]	-	13	100
Ripiro	IL, MG, KW	Mar-19	29	19[b]	25	77	90
	IL, MG, KW	May-19	30	17[b]	18	70	97
	IL, MG, KW	Jul-19	30	12[b]	9	37	80
	IL, MG, KW	Sep-19	30	14[b]	13	37	73
	IL, MG, KW	Nov-19	30	17[b]	17	40	87
	IL, MG, KW	Jan-20	30	19[b]	20	33	73
Foxton	-	Mar-19	3	19[a]	-	33	33
Oreti	-	Feb-19	40	16[a]	-	3	88

[a]Mean monthly sea surface temperature (11 µ daytime), retrospectively obtained from NOAA (MODIS-Aqua) and extracted using SeaDAS v.7.5.3. Based on *c.* 1232 km^2 bounding box encompassing study area.
[b]Gathered on site

4.4.3 Abundance Patterns of Toheroa IMCs

Quantitative PCR based on the 16S rRNA gene revealed differences in the abundance of *Endozoicomonas* spp. in geographically and locally separated populations. Moreover, qPCR revealed temporal variability of *Endozoicomonas* spp. abundance in toheroa at Ripiro Beach sampled between March 2019 and January 2020. A higher prevalence was detected by qPCR than observed by histology across all sites (Table 4.1). The other exception was Ninety Mile Beach, where histology prevalence was 13% and qPCR detection was 100%. The temporal variation of IMC prevalence detected via histology was complimented by qPCR, with the highest number of qPCR positive toheroa in May 2019 (97%) and the lowest in September 2019 and January 2020 (both 73%).

Quantitative PCR also revealed varying *Endozoicomonas* spp. abundance between sampling locations based on 16S rRNA gene copy numbers (Fig. 4.5). A Kruskal-Wallis test indicated a statistically significant difference between sampling locations (X^2 = 37.46, df = 4, p = <0.001). Further, Dunn tests releveled that abundance was greatest in Ripiro (March) and Ninety-Mile Beach (November) (Fig. 4.5). The lowest gene copy numbers were in Foxton, Oreti and Ripiro Beach (November) specimens. The specimens with the joint highest numbers of gene copies were collected from Ripiro (March) and Ninety Mile (November) (Z = -0.7, p = 1.00), which had an order of at least one log greater than the joint lowest, Oreti Beach and Ripiro (November) (Z = -0.1, p = 1.00).

Based on *Endozoicomonas* spp. 16S rRNA gene copy numbers pooled for each site at Ripiro Beach (Island, Mahuta Gap, and Kopawai), overall a statistically significant difference was found (X^2 = 7.84, df = 2, p = 0.02). Dunn tests revealed samples from Kopawai had the greatest gene copy number compared to samples from Mahuta Gap (Z = 2.4, p = 0.024) and Island (Z = -2.4, p = 0.022). See Tables D.1-D.4 for further details. Seasonal patterns of *Endozoicomonas* spp. abundance in toheroa tissues were found for the Mahuta Gap (X^2 = 27.12, df = 5, p = <0.001) and Kopawai (X^2 = 23.57, df = 5, p = <0.001) sites. At the Island site, no statistically significant seasonal pattern was identified (X^2 = 8.45, df = 5, p = 0.13), though abundance varied greatly between individuals sampled at the same time and between sampling occasions (Fig. 4.6). At Mahuta Gap and Kopawai, the greatest seasonal variation is observed between summer (March) and autumn/winter (July and September). A significant drop in *Endozoicomonas* spp. gene copies can be seen at these sites, which is not represented at the Island site (Fig. 4.6 & Tables D.5 & D.6). For instance, in September the median number of gene copies recorded in toheroa from Mahuta Gap was 5, compared to 29,885 in May (Z = 4.3, p = <0.001). Similarly, at Kopawai, the median number of *Endozoicomonas* spp. gene copies detected in toheroa tissues in September was 673, compared to 93,453 in March (Z = 3.4, p = 0.005). Moving towards summer (January), gene copy numbers recorded in toheroa tissues from Mahuta Gap and Kopawai specimens increased to levels like that of counterparts collected pre-autumn/winter at these sites (Fig. 4.6).

Table 4.2. Phylogenetic distance matrix of *Endozoicomonas* spp. in toheroa from Foxton (n = 1), Oreti (n = 4), Ripiro (n = 11), and Ninety Mile Beach (n = 3). Sequences from Howells et al. (2021) derived from several shellfish species are included in the matrix. NZ-IMC Clam (*A. stutchburyi, P. australis, P. subtriangulata, P. donacina, D. anus*), NZ-IMC Scallop (*P. novaezelandiae*) and NZ-IMC Mussel (*P. canaliculus*). Figures are genetic relatedness expressed as percentage (%) identity match.

	Ninety-Mile	**Ripiro**	**Foxton**	**Oreti**	**NZ-IMC Clam**	**NZ-IMC Scallop**
Ripiro	100	100				
Foxton	100	100	100			
Oreti	99.2	99.2	99.2			
NZ-IMC Clam	100	100	100	99.2	100	
NZ-IMC Scallop	97.1	97.1	97.1	97.1	97.1	
NZ-IMC Mussel	93.6	93.6	93.6	94.2	93.6	95.1

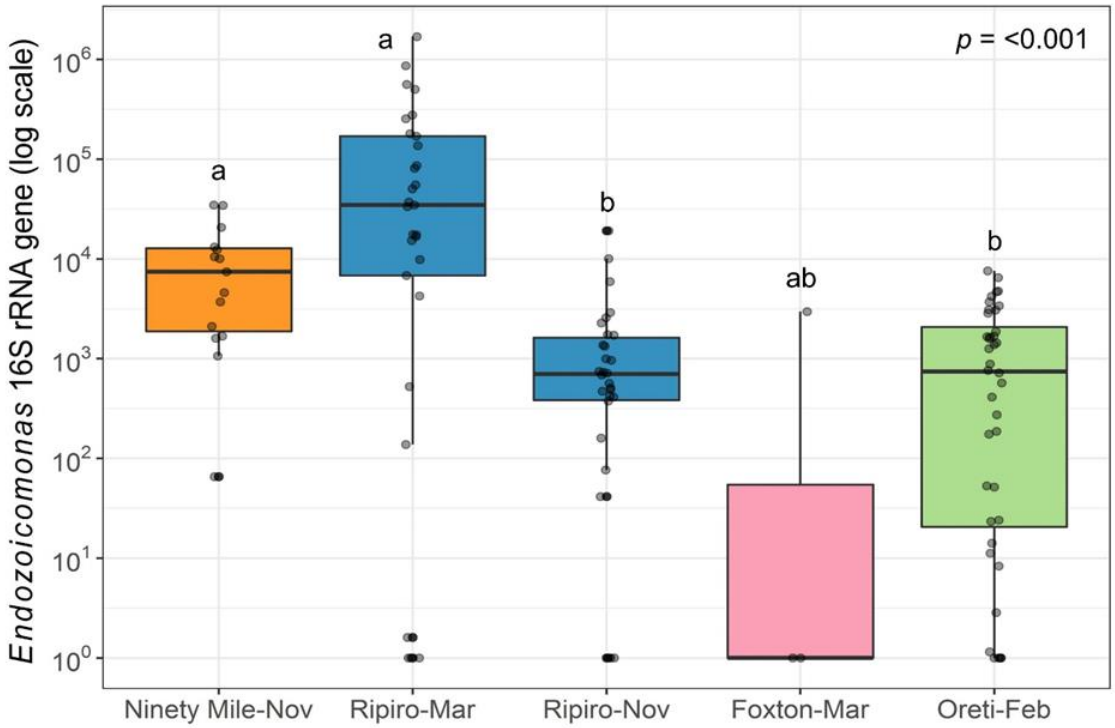

Fig. 4.5. Geographic and temporal variation of *Endozoicomonas* spp. abundance in toheroa tissues based on copy numbers of the *Endozoicomonas* 16S rRNA gene (qPCR). Four significant toheroa sites around Aotearoa are represented: Oreti Beach (*n* = 40), Foxton Beach (*n* = 3), Ripiro Beach (March and November) (*n* = 59) and Ninety Mile Beach or Te-Oneroa-a-Tōhē (*n* = 15). Gene copy numbers are log transformed. Box plots represent gene copy numbers over time and between sites, line: median, box: interquartile range, whiskers: min/max, dots: possible outliers. Kruskal-Wallis test *p*-values are shown (top right). If boxes do not share letters, corresponding distributions are significantly different (Dunn test, Bonferroni correction).

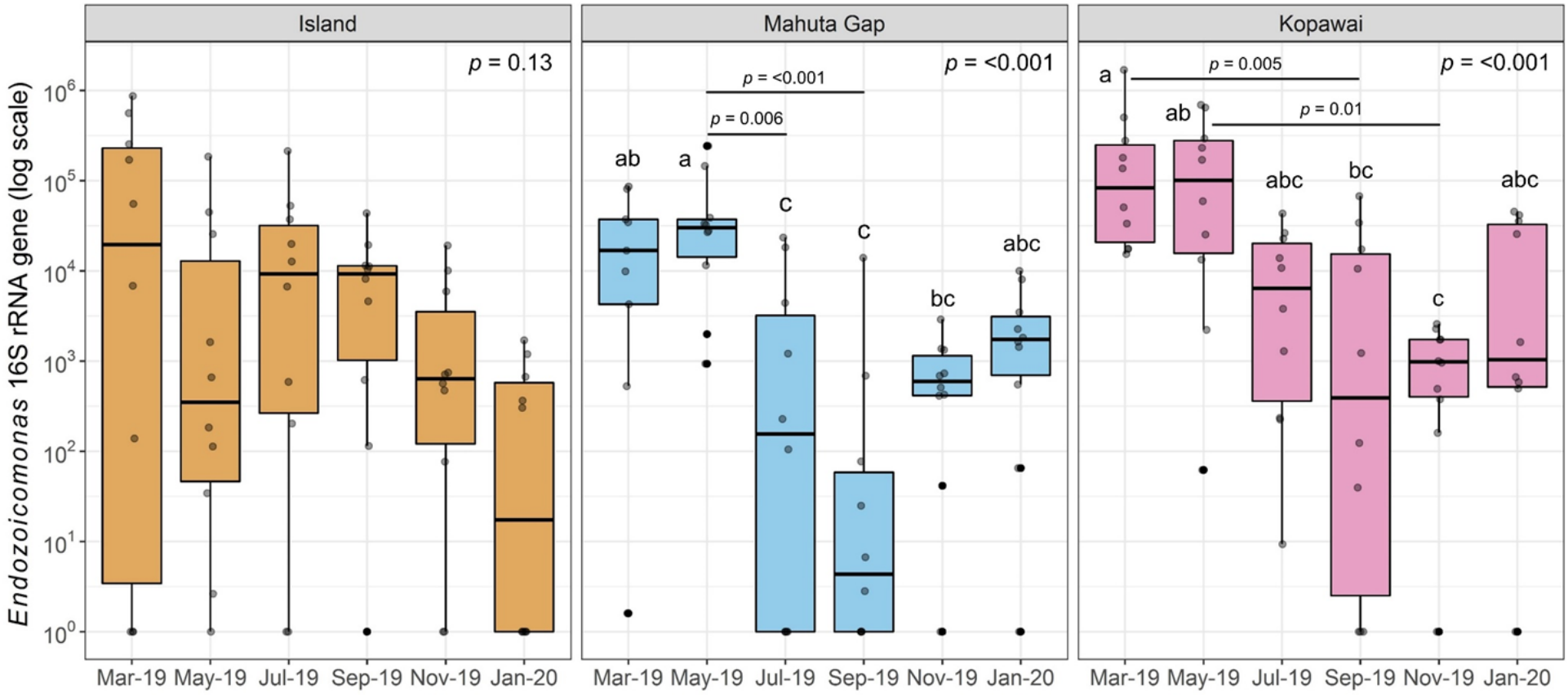

Fig. 4.6. Seasonal patterns of *Endozoicomonas* spp. abundance in toheroa tissues. Three sites at Ripiro Beach are represented, Island, Mahuta Gap and Kopawai, *n* = 10 for each box (except Mahuta Gap in Mar-19 where *n* = 9). Line: median, box: interquartile range, whiskers: min/max, dots: possible outliers. Kruskal-Wallis test *p*-values are shown (top right). If boxes do not share letters, corresponding distributions are significantly different (Dunn test).

Toheroa bed density estimates (m^2) for sites at Ripiro Beach in November 2019 are shown in Table 4.3. A Kruskal-Wallis test indicated that *Endozoicomonas* spp. abundance in toheroa tissues did not differ significantly (p = >0.8) between sites in November 2019.

Table 4.3. Toheroa bed density (mean and standard error) at three sites at Ripiro Beach in November 2019 and corresponding *Endozoicomonas* spp. gene copies detected in toheroa tissues from specimens gathered at the same time.

	Toheroa bed density (m^2)		***Endozoicomonas* spp. gene copies**		**Prevalence (%)**
Site	Mean	SE	Median	Range	qPCR-positive
Island	224	49.9	639	0-19087	80
Mahuta Gap	65	21.1	597	0-2891	90
Kopawai	284	32.2	977	0-2564	90

4.5 Discussion

This study set out to characterise the IMCs present in toheroa populations across Aotearoa and gather a benchmark of their abundance in remaining toheroa populations. The consensus 16S rRNA gene sequence for the North Island (Ninety Mile, Ripiro, and Foxton Beach) was 100% identical to the sequence previously reported by Howells et al. (2021) from toheroa, and several other clam spp. (Fig. 4.3, 4.4 & Table 4.2). Both unique sequences reported here were closely related to *Endozoicomonas elysicola* (Fig. 4.3), isolated from the sea slug *Elysia ornate* (Kurahashi and Yokota, 2007), and collected off the coast of Japan. Genetic distances indicated that the *Endozoicomonas* spp. from toheroa (Northern sites and Oreti) are similar to *Endozoicomonas* spp. reported in New Zealand scallops (*P. novaezelandiae*) (Fig. 4.3). The two sequences from this study were differently related to *Endozoicomonas* spp. reported in green-lipped mussels, with the Oreti sequence being genetically more similar (94.2%) than the sequence for northern toheroa (93.6%). It is possible that these differences represent different *Endozoicomonas* species or strains in toheroa. Howells et al. (2019) recently showed using high throughput sequencing that multiple *Endozoicomonas* spp. could be present in several Aotearoa shellfish species, including toheroa and other members of the *Paphies* genus, *P. subtriangulata* (tuatua), and *P. australis* (pipi).

Phylogenetic distances between the sequences in this study and those previously reported in other marine organisms provide conflicting evidence of a geographic pattern of genetic dissimilarity. For instance, the sequences in this study were most genetically similar to those previously reported in shellfish from Aotearoa (Howells et al., 2021). The next most closely related sequence was *E. elysicola*, reported

from Japan (Kurahashi and Yokota, 2007), followed by *E. montiporae* isolated from a coral from southern Taiwan (Yang et al., 2010). Three sequences were found to be nearly equally dissimilar (*c.* 94%) to those reported here, *Endozoicomonas* sp. isolate PM28062 (NCBI accession no. KX780138.1) reported in king scallops (*P. maximus*) from the Lyme Bay MPA, United Kingdom (Cano et al., 2018), *Candidatus* Endonucleobacter bathymodioli isolated from bathymodiolin mussels, from the Gulf of Mexico (Zielinski et al., 2009) and *Endozoicomonas* sp. isolated from green-lipped mussels from Aotearoa (Howells et al., 2021). In this way, a geographic pattern of genetic dissimilarity appears to exist, with greater genetic difference with increasing geographic distance from Aotearoa, except for the *Endozoicomonas* sp. isolate from green-lipped mussels from Aotearoa (Fig. 4.3).

While the genus *Endozoicomonas* is typically associated with the bacterial community of corals (Ding et al., 2016; van de Water et al., 2017; Ziegler et al., 2016), *Endozoicomonas* spp. have also been recorded in a variety of marine species (Neave et al., 2016, and references therein), including marine molluscs (Cano et al., 2020; Howells et al., 2021). Since the description of the genus *Endozoicomonas* (Kurahashi and Yokota, 2007), they have been shown to be diverse endosymbionts with a global distribution (Neave et al., 2016). Their functional diversity appears to be extensive too (Neave et al., 2017), with *Endozoicomonas* spp. associated with host nutrition and health, biogeochemical cycling, and antibiotic production (reviewed in Neave et al., 2016). Links to disease have been made in fish (Mendoza et al., 2013), corals (Ziegler et al., 2016) and shellfish (Cano et al., 2020; Cano et al., 2018; Hooper et al., 2019; Howells et al., 2021). Moreover, Schill et al. (2017) found that the gill microbiome of blue mussel, *Mytilus edulis* in Barnegat Bay, New Jersey was dominated by *Endozoicomonas* spp., with 41.9-90.3% of the gill bacterial community and 4-71.8% of the digestive bacterial community consisting of *Endozoicomonas* spp. (Schill et al., 2017). Similarly, Rossbach et al. (2019) found that the bacterial community of giant clam *Tridacna maxima* gills from the Red Sea were dominated by '*Endozoicomonadaceae'* taxa, a recently proposed family including the genus *Endozoicomonas* (Bartz et al., 2018). While there is substantial evidence that *Endozoicomonas* spp. are important endosymbionts in several hosts, genome decay has been reported in several strains by Qi et al. (2018), and a small draft genome (4.83 Mb) was reported by Cano et al. (2018) in *P. maximus* compared to other published strains (>5.6 Mb, Neave et al., 2014). A loss of regulatory genes, metabolic capacity, and an expansion of virulence genes (Cano et al., 2018; Qi et al., 2018) suggests some strains might be undergoing a niche shift.

Quantitative PCR revealed a seasonal pattern of *Endozoicomonas* spp. abundance, with specimens collected in March 2019 (end of summer) presenting the highest number of *Endozoicomonas* spp. 16S rRNA gene copies (Fig. 4.6 & Table 4.4).

For specimens gathered from Kopawai and Mahuta Gap, similar seasonal patterns were found (Fig. 4.6) with substantially decreased *Endozoicomonas* abundance in tissues in July and September (winter/spring). This could be attributed to seasonality (see air temperature, Table 4.1). However, this pattern was not observed for all sites. For specimens gathered at Island, no statistically significant difference of *Endozoicomonas* spp. abundance was found over time (Fig. 4.6).

Table 4.4. Median number of *Endozoicomonas* spp. gene copies determined from toheroa tissues (qPCR) calculated for sites with freshwater streams present (Kopawai and Mahuta Gap) and typically no freshwater outflow present (Island). Total rainfall 30 days prior to specimen collection was obtained from www.nrc.gov.nz. Rainfall data was obtained from the closest rainfall station at Kai Iwi Lakes *c.* 10 km from the closest site at Ripiro Beach.

	Total rainfall (mm)	**Median *Endozoicomonas* spp. gene copies**	
		Freshwater stream present	No freshwater stream
Late-summer (Mar-19)	31	34491	30961
Mid-winter (Jul-19)	184	1247	9665
Early-spring (Sept-19)	72	32	9246

A reason for this disparity could be freshwater outflow. For example, van de Water et al. (2017) found that the microbiome of soft corals in the Mediterranean were susceptible to manipulation from local disturbance. The microbiome of coral specimens was typically dominated by *Endozoicomonas*, but in Majorca (Spain) and Portofino (Italy), freshwater outflow in the form of submarine groundwater discharge after heavy rains between sampling periods (and subsequent nutrient influx) were linked to altered bacterial communities, where *Endozoicomonas* spp. abundance was considerably lower (van de Water et al., 2017). Toheroa tend to aggregate in dense beds close to or within freshwater streams (Beentjes, 2010a; Beentjes, 2010b; Ross et al., 2018a; Williams et al., 2013a). This reduction in *Endozoicomonas* spp. abundance in winter could be attributed to flushing from freshwater streams, which flow over toheroa beds. This 'flushing' could substantially lower the salinity of pore water in toheroa beds (Cope, 2018) creating unfavourable conditions for *Endozoicomonas* species outside of hosts. Additionally, Mahuta Gap and Kopawai sites have consistent freshwater streams that flow over toheroa beds, compared to Island where the freshwater flow could be described as 'ephemeral' or 'transient'. Following the detection of this link, total rainfall for the 30 days prior to the day of sampling was obtained for select months (Table 4.4). In March, where *Endozoicomonas* spp. abundance was greatest, the highest air temperature was

recorded during site visits (25 ºC). Furthermore, median *Endozoicomonas* spp. gene copy numbers do not differ greatly between stream-bearing sites and Island site in summer (Table 4.4). In winter however, median gene copy count is much lower overall at stream-bearing sites, where the median number of *Endozoicomonas* spp. gene copies was found to be almost eight times lower than for Island specimens (Table 4.4). This difference is even more pronounced in early spring, while the median number of *Endozoicomonas* spp. gene copies for Island remained stable at *c.* 9000 copies (Table 4.4). It is possible this is attributed to a higher volume of freshwater in consistent streams due to increased precipitation (Table 4.4). Interestingly, relatively low mean *Endozoicomonas* spp. abundance was reported in Oreti Beach toheroa tissues 1512 ±SE 305 (16S rRNA gene copies), despite being collected in summer (Fig. 4.5), when the highest abundance was recorded for the Ripiro Beach populations (Fig. 4.6). Average sea surface temperatures are lower at this location compared to northern sites, given its comparatively low latitude (Fig. 4.1 & Table 4.1). However, robust toheroa beds at Oreti Beach have also been linked with freshwater outflow (Beentjes, 2010b). Additionally, the water table is comparatively high at this beach (P. Ross, personal observation) which could be influencing *Endozoicomonas* spp. abundance continually by modifying the salinity profile in toheroa beds or introducing nutrients from terrestrial environments.

Links to freshwater flows and toheroa health have been made by researchers previously (Smith, 2013; Williams et al., 2013b). Freshwater streams modify habitats that are favourable to toheroa (Cope, 2018), and rainfall has been linked to increased toheroa condition via increased nutrient delivery from land and subsequent phytoplankton blooms (Cassie, 1955). As such, the tentative link drawn between *Endozoicomonas* spp. abundance in toheroa and freshwater outflow could be attributed to nutrient pollution from terrestrial systems (van de Water et al., 2017) or nutrient availability (Rossbach et al., 2019) rather than salinity profile modulation. Experimental study of *Endozoicomonas* endosymbionts in toheroa and other Aotearoa shellfish should therefore consider salinity and nutrient pollution/availability as potential modulators of their abundance in hosts.

Host tissue cells of shellfish infected with intracellular microcolonies of bacteria are usually detected in the gills and digestive glands (Cano et al., 2020; Carballal et al., 2001; Ceuta and Boehs, 2012; Zhu et al., 2012), as was the case here (Fig. 4.2). Some studies have therefore concluded that transmission is probably faecal-oral, like *C.* X. californiensis (Crosson et al., 2014; Friedman et al., 2002). Hooper et al. (2019) showed the relatively long capacity of *Endozoicomonas* spp. to survive outside of *P. maximus* hosts, coupled with large amounts of shedding into the water column could facilitate horizontal transmission between hosts. Considering this, a crude measurement of toheroa bed density was taken at the Ripiro Beach sites to assess whether bed density contributed to *Endozoicomonas* spp. prevalence and intensity, as it does for other marine

pathogens, for example, *Bonamia ostreae* in *Ostrea edulis* (Engelsma et al., 2010). Density estimates are shown in Table 4.3, along with *Endozoicomonas* spp. gene copy information from toheroa sampled on the same occasion. Dunn tests indicated mean gene copy numbers did not differ significantly between sampling sites on this occasion, despite variation of bed density (Table 4.3). For instance, mean density of toheroa at Kopawai was 219 per m^2 higher than the estimate for Mahuta Gap despite little difference in *Endozoicomonas* spp. gene copy range or prevalence (Table 4.3). Suggesting population density likely has little bearing on *Endozoicomonas* spp. abundance/prevalence in toheroa populations.

Histologically, like many other cases where IMCs have been detected, no immune response was associated with inclusions (Cano et al., 2020; Carballal et al., 2001; Dorfmeier et al., 2015; Horwitz et al., 2016). Accumulations of lipofuscin were often observed in the gill and digestive gland epithelium of toheroa (Fig. 4.2), it is presumed this is attributed to aging and tissue turnover (end-product of lysosomal digestion), but could be linked to environmental parameters (Lohrmann et al., 2019, and references therein). Further, specimens were also asymptomatic. No gross signs of infection were apparent, again typical for IMCs (Cano et al., 2020). Many examples elsewhere indicate that animals can be asymptomatic, while IMC intensity can be relatively high (Dorfmeier et al., 2015; Horwitz et al., 2016; Tinelli et al., 2020; Wetchateng et al., 2010). On the other hand, reports have also suggested that intracellular bacterial infections in shellfish have the capacity to cause mass mortalities (Cano et al., 2018; Le Gall et al., 1988; Villalba et al., 1999), even in the absence of obvious environmental drivers and while infection rates remained relatively stable. For example, Zhu et al. (2012) associated '*Rickettsia*-like' IMCs with mass mortalities of farmed blood clams, *Tegillarca granosa* in China, at temperatures ranging from 16-31ºC with the highest mortality rate (100%) recorded at 20ºC. Similarly, infection intensity of *P. maximus* from Lyme Bay, where mortalities had been attributed to *Endozoicomonas* spp. (Cano et al., 2018), were not substantially different seasonally, outside of mortality events (Hooper et al., 2019). Additionally, *Endozoicomonas* abundance in many apparently healthy toheroa reported here, were not substantially different from those reported by Howells et al. (2021) for mortality specimens of various Aotearoa shellfish. For instance, the max number of *Endozoicomonas* spp. 16S rRNA gene copies found in toheroa tissues in this study was 1,688,081 and the max for mortality specimens (pipi, *P. australis*) reported by Howells et al. (2021) was 1,370,000 (identical protocol used herein). The sequences reported in these instances were identical (Fig. 4.3), and therefore could indicate differential tolerance/susceptibility to *Endozoicomonas* spp. between hosts.

What these cases, and the present study highlight, is that virulence and pathogenicity of *Endozoicomonas* spp. cannot be explained by prevalence and intensity

alone. The aetiology of these potential pathogens is likely complex. Cano et al. (2018) postulate that temperature could be a driver. At the same time, many IMC-linked mortality events of Aotearoa shellfish have been reported in the austral-summer (Howells et al., 2019). Temporal patterns observed for some sites here, indicate temperature may be influencing *Endozoicomonas* spp. abundance in toheroa tissues (Fig. 4.6), but the case for freshwater influx/nutrient availability modulation is compelling (Table 4.4). Seasonal patterns of IMCs observed in geoducks (*Panopea generosa*) in Washington State by Dorfmeier et al. (2015) were site specific (like this study, Fig. 4.6) indicating that, more than just temperature alone is driving infection rates and intensity. Harvell and Lamb (2020) mention the holobiont properties of organisms play an important role in disease manifestation and progression. Therefore, linking environmental risk factors to a single pathogen (like IMCs) neglects the complexity of the microbiome in disease progression (Bass et al., 2019). In the case of IMCs, environmental conditions which modulate/disrupt the microbiome (as well as host traits), should therefore be considered when attempting to determine risk factors contributing to disease progression. The seasonal pattern of *Endozoicomonas* spp. abundance observed here was in the absence of reported mortalities, but the potential for *Endozoicomonas* spp. to cause mortality in toheroa cannot be ruled out. Investigations of the aetiology of these potential pathogens *ex situ* are needed to answer this question, like those carried out on *C.* X. californiensis (Crosson and Friedman, 2018; Moore et al., 2000). Furthermore, to-date many of the links between IMCs and risk factors have been made using histopathology to determine intensity/prevalence (Cano et al., 2018; Dorfmeier et al., 2015; Zhu et al., 2012). Both Howells et al. (2021) and Hooper et al. (2019) show that *Endozoicomonas* prevalence can be high in molluscs while intensity varies greatly. A quantitative approach to determine the abundance of *Endozoicomonas* spp. in hosts is therefore necessary. Additionally, in this study qPCR prevalence of *Endozoicomonas* spp. for Oreti Beach specimens was 88%, but histology (IMC) prevalence was only 3% (Table 4.1), suggesting that qPCR-positive is not indicative of pathomorphological changes in hosts (Fig. 4.2). The sequence determined for Oreti toheroa was different to those reported for northern toheroa (Fig. 4.3), it is possible that differential pathogenesis between northern and southern toheroa is attributed to *Endozoicomonas* strains that differ in pathogenicity. Therefore, while a quantitative approach is needed, the continued application of routine histology is also required to reveal what abundance means for pathogenesis in host tissues. Similarly, early stages of infection are not detectable by histology; infection prevalence could therefore be underestimated if histology alone were used for diagnosis.

Farming of threatened marine species has recently been highlighted as an often-neglected conservation tool (Gentry et al., 2019). Toheroa aquaculture to bolster populations and for commercial enterprise is a potentially viable option and interest has

been expressed by various Māori groups (Ross et al., 2018a). Discovering what function *Endozoicomonas* spp. play in toheroa life histories will contribute to the success of both *in situ* restoration and restorative/commercial farming. For example, if *Endozoicomonas* spp. are important endosymbionts within toheroa tissues, as they are in other marine invertebrates (Neave et al., 2016; Rossbach et al., 2019; Schill et al., 2017), knowledge of their role could alter restorative approaches e.g., encouraging their proliferation. Alternatively, if pathogenic, ensuring that risk factors are mitigated (*in situ*) and that virulence can be reduced (aquaculture) will become important for managing toheroa health.

4.6 Conclusion

Intracellular microcolonies of bacteria in toheroa tissues were confirmed as *Endozoicomonas* using ISH, PCR, and gene sequencing. Quantitative PCR revealed site and seasonal variation of *Endozoicomonas* spp. abundance in toheroa tissues. Local conditions were found to have a considerable effect on *Endozoicomonas* spp. abundance, and links were made to freshwater outflow. Freshwater streams on high-energy beaches are the favoured habitat of toheroa, but land-use (e.g., *Pinus radiata* forestry) close to these habitats in northern Aotearoa has substantially changed stream features (Williams et al., 2013b). If streams are modifying pathogen/endosymbiont abundance in hosts, their modification or reduction could have unforeseen implications for the health and survival of toheroa. Exploration of the toheroa-associated bacterial community would help to identify the role *Endozoicomonas* spp. play in toheroa hosts and shed light on the impact anthropogenic land use change is having on the composition and function of the toheroa microbiome. Experimental study of *Endozoicomonas* spp. in Aotearoa shellfish should be conducted *ex situ* to explore possible drivers of disease on-set. Similarly, the use of gene expression profiling could greatly improve our understanding of these potential endosymbionts and the part they play within the shellfish mortality landscape in Aotearoa.

4.7 References

Bartz, J.-O., et al., 2018. *Parendozoicomonas haliclonae* gen. nov. sp. nov. isolated from a marine sponge of the genus *Haliclona* and description of the family *Endozoicomonadaceae* fam. nov. comprising the genera *Endozoicomonas*, *Parendozoicomonas*, and *Kistimonas*. Systematic and Applied Microbiology. 41, 73-84.

Bass, D., et al., 2019. The Pathobiome in Animal and Plant Diseases. Trends in Ecology & Evolution. 34, 996-1008.

Beentjes, M. P., 2010a. Toheroa survey of Bluecliffs Beach, 2009, and review of historical surveys. New Zealand Fisheries Assessment Report 2010/7. 42.

Beentjes, M. P., 2010b. Toheroa survey of Oreti Beach, 2009, and review of historical surveys. New Zealand Fisheries Assessment Report 2010/6. 40.

Ben-Horin, T., et al., 2013. Variable intertidal temperature explains why disease endangers black abalone. Ecology. 94, 161-168.

Cano, I., et al., 2020. Cosmopolitan Distribution of *Endozoicomonas*-Like Organisms and Other Intracellular Microcolonies of Bacteria Causing Infection in Marine Mollusks. Frontiers in Microbiology. 11, 2778.

Cano, I., et al., 2018. Molecular Characterization of an *Endozoicomonas*-Like Organism Causing Infection in the King Scallop (*Pecten maximus* L.). Applied and Environmental Microbiology. 84, e00952-17.

Carballal, M. J., et al., 2001. Parasites and pathologic conditions of the cockle *Cerastoderma edule* populations of the coast of Galicia (NW Spain). Journal of Invertebrate Pathology. 78, 87-97.

Cassie, R. M., 1955. Population Studies on the Toheroa, *Amphidesma ventricosum* Gray (Eulamellibranchiata). Marine and Freshwater Research. 6, 348-391.

Castinel, A., et al., Review of disease risks for New Zealand shellfish aquaculture: Perspectives for management. Cawthron Report 2297. Prepared for Ministry for Business, Innovation and Employment. Cawthron Institute, Nelson, NZ, 2014, pp. 31.

Ceuta, L. O., Boehs, G., 2012. Parasites of the mangrove mussel *Mytella guyanensis* (Bivalvia: Mytilidae) in Camamu Bay, Bahia, Brazil. Brazilian Journal of Biology. 72**,** 421-427.

Cope, J., The modification of toheroa habitat by streams on Ripiro Beach. MSc. University of Waikato, Hamilton, New Zealand, 2018, pp. 126.

Crosson, L. M., Friedman, C. S., 2018. Withering syndrome susceptibility of northeastern Pacific abalones: A complex relationship with phylogeny and thermal experience. Journal of Invertebrate Pathology. 151**,** 91-101.

Crosson, L. M., et al., 2014. Abalone withering syndrome: distribution, impacts, current diagnostic methods and new findings. Diseases of Aquatic Organisms. 108**,** 261-270.

da Silva, P. M., et al., 2015. Survey of Pathologies in *Crassostrea gasar* (Adanson, 1757) Oysters from Cultured and Wild Populations in the São Francisco Estuary, Sergipe, Northeast Brazil. Journal of Shellfish Research. 34**,** 289-296.

Darriba, S., et al., 2012. Phage particles infecting branchial Rickettsiales-like organisms in banded carpet shell *Polititapes virgineus* (Bivalvia) from Galicia (NW Spain). Diseases of Aquatic Organisms. 100**,** 269-272.

Di, G. L., et al., 2016. Pathology and physiology of *Haliotis diversicolor* with withering syndrome. Aquaculture. 453**,** 1-9.

Ding, J.-Y., et al., 2016. Genomic Insight into the Host–Endosymbiont Relationship of *Endozoicomonas montiporae* CL-33T with its Coral Host. Frontiers in Microbiology. 7**,** 251.

Dinno, A., 2015. Nonparametric pairwise multiple comparisons in independent groups using Dunn's test. Stata Journal 15**,** 292-300.

Dinno, A., Dinno, M., Package 'dunn. test'. CRAN Repository, Vol. 10, 2017.

Dorfmeier, E. M., et al., 2015. Temporal and Spatial Variability of Native Geoduck (*Panopea generosa*) Endosymbionts in the Pacific Northwest. Journal of Shellfish Research. 34**,** 81-90.

Engelsma, M. Y., et al., 2010. Epidemiology of *Bonamia ostreae* infecting European flat oysters *Ostrea edulis* from Lake Grevelingen, The Netherlands. Marine Ecology Progress Series. 409**,** 131-142.

Fournier, P.-E., Raoult, D., 2009. Current Knowledge on Phylogeny and Taxonomy of *Rickettsia* spp. Annals of the New York Academy of Sciences. 1166**,** 1-11.

Friedman, C. S., et al., 2000. '*Candidatus* Xenohaliotis californiensis', a newly described pathogen of abalone, *Haliotis* spp., along the west coast of North America. International Journal of Systematic and Evolutionary Microbiology. 50**,** 847-855.

Friedman, C. S., et al., 2002. Transmission of withering syndrome in black abalone, *Haliotis cracherodii* leach. Journal of Shellfish Research. 21**,** 817-824.

Gardner, G. R., et al., 1995. Association of Prokaryotes with Symptomatic Appearance of Withering Syndrome in Black Abalone *Haliotis cracherodii*. Journal of Invertebrate Pathology. 66**,** 111-120.

Gentry, R. R., et al., 2019. Looking to aquatic species for conservation farming success. Conservation Letters. 12**,** e12681.

Gollas-Galvan, T., et al., 2014. *Rickettsia*-like organisms from cultured aquatic organisms, with emphasis on necrotizing hepatopancreatitis bacterium affecting penaeid shrimp: an overview on an emergent concern. Reviews in Aquaculture. 6**,** 256-269.

Harvell, C. D., Lamb, B. J., Disease outbreaks can threaten marine biodiversity. In: R. B. Silliman, D. K. Lafferty, Eds., Marine Disease Ecology. Oxford University Press, Oxford, United Kingdom, 2020, pp. 18.

Hewson, I., et al., 2014. Densovirus associated with sea-star wasting disease and mass mortality. Proceedings of the National Academy of Sciences of the United States of America. 111**,** 17278.

Hine, P. M., Diggles, B. K., 2002a. The distribution of *Perkinsus olseni* in New Zealand bivalve molluscs. Surveillance. 29**,** 8-11.

Hine, P. M., Diggles, B. K., 2002b. Prokaryote infections in the New Zealand scallops *Pecten novaezelandiae* and *Chlamys delicatula*. Diseases of Aquatic Organisms. 50**,** 137-144.

Hine, P. M., Wesney, B., 1997. Virus-like particles associated with cytopathology in the digestive gland epithelium of scallops *Pecten novaezelandiae* and toheroa *Paphies ventricosum*. Diseases of Aquatic Organisms. 29**,** 197-204.

Hooper, P. M., et al., 2019. Shedding and survival of an intracellular pathogenic *Endozoicomonas*-like organism infecting king scallop *Pecten maximus*. Diseases of Aquatic Organisms. 134**,** 167-173.

Horwitz, R., et al., 2016. Characterization of an intracellular bacterium infecting the digestive gland of the South African abalone *Haliotis midae*. Aquaculture. 451**,** 24-32.

Howells, J., et al., 2021. Intracellular bacteria in New Zealand shellfish are identified as *Endozoicomonas* species. Diseases of Aquatic Organisms. 143**,** 27-37.

Howells, J., et al., Investigation of *Rickettsia*-like organisms in New Zealand wild shellfish. Biosecurity New Zealand, Ministry for Primary Industries, Wellington, NZ, 2019, pp. 58.

Johnson, M., et al., 2008. NCBI BLAST: a better web interface. Nucleic Acids Research. 36**,** W5-9.

Kearse, M., et al., 2012. Geneious Basic: An integrated and extendable desktop software platform for the organization and analysis of sequence data. Bioinformatics. 28**,** 1647-1649.

Kurahashi, M., Yokota, A., 2007. *Endozoicomonas elysicola* gen. nov., sp. nov., a γ-proteobacterium isolated from the sea slug *Elysia ornata*. Systematic and Applied Microbiology. 30**,** 202-206.

Lane, H. S., et al., 2016. *Bonamia ostreae* in the New Zealand oyster *Ostrea chilensis*: a new host and geographic record for this haplosporidian parasite. Diseases of Aquatic Organisms. 118**,** 55-63.

Le Gall, G., et al., 1988. Branchial Rickettsiales-like infection associated with a mass mortality of sea scallop *Pecten maximus*. Diseases of Aquatic Organisms. 4**,** 229-232.

Lohrmann, K. B., et al., 2019. Histopathological assessment of the health status of *Mytilus chilensis* (Hupé 1854) in southern Chile. Aquaculture. 503**,** 40-50.

Marcos-Lopez, M., et al., 2017. *Piscirickettsia salmonis* infection in cultured lumpfish (*Cyclopterus lumpus* L.). Journal of Fish Diseases. 40**,** 1625-1634.

McKinnon, S. L. C., Olsen, D. L., 1994. Review of the Southland toheroa fishery. New Zealand Ministry of Agriculture and Fisheries. New Zealand fisheries management: Regional series. 3**,** 18.

Mendoza, M., et al., 2013. A novel agent (*Endozoicomonas elysicola*) responsible for epitheliocystis in cobia *Rachycentrum canadum* larvae. Diseases of Aquatic Organisms. 106**,** 31-37.

Miskelly, C. M., Legal protection of New Zealand's indigenous aquatic fauna–an historical review. Tuhinga, Vol. 27. Te Papa Press, Wellington, NZ, 2016, pp. 81-115.

Moore, J. D., et al., 2002. Withering syndrome and restoration of southern California abalone populations. CalCOFI Reports. 43**,** 112-119.

Moore, J. D., et al., 2000. Withering syndrome in farmed red abalone *Haliotis rufescens*: Thermal induction and association with a gastrointestinal *Rickettsiales*-like prokaryote. Journal of Aquatic Animal Health. 12**,** 26-34.

Murton, B., 2006. 'Toheroa Wars': Cultural politics and everyday resistance on a northern New Zealand beach. New Zealand Geographer. 62**,** 25-38.

Neave, M. J., et al., 2016. Diversity and function of prevalent symbiotic marine bacteria in the genus *Endozoicomonas*. Applied Microbiology and Biotechnology. 100**,** 8315-8324.

Neave, M. J., et al., 2014. Whole-genome sequences of three symbiotic *endozoicomonas* strains. Genome Announcements. 2**,** e00802-14.

Neave, M. J., et al., 2017. *Endozoicomonas* genomes reveal functional adaptation and plasticity in bacterial strains symbiotically associated with diverse marine hosts. Scientific Reports. 7**,** 40579.

Norton, J. H., et al., 1993. Mortalities in the Giant Clam *Hippopus hippopus* Associated with Rickettsiales-like Organisms. Journal of Invertebrate Pathology. 62**,** 207-209.

Qi, W., et al., 2018. Ca. *Endozoicomonas cretensis*: A Novel Fish Pathogen Characterized by Genome Plasticity. Genome Biology and Evolution. 10**,** 1363-1374.

Redfearn, P., Biology and distribution of the toheroa, *Paphies* (Mesodesma) *ventricosa* (Gray). Fisheries Research Bulletin No. 11. New Zealand Ministry of Agriculture and Fisheries, 1974, pp. 51.

Ross, P. M., et al., 2018a. The biology, ecology and history of toheroa (*Paphies ventricosa*): a review of scientific, local and customary knowledge. New Zealand Journal of Marine and Freshwater Research. 52**,** 196-231.

Ross, P. M., et al., 2018b. First detection of gas bubble disease and *Rickettsia*-like organisms in *Paphies ventricosa*, a New Zealand surf clam. Journal of Fish Diseases. 41**,** 187-190.

Rossbach, S., et al., 2019. Tissue-Specific Microbiomes of the Red Sea Giant Clam *Tridacna maxima* Highlight Differential Abundance of *Endozoicomonadaceae*. Frontiers in Microbiology. 10**,** 2661.

Rozas, M., Enriquez, R., 2014. Piscirickettsiosis and *Piscirickettsia salmonis* in fish: a review. Journal of Fish Diseases. 37**,** 163-188.

Schill, W. B., et al., 2017. *Endozoicomonas* Dominates the Gill and Intestinal Content Microbiomes of *Mytilus edulis* from Barnegat Bay, New Jersey. Journal of Shellfish Research. 36**,** 391-401.

Smith, S., Factors influencing the abundance of Toheroa (*Paphies ventricosa*) on Northland beaches: Perspectives from the beach. In: J. Williams, et al., Review of factors affecting the abundance of toheroa (*Paphies ventricosa*). New Zealand Aquatic Environment and Biodiversity Report No. 114, 2013, pp. 76.

Sun, J. F., Wu, X. Z., 2004. Histology, ultrastructure, and morphogenesis of a *rickettsia*-like organism causing disease in the oyster, *Crassostrea ariakensis* gould. Journal of Invertebrate Pathology. 86**,** 77-86.

Team, R. C., R: A language and environment for statistical computing. R Foundation for Statistical Computing, Vienna, Austria, 2013.

Thrupp, T. J., et al., 2016. A novel bacterial infection of the edible crab, *Cancer pagurus*. Journal of Invertebrate Pathology. 133**,** 83-86.

Tinelli, A., et al., 2020. Histological features of *Rickettsia*-like organisms in the European flat oyster (*Ostrea edulis* L.). Environmental Science and Pollution Research. 27**,** 882-889.

Travers, M. A., et al., 2015. Bacterial diseases in marine bivalves. Journal of Invertebrate Pathology. 131**,** 11-31.

van de Water, J. A. J. M., et al., 2017. Comparative Assessment of Mediterranean Gorgonian-Associated Microbial Communities Reveals Conserved Core and Locally Variant Bacteria. Microbial Ecology. 73**,** 466-478.

Villalba, A., et al., 1999. Branchial *rickettsia*-like infection associated with clam *Venerupis rhomboides* mortality. Diseases of Aquatic Organisms. 36**,** 53-60.

Wetchateng, T., et al., 2010. Withering syndrome in the abalone *Haliotis diversicolor supertexta*. Diseases of Aquatic Organisms. 90**,** 69-76.

Wickham, H., 2009. ggplot2: Elegant Graphics for Data Analysis. Springer, New York.

Williams, J., et al., Distribution and abundance of toheroa (*Paphies ventricosa*) and tuatua (*P. subtriangulata*) at Ninety Mile Beach in 2010 and Dargaville Beach in 2011. Ministry of Primary Industries, Wellington, 2013a, pp. 52.

Williams, J. R., et al., Review of factors affecting the abundance of toheroa (*Paphies ventricosa*). New Zealand Aquatic Environment and Biodiversity Report No. 114, 2013b, pp. 76.

Wu, X., et al., 2005. Purification and antigenic characteristics of a *rickettsia*-like organism from the oyster *Crassostrea ariakensis*. Diseases of Aquatic Organisms. 67**,** 149-154.

Yang, C. S., et al., 2010. *Endozoicomonas montiporae* sp. nov., isolated from the encrusting pore coral *Montipora aequituberculata*. International Journal of Systematic and Evolutionary Microbiology. 60**,** 1158-1162.

Zhu, Z. W., et al., 2012. *Rickettsia*-like organism infection associated with mass mortalities of blood clam, *Tegillarca granosa*, in the Yueqing Bay in China. Acta Oceanologica Sinica. 31**,** 106-115.

Ziegler, M., et al., 2016. Coral microbial community dynamics in response to anthropogenic impacts near a major city in the central Red Sea. Marine Pollution Bulletin. 105**,** 629-640.

Zielinski, F. U., et al., 2009. Widespread occurrence of an intranuclear bacterial parasite in vent and seep bathymodiolin mussels. Environmental Microbiology. 11**,** 1150-1167.

Chapter 5
The Bacterial Community in a Threatened Beach Clam Endemic to Aotearoa (New Zealand)

Mahuta Gap, Ripiro Beach

5.1 Abstract

Habitat degradation is multifaceted, the indirect effects of an action are often difficult to predict and directly attribute to a single cause. In Aotearoa (New Zealand), the toheroa is an endemic beach clam that remains threated following overfishing in the 20th century. Today their populations remain in a precarious position despite protective measures in place for more than four decades. Potential reasons for this are habitat change and degradation. Agriculture (e.g., pine plantation) has been associated with the reduction of freshwater streams on long beaches in Te Tai Tokerau (Northland). Studies of the biology and ecology of toheroa have emphasised the importance of these freshwater flows for toheroa, though the precise reason is currently unknown. Previous work identified health related differences in sites where freshwater flows were present and absent. Here, the microbiome (composite: gill and digestive gland) of toheroa is explored across four remaining toheroa populations; Te-Oneroa-a-Tōhē (*n* = 6), Ripiro Beach (*n* = 15), Foxton Beach (*n* = 1), and Oreti Beach (*n* = 6).

The core microbial community (9 Phyla and 18 Families) in toheroa tissues differed between geographically separated sites. Locally, however, bacterial communities were considerably different even between relatively close toheroa beds (*c.* 10 km) on the same beach. Freshwater outflow was linked to differing bacterial communities. The most highly represented taxa detected in the toheroa microbiome was *Spirochaetaceae*, accounting for the top three OTUs present in 95% of specimens, suggesting a significant role within the toheroa holobiont. Recent research identified *Endozoicomonas* spp. as a potential pathogen in toheroa. In the present study, 2.1% (range: 0-17.9%) of the relative abundance of the toheroa microbiome was assigned to the bacterial genus *Endozoicomonas.* This taxon was also identified as a key indicator species between sites without freshwater streams and stream-bearing sites.

5.2 Introduction

In hosts, bacteria regulate resistance to, and contribute to, disease (Bass et al., 2019), and many biogeochemical cycles within host cells are driven by symbiotic bacteria (Neave et al., 2016; Tandon et al., 2020). In this way, bacteria contribute to host survival and homeostasis. Bacterial community composition and function studies of threatened (West et al., 2019) and farmed species (Desai et al., 2012; Ghanbari et al., 2015) are primarily carried out to assess host health. In threatened species like the kākāpō, *Strigops habroptilus* (a critically endangered parrot endemic to Aotearoa), interrogation of faecal microbiota has been used to advise conservationists on nutritional supplements/translocations (Perry et al., 2017). For similar applications, DNA metabarcoding approaches are often used to guide nutrition in terrestrial farming (Singh

and Trivedi, 2017). The uptake of high-throughput sequencing approaches for aquaculture has been rapid too (Desai et al., 2012; Llewellyn et al., 2014). Establishing what is 'healthy' in marine species is a particularly challenging task, but microbiome typing and subsequent diversity indices and functional profiling offer powerful tools for health assessment at a wider resolution than single pathogen approaches (i.e., Sanger sequencing or qPCR) (Carnegie et al., 2016).

Bacteria are drivers and modulators of numerous metabolic processes within their hosts. In corals, bacteria perform functional roles in antimicrobial activity (Morrow et al., 2015), bleaching defence, and various biogeochemical processes (reviewed in Bourne et al., 2016). In other marine invertebrates, metabolic processes are underpinned by gut microbiota and their respective functional roles. This is evident from various explorations of the gut microbiota in crustaceans such as penaeid shrimp (Holt et al., 2020), as well as finfish (Ghanbari et al., 2015; Mouchet et al., 2012), and molluscs e.g., the black-lipped pearl oyster, *Pinctada margaritifera* and Pacific oysters, *Crassostrea virginica* (Dubé et al., 2019; King et al., 2012). It is generally accepted that a diverse microbiome (community and function) is an indication of overall 'good health' in a host. The reverse is a host microbiome dominated by few taxa, where opportunistic and (or) pathogenic bacteria account for a significant proportion of all taxa present (dysbiosis). This approach to disease in hosts, which recognises the interactions between hosts and host-associated microbes (bacteria, fungi, viruses, and archaea), is an update to the previously described epidemiological triad, which examined disease as an interaction between host, pathogen, and environment (Snieszko, 1974). Instead, the 'pathobiome', a term that strives to move away from a single-pathogen concept has been suggested (Bass et al., 2019). This approach encompasses the epidemiological triad described by Snieszko (1974) but moves to incorporate host-microbe and environment-microbe interactions within each facet of the original model (Bass et al., 2019; Lane et al., 2020). Without adaptive immune systems, bivalve molluscs rely on innate immunity (e.g., antimicrobial peptides and host microbiomes) as a defensive mechanism against invading pathogens (Pierce and Ward, 2018). Therefore, knowledge of shellfish host-associated bacterial communities provides a lens with which host stress, immunity, and overall health can be viewed.

Wild shellfish are comparatively understudied in the aquatic disease sphere in Aotearoa. Aquaculture is a considerable economic driver of shellfish disease research, explaining the comparatively developed research capacity in this area (Castinel et al., 2019; Lane et al., 2020; Nguyen et al., 2019). Some exceptions exist, for instance, numerous disease ecology studies focusing on digenean trematodes in the Aotearoa cockle (*Austrovenus stutchburyi*) (Babirat et al., 2004; Mouritsen, 2002) have been carried out. Furthermore, while attempting to find a source of tetrodotoxin (TTX) in an

important Aotearoa clam, pipi (*Paphies australis*), Biessy et al. (2020) also provided one of the first in-depth national studies of the bacterial community in a wild shellfish species from Aotearoa. Pipi are in the *Paphies* genus, an endemic family of clams to Aotearoa that includes northern tuatua (*P. subtriangulata*), southern tuatua (*P. donacina*), and toheroa (*P. ventricosa*). All four of these clams represent ecologically important beach (tuatua and toheroa) and estuary (pipi) constituents. At the same time, they are all regionally important kai moana and of cultural significance to tangata whenua (Māori: Indigenous people of Aotearoa). However, in recent years, there has been an apparent upsurge in the number of unexplained shellfish mass mortality events (MMEs) in Aotearoa (Howells et al., 2021; Chapter 2). All members of the *Paphies* genus have been implicated in these MMEs, including the threatened toheroa.

On many beaches where the toheroa was once highly abundant, they are now absent (Muriwai) or populations are diminished (Kāpiti-Horowhenua) (reviewed in Ross et al., 2018a). One of the main contributing factors was overharvesting in the previous century, yet the fishery (both recreational and commercial) has been closed for decades. Among several potential factors contributing to their continued depressed state, disease has been identified as a potential barrier to their recovery (Ross et al., 2018b). Toheroa beds are often found concentrated at freshwater streams (seeps or overland flows), at higher densities than outside of stream associated habitats (Beentjes, 2010; Williams et al., 2013). The exact reasons for this habitat 'selection' are unknown, though studies have suggested thermal protection from desiccation (Cope, 2018) and altered beach morphology that concentrates toheroa spat and phytoplankton via embayment (Cope, 2018; Ross et al., 2018a; Williams et al., 2013) as explanations of their abundance in these areas. However, the reduction of freshwater streams and associated recesses in the beach, linked to *Pinus radiata* forestry (Williams et al., 2013) and diversions for agriculture purposes (Ross et al., 2018a) in Te Tai Tokerau (Northland), may be affecting remaining populations. The implications of this habitat modification for toheroa intrinsic health are unknown.

In this study, the bacterial community of toheroa is characterised in specimens from key remaining populations in the North and South Islands of Aotearoa (Fig. 5.1). The core toheroa microbiome is described, and an exploration of how locally different environmental conditions can modulate the microbiome of toheroa was carried out.

5.3 Methods

5.3.1 Specimen Collection

Toheroa (28 in total) were sampled from (Fig. 5.1 & Table 5.1) Te-Oneroa-a-Tōhē (Ninety-Mile Beach) in the far north (November 2019; n = 6), Ripiro Beach

(Kaipara; September 2019; *n* = 15), Foxton Beach in the lower North Island (March 2019; *n* = 1), and Oreti Beach in the far south (February 2019; *n* = 6). These were subsamples from previous chapters (Chapters 3 & 4). At Ripiro Beach, five toheroa were collected from each of three sites (Island, Mahuta Gap, and Kopawai). Sampled toheroa were sectioned from anterior to posterior (encompassing all major organs). One-half was placed in 70% EtOH for DNA extraction. The other half was for histopathology, with tissues fixed in 10% formalin for a maximum of 48 hrs, trimmed and placed in tissue cassettes with 70% EtOH. Haematoxylin and eosin (H&E) staining and slide preparation was carried out at SVS Laboratories Ltd. (Hamilton, NZ). Stained tissues were viewed using an Olympus BX53. For comparison with the toheroa microbiome, certain health factors recorded via histology in Chapter 3 are reproduced here. These include sex, mucous cell hyperplasia, ciliate infiltration, and intracellular microcolonies of bacteria (IMCs) intensity.

5.3.2 DNA Extraction and PCR Amplification

Tissue from toheroa gills (20 mg) and digestive gland (5 mg) was excised for DNA extraction. Gill and digestive gland tissues (25 mg combined) were macerated using a scalpel and transferred into 1.5 ml microcentrifuge tubes. Tissue digest buffer (180 µl) and digest enzyme (20 µl proteinase K) were added to each sample and lysed overnight at 56 °C on a heat-shaking platform. DNA extraction was carried out using the QIAamp® DNA Mini Kit (Qiagen, Valencia, CA, USA), following manufacturer's instructions. The presence of amplifiable DNA within the extract was confirmed by using an 18S rRNA internal control (Life Technologies, Ribosomal 18S rRNA Endogenous Control). Extracted DNA was quantified using the Qubit fluorometer high sensitivity double stranded DNA protocol (Life Technologies, Auckland). DNA was stored at -20°C until further analyses.

Polymerase chain reaction (PCR) was used to amplify the V4-V5 regions of the 16S rRNA gene from extracted DNA using the primer set F515 (5'CCATCTCATCCCTGCGTGTCTCCGACTCAG-unique IonCode barcode-GATGTGCCAGCMGCCGCGGTAA-3') and R926 (5'-CCACTACGCCTCCGCTTTCC TCTCTATGGGCAGTCGGTGATCCGYCAATTYMTTTRAGTTT-3') (IDT, New Zealand). Each PCR reaction contained 9.1 µL molecular-grade ultrapure water, 2.4 µL dNTPs (2 mM) (Invitrogen Ltd, NZ), 2.4 µL 10x PCR buffer (Invitrogen), 2.4 µL $MgCl_2$ (50 mM) (Invitrogen), 0.4 µL of each primer (10 mM) (Integrated DNA Technologies, Inc), 0.8 µL bovine serum albumin (BSA) (Promega Corporation, USA), 0.1 µL Taq DNA polymerase (Invitrogen) and 2 µL of genomic DNA template (5 ng μl^{-1}). A lower DNA template concentration (1 ng μl^{-1}) was used for three samples to account for PCR inhibition. Reactions were performed in triplicate for each sample with the following thermocycler

conditions: 3 min initial denaturation at 94°C, followed by 30 cycles of 45 s at 94°C, 1 min at 50°C, and 1.5 min at 72°C, with a final 10 min elongation at 72°C. A positive (internal control made available from another study previously conducted at the Thermophile Research Unit, Hamilton) and a negative control (molecular-grade ultrapure water) was run in every PCR. Triplicate reactions were pooled, and the PCR products were verified on a 1% SYBR Safe stained agarose gel. Wells were loaded with 5 µL PCR product and 2 µL 3x loading dye (Invitrogen). Gels were run for 25 min at 70 V with a 1 KB+ ladder and visualised using an Alpha Imager. Amplicons were stored at -20°C until sequencing (~3 months).

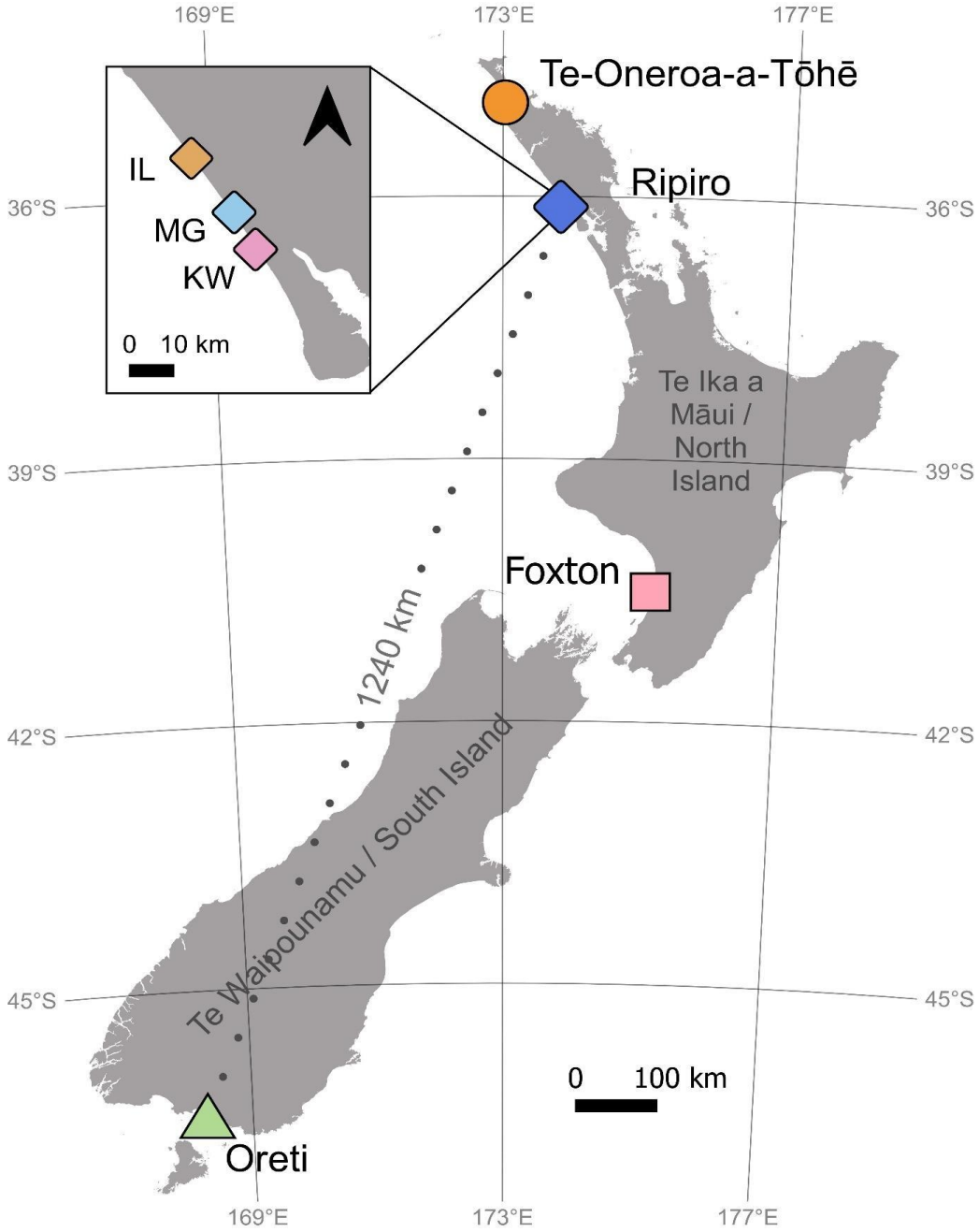

Fig. 5.1. Location of study sites around Aotearoa (New Zealand). IL: Island, MG: Mahuta Gap, and KW: Kopawai. Te-Oneroa-a-Tōhē: Ninety-Mile Beach. Spatial data obtained from DIVA-GIS. CRS: WGS 84 (EPSG: 4326).

Table 5.1. Site information and details of specimens gathered for this study.

Location	Site	ID	Date	*n*	Stream	Description
Ninety-Mile (Te-Oneroa-a-Tōhē)	-	Nine. 1-6	Nov-19	6	no	Ninety-Mile Beach or Te-Oneroa-a-Tōhē is the farthest north of the sampling sites here, toheroa beds typically found close to streams like Ripiro Beach.
Ripiro	Island (IL)	IL.1-5	Sep-19	5	no	Northern-most sampling site on Ripiro Beach, consistent stream not present, bed typically high on beach and outside of stream path.
	Mahuta Gap (MG)	MG.1-5	Sep-19	5	yes	Most consistent stream and bed out of Ripiro Beach sites, stream typically has the largest overland flow out of Ripiro beach sites.
	Kopawai (KW)	KW.1-5	Sep-19	5	yes	Freshwater stream is inconsistent in size and source is a small lake. Toheroa bed is typically low at this site.
Foxton	-	Fox. 1	Mar-19	1	no	Toheroa are sparsely distributed, not in dense beds as in other sites. Population is in precarious state, robust beds are not longer present.
Oreti	-	ORE. 4 & 6	Feb-19	6	no	Unlike northern sites, toheroa at Oreti Beach are not densely grouped at freshwater flows, adults tend to be much larger (*c.* 115 mm) than elsewhere. Animals tend to be lower on beach.

PCR amplicon concentration for each sample was normalized and purified using a SequelPrep Normalization Kit, following the manufacturer's instructions (Life Technologies, Auckland). DNA sequencing was undertaken at the Waikato DNA Sequencing Facility (University of Waikato, Hamilton) using an Ion-Torrent Personal Genome Machine (PGM) DNA sequencer with an Ion 318v2 chip (Life Technologies). Raw sequences were filtered in mothur to remove long and short reads and reads with excessive homopolymers (Schloss et al., 2009). A total of 1,519,764 sequences (250 bp) were quality filtered using USEARCH (Edgar, 2010). High quality reads (274,069) were then clustered into operational taxonomic units (OTUs) at a similarity threshold of 97%. OTUs (FASTA) were classified using SILVA Incremental Aligner (SINA) (v. 1.2.11) (Pruesse et al., 2007; Quast et al., 2013). The minimum query identity was 80% and taxonomic placements at <70% identity match were assigned 'unknown'. Taxonomic classifications were obtained at kingdom, phylum, class, order, family, and genus level. Sequences were filtered for chloroplast, mitochondria, Archaea, Eukaryota, singletons and 'unknown', leaving a total of 553 OTUs, with an average of 9990 reads per sample (n = 24). Four samples were removed from any further analyses due to considerably lower reads (<2000). A 'phyloseq' object was created using taxonomic data, OTU count table, and metadata (McMurdie and Holmes, 2013). Statistical analyses of bacterial community data were carried out in RStudio (R Core Team, 2013).

5.3.3 Data Analysis and Visualisation

Prior to statistical analyses, OTU counts were normalised using scaling with ranked subsampling (SRS) (Beule and Karlovsky, 2020). To examine the microbial community composition between geographically and locally separated study sites, several diversity indices were used. Following taxonomic assignment to 16S rRNA sequences, taxonomy combined with OTU count tables were used to establish community indices of alpha diversity (Shannon and Simpson), and richness (Chao1), using the 'phyloseq' and 'microbiome' packages (Lahti et al., 2017; McMurdie and Holmes, 2013). Using the same packages in RStudio, stacked barplots were created based on the relative abundance of the top 10 taxa at both family and genus levels, all other taxa were merged as 'Other'. The Bray-Curtis dissimilarity index was used to measure dissimilarity between the bacterial communities in toheroa tissues sampled from different populations (locally and geographically). Normalised OTU counts were $\log_{10}(x+1)$ transformed prior to dissimilarity index use. Hierarchical clustering and non-metric multi-dimensional scaling (NMDS) were used to visualise dissimilarity between samples based on the Bray-Curtis index. To establish whether dissimilarities of the microbial community in the toheroa composite microbiome was statistically different between sampled study sites (Ninety-Mile Beach and Ripiro sub sites), permutational

multivariate analysis of variance (PERMANOVA) was performed using the 'vegan' package (Oksanen et al., 2020) in RStudio. Additionally, indicator species (OTUs) were predicted using the 'multiplatt' function with 9999 permutations via the 'indicspecies' package in R (De Cáceres et al., 2020; De Cáceres et al., 2010). A heatmap based on relative abundances of several top indicator species was subsequently constructed. Significance level for all statistical analyses was 95%.

Several other statistical and graphical packages were used to produce figures and manipulate data in the R statistical environment, including 'ggplot2' (Wickham, 2009) and 'ggdendro' (de Vries and Ripley, 2020). The core microbiome was deduced by filtering for OTUs present in 70% of specimens. The top 10 of these (relative abundance) were compared against published sequences using the NCBI nucleotide BLAST tool (Johnson et al., 2008). Top OTUs (sequences) were then used to create a phylogenetic tree to compare phylogeny of the top OTUs to similar marine bacteria in the NCBI database. Sequences were aligned (93% similarity) and a phylogenetic tree was constructed based on 100,000 bootstrapped replicates (Appendix, Fig. E.1. & Table E.1).

5.4 Results

The microbiome (composition) of toheroa varied both between beaches and between beds at a single beach (Figs. 5.2 and 5.3). At the family level, *Spirochaetaceae* was the most highly represented taxa in the toheroa microbiome regardless of study site. *Mycoplasmataceae* was the second most abundant taxa in Ripiro, Oreti, and Foxton specimens, while *Endozoicomonadaceae* (Bartz et al., 2018), were second most abundant in Te-Oneroa-a-Tōhē toheroa. *Pseudoalteromonadaceae* was relatively abundant in Oreti specimens. Similarly, *Fusobacteriaceae* was comparatively abundant in the single Foxton specimen (n = 1). *Vibrionaceae*, relatively abundant in Oreti specimens, was recorded at lower levels at Foxton and Ninety-Mile Beach but was not recorded at Ripiro. At the genus level, unclassified *Spirochaetaceae* and *Spirochaeta*-2 were most abundant taxa at sites other than Oreti where *Spirochaeta*-2, *Vibrio* and *Mycoplasma* were the most abundant taxa. *Mycoplasma* was present in all specimens and the most abundant taxa in MG.3 from Ripiro. This same sample also recorded the highest abundance of *Psychrilyobacter*.

Endozoicomonas was most abundant in Te-Oneroa-a-Tōhē specimens and present at comparably low abundances at other sites. *Vibrio* were abundance in the two Oreti Beach specimens, and in single specimens from Te-Oneroa-a-Tōhē and Foxton. *Synechococcus* CC9902 (Hamilton et al., 2014) was recorded at higher abundances at Kopawai and Mahuta Gap than at other sites. Microbial sequences not aligned to the ten most common families or genera were classified as 'other' and this component of the

microbiome was much greater at Oreti than at other sites (Fig. 5.2 & 5.3), indicating a potentially dissimilar core microbiome to the other specimens collected from the North Island. See Table E.1 for sequence details of the top 10 OTUs.

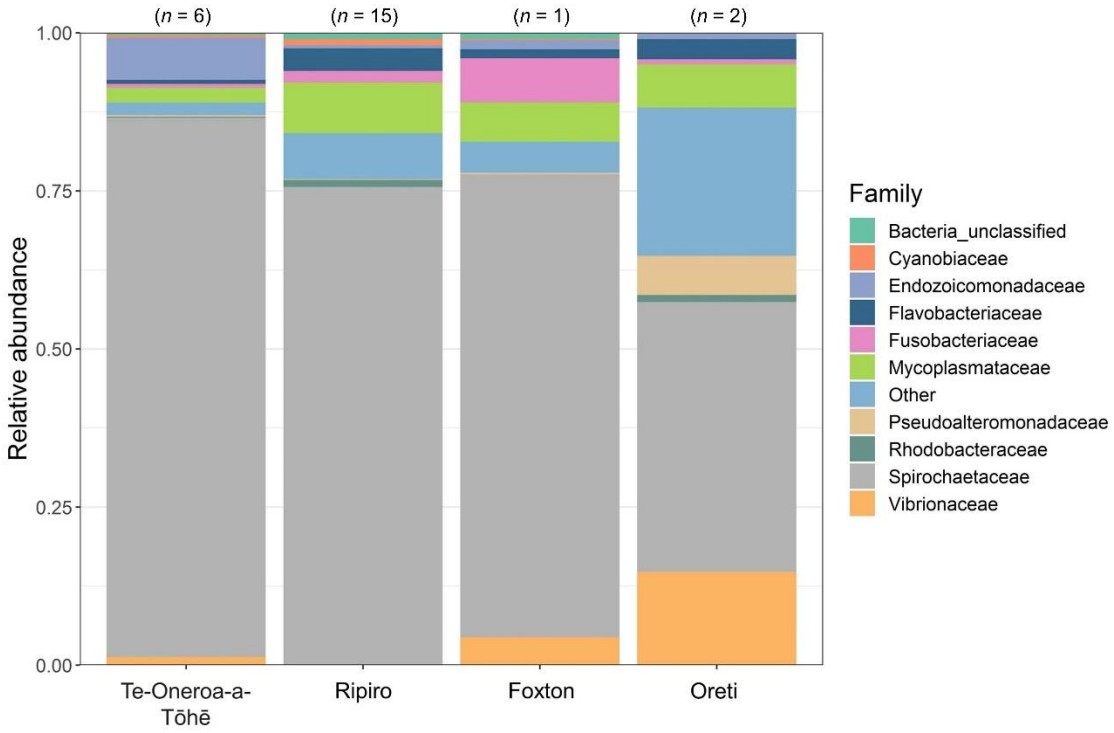

Fig. 5.2. Stacked barplots showing the relative abundance of the top 10 bacterial 16S ribosomal RNA OTUs, at the family level (composite microbiome). Samples are clustered based on study site/beach. Sample sizes are shown above bars.

5.4.1 Beta Diversity

Oreti Beach specimens (*n* = 2) were substantially dissimilar from all other samples examined herein (NMDS, stress = 0.1) (Fig. 5.4). This observation was clearer still when hierarchical clustering was used to visualise differences/similarity between samples (Fig. 5.5). The two Oreti specimens cluster closely and are the furthest distance from all other specimens (>0.6) (Fig. 5.5). Surprisingly, hierarchical clustering indicates most specimens (3 of 5) from Island (Ripiro Beach) are more dissimilar to specimens from Kopawai and Mahuta Gap (Ripiro Beach), than to specimens sampled from Ninety-Mile Beach. Clustering also shows that these three samples are not only more similar to specimens gathered from Ninety-Mile Beach, but also that specimens from Mahuta Gap and Kopawai are more similar to specimens from Oreti than they are to three of the Island samples (Bray-Curtis distance = 0.8). This clustering can also be observed in the NMDS ordination. Ellipses could not be calculated for Oreti and Foxton due to lack of replication (Fig. 5.4).

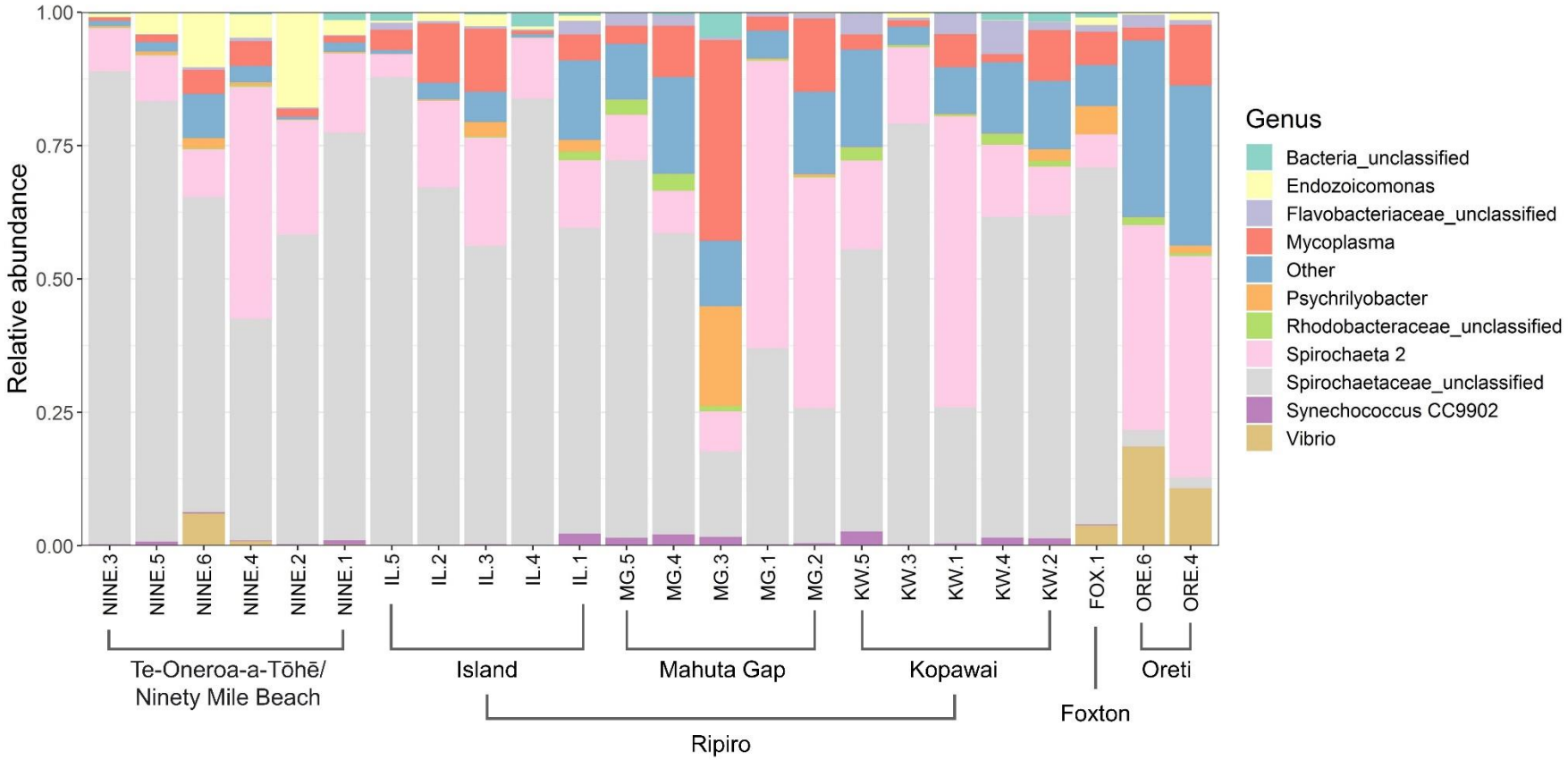

Fig. 5.3. Stacked barplots showing the relative abundance of the top 10 bacterial 16S ribosomal RNA OTUs, at the genus level (composite microbiome). Samples are clustered based on study site/beach. Fox: Foxton Beach, IL: Island, MG: Mahuta Gap, KW: Kopawai, Nine: Ninety-Mile Beach (Te-Oneroa-a-Tōhē), ORE: Oreti Beach.

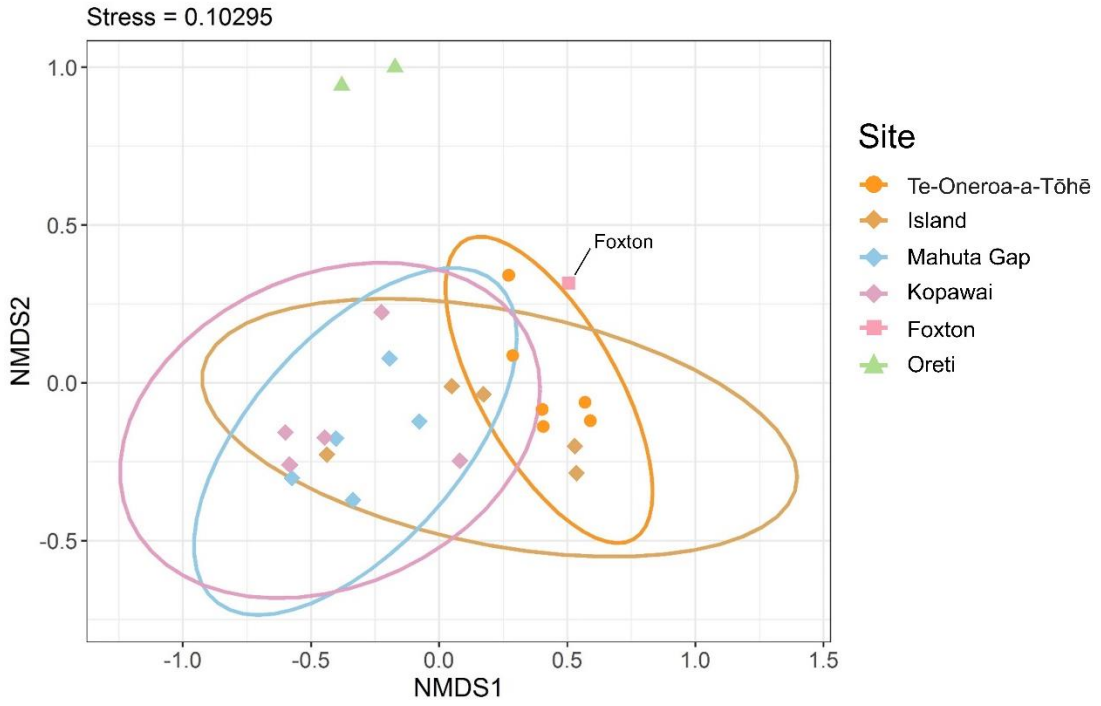

Fig. 5.4. Non-metric multidimensional scaling (NMDS) based on Bray-Curtis dissimilarity index. Constructed using 16S rRNA community data derived from the toheroa composite microbiome (gill and digestive gland). Normalised OTU counts were log10(x+1) transformed prior to index calculation. Shapes represent beaches and different colours represent sampled sites.

A PERMANOVA model identified site as a considerable contributor to dissimilarity ($F = 3.3$, $df = 3$, $p = 0.001$). Indicator species analysis was subsequently used to identify key taxa contributing to site-specific dissimilarity. Foremost, the most indicator species associated to a group or combination of groups was for Kopawai and Mahuta Gap combined (35 taxa). OTU74 (family: *Neisseriaceae*), OTU70 (family: *Desulfocapsaceae*) and OTU37 (family: *Flavobacteriaceae*) were the top three taxa for this combination of groups with an Indval score >0.9 (p <0.001). When Island was added to the group (i.e., all Ripiro Beach sites), 21 taxa were identified as indicator species compared to Ninety-Mile Beach. The top two were OTU38 (family: *Desulfocapsaceae*) (0.961, $p = 0.006$) and OTU83 (family: *Desulfosarcinaceae*) (0.952, $p = 0.001$). Separately, grouping Island and Kopawai, the top indicator species identified was OTU99 (family: *Saprospiraceae*) (0.862, $p = 0.028$). OTU118 was identified as the top indicator taxa for Ninety-Mile Beach (0.707, $p = 0.038$), taxonomically assigned to *Cobetia* (family: *Halomonadaceae*). Finally, for a combination of groups: Island, Kopawai, and Ninety-Mile Beach (i.e., excluding Mahuta Gap) OTU5 (*Endozoicomonas* spp.) identified as the sole indicator species (0.957, $p = 0.002$). The relative abundances of indicator taxa have been used to construct a heatmap (Fig. 5.6). Despite not being included in indicator species analysis, Oreti and Foxton samples were included for comparison of indicator OTUs. Interestingly, when

Kopawai, Mahuta Gap, and Ninety-Mile Beach were grouped, one indicator species OTU20 (*Pseudoalteromonas* spp.) was highlighted. When compared with other samples (Fig. 5.6), there is clear difference in abundance between sites, but interestingly, the Oreti Beach samples both have the highest relative abundance despite not being included in analyses (Figs. 5.2, 5.3 & 5.6).

5.4.2 Alpha Diversity

Alpha diversity indices were used to interrogate variation of richness and diversity between samples (Fig. 5.7). Kruskal-Wallis tests indicated that bacterial diversity in toheroa tissues did not differ significantly between study sites (p = >0.05). Richness estimates did differ significantly between study sites (p = 0.02), with estimates for Kopawai and Mahuta Gap specimens significantly greater than that for Ninety-Mile Beach (Fig. 5.7). Due to a lack of replication, Oreti (n = 2) and Foxton (n = 1) beach specimens were not included in statistical analyses. However, it should be noted that Shannon diversity estimates for Oreti Beach specimens were greatest (median = 2.51, ±SE 0.1), closely followed by Kopawai and Mahuta Gap (Fig. 5.7, Table E.2).

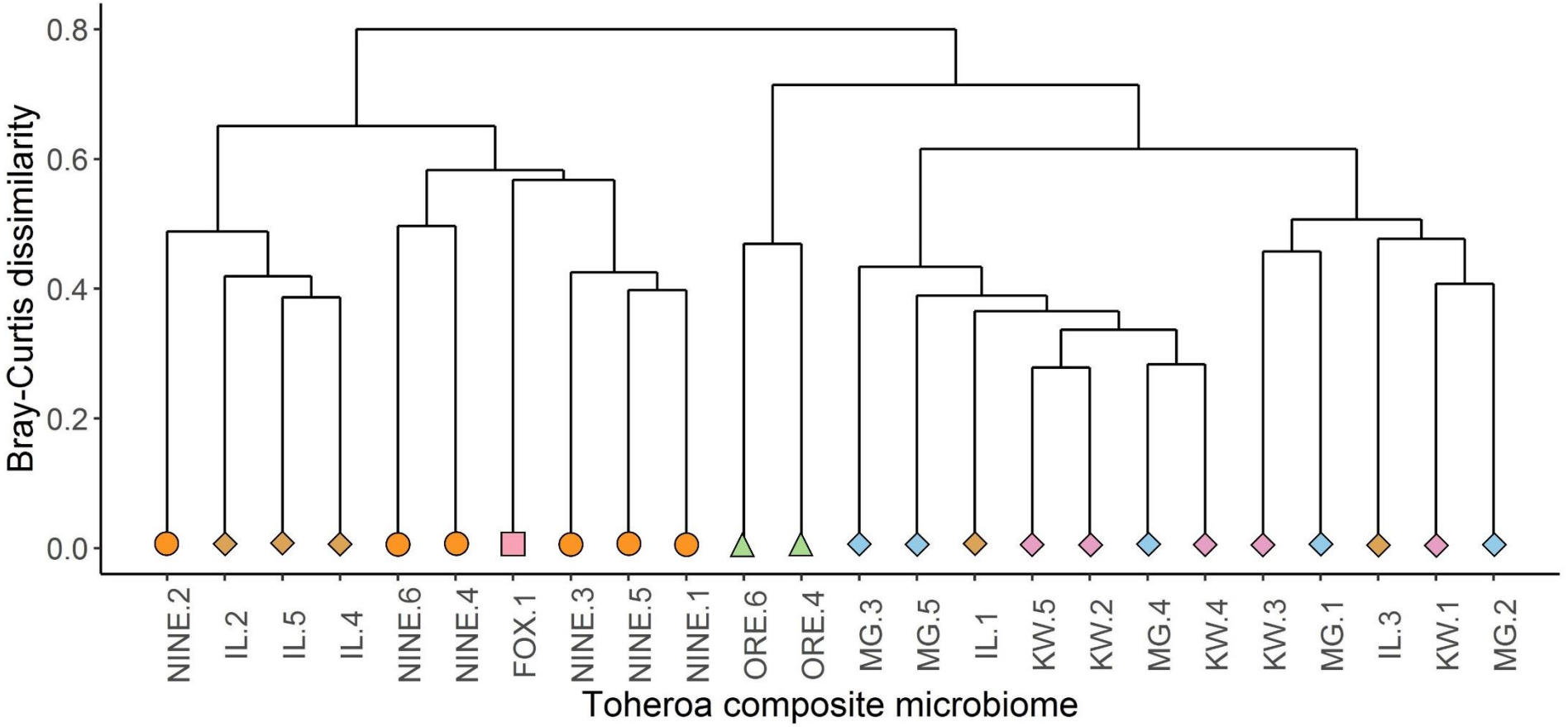

Fig. 5.5. Complete linkage hierarchical clustering based on Bray-Curtis dissimilarities of relative OTU proportions. Constructed using Bray-Curtis dissimilarity index based on the composite microbiome of toheroa (gill and digestive gland) log10(x+1) transformed. IL: Island, MG: Mahuta Gap, KW: Kopawai, Nine: Ninety-Mile Beach (Te-Oneroa-a-Tōhē), Fox: Foxton, Ore: Oreti Beach. Node colour represents sites. Shape corresponds to beach (Fig. 5.1).

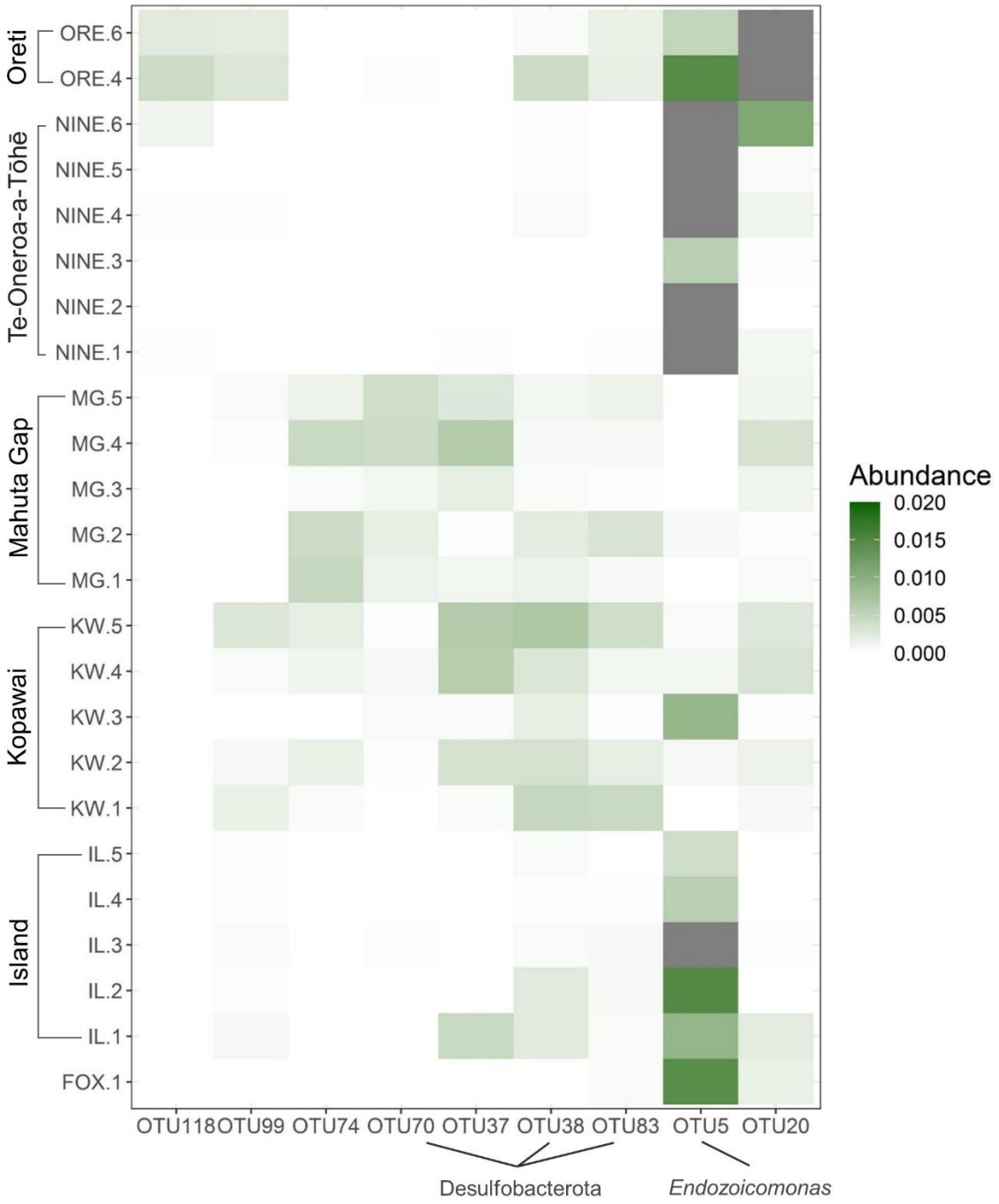

Fig. 5.6. Relative abundance (%) of several top indicator species (OTUs) identified by 'indicspecies' (De Cáceres et al., 2020). Oreti and Foxton Beach specimens were not included in indicator species analysis but are included here for comparison. Relative abundance >0.02 (2%) is represented by a grey tile for respective samples.

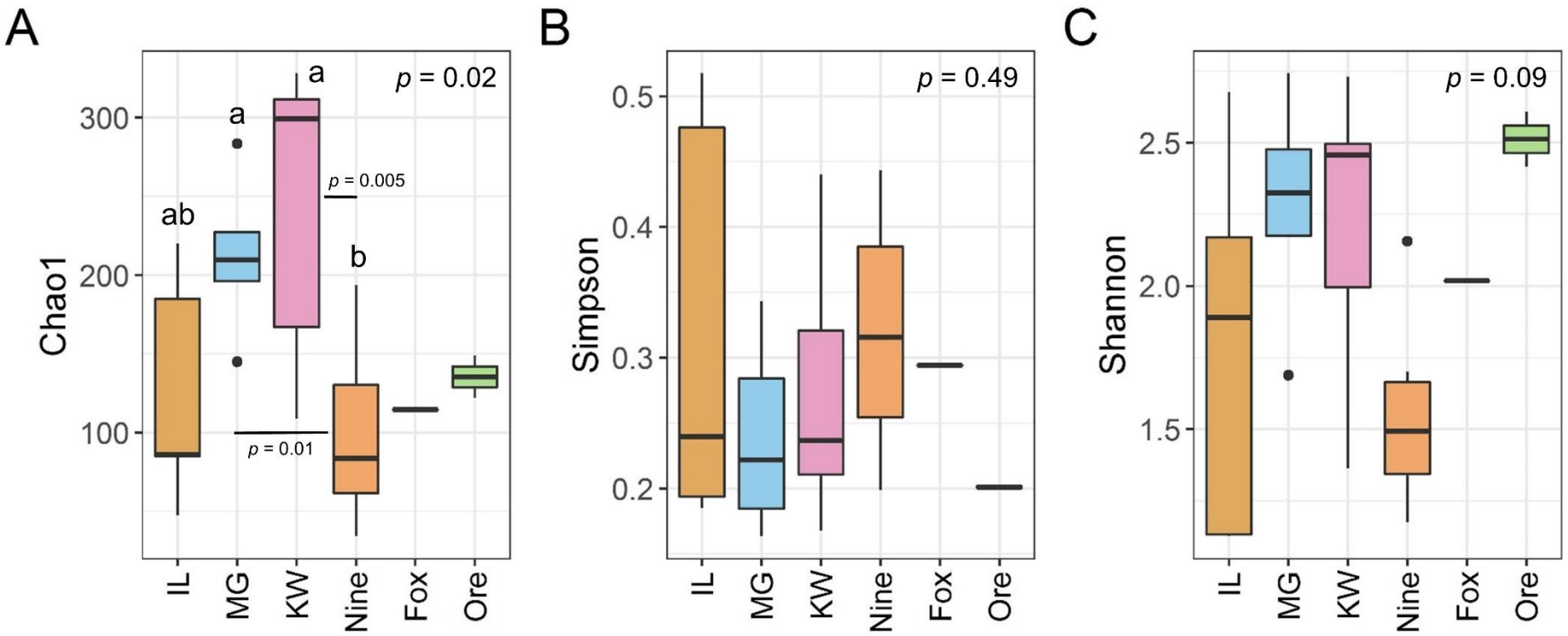

Fig. 5.7. Boxplots comparing alpha diversity constructed using the composite microbiome of toheroa. A: Chao1 richness, B: Simpson diversity index, C: Shannon diversity index. Line: median, box: interquartile range, whiskers: min/max, dots: possible outliers. Kruskal-Wallis test *p*-values are shown in top left corners. If boxes do not share letters, corresponding distributions are significantly different (Dunn test, significance level: 95%). IL: Island, MG: Mahuta Gap, KW: Kopawai, Nine: Ninety-Mile Beach, Fox: Foxton, Ore: Oreti Beach.

5.5 Discussion

The bacterial community of toheroa was described in detail, for the first time, in this study. The most abundant taxa were from the families *Spirochaetaceae* (mean = 75%, range = 24-97%) and *Mycoplasmataceae* (mean = 6%, range = 1-38%). At the genus level, this could be broken down to *Spirochaeta*-2, unclassified *Spirochaetaceae*, and *Mycoplasma*. Both *Spirochaetaceae* and *Mycoplasmataceae* are common dominant constituents of the bacterial community of bivalve molluscs (Dubé et al., 2019; Nguyen et al., 2020; Offret et al., 2020; Pierce and Ward, 2018). For example, this study echoes findings of recent study of the pipi (*P. australis*) microbiome, where *Spirochaetaceae* and *Mycoplasmataceae* were found to be the most abundant taxa present in the gill and digestive gland, respectively (Biessy et al., 2020). As the present study was based on the composite of gill and digestive gland it is not possible to discern tissue-specific microbial communities, though given the findings of Biessy et al. (2020) it is possible to venture that the abundance of these taxa herein are likely attributed to the same respective tissues. Geographic differences in bacterial communities were immediately apparent. Namely the presence of *Vibrionaceae*/*Vibrio* taxa at comparatively high abundance in South Island specimens from Oreti Beach (potentially due to survivor bias). Again, this finding echoes Biessy et al. (2020) where a high abundance of *Vibrionaceae* was found in the siphons of specimens from Aparima (Riverton), *c.* 10 km from Oreti Beach. Additionally, bacteria in the genus *Endozoicomonas* were found to be differentially abundant, with greatest abundance in Ninety-Mile Beach specimens. Importantly, *Synechococcus* CC9902 was also found to be in the top 10 taxa (in terms of relative abundance) in several specimens from Ripiro and Ninety-Mile Beach. Biessy et al. (2020) strived to identify possible culprits associated with tetrodotoxin (TTX) in pipi. The authors identified several possible candidates based on interrogation of the bacterial community of pipi siphons and digestive gland, including *Synechococcus* CC9902. Its role in TTX production remains unknown but raises potential safety implications for consumers of toheroa.

Geographic and local differences were expected due to differential environmental influences (e.g., Nguyen et al., 2020; Offret et al., 2020), but some curious similarities and dissimilarities were observed. For instance, an ordination based on Bray-Curtis dissimilarity index clustered all North Island specimens closely, but the Oreti samples (*n* = 2), the only South Island samples presented herein, clustered separately (also see Fig. 5.5). Interestingly, hierarchical clustering placed samples geographically disjoined (*c.* 1240 km) closer together (more similar) than specimens from the same beach (10 km apart). Namely, three Island samples were found to be more similar to Ninety-Mile Beach specimens than to all other Ripiro Beach specimens. Additionally, this clustering showed that there is an overall split in sample similarity (Fig. 5.5). Most of the Ripiro Beach

specimens are clustered closely. This cluster is more similar in community composition to the two Oreti Beach specimens than to all other samples collected from the North Island (Fig. 5.5), even three from the same beach (Table 5.1). On closer examination of relative abundances of indicator taxa (Fig. 5.6), the extent that key taxa are driving this dissimilarity is clear. Foremost, there is a striking difference in the relative abundance of OTU5 (*Endozoicomonas* spp.) between sites, a distinct relative absence from both the Kopawai and Mahuta Gap specimens is obvious (apart from one Kopawai specimen).

The site specific differences in bacterial community composition described here must be treated with caution. Due to low sample numbers, variation within sites due to health related factors, could not be explored. Within site variability is evident when the community composition (taxa and relative abundance) are examined (see MG.3 in Fig. 5.3, for example). This is variability is clearer still when viewing the alpha diversity metrics in Fig. 5.7. A wide range of health related factors could influence microbial composition between toheroa hosts within the same site, these include parasitism, sex, and diet to name a few. Some of these factors, explored in the same specimens in Chapter 3, are included in Table 5.2 and discussed further below.

5.5.1 Sulfur-cycling Symbionts

For several taxa identified as indicator species (i.e., OTUs 99, 74, 70, 37, 38, and 83) there is a clear association with Kopawai and Mahuta Gap compared to all other sites/beaches. Of these, three are particularly interesting. OTUs 70, 38, and 83 were taxonomically assigned to the phylum Desulfobacterota. It is possible that the reason for this is due to algae blooms that are typical in autumn (austral) on Ripiro Beach (Williams et al., 2013). Dense mats of dead algae cover the mid- to low-intertidal of beach (pers. obs.), which likely increases bacterial decomposition following an influx of decaying organic matter. Increased bacterial respiration probably explains the presence of sulfate-reducing bacteria (Desulfobacterota) within the bacterial community of toheroa as oxygen is depleted within toheroa beds and sulfur (SO_4^{2-}) reduction rates increase e.g., van Erk et al. (2020) provide a kelp and sandy beach ecosystem parallel. It is therefore suggested, that the detection of Desulfobacterota taxa in the toheroa bacterial community is due to environmental exposure rather than a fundamental constituent of bacterial community of toheroa. Supported by the considerably lower relative abundance of Desulfobacterota OTUs within the toheroa composite microbiome. For example, in Brittany, France the bacterial community of the Manila clam (*Ruditapes phlippinarum*) digestive gland was dominated by taxa of the Orders Mycoplasmatales and Rickettsiales, not reflective of the surrounding sediment that was dominated by Desulfobacterales (36%) (Offret et al., 2020).

Interestingly, links to the sulfur cycle were made elsewhere too. When the sequence of OTU3 (average relative abundance: 20.2%) was compared to published sequences (NCBI), a moderate identity was found to a spirochaete endosymbiont (88.8%, AJ620512.1) found in a gut-less worm (Oligochaeta) (Blazejak et al., 2005; Cano et al., 2020). Additionally, some *Endozoicomonas* spp. (OTU5) are associated with sulfur-cycling roles in coral hosts (Tandon et al., 2020). Both Spirochaetales and *Endozoicomonas* taxa together have been shown to be dominant symbionts of other marine organisms i.e., red coral *Corallium rubrum* (van de Water et al., 2016). Given the multiple links between the toheroa-associated bacterial community and well-known symbionts (particularly sulfur-cycling symbionts), future work in this area should consider their potential importance for toheroa health.

5.5.2 Mucus and the Genera Vibrio *and* Pseudoalteromonas

The bacterial genus *Pseudoalteromonas* (100% identity, MT645493.1) was detected at relatively high abundance (5 and 7%) in Oreti Beach specimens, despite being found in several other samples at lower abundances (OTU20, Fig. 5.6). The functional role of this genus within the toheroa-associated bacterial community is unknown. However, many strains produce bioactive compounds with anti-bacterial, -fungal, -fouling, and algicidal activity (Atencio et al., 2018; Offret et al., 2016). Furthermore, the genus *Pseudoalteromonas* currently hosts 41 species, 16 of which are antimicrobial metabolite producers (reviewed in Offret et al., 2016). In fact, several probiotics have been developed using *Pseudoalteromonas* spp. to reduce pathogen burden (*Vibrio* spp.) in bivalve aquaculture (Kesarcodi-Watson et al., 2012; Offret et al., 2019; Prado et al., 2010). For example, Offret et al. (2019) showed the efficacy of a *Pseudoalteromonas* strain (hCg-6) isolated from mollusc haemolymph against *Vibrio harveyi* (ORM4) in European abalone (*Haliotis tuberculata*). Interestingly, the three specimens found to have the highest relative abundance of *Vibrio* spp. were also found to host the highest relative abundance of *Pseudoalteromonas* species. This mirrors the findings of Biessy et al. (2020) again. A tentative link can be drawn between the presence and relative abundance of *Vibrio* and *Pseudoalteromonas* spp. in the pipi siphon bacterial community (see Riverton and Waihi, Biessy et al., 2020). This link could be casual rather than causal, but it is possible that these bacteria co-occur in the bacterial community of *Paphies* calms owed to the remediating effects of *Pseudoalteromonas* spp. against several *Vibrio* strains (Kesarcodi-Watson et al., 2012; Offret et al., 2016; Offret et al., 2019). In the Sydney rock oyster (*Saccostrea glomerata*), Nguyen et al. (2020) also found an association between *Pseudoalteromonas* and *Vibrio* spp., where the authors noted greater relative abundance of these taxa in Queensland unknown (QX) disease-susceptible oysters versus QX disease-resistant oysters. Another analogue can be

drawn, this time to corals. The antimicrobial properties of coral mucus associated bacteria have been explored in the past (Shnit-Orland et al., 2012) with links to *Pseudoalteromonas* spp. as a key inhibitor of *Vibrio* spp. (Nissimov et al., 2009; Vizcaino et al., 2010). For example, Nissimov et al. (2009) showed that a *Pseudoalteromonas* sp. isolated from the coral mucus of *Oculina patagonica* was the greatest inhibitor of *Vibrio shiloi* out of nine isolates that inhibited *V. shiloi* growth. Interestingly, specimens in this study that were found to have a high relative abundance of *Pseudoalteromonas* (Fig. 5.6) were also observed to have the highest intensity of mucous cell hyperplasia i.e., 'ORE.4', 'ORE.6', and 'NINE.5' (Table 5.2 & Figs. 5.8 & E.2).

This link can only be speculated on here, but it does create an interesting avenue for further exploration of the mucus bacterial community associated with toheroa. Excessive mucus production was observed in many toheroa specimens (98% prevalence in Oreti Beach specimens, n = 40) during a histopathology screening of toheroa (Chapter 3, Fig. C.2). The bacterial community associated with said mucus likely provide antibacterial properties as reported in other taxa e.g., teleost and elasmobranch fishes (reviewed in Tiralongo et al., 2020). Therefore, its role within the toheroa holobiont may be crucial for toheroa microbial homeostasis and health (Allam and Pales Espinosa, 2016). Mucus production in several marine species is used as a first line of defence (Allam and Pales Espinosa, 2016; Dash et al., 2018; Shnit-Orland and Kushmaro, 2009; Tiralongo et al., 2020). Like molluscs, corals do not possess an adaptive immune system, instead associated-microbial communities in hosts (holobiont) provide defence (Mydlarz et al., 2010; Reed et al., 2010). Primarily, mucus sloughs and traps microbes but it also provides a medium for antimicrobial metabolite-producing bacteria (innate immunity) that can reduce or remediate the impact of opportunistic pathogens (Allam and Pales Espinosa, 2016; Dash et al., 2018). In numerous mollusc species, mucus has been reported as a facilitator of bacterial symbiotic relationships (Allam and Pales Espinosa, 2016). For instance, as a regulator of *Perkinsus marinus* virulence in Pacific oysters (*C. virginica*) (Pales Espinosa et al., 2014). It therefore is probable that the observational link between *Pseudoalteromonas* and *Vibrio* spp., and mucous cell hyperplasia in toheroa, is due to defensive mucus production. Further study of toheroa health, or the health of other *Paphies* clams in Aotearoa, could consider mucus and mucus-associated bacterial communities as a possible defensive mechanism against pathogens.

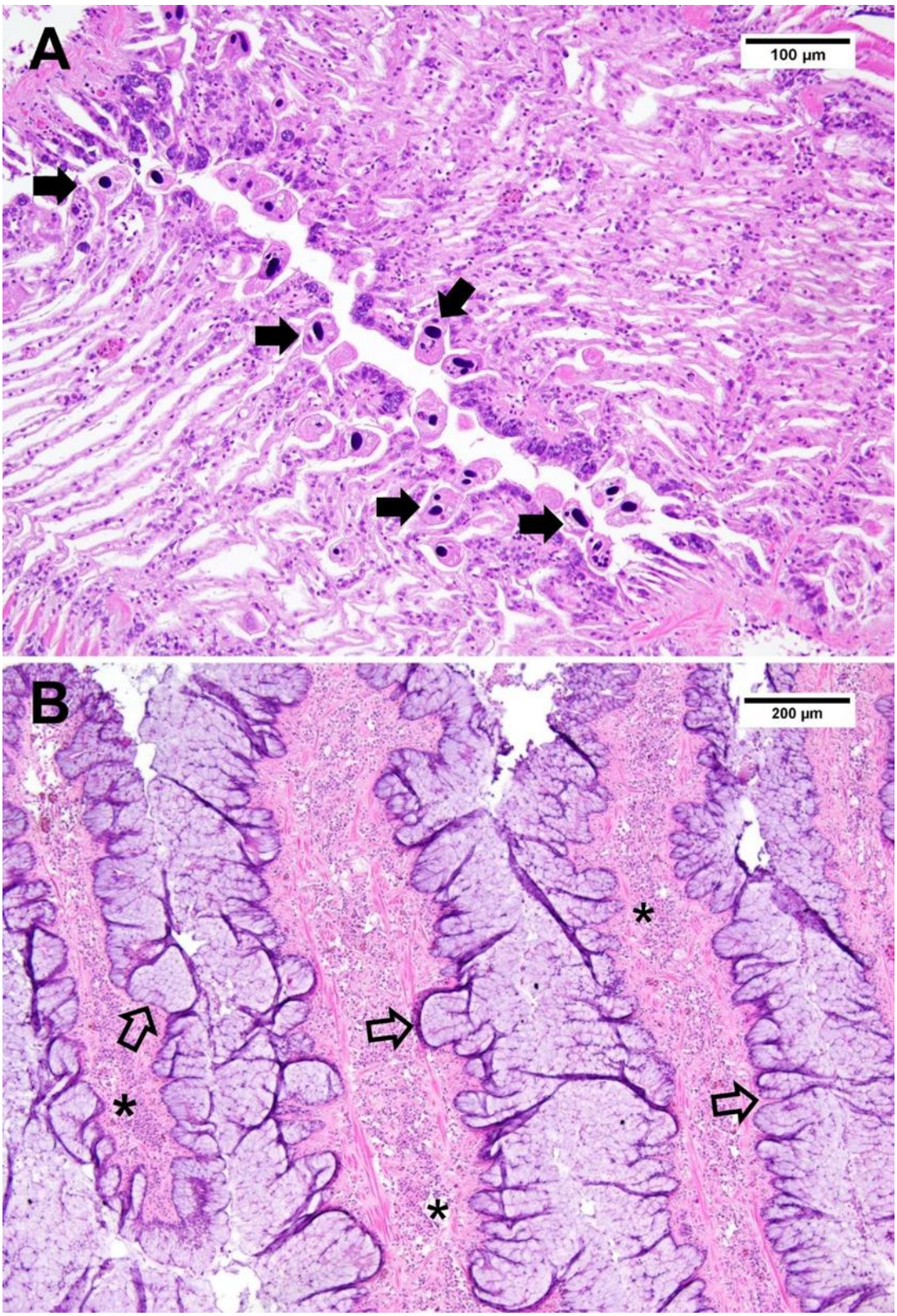

Fig. 5.8. Histology of toheroa gills (stained with H&E) at x10 and x20 magnification. Viewed using an Olympus BX53. A) Shows the presence of gill ciliates in specimens gathered from Mahuta Gap in September 2019 (MG.1). Gill ciliates were at particularly high intensity in the five specimens from Mahuta Gap at c. 15-20 gill ciliates present per field of view at x20 magnification. B) Mucous cell (goblet) hyperplasia (hollow arrows) in the suprabranchial chamber of an Oreti specimen (ORE.6). Asterisks: haemocytes within muscle fibres.

Table 5.2. Histological observations in toheroa tissue sections. Counts (*n)* of intracellular microcolonies (IMCs) of bacteria and gill ciliates are totals in the gills of respective specimens.

Site	Sample	Sex	IMCs (*n*)	Ciliates (*n*)	Mucous cell hyperplasia
Ninety-Mile (Te-Oneroa-a-Tōhē)	NINE.1	Male	8	>100	Low
	NINE.2	Female	-	>100	Low
	NINE.3	Female	-	-	High
	NINE.4	Female	-	-	Low
	NINE.5	Male	-	>100	High
	NINE.6	Male	-	-	Moderate
Island	IL.1	Male	3	-	Low
	IL.2	Female	11	-	Low
	IL.3	Female	-	-	Low
	IL.4	Male	44	-	Low
	IL.5	Female	-	-	Low
Mahuta Gap	MG.1	Male	-	>100	Moderate
	MG.2	Male	5	>100	Low
	MG.3	Male	-	>100	Low
	MG.4	Male	-	>100	Low
	MG.5	Male	6	>100	Low
Kopawai	KW.1	Female	-	-	Moderate
	KW.2	Male	-	-	Low
	KW.3	Male	-	-	Low
	KW.4	Female	8	>100	Low
	KW.5	Female	9	>100	Low
Foxton	FOX.1	Male	4	-	High
Oreti	ORE.4	Male	-	-	Moderate
	ORE.6	Male	-	-	High

5.5.3 Freshwater Streams and the Toheroa Microbiome

A striking difference in relative abundance of *Endozoicomonas* spp. was detected between study sites. Namely, the relative absence of *Endozoicomonas* spp. in Kopawai and Mahuta Gap specimens compared to other study sites (OTU5, Fig. 5.6). In terms of site-specific effects that could be driving this change, Kopawai and Mahuta Gap both have sizable streams (Table 5.1), compared to all other sites used in this study. In Chapter 4, it was suggested that *Endozoicomonas* spp. abundance patterns were likely driven by salinity/freshwater exposure more than temperature in toheroa. This effect would not be surprising, given studies of coral (van de Water et al., 2017), jellyfish and mussel microbiomes (Daniel and Ana, 2020) have linked *Endozoicomonas* spp. dominance or absence to salinity/freshwater. For instance, when the microbial community composition of a coastal hydrological system was investigated (Adyasari et al., 2020), the authors found that the primary factor driving microbial community

dynamics was salinity. In the Sydney rock oyster, Nguyen et al. (2020) found that *Endozoicomonas* spp. was also a significant driver in microbiota dissimilarity between location and seasons. Furthermore, the authors found that *Endozoicomonas* spp. relative abundance was considerably higher in QX disease-resistant oysters than in their disease-susceptible counterparts. In corals and sponges, *Endozoicomonas* spp. are often treated as an important constituents of host microbiota (Neave et al., 2016; Neave et al., 2017; Nishijima et al., 2013), whereas in fish and shellfish, *Endozoicomonas* spp. are often considered potentially pathogenic (Cano et al., 2020; Hooper et al., 2019; Howells et al., 2021; Mendoza et al., 2013).

More and more microbiome studies of marine molluscs are showing *Endozoicomonas* spp. to be dominant (Daniel and Ana, 2020; Schill et al., 2017) or highly abundant taxa (Dubé et al., 2019; Nguyen et al., 2020) in host-associated bacterial communities. Dubé et al. (2019) go further, mentioning that the relative abundance of *Endozoicomonas* spp. in the oyster microbiome suggests particular importance for host health. Similarly, Nguyen et al. (2020) note the dominance of *Endozoicomonas* spp. in many coral and sponge-associated microbiomes, calling for research into their functional role in oyster hosts. When the microbiome of the Red Sea giant clam (*Tridacna maxima*) was investigated, authors found high abundance of OTUs assigned to *Endozoicomonadaceae*, particularly in the gills (Rossbach et al., 2019). Taxonomy-based functional inference indicated that *Endozoicomonadaceae* play a role in nitrogen cycling and uptake in *T. maxima* gill tissues (Rossbach et al., 2019). Therefore, it is possible that *Endozoicomonas* spp. in the bacterial community of toheroa are similarly important constituents for toheroa homeostasis, health, and survival, where 'infection levels' (Chapter 4) are instead microbiome modulation (compositional and/or functional disturbance) in response to changing intrinsic demands (biogeochemical cycling).

The potential influence of freshwater exposure on the toheroa-associated bacterial community was noticed elsewhere too. For Mahuta Gap specimens (the site with the most consistent stream), one of the top indicator taxa identified was OTU247, *Bacteriovoracaceae* (0.78, p = 0.021) which are typically associated with soil and freshwater (Davidov and Jurkevitch, 2004). Though many marine *Bacteriovoracaceae* taxa exist too (Pineiro et al., 2007). A search in the using BLAST (NCBI) indicated that OTU247 was 97.2% identity to *Bacteriovorax* sp. MER21 (DQ631740.1) (Pineiro et al., 2007). Interestingly, *Bacteriovoracaceae* (and other *Bdellovibrio* and like organisms, BALOs) are often associated with protozoan grazers in aquatic systems (Johnke et al., 2017; Paix et al., 2019). Here, ciliates (protozoa) were observed in high abundance in the gills of toheroa and primarily in Mahuta Gap specimens (Table 5.2 and Fig. 5.8). Protozoan gill ciliates in molluscs are in turn, often associated with slow flowing water with high nutrient loads. Gill ciliates attach to gills via hooks, predating on bacteria that

pass through the water channels in the gills of hosts (Fig. 5.8). One possible mechanism behind the differential relative abundance of *Bacteriovorax* spp. in Mahuta Gap specimens is delivery/retention by ciliates as a vector. When the gill was extracted, the bacterial community of associated parasites (ciliates) was unavoidably included. Gill ciliates could be selectively grazing on *Bacteriovorax* spp. or environmental exposure at Mahuta Gap might simply be higher. Regardless of delivery route, observations of parasites at such high abundances highlights the need for multi-disciplinary approaches to health assessments. For instance, in the present study the potential modifying influence of gill ciliates by predation on bacteria would not be acknowledged were it not for routine histopathology being used alongside DNA metabarcoding. Furthermore, *Bacteriovorax* spp. are predatory bacteria (Chen et al., 2012). By feeding on Gram-negative bacteria (e.g., *Vibrio* spp.), they have been shown to shape the bacterial community of hosts (Chen et al., 2011; Chen et al., 2012). It is possible that *Bacteriovorax* taxa are also modulating the toheroa microbiome in the same way predatory gill ciliates potentially are. Alongside environmental, parasitic, and host modulation (mucus production) effects, predatory bacteria should be considered as modifiers of the toheroa microbiome in the future.

The association made between several taxa and freshwater outflow presence or absence raises potential implications for the ongoing recovery effort for toheroa. Key bacteria taxa in several freshwater-associated toheroa specimens were missing from counterparts not exposed to freshwater outflow and vice-versa. In some samples, this difference was so striking that geographically separated specimens (*c.* 1240 km) hosted more similar bacterial communities, than local specimens. Additionally, richness estimates of bacterial communities were typically higher for specimens gathered at stream-bearing sites (Fig. 5.7). This link remains tentative, a variety of health related features (Table 5.2) that could not be statistically tested here, are likely influencing community composition in kind with a variety of site specific environmental parameters.

Though the function of taxa present in the toheroa bacterial community was not examined in the present study, functional profiles are likely modified in-kind with bacterial community composition (urchins: Brothers et al., 2018; sea stars: Lloyd and Pespeni, 2018). Declining toheroa abundance on Te Tai Tokerau beaches has been associated with decreased abundance of freshwater flows (Chapter 1). For instance, Williams et al. (2013) reported that land use change had reduced the number of streams on Ripiro Beach from 15 to 9 (not encompassing the entire beach) and from 83 to 30 on Ninety-Mile Beach, based on historical maps from c.1950. The results presented here, highlight how the toheroa bacterial community could be impacted, in turn raising questions for the future recovery of toheroa. Namely, what impact reduced freshwater flows have on the

function of the toheroa microbiome? Moreover, what knock-on effect this modification has on toheroa defence, health, and survival?

5.6 Recommendations

1. The link between toheroa life histories and freshwater flows remains an interesting facet of their ecology worthy of further exploration. Understanding the functional diversity of the toheroa microbiome, and how it is modified indirectly by freshwater outflow (and other factors i.e., sex, diet, and parasite loads), will aid investigations of toheroa health in the future. A comprehensive understanding of the tissue-specific functional profile of the toheroa microbiome will also inform health related study of toheroa if conservation aquaculture as a recovery tool is explored in the future.
2. An investigation into TTX concentrations in toheroa should be conducted following the report of high abundances of *Synechococcus* CC9902 in toheroa and following the findings of Biessy et al. (2020). If *Synechococcus* CC9902 is the TTX producing culprit in *Paphies* clams, then there are potential safety concerns for consumers of toheroa that require further investigation.
3. Multiple taxa identified in the toheroa bacterial community were closely related to bacteria that fulfil sulfur-cycling roles in the environment (Desulfobacterota) or in host cells (endosymbionts). It is possible, like other infaunal marine molluscs that toheroa intermittently depend on chemosymbiosis for nutrition (e.g., van der Geest et al., 2014). Future studies of toheroa health should consider the significance of sulfur-cycling symbionts for toheroa health and growth.
4. Mucous cell hyperplasia, subsequent excess mucus production, and the cautious links to *Pseudoalteromonas* and *Vibrio* spp., raises a new avenue for research of toheroa health. Due to the protected status of toheroa, and the depressed state of several populations, exploration of mucus-associated bacteria of toheroa offers a non-invasive health assessment route. If, alike other mucus producing marine species, mucus provides the first line of defence, the structural and functional diversity of the mucus microbiome could prove useful for monitoring toheroa health.
5. Parasitic grazing protozoa (gill ciliates) and predatory bacteria (*Bacteriovorax* spp.) should be considered potential intrinsic modifiers of the toheroa microbiome in the future. Although the effect on taxa present appears slight, functional profiles may be modified if specific taxa are being predated on. Health studies on Aotearoa shellfish should continue to use traditional histology as alongside powerful molecular tools.

6 Previous research of *Endozoicomonas* spp. in toheroa treated the bacteria as a potential pathogen (Howells et al., 2021; Chapter 4). However, it is entirely possible that *Endozoicomonas* spp. fill an important functional role within the toheroa bacterial community. Several streams of research including whole-genome sequencing, gene expression analyses, and *ex situ* experimentation focusing on *Endozoicomonas* spp. (co-infection and stress gradients), would provide valuable insight into the role of *Endozoicomonas* spp. in Aotearoa shellfish.

5.7 References

Adyasari, D., et al., 2020. Microbial community composition across a coastal hydrological system affected by submarine groundwater discharge (SGD). PLOS ONE. 15**,** e0235235.

Allam, B., Pales Espinosa, E., 2016. Bivalve immunity and response to infections: Are we looking at the right place? Fish & Shellfish Immunology. 53**,** 4-12.

Atencio, L. A., et al., 2018. Antimicrobial-producing *Pseudoalteromonas* from the marine environment of Panama shows a high phylogenetic diversity and clonal structure. Journal of Basic Microbiology. 58**,** 747-769.

Babirat, C., et al., 2004. Equal partnership: two trematode species, not one, manipulate the burrowing behaviour of the New Zealand cockle, *Austrovenus stutchburyi*. Journal of Helminthology. 78**,** 195-199.

Bass, D., et al., 2019. The Pathobiome in Animal and Plant Diseases. Trends in Ecology & Evolution. 34**,** 996-1008.

Beentjes, M. P., 2010. Toheroa survey of Oreti Beach, 2009, and review of historical surveys. New Zealand Fisheries Assessment Report 2010/6. 40.

Beule, L., Karlovsky, P., 2020. Improved normalization of species count data in ecology by scaling with ranked subsampling (SRS): application to microbial communities. PeerJ. 8**,** e9593.

Biessy, L., et al., 2020. Seasonal and Spatial Variations in Bacterial Communities From Tetrodotoxin-Bearing and Non-tetrodotoxin-Bearing Clams. Frontiers in Microbiology. 11**,** 1860.

Blazejak, A., et al., 2005. Coexistence of bacterial sulfide oxidizers, sulfate reducers, and spirochetes in a gutless worm (Oligochaeta) from the Peru margin. Applied and Environmental Microbiology. 71**,** 1553-1561.

Bourne, D. G., et al., 2016. Insights into the Coral Microbiome: Underpinning the Health and Resilience of Reef Ecosystems. Annual Review of Microbiology. 70**,** 317-340.

Brothers, C. J., et al., 2018. Ocean warming alters predicted microbiome functionality in a common sea urchin. Proceedings of the Royal Society B: Biological Sciences. 285**,** 1881.

Cano, I., et al., 2020. Cosmopolitan Distribution of *Endozoicomonas*-Like Organisms and Other Intracellular Microcolonies of Bacteria Causing Infection in Marine Mollusks. Frontiers in Microbiology. 11**,** 2778.

Carnegie, R. B., et al., 2016. Managing marine mollusc diseases in the context of regional and international commerce: policy issues and emerging concerns. Philosophical Transactions of the Royal Society B: Biological Sciences. 371**,** 20150215.

Castinel, A., et al., 2019. Disease threats to farmed green-lipped mussels *Perna canaliculus* in New Zealand: review of challenges in risk assessment and pathway analysis. Aquaculture Environment Interactions. 11**,** 291-304.

Chen, H., et al., 2011. Prey bacteria shape the community structure of their predators. The ISME Journal. 5**,** 1314-1322.

Chen, H., et al., 2012. Predatory *Bacteriovorax* Communities Ordered by Various Prey Species. PLOS ONE. 7**,** e34174.

Cope, J., The modification of toheroa habitat by streams on Ripiro Beach. MSc. University of Waikato, Hamilton, New Zealand, 2018, pp. 126.

Daniel, F. R. C., Ana, R. M. P., 2020. Marine lake populations of jellyfish, mussels and sponges host compositionally distinct prokaryotic communities. Hydrobiologia. 878, 3409–3425.

Dash, S., et al., 2018. Epidermal mucus, a major determinant in fish health: a review. Iranian journal of veterinary research. 19**,** 72-81.

Davidov, Y., Jurkevitch, E., 2004. Diversity and evolution of *Bdellovibrio*-and-like organisms (BALOs), reclassification of *Bacteriovorax starrii* as *Peredibacter starrii* gen. nov., comb. nov., and description of the *Bacteriovorax–Peredibacter* clade as *Bacteriovoracaceae* fam. nov. International Journal of Systematic and Evolutionary Microbiology. 54**,** 1439-1452.

De Cáceres, M., et al., Package 'indicspecies'. Relationship Between Species and Groups of Sites, 2020. CRAN Repository. pp, 32.

De Cáceres, M., et al., 2010. Improving indicator species analysis by combining groups of sites. Oikos. 119**,** 1674-1684.

de Vries, A., Ripley, B., D., ggdendro: Create Dendrograms and Tree Diagrams Using 'ggplot2'. 2020.

Desai, A. R., et al., 2012. Effects of plant-based diets on the distal gut microbiome of rainbow trout (*Oncorhynchus mykiss*). Aquaculture. 350-353**,** 134-142.

Dubé, C. E., et al., 2019. Microbiome of the Black-Lipped Pearl Oyster *Pinctada margaritifera*, a Multi-Tissue Description With Functional Profiling. Frontiers in Microbiology. 10**,** 1548.

Edgar, R. C., 2010. Search and clustering orders of magnitude faster than BLAST. Bioinformatics. 26**,** 2460-2461.

Ghanbari, M., et al., 2015. A new view of the fish gut microbiome: Advances from next-generation sequencing. Aquaculture. 448**,** 464-475.

Holt, C. C., et al., 2020. Understanding the role of the shrimp gut microbiome in health and disease. Journal of Invertebrate Pathology. 107387.

Hooper, P. M., et al., 2019. Shedding and survival of an intracellular pathogenic *Endozoicomonas*-like organism infecting king scallop *Pecten maximus*. Diseases of Aquatic Organisms. 134**,** 167-173.

Howells, J., et al., 2021. Intracellular bacteria in New Zealand shellfish are identified as *Endozoicomonas* species. Diseases of Aquatic Organisms. 143**,** 27-37.

Johnke, J., et al., 2017. Killing the killer: predation between protists and predatory bacteria. FEMS Microbiology Letters. 364**,** fnx089.

Johnson, M., et al., 2008. NCBI BLAST: a better web interface. Nucleic Acids Research. 36**,** W5-9.

Kesarcodi-Watson, A., et al., 2012. Protective effect of four potential probiotics against pathogen-challenge of the larvae of three bivalves: Pacific oyster (*Crassostrea gigas*), flat oyster (*Ostrea edulis*) and scallop (*Pecten maximus*). Aquaculture. 344-349**,** 29-34.

King, G. M., et al., 2012. Analysis of Stomach and Gut Microbiomes of the Eastern Oyster (*Crassostrea virginica*) from Coastal Louisiana, USA. PLOS ONE. 7**,** e51475.

Lahti, L., et al., 2017. Tools for microbiome analysis in R. Version. 1**,** 504.

Lane, H. S., et al., 2020. Aquatic disease in New Zealand: synthesis and future directions. New Zealand Journal of Marine and Freshwater Research. 1-42.

Llewellyn, M. S., et al., 2014. Teleost microbiomes: the state of the art in their characterization, manipulation and importance in aquaculture and fisheries. Frontiers in Microbiology. 5**,** 207.

Lloyd, M. M., Pespeni, M. H., 2018. Microbiome shifts with onset and progression of Sea Star Wasting Disease revealed through time course sampling. Scientific Reports. 8**,** 16476.

McMurdie, P. J., Holmes, S., 2013. phyloseq: An R Package for Reproducible Interactive Analysis and Graphics of Microbiome Census Data. PLOS ONE. 8**,** e61217.

Mendoza, M., et al., 2013. A novel agent (*Endozoicomonas elysicola*) responsible for epitheliocystis in cobia *Rachycentrum canadum* larvae. Diseases of Aquatic Organisms. 106**,** 31-37.

Morrow, K. M., et al., 2015. Natural volcanic CO_2 seeps reveal future trajectories for host–microbial associations in corals and sponges. The ISME Journal. 9**,** 894-908.

Mouchet, M. A., et al., 2012. Genetic difference but functional similarity among fish gut bacterial communities through molecular and biochemical fingerprints. FEMS Microbiology Ecology. 79**,** 568-580.

Mouritsen, K. N., 2002. The parasite-induced surfacing behaviour in the cockle *Austrovenus stutchburyi*: a test of an alternative hypothesis and identification of potential mechanisms. Parasitology. 124**,** 521-528.

Mydlarz, L. D., et al., 2010. What are the physiological and immunological responses of coral to climate warming and disease? The Journal of Experimental Biology. 213**,** 934.

Neave, M. J., et al., 2016. Diversity and function of prevalent symbiotic marine bacteria in the genus *Endozoicomonas*. Applied Microbiology and Biotechnology. 100**,** 8315-8324.

Neave, M. J., et al., 2017. *Endozoicomonas* genomes reveal functional adaptation and plasticity in bacterial strains symbiotically associated with diverse marine hosts. Scientific Reports. 7**,** 40579.

Nguyen, T. V., et al., 2019. Omics approaches to investigate host–pathogen interactions in mass mortality outbreaks of *Crassostrea gigas*. Reviews in Aquaculture. 11**,** 1308-1324.

Nguyen, V. K., et al., 2020. The Sydney rock oyster microbiota is influenced by location, season and genetics. Aquaculture. 527**,** 735472.

Nishijima, M., et al., 2013. *Endozoicomonas numazuensis* sp. nov., a gammaproteobacterium isolated from marine sponges, and emended description of the genus *Endozoicomonas* Kurahashi and Yokota 2007. International Journal of Systematic and Evolutionary Microbiology. 63**,** 709-714.

Nissimov, J., et al., 2009. Antimicrobial properties of resident coral mucus bacteria of *Oculina patagonica*. FEMS Microbiology Letters. 292**,** 210-215.

Offret, C., et al., 2016. Spotlight on Antimicrobial Metabolites from the Marine Bacteria *Pseudoalteromonas*: Chemodiversity and Ecological Significance. Marine drugs. 14**,** 129.

Offret, C., et al., 2020. The marine intertidal zone shapes oyster and clam digestive bacterial microbiota. FEMS Microbiology Ecology. 96**,** fiaa078.

Offret, C., et al., 2019. Protective Efficacy of a *Pseudoalteromonas* Strain in European Abalone, *Haliotis tuberculata*, Infected with *Vibrio harveyi* ORM4. Probiotics and Antimicrobial Proteins. 11**,** 239-247.

Paix, B., et al., 2019. Diversity, Dynamics, and Distribution of *Bdellovibrio* and Like Organisms in Perialpine Lakes. Applied and Environmental Microbiology. 85**,** e02494-18.

Pales Espinosa, E., et al., 2014. Pallial mucus of the oyster *Crassostrea virginica* regulates the expression of putative virulence genes of its pathogen *Perkinsus marinus*. International Journal for Parasitology. 44**,** 305-317.

Perry, E. K., et al., 2017. The Low-Diversity Fecal Microbiota of the Critically Endangered Kākāpō Is Robust to Anthropogenic Dietary and Geographic Influences. Frontiers in Microbiology. 8**,** 2033.

Pierce, M. L., Ward, J. E., 2018. Microbial Ecology of the Bivalvia, with an Emphasis on the Family Ostreidae. Journal of Shellfish Research. 37**,** 793-806.

Pineiro, S. A., et al., 2007. Global survey of diversity among environmental saltwater *Bacteriovoracaceae*. Environmental Microbiology. 9**,** 2441-2450.

Prado, S., et al., 2010. Review of probiotics for use in bivalve hatcheries. Veterinary Microbiology. 145**,** 187-197.

Pruesse, E., et al., 2007. SILVA: a comprehensive online resource for quality checked and aligned ribosomal RNA sequence data compatible with ARB. Nucleic Acids Research. 35**,** 7188-7196.

Quast, C., et al., 2013. The SILVA ribosomal RNA gene database project: improved data processing and web-based tools. Nucleic Acids Research. 41**,** D590-D596.

Reed, K. C., et al., 2010. Coral immunology and resistance to disease. Diseases of Aquatic Organisms. 90**,** 85-92.

Ross, P. M., et al., 2018a. The biology, ecology and history of toheroa (*Paphies ventricosa*): a review of scientific, local and customary knowledge. New Zealand Journal of Marine and Freshwater Research. 52**,** 196-231.

Ross, P. M., et al., 2018b. First detection of gas bubble disease and *Rickettsia*-like organisms in *Paphies ventricosa*, a New Zealand surf clam. Journal of Fish Diseases. 41**,** 187-190.

Rossbach, S., et al., 2019. Tissue-Specific Microbiomes of the Red Sea Giant Clam *Tridacna maxima* Highlight Differential Abundance of *Endozoicomonadaceae*. Frontiers in Microbiology. 10**,** 2661.

Schill, W. B., et al., 2017. *Endozoicomonas* Dominates the Gill and Intestinal Content Microbiomes of *Mytilus edulis* from Barnegat Bay, New Jersey. Journal of Shellfish Research. 36**,** 391-401.

Schloss, P. D., et al., 2009. Introducing mothur: Open-Source, Platform-Independent, Community-Supported Software for Describing and Comparing Microbial Communities. Applied and Environmental Microbiology. 75**,** 7537-7541.

Shnit-Orland, M., Kushmaro, A., 2009. Coral mucus-associated bacteria: a possible first line of defense. FEMS Microbiology Ecology. 67**,** 371-380.

Shnit-Orland, M., et al., 2012. Antibacterial Activity of *Pseudoalteromonas* in the Coral Holobiont. Microbial Ecology. 64**,** 851-859.

Singh, B. K., Trivedi, P., 2017. Microbiome and the future for food and nutrient security. Microbial biotechnology. 10**,** 50-53.

Snieszko, S. F., 1974. The effects of environmental stress on outbreaks of infectious diseases of fishes. Journal of Fish Biology. 6**,** 197-208.

Tandon, K., et al., 2020. Comparative genomics: Dominant coral-bacterium *Endozoicomonas acroporae* metabolizes dimethylsulfoniopropionate (DMSP). The ISME Journal. 14**,** 1290-1303.

Team, R. C., R: A language and environment for statistical computing. R Foundation for Statistical Computing, Vienna, Austria, 2013.

Tiralongo, F., et al., 2020. Skin Mucus of Marine Fish as a Source for the Development of Antimicrobial Agents. Frontiers in Marine Science. 7**,** 760.

van de Water, J. A. J. M., et al., 2016. Spirochaetes dominate the microbial community associated with the red coral *Corallium rubrum* on a broad geographic scale. Scientific reports. 6**,** 27277.

van de Water, J. A. J. M., et al., 2017. Comparative Assessment of Mediterranean Gorgonian-Associated Microbial Communities Reveals Conserved Core and Locally Variant Bacteria. Microbial Ecology. 73**,** 466-478.

van der Geest, M., et al., 2014. Nutritional and reproductive strategies in a chemosymbiotic bivalve living in a tropical intertidal seagrass bed. Marine Ecology Progress Series. 501**,** 113-126.

van Erk, M. R., et al., 2020. Kelp deposition changes mineralization pathways and microbial communities in a sandy beach. Limnology and Oceanography. 65**,** 3066-3084.

Vizcaino, M. I., et al., 2010. Antimicrobial resistance of the coral pathogen *Vibrio coralliilyticus* and Caribbean sister phylotypes isolated from a diseased octocoral. Microbial Ecology. 59**,** 646-657.

West, A. G., et al., 2019. The microbiome in threatened species conservation. Biological Conservation. 229**,** 85-98.

Wickham, H., 2009. ggplot2: Elegant Graphics for Data Analysis. Springer, New York.

Williams, J. R., et al., Review of factors affecting the abundance of toheroa (*Paphies ventricosa*). New Zealand Aquatic Environment and Biodiversity Report No. 114, 2013, pp. 76.

Chapter 6
Do Freshwater Streams Deliver Trace Metal Pollution to a Threatened Intertidal Beach Clam?

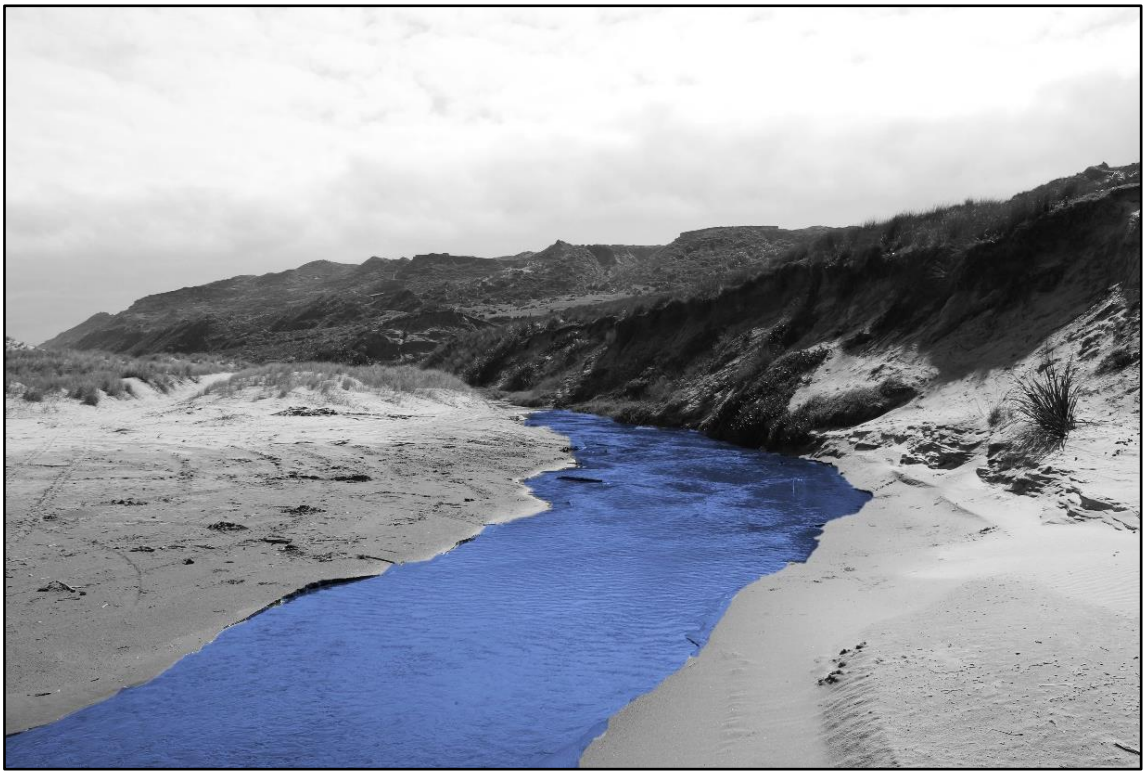

Freshwater flowing onto the beach
Kopawai, Ripiro Beach

6.1 Abstract

Toheroa beds are typically found where freshwater streams flow onto the beach, suggesting habitat requirements linked to the presence of freshwater outflow. Consequently, these same streams may be delivering terrestrial pollutants to toheroa habitats. To investigate what influence streams might be having on pollutant delivery, trace metal concentrations were determined in toheroa tissue (foot, *n* = 30) and surface sediments (*n* = 12) within streams (encompassing stream water) at Ripiro Beach using inductively coupled plasma-mass spectrometry (ICP-MS). Toheroa is te reo Māori for 'long tongue' this is due to its size, relative to the entire body mass of toheroa, the foot is therefore often the most readily consumed part of toheroa.

Analyses of trace metals (Pb, Fe, Mn, Cr, Co, Ni, Cu, Zn, V, As, Se, and Mg) in surface sediments (i.e., sand) within stream outflows indicated little delivery potential of trace metal pollution to toheroa beds, likely due to a combination of trace metal deposition, beach topography, and hydrology. Instead, seasonal variation of trace metal concentrations in toheroa soft tissues at three sites, suggests exposure from the ocean and diet override the potential effects of freshwater stream delivery. Overall, the metal pollution index (MPI) indicated a relatively low trace metal load in toheroa soft tissues, and low levels of trace metal pollution in surface sediment. Furthermore, the hazard quotient (HQ) was low *c.* 3.04, suggesting little exposure risk to humans from the consumption of toheroa.

6.2 Introduction

Trace metals are naturally present in the environment at low levels, and generally, very small amounts are required by marine organisms for their biogeochemical processes. However, when excess quantities of metals are introduced by either natural or anthropogenic processes the effects can be toxic, and potentially lethal (Bennett et al., 2001; Calabrese et al., 1973). Metal pollution is a growing issue in marine systems due to the persistent nature of many trace metals, and their continued discharge (Luoma and Rainbow, 2008). Marine organisms primarily uptake trace metals through their diet (Rainbow and Wang, 2001; Wang, 2002), where elements are incorporated into soft tissues and shells (biomineralization) during their formation (via aqueous or dietary exposure). For this reason, sedentary organisms in coastal habitats are often used as biomonitors to assess bioavailable levels of certain trace metals. Less studied, are the health implications of excess trace metal exposure for hosts (Abdou et al., 2020; Beiras and Albentosa, 2004; Chora et al., 2009; Stewart et al., 2021). Instead, focus is often placed on organisms that are consumed by humans (Jonathan et al., 2017; Squadrone

et al., 2016), and the subsequent health risk for consumers (Liu et al., 2018; Liu et al., 2017b; Wang et al., 2018).

In bivalves, overexposure to trace metals is known to impact health and reproduction. For example, high levels of Hg, Cu, Zn, Cd, and Pb in *Ruditapes decussatus* and *Mytilus galloprovincialis* has been associated with decreased embryogenesis (Beiras and Albentosa, 2004). The authors in this case found, that despite the perceived 'toxicity' of certain trace metals (e.g., Hg and Pb), Cu, followed by Zn likely posed the greatest risk to reproductive success (Beiras and Albentosa, 2004). Similarly, Wang et al. (2009) showed how the reproductive potential (embryogenesis, survival, growth, and metamorphosis of larvae) of *Meretrix meretrix* could be impeded by the ecotoxicological effects of Cd, Hg, and Pb. The biochemical implications of exposure to increased Cd concentration in *R. decussatus* via proteomic analysis (Chora et al., 2009) showed that Cd has the capacity to induce major changes in proteins associated with cell maintenance, metabolism, and cytoskeletal maintenance (Chora et al., 2009). Furthermore, complex additive and interactive relationships can exist between pathogens, hosts, and bioavailable trace metals. For instance, Ivanina et al. (2011) examined the interactive effects of hypoxia and Cd in *Crassostrea virginica*. The authors recorded a higher abundance of *Vibrio parahaemolyticus* and *Vibrio vulnificus* associated with increased Cd exposure. Importantly, they also found that prolonged hypoxia exposure increased Cd uptake (Ivanina et al., 2011), illustrating the synergistic effects environmental conditions can have on trace metal uptake rates and therefore pathogen-host interactions.

The toxic effects of overexposure to several trace metals in humans are well known (reviewed by Bosch et al., 2016). Because many bivalves are both filter feeders and sedentary (or exhibit limited mobility), they are considered susceptible to pollutant and toxin bioavailability and to pathogens. Consequently, many bivalve shellfish constitute good biomonitors of environmental pollution (Boening, 1999; Goldberg et al., 1978; Hamed and Emara, 2006; Rainbow and Phillips, 1993). Human consumption risks are generally associated with biotoxin-producing microalgae in the form of harmful algae blooms (HABs) (O'Mahony, 2018). For trace metals, government regulatory agencies often set safe exposure limits, as the risks of overexposure are well known (Liu et al., 2017a; Wang et al., 2018). As exposure risk is based on consumption (dose), generally the risk to consumers is low. Subsistence fishers and coastal Indigenous communities, however, are generally at higher risk due to greater consumption of wild-caught food (Cisneros-Montemayor et al., 2016; Phillips et al., 2014; Stewart et al., 2011). As diets are expected to shift in coming decades, and as reliance on seafood products (especially farmed) as a source of animal protein increases (Costello et al., 2020; Willer and Aldridge, 2020), this risk will inevitably grow too.

The toheroa is endemic to Aotearoa. At present, harvesting toheroa is limited (customary take only) following exploitive commercial and recreational harvesting in the 20th century that significantly reduced populations. Toheroa beds often occur in association with freshwater flows on high-energy surf beaches (Beentjes, 2010; Ross et al., 2018; Williams et al., 2013a; Williams et al., 2013b). The ecological processes underpinning this habitat 'selection' are not known, though associations to health (Chapters 4 & 5), food availability, beach morphology, and reduced desiccation risk (Cope, 2018) have been made. Despite a moratorium of the fishery, toheroa populations have not recovered. Water quality of associated freshwater streams has been identified as a potential factor contributing to the limited recovery of toheroa (Ross et al., 2018; Williams et al., 2013b), but has not yet been studied. Given that there appears to be a reliance on freshwater streams for toheroa life histories, it is reasonable to suggest that any reduction in freshwater flow or quality, could negatively affect toheroa populations. While streams may be modulating pathogen/symbiont abundance (Chapters 4 & 5), reducing temperatures (and thus lowering desiccation risk), and increasing food availability (Cope, 2018), they could also be delivering pollutants (e.g., excess trace metals) to toheroa beds in the intertidal zone.

To better understand this possible contaminant pathway, in this preliminary study I explore the role streams play as a source of trace metal pollution for toheroa, while also providing a benchmark of trace metal concentrations in toheroa. Given that toheroa have long been an important source of food (and continue to be consumed via a customary fishery), a risk assessment for consumption based on selected trace metals is also presented. Consequently, three questions are asked in this study:

Q1. Is there a **seasonal difference** in trace metal concentrations in toheroa tissues that could be attributed to rainfall, greater freshwater outflow, and subsequently increased delivery of terrestrial pollution to toheroa beds?

Q2. Is there a difference in trace metal concentrations in **toheroa tissues** and in **surface sediments between sites** that could be attributed to different land use adjacent to toheroa beds?

Q3. Are trace metal concentrations in toheroa tissues at levels that could be considered harmful to **toheroa and (or) human health?**

6.3 Methods

6.3.1 Study Site and Specimen Collection

The questions detailed above, arose following observations made during site visits and analyses for previous chapters of this thesis. Therefore, due to time and budget

constraints, foot tissues from toheroa specimens gathered for previous studies (Chapters 3 & 4) were used for this study. The rationale for this was also due to the fact the foot of toheroa is the most readily consumed part of toheroa due to its size relative to the entire body mass of toheroa. Toheroa were sampled at three streams associated toheroa beds (Island (IL), Mahuta Gap (MG), and Kopawai (KW)) along Ripiro Beach (Fig. 6.1) in March 2019 (*n* = 15, 5 from each site) and September 2019 (*n* = 15, 5 from each site). Adult toheroa (*c.* 70 mm) were targeted for sampling and the collection of toheroa within beds was haphazard at each given site. Due to protections on toheroa, collections were conducted under a special permit issued by Fisheries New Zealand (permit no. SP706-2).

The three sites differed both, in stream volume, and adjacent land use. The Island site was the lowest volume stream, entering the beach after flowing through agricultural land (pasture) and a wetland. Mahuta Gap has the highest volume stream. The stream is present year-round (pers. obs.) and is used as a vehicle access way to the beach via 'Mahuta Gap Road'. Land use close-by is agricultural (cattle pasture). At Kopawai, the stream is of intermediate volume, and is consistently present, but typically not as wide as the stream present at Mahuta Gap. The stream at Kopawai comes from primarily groundwater sources, as opposed to Mahuta Gap and Island, which could be more accurately described as overland flows. A small lake (*c.* 320 m across its longest axis) sits above the Kopawai site. Adjacent land use is also pasture farmland.

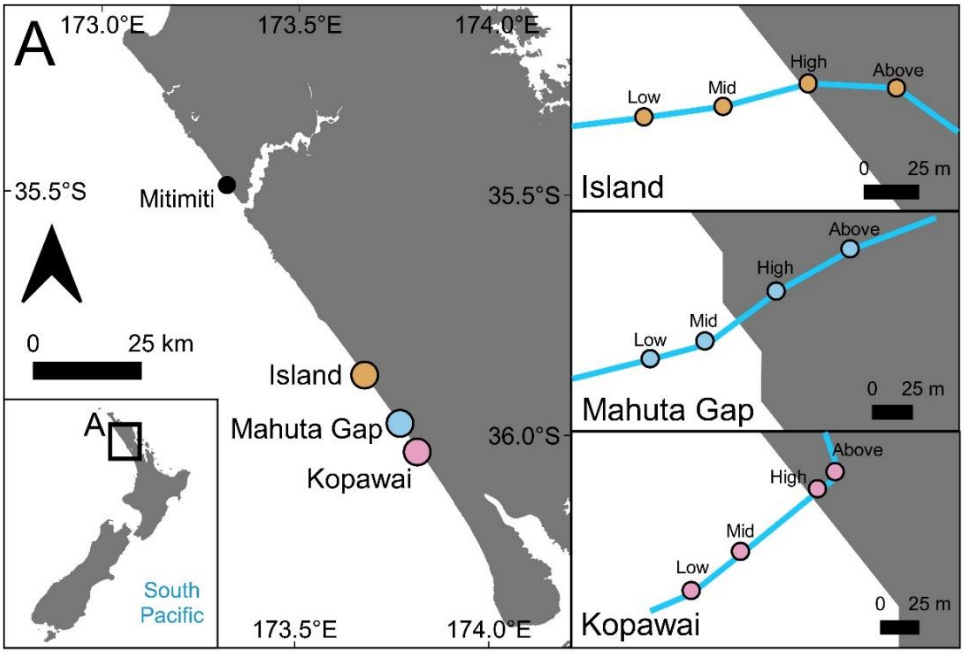

Fig. 6.1. Study location on Ripiro Beach, Te Tai Tokerau. Map shows the three sites used in this study, Island, Mahuta Gap, and Kopawai (left). Sediment sampling locations are also shown at each stream, as well as an indicative flow path (right). Surface sediment was sampled at four stations along a gradient from the respective toheroa bed at 'Low' to above the point which the stream enters the beach 'Above'. Spatial data obtained from DIVA-GIS. CRS: WGS 84 (EPSG: 4326).

Sediment (sand) samples (*n* = 4) were gathered in September 2020 at each of the three sites (Fig. 6.1 & 6.2) (3 x 4 = 12). A small corer was used to extract *c.* 70 cm^3 of surface sediment (top 0-10 cm) within the streams, encompassing surface stream water, at four stations at each site (four stations and three sites: *n* = 12, Fig. 6.2) to establish what trace elements are potentially being delivered to toheroa beds via freshwater influx. Samples were taken along a gradient from *c.* 50 m above (towards land) where the stream enters the beach, hereafter referred to as 'Above', to each respective toheroa bed, referred to as 'Low'. Two stations were sampled in between these, 'High': the high-tide mark and 'Mid': halfway between the toheroa bed (Low) and the High station (Fig. 6.1 & 6.2).

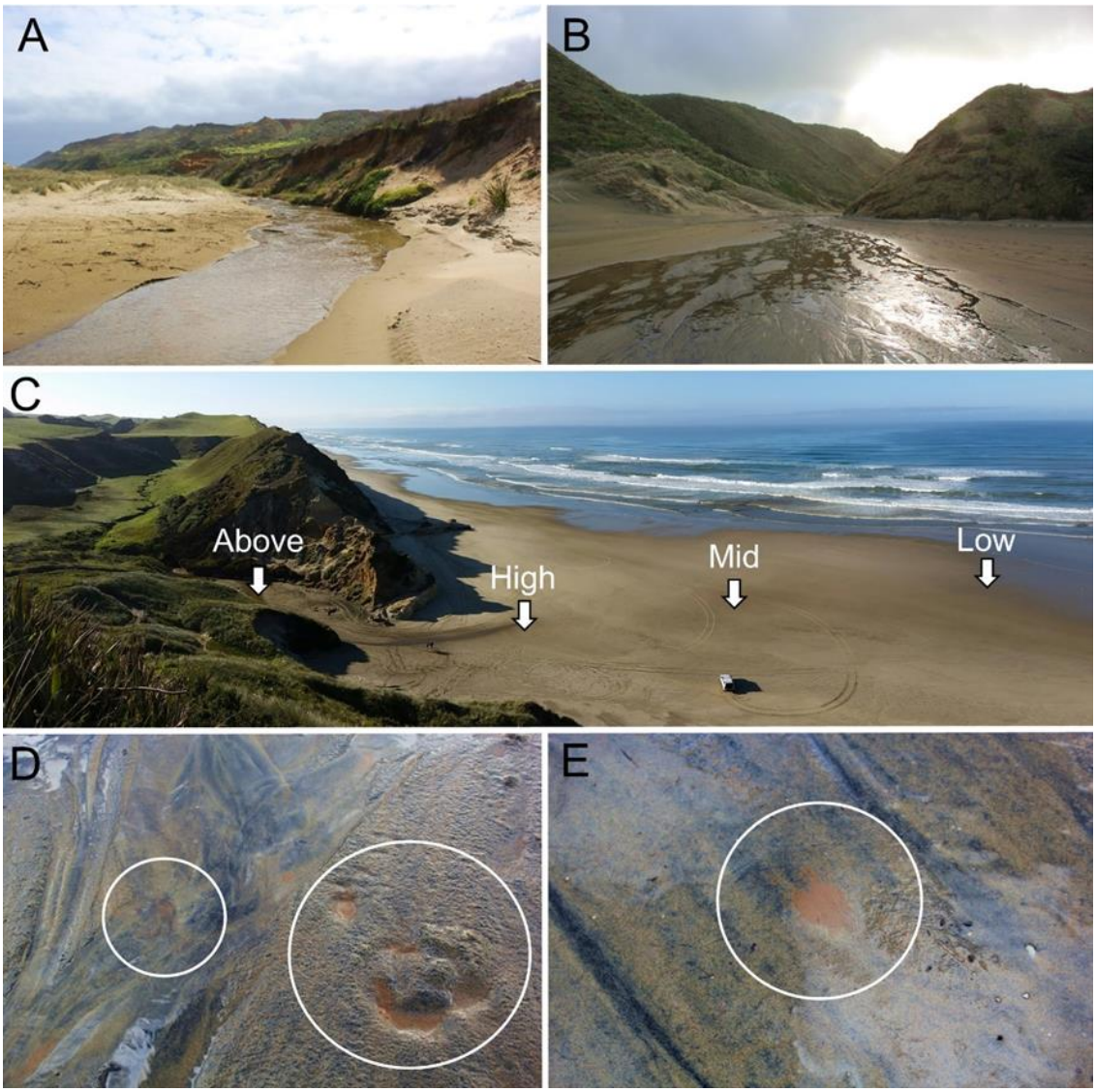

Fig. 6.2. Site photographs taken in September 2020 on Ripiro Beach, using a Canon EOS 60D. A: Kopawai 'Above' station. B: Mahuta Gap Road entrance to Ripiro Beach (High station). C: Island site on Ripiro Beach (photograph: P. Ross). Sediment sampling stations are shown. D & E: Apparent Fe(III) deposits (circled) within the stream at Kopawai. Black sand (titanomagnetite), typical of North Island west coast beaches of Aotearoa, owed to volcanic activity (Taranaki) and titanium (Ti) and iron (Fe).

6.3.2 Sample Storage and Preparation

Foot tissues (*n* = 30 in total) were stored frozen (-18 ºC) until preparation for chemical analysis. Prior to analysis via ICP-MS, foot tissues were weighed (to the nearest 0.001 g) and freeze-dried (Lyovapor™ L-200) to aid chemical digestion. Tissue moisture content was determined using mass (g) of specimens pre- and post-freeze drying. Similarly, sediment samples (*n* = 12 in total) were weighed pre- and post-drying to determine moisture content.

6.3.3 Digestion and Chemical Analysis (ICP-MS)

Preparation and chemical analyses by ICP-MS of soft tissue and sediment samples was undertaken at the University of Waikato Mass Spectrometry Facility (Hamilton, NZ). 0.2 g of freeze-dried tissue sample (*c.* 1 g wet weight) and 0.65 ml of double distilled HNO_3 (70%) were added into 50 ml calibrated vials. Vials were heated at 80 °C for one hour. After cooling (to room temperature), 0.6 ml H_2O_2 (30%) was added to vials. Vials were heated again at 80 °C for one hour. After cooling (to room temperature), 0.4 ml H_20_2 was added, and vials were heated a third time at 80 °C for 30 mins. Samples were diluted to a final volume of 20 ml with ultrapure H_20 (Type-1 18 mΩ). After drying at 50 °C for one week, sediment samples were ground with mortar and pestle until no lumps remained. Then, 0.2 g of ground sediment was weighed into clean 50 ml calibrated vials. 1 ml HNO_3 and 0.33 ml HCL (Aqua regia) was added to each sample and samples were left overnight. Samples were then heated at 50 °C for one hour, then 50 ml of ultrapure H_2O (Type-1 18 mΩ) was added to each vial. Sediment samples were centrifuged for 10 mins at 4000 rpm, 10 ml of the supernatant was then added to clean 15 ml tubes for analysis.

Elemental concentrations of ^{208}Pb, ^{56}Fe, ^{55}Mn, ^{52}Cr, ^{59}Co, ^{60}Ni, ^{65}Cu, ^{68}Zn, ^{51}V, ^{91}As, and ^{82}Se (and ^{24}Mg in sediment) were determined in toheroa foot tissues and sediment samples using an Agilent 8900 with a triple-quadrupole (QQQ) Inductively Coupled Plasma–Mass Spectrometer, ICP-MS [Agilent, USA].

6.3.3.1 Quality Assurance

All elements analysed herein were above the limit of detection (LOD). Certified reference material (CRM) ERM®-CE278K (wild mussels, *Mytilus edulis*) from The European Commission, Joint Research Centre (JRC) Institute for Reference Materials and Measurements (IRMM), and method blanks were prepared and analysed alongside the tissue and sediment samples. The observed concentrations of the CRM were in close

alignment with the certified values (Table 6.1) apart from Se. Selenium was subsequently removed from analyses of toheroa foot tissue. The recovery of Fe was also poor (Table 6.1), but Fe was retained for analyses in foot tissue due to perceived importance to the study. However, caution should be placed on its interpretation.

Table 6.1. Observed concentrations versus certified values obtained using certified reference material ERM® -CE278k (European Commission, Joint Research Centre). Values in μg g^{-1}.

Element	Certified value (±SD)	This study
As	6.7 (0.4)	8.14
Cr	0.73 (0.22)	0.43
Cu	5.98 (0.27)	5.76
Fe	161 (8)	**98.9**
Mn	4.88 (0.24)	4.53
Ni	0.69 (0.15)	0.56
Pb	2.18 (0.18)	1.84
Se	1.62 (0.12)	**1.14**
Zn	71 (4)	55.62

6.3.4 Metal Pollution Index and Hazard Quotient

The metal pollution index (MPI) (Usero et al., 1996) was used to compare trace element pollution exposure between sites on Ripiro Beach, which were calculated for each sample/site as follows:

$$MPI = (Cf_1 \times Cf_2 \ldots Cf_n)^{\frac{1}{n}}$$

Cf_n is the concentration of a given element *n* in a sample. The higher the MPI score, the more polluted a site or station is considered to be. Here, the MPI was used to examine trace metal pollution between sites where freshwater streams that flow through agricultural land, flow onto the beach and over toheroa beds. MPI scores were calculated for each specimen and sediment sample.

To examine the relative hazard of consumption of toheroa tissue based on trace metal concentrations, the Hazard Quotient (HQ) was used (de Souza et al., 2011; Liu et al., 2017a). The HQ is essentially a ratio between exposure of a given element and the average daily reference dose provided by government agencies. A HQ score <1 is considered low, >9.9 moderate, >19.9 high, and >100 is considered critical. Here, the HQ was calculated based on trace metal concentrations (Cr, Cu, Zn, As, and Pb) derived

from the foot tissue only. Due to depuration, partitioning and soft tissue turnover, potentially hazardous trace metal concentrations have likely been missed here (Marsden et al., 2014; Okazaki and Panietz, 1981), and a different HQ score would be found if the entire visceral mass was analysed instead. The following formula was used to calculate the Hazard Quotient:

$$HQ = \frac{(C \times dose)}{(RfDo \times 70\ kg)}$$

C is the trace metal concentration derived from the foot tissue of toheroa (mg kg^{-1}), expressed as wet weight converted from dry weight. Following Liu et al. (2017a), *dose* was taken to be 0.3 kg wet weight per day for adults. *RfDo* is the average daily reference dose for a given metal per day (mg kg^{-1} per day). The *RfDo* values for Cr, Cu, Zn, As, Cd, Hg, and Pb are 0.003, 0.02, 0.3, 0.003, 0.001, 0.0001, and 0.0036 mg/kg, respectively (Liu et al., 2017a). The HQ scores were categorised as per Liu et al. (2017a) and summed to get a total HQ value to assess interactive risks of multiple metals (Chien et al., 2002).

6.3.5 Statistical Analyses

Permutational Multivariate Analysis of Variance (PERMANOVA) (permutations = 999) based on Euclidean distance was used to assess trace metal dissimilarity between study sites and sampling months explained trace metal concentration variation in foot tissue. PERMANOVA was also applied to sediment samples gathered in September 2020. All trace metal concentration data was transformed (square root) prior to multivariate analysis. To visualise dissimilarity between study sites and months for sediment and foot tissue based on trace element concentrations, Non-metric Multidimensional Scaling (NMDS) ordinations were constructed (Euclidean distance). To examine site-specific differences in trace metal concentrations in foot tissue and sediment, One-way Analysis of Variance (ANOVA) was used. Where statistically significant differences were detected (p = <0.05), Tukey's post-hoc tests were used to further interrogate where statistical differences lay. If test assumptions were violated, Kruskal-Wallis and Dunn tests were used (Dinno and Dinno, 2017). To determine whether trace metal concentrations differed significantly in toheroa foot tissue between March and September 2019, unpaired t-tests were used (significance level = <0.05), if test assumptions were violated Mann-Whitney U-tests was used instead. Sites were pooled for analyses, thus seasonal differences are based on Ripiro Beach (n = 30).

Spearman's correlation was used to examine the relationship between trace element concentrations in foot tissue and sediment.

All statistical analyses were carried out in RStudio (R Core Team, 2013). Multivariate analysis and ordinations were constructed using the package 'vegan' (Oksanen et al., 2019). All data visualisation was achieved using the package 'ggplot2' (Wickham, 2009), ANOVA and t-tests were carried out using base R. Correlation matrices were constructed using the package 'corrplot' (Wei et al., 2017).

6.4 Results

Trace metal concentrations in both sediment and toheroa tissue varied with site and season. Due to recovery and limits of detection, the elements focused on for analyses were Pb, Fe, Mn, Cr, Co, Ni, Cu, Zn, V, and As (and Mg in the sediment).

6.4.1 Toheroa Tissue

Trace metal concentrations in foot tissues were analysed separately for sampling months (March and September), and compared between sites. In March 2019, concentrations of trace metals varied significantly between study sites. Pb, Fe, Co, Ni, Cu, and Zn concentrations varied between sites (p <0.05), though most recorded differences were only marginally different. The exception was Co (p = 0.005) which was recorded in greater concentrations in specimens collected at Island than at Mahuta Gap and Kopawai (Fig. 6.2). Concentrations of Mn, Cr, V, and As did not differ significantly between sampling sites in March 2019 (p >0.05). From specimens gathered in September 2019, although there was some variation in trace metal concentrations in foot tissue between sites, only Pb concentration varied significantly between sites (p = 0.02). With a significantly higher Pb concentration determined for Kopawai specimens compared to Mahuta Gap specimens (p = 0.01). Trace metals other than Pb and Ni, were generally recorded at similar concentration across sites in September (Fig. 6.3). For some elements (Fe, Ni, Cu, As, Pb, and Cr), concentrations varied significantly between March and September (Table 6.2 & F.1). This difference was highly significant (p = <0.001) for Pb and Cu, which were recorded at higher concentrations in toheroa in March, and Ni, which was present at higher concentrations in September. To aid interpretation of trace metal concentrations of the ten elements examined in toheroa tissue herein, permutational multivariate analysis of variance (PERMANOVA) was used. A model was created using site and sampling month. Permutational testing indicated that site was not a significant explanatory variable for trace element dissimilarity (F = 2.6, df = 2, p = 0.061), but that sampling month (March and September) did significantly contribute dissimilarity (F = 6.0, df = 1, p = 0.020) in the model (visualised using NMDS, Fig. 6.5). An interaction

term (site and month) indicated little interactive effects (F = 1.8, df = 2, p = 0.160). Overall, trace metal concentrations in toheroa were low, relative to concentrations reported from other bivalves (Table 6.3).

6.4.2 Hazard quotient

The hazard quotient (HQ) was used to assess the potential risk associated with the consumption of trace metals within toheroa tissues. HQ scores were relatively low (Table 6.4). The HQ scores obtained for Cr, Cu, Zn, and Pb were less than 0.25. The only exception was arsenic, where a moderate HQ score was obtained regardless of sampling site or season (range = 2.4-2.94).

6.4.3 Sediment

Elemental concentrations in sediment observed here were compared to those observed in other studies (Table 6.5). Direct comparisons of these results are challenging due to differing methods, locations, and reporting, however, concentrations reported here were generally lower (Table 6.5). To examine the potential delivery of trace elements from streams to toheroa beds, elemental concentrations of sediment gathered along a transect from the stream source to toheroa beds were visualised using point and line plots (Fig. 6.6) and barplots (Fig. F.1). Evident from figures 6.6 and F.1, concentrations fluctuated between sampling area and site. Only one sample was gathered at each station, therefore formal statistical analyses were not conducted. One-way analysis of variance based on pooled station concentrations revealed that concentrations of Cr (p = 0.045) and Ni (p = 0.047) varied significantly between study sites, though only marginally so.

A PERMANOVA model was constructed to assess trace metal concentrations derived from sediment (n = 12) using Pb, Fe, Mn, Cr, Co, Ni, Cu, Zn, V, and As. The model indicated site was not a significant contributor to dissimilarity of trace metal concentrations in sediment (F = 1.2, df = 2, p = 0.354) (Fig. 6.5).

Table 6.2. Results from Unpaired t-tests and Mann-Whitney U-tests based on trace metal concentrations derived from toheroa foot tissue in March and September 2019. Tests conducted on pooled sample concentrations for three sites (n = 15 for each month), p significant at <0.05. Total rainfall 30 days prior to specimen collection was obtained from www.nrc.gov.nz (March 2019: 31 mm, September 2019: 72 mm). Rainfall data was obtained from the closest rainfall station at Kai Iwi Lakes *c.* 10 km from the closest site at Ripiro Beach.

Element	t	df	*p*	Change
Fe	2.34	28	**0.027**	Mar > Sept
Co	1.44	28	0.161	-
Ni	-4.82	28	**<0.001**	Sept > Mar
Cu	5.79	28	**<0.001**	Mar > Sept
Zn	1.63	28	0.115	-
As	2.14	28	**0.041**	Mar > Sept
	W	**df**	***p***	
V	92	28	0.412	-
Pb	210	28	**<0.001**	Mar > Sept
Mn	130	28	0.486	-
Cr	180	28	**0.004**	Mar > Sept

6.4.4 Marine Pollution Index

MPI scores were low (<0.25) for all study sites and sampling events based on trace metal concentrations in toheroa foot tissues (Table 6.3). Compared to MPI scores calculated using data from different studies for other clam spp., the MPI scores here were much lower (Table 6.3), but it is important to consider these were based on the foot tissue alone herein. The MPI calculated for sediment samples was substantially higher than the scores obtained for toheroa tissues (Table. F.2). To assess the capacity of streams to deliver elemental contamination to toheroa beds, the MPI was calculated for each station at each study site (Fig. 6.7, Table F.2). Examination of individual MPI scores along beach profiles (Fig. 6.7) revealed relatively consistent patterns in trace metal distribution, apart from the 'High' station at Kopawai (Fig. 6.7). When sediment MPI scores were compared between study sites, no statistically significant difference in pollution index score was found ($F = 1.14$, $df = 2$, $p = 0.36$).

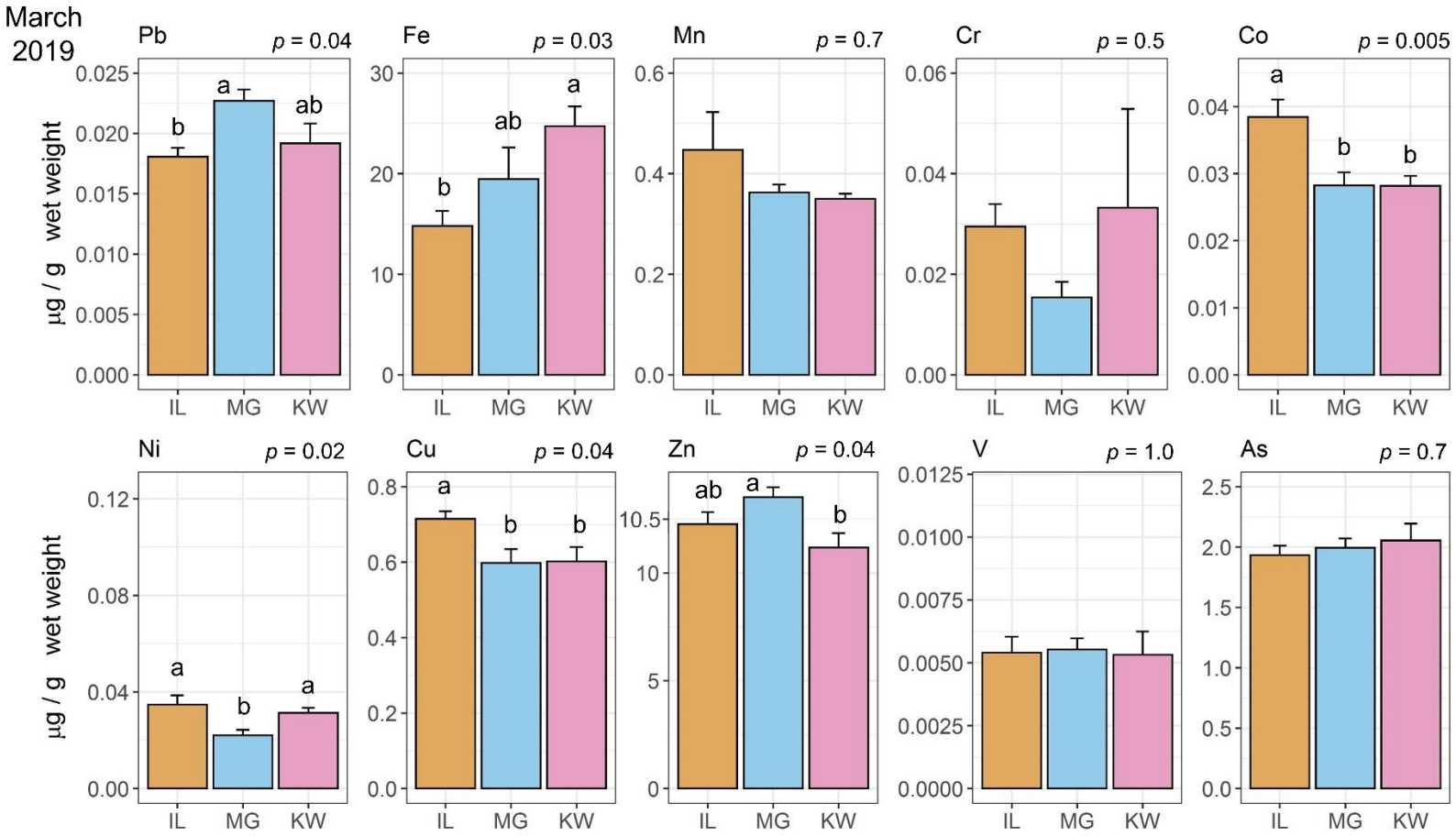

Fig. 6.3. Trace metal concentrations in toheroa foot tissues sampled in March 2019 from IL: Island, MG: Mahuta Gap, and KW: Kopawai on Ripiro Beach. Bars show mean conc. (n = 5) and standard error. Concentrations are given in µg g^{-1} wet weight. One-way ANOVA p-values are shown above each plot. If boxes do not share letters, corresponding distributions are significantly different (Tukey's post-hoc test, p-adj). For Mn, Kruskal-Wallis test was carried out. For reference, maximum levels of metal contaminants in molluscs stipulated by Australia New Zealand Food Standards (FSANZ) Code are 0.1 µg g^{-1} for As and 2 µg g^{-1} for Pb.

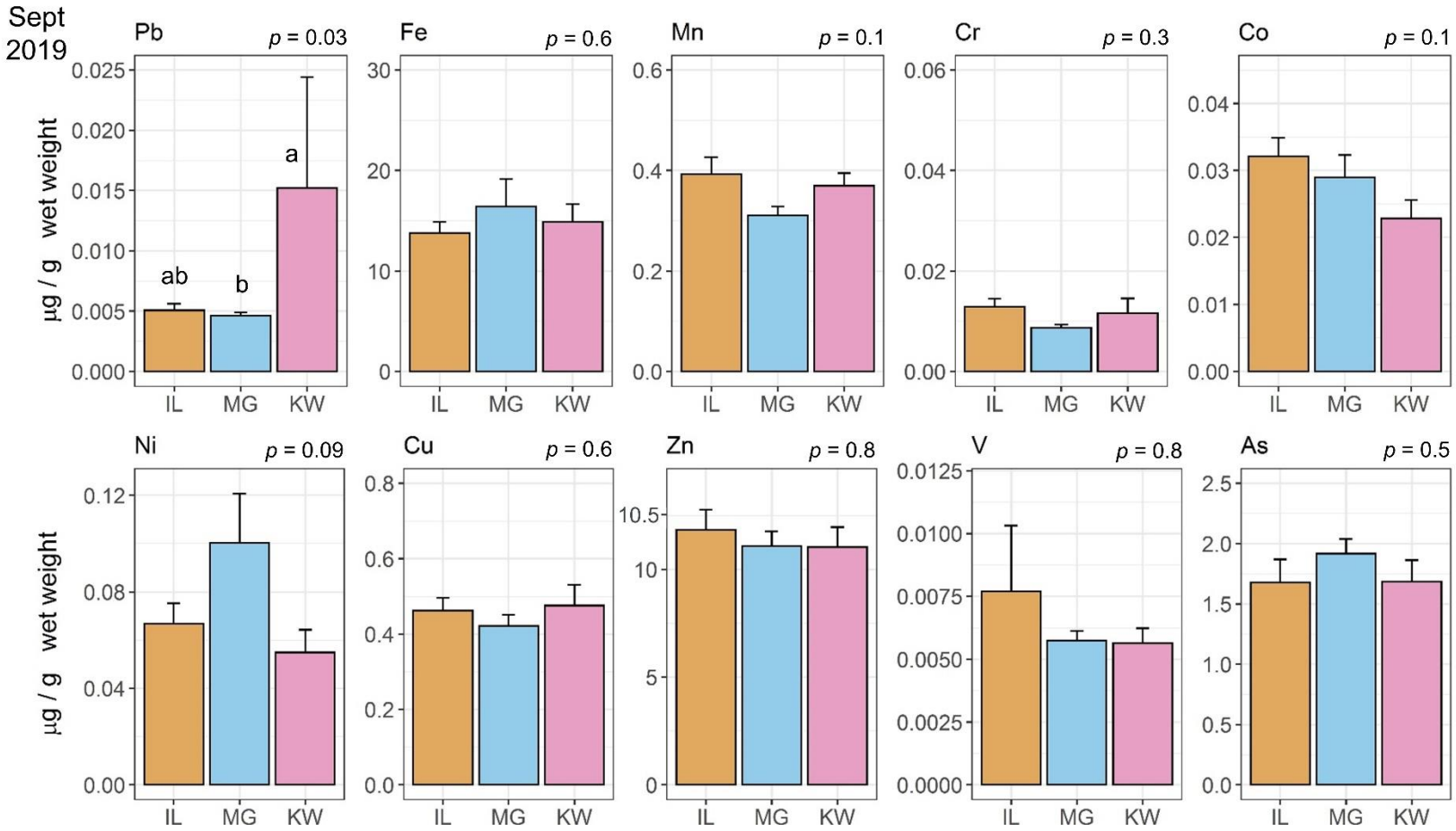

Fig. 6.4. Trace metal concentrations in toheroa foot tissues sampled in September 2019 from IL: Island, MG: Mahuta Gap, and KW: Kopawai on Ripiro Beach. Bars show mean conc. (n = 5) and standard error. Concentrations are given in µg g^{-1} wet weight. One-way ANOVA p-values are shown above each plot. If boxes do not share letters, corresponding distributions are significantly different (Tukey's post-hoc test, p-adj). For Pb, and V, Kruskal-Wallis tests were carried out. Dunn's post-hoc test was carried out for Pb. For reference, maximum levels of metal contaminants in molluscs stipulated by Australia New Zealand Food Standards (FSANZ) Code are 0.1 µg g^{-1} for As and 2 µg g^{-1} for Pb.

Table 6.3. Trace element concentrations derived from various marine clam species. MPI and HQ (hazard quotient) are also given. The HQ index was calculated herein using trace metal concentrations for Cr, Cu, Zn, As, and Pb. The total HQ index score in Liu et al. (2017a) included the elements Hg and Cd but were removed to be comparable to Usero et al. (2005) and this study. The HQ index calculated in Liu et al. (2017a) was based on an average adult weight of 60 kg, for this study and the calculation for Usero et al. (2005), 70 kg was used. For comparability, the MPI was calculated using concentrations for Cr, Mn, Co, Ni, Cu, Zn, As, and Pb. Values are in μg g^{-1} (wet weight), mean and standard deviation (± SD) are shown for this study.

	This study	**Nielsen and Nathan (1975)**	**Nielsen and Nathan (1975)**	**Liu et al. (2017a)**	**Liu et al. (2017a)**	**Liu et al. (2017a)**	**Usero et al. (2005)**	**Usero et al. (2005)**
Location	Ripiro Beach, Aotearoa	Te Waewae Bay & Oreti Beach, NZ	Tauranga, Aotearoa	Laizhou Bay, China	Laizhou Bay, China	Laizhou Bay, China	Southern Spain	Southern Spain
Taxa	Toheroa[1] (*P. ventricosa*)	Toheroa[2] (*P. ventricosa*)	Tuatua[2] (*P. subtriangulata*)	Ark clam[3] (*Scapharca subcrenata*)	Surf clam[3] (*Mactra veneriformis*)	Manila clam[3] (*Ruditapes phlippinarum*)	Wedge clam[2] (*Donax trunculus*)	Venus clam[2] (*Chamelea gallina*)
Pb	0.014 (0.01)	0.8	0.9	0.1	0.21	0.22	2.98	1.02
Fe	17.3 (5.8)	79	43	-	-	-	-	-
Mn	0.37 (0.1)	-	-	-	-	-	-	-
Cr	0.019 (0.02)	-	-	0.25	0.48	0.38	0.97	0.57
Co	0.03 (0.01)	-	-	-	-	-	-	-
Ni	0.052 (0.03)	-	-	-	-	-	0.98	1.54
Cu	0.57 (0.2)	1.7	1.4	1.17	1.11	1.78	142	30.4
Zn	13.4 (2.0)	9.8	7.2	17.5	9.89	21.4	86.6	58.3
As	1.88 (0.3)	-	-	3.04	1.16	3.08	6.92	5.13
V	0.006 (0.002)	-	-	-	-	-	-	-
MPI	0.18 (0.03)	-	-	2.91	3.15	3.94	3.21	2.03
HQ total	3.04	-	-	25.8†	10.4†	26.5†	46.8†	16.8†

[1]Foot tissue
[2]Visceral mass
[3]Muscle tissue
†Calculated or recalculated herein

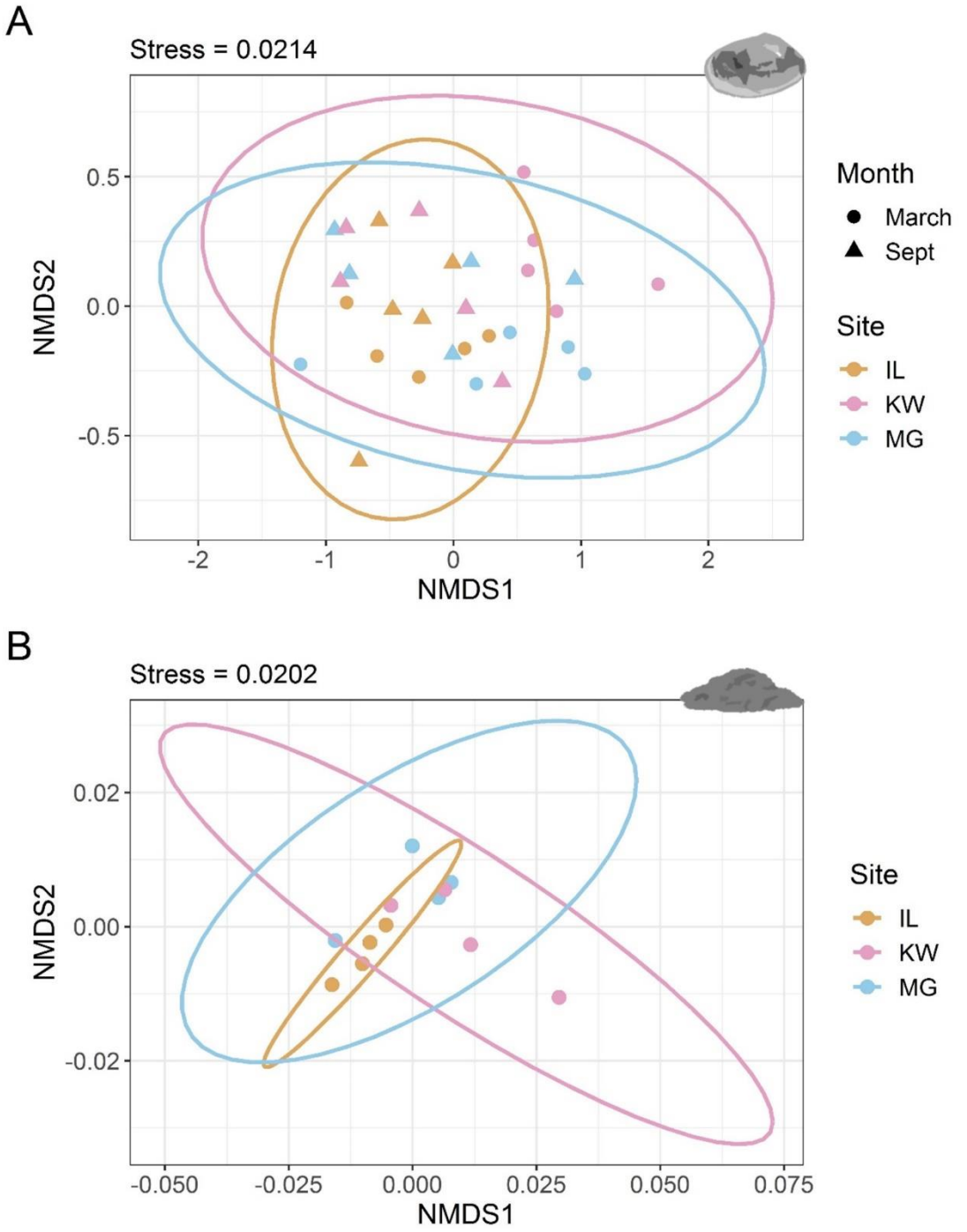

Fig. 6.5. Non-metric Multi-dimensional Scaling (NMDS) ordinations based on Euclidean distance matrices. A: ordination constructed using TE concentrations derived from foot tissue from specimens gathered in March and September 2019. B: ordination constructed using TE concentrations derived from surface sediment. Stress values are shown above each plot (<0.05 indicates excellent representation of dissimilarities). IL: Island, MG: Mahuta Gap, KW: Kopawai.

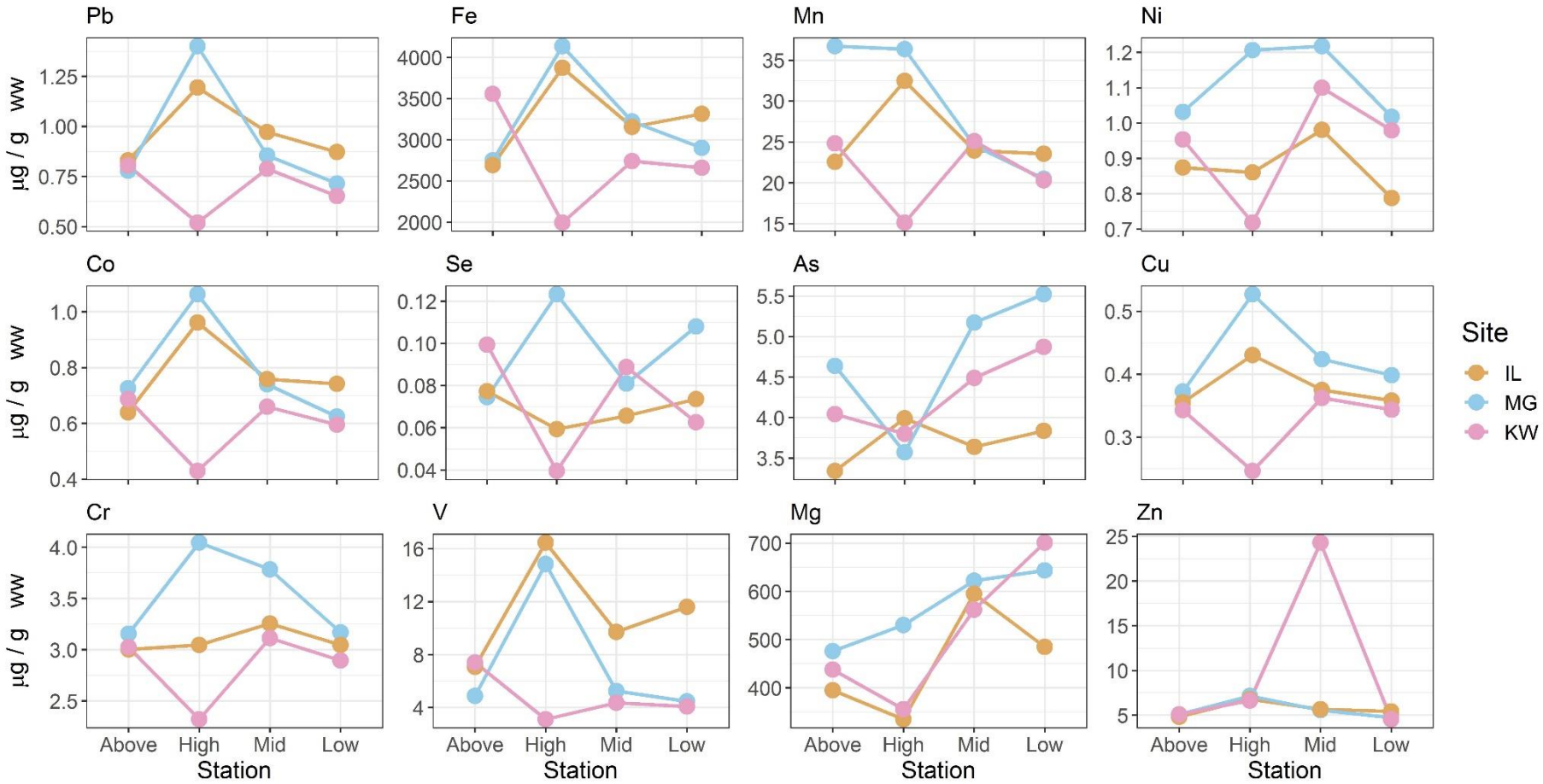

Fig. 6.6. Point and line plots showing element concentrations derived from sediment samples gathered in streams from Ripiro Beach in September 2020. Each point represents a single sample, *n* = 4 for each study site (IL: Island, MG: Mahuta Gap, KW: Kopawai). Sediment samples gathered at four stations at each site (see Figs. 6.1 & 6.2 for details). Mass given in µg g^{-1} wet weight.

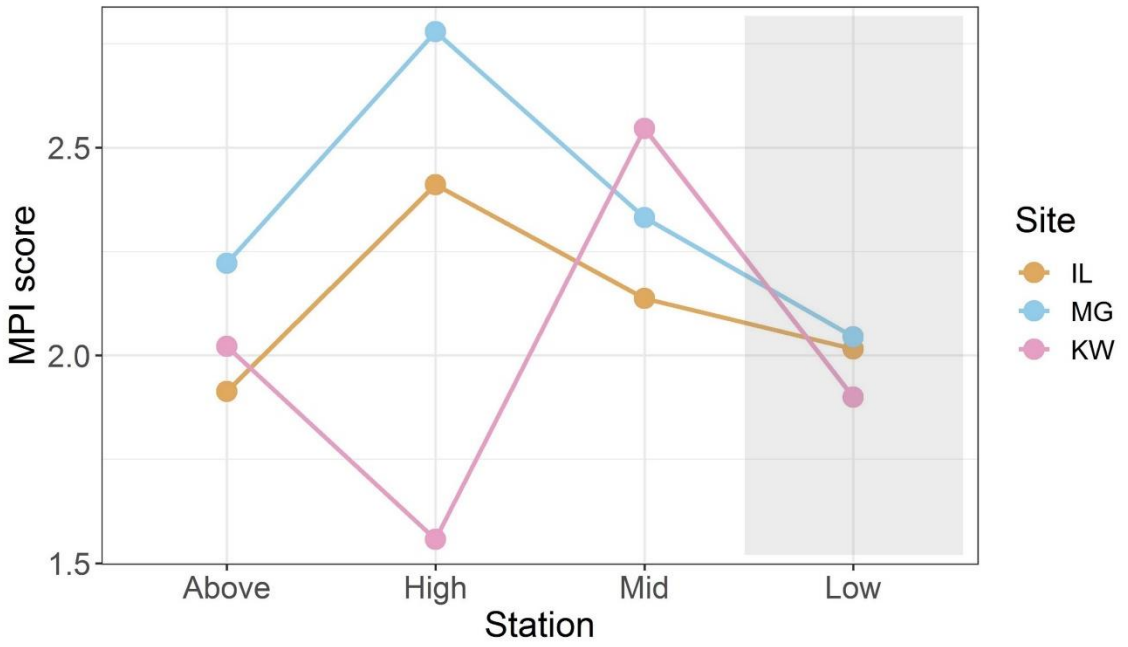

Fig. 6.7. MPI scores derived from sediment samples gathered from three sites on Ripiro Beach, IL: Island, MG: Mahuta Gap, and KW: Kopawai. MPI scores were derived for sediment samples taken at different stations along a gradient, moving from freshwater stream sources, towards the low-intertidal zone. See Fig. 6.1 and 6.2 for details. Shaded area: approximate location of toheroa beds.

Table 6.4. Hazard quotient (HQ) for Cr, Cu, Zn, As, and Pb based on concentrations of toheroa foot tissue. Independent HQ scores calculated for each site and month of toheroa sampling. HQ total is the sum of HQ scores for each element for a given site/month. A HQ score <1 is considered low, >9.9 moderate, >19.9 high, and >100 is considered critical.

Site	Month	Cr	Cu	Zn	As	Pb	HQ Total
Island	March	0.05	0.17	0.20	2.76	0.02	3.20
	Sept	0.02	0.10	0.19	2.40	0.01	2.71
Mahuta Gap	March	0.03	0.14	0.22	2.85	0.03	3.26
	Sept	0.01	0.09	0.18	2.74	0.01	3.03
Kopawai	March	0.06	0.14	0.18	2.94	0.02	3.33
	Sept	0.02	0.10	0.18	2.41	0.02	2.73

Table 6.5. Comparison of trace element concentrations derived from marine surface sediments in different ecotypes in different locations globally. Mean concentrations and standard deviation (± SD) are given (µg g^{-1}) or ranges (min-max). Figures provided for this study are based on wet weight. Referenced studies are either dry weight or presumed dry weight if not specified. LOD: limit of detection.

	This study	**Trefry et al. (2014)**	**Khan et al. (2017)**	**Bastakoti et al. (2018)**	**Kumar et al. (2017)**	**Nobi et al. (2010)**
Location	Ripiro Beach, Aotearoa	Chukchi Sea, Alaska[1]	Cox's Bazar, Bangladesh[2]	Mangawhai, Aotearoa[3]	SE coast, India[4]	Andaman Islands, India[5]
Pb	0.86 (0.2)	11 (2)	-	0.72 (0.45)	11.8–23.0	below LOD
Fe	3083 (588)	-	-	1558 (298)	-	508–3930
Mn	25 (6.5)	353 (100)	-	-	415–843	23–525
Ni	0.98 (0.2)	25 (7)	-	-	39–60	2.2–2.9
Co	0.72 (0.2)	-	17 (6.4)	-	5.8–13.5	0.82–0.88
Se	0.079 (0.02)	0.75 (0.17)	-	-	-	-
As	4.24 (0.7)	14.7 (6.2)	3.4 (2.2)	54.74 (1.96)	-	-
Cu	0.38 (0.1)	13 (4)	-	6.71 (2.36)	1.3–15.7	6.6–7.0
Cr	3.15 (0.4)	71 (18)	866 (637)	-	108–273	5.8–9.6
V	7.77 (4.4)	104 (30)	-	-	-	-
Mg	511 (117)	-	-	-	-	2018–6204
Zn	7.15 (5.5)	71 (21)	214 (162)	10.6 (0.85)	40–73	10.4–27.7

[1]Surface sediment in deep ocean (>50 m)
[2]Surface sediment on sandy beach (0-30 cm)
[3]Island site; outside of mangrove habitat within estuary; surface sediment (0-10 cm)
[4]Surface sediment; range given over eight sites
[5]Surface sediment (0-10 cm); sandy beach ecosystem

6.4.5 Spearman's Correlation

Spearman's correlation was used to examine relationships between trace element concentrations in toheroa tissues and sediment. In toheroa tissues, significant relationships between elemental concentrations differed in March and September. In March, Cr was positively correlated with Ni and Cu (rho = 0.7, p = <0.05). In September, Mn and As (rho = -0.79, p = <0.001), Co and Zn (rho = 0.81, p = <0.001), and As and Zn (rho = 0.71, p = 0.003), were all significantly correlated. In sediment samples gathered in September 2020, V and Fe (rho = 0.87, p = <0.001), Cr and Cu, (rho = 0.83, p = 0.001), Fe and Co (rho = 0.86, p = <0.001), Fe and Pb (rho = 0.82, p = 0.001), and Co and Pb (rho = 0.94, p = <0.001) were all significantly correlated. For brevity, only correlations with a rho value ≥0.7 for the toheroa tissues and ≥0.8 for the sediment samples have been expanded on here. See Appendix F for further details (Figs. 6.8 & F.2, Tables F.3 & F.4).

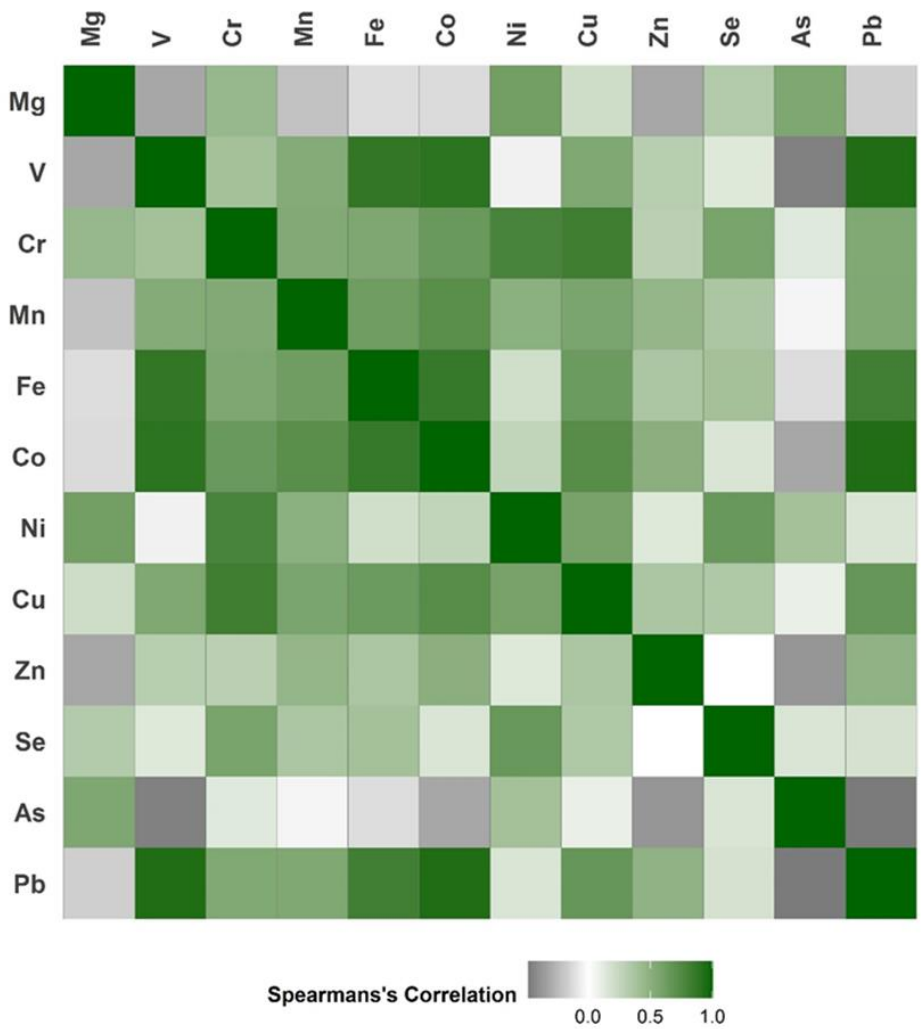

Fig. 6.8. Correlation matrix constructed using Spearman's correlation, showing the relationship between detected elements in sediment collected from streams on Ripiro Beach in September 2020. Heatmap shows positive and negative correlations between respective trace metals.

6.5 Discussion

Metal pollution is a persistent issue in marine ecosystems and from both ecological and human health perspectives, is a growing problem (Luoma and Rainbow, 2008; Wang et al., 2013). Bivalve molluscs uptake metals into shells and soft tissues, with potentially detrimental health effects when the bioavailability of certain elements is in excess (Beiras and Albentosa, 2004; Chora et al., 2009; Stewart et al., 2021). The problem is expected to get worse for marine bivalves under climate change scenarios as decreasing ocean pH is expected to exacerbate the effects of metal contamination by influencing metal speciation (bioavailability), uptake rates, and toxicity (Millero et al., 2009; Roberts et al., 2013; Sezer et al., 2020).

6.5.1 Q1: Seasonal Variability (Toheroa Tissues)

In this study, trace metal concentrations in toheroa foot tissues varied minimally between sites, but significantly between sampling occasions. Some site-specific differences were identified in March (Pb, Fe, Co, Ni, Cu, and Zn), whereas only lead (Pb) concentrations varied significantly between study sites in September. Multivariate analyses identified the time of sampling as a significant contributor to dissimilarity, but not where the specimens were collected (Fig. 6.5), with significantly higher or lower concentrations of various trace metals in toheroa tissues recorded in September and March sampling events (Table 6.2).

If streams were delivering considerable levels of trace metal contamination to toheroa beds, it was expected that this would be represented in the September specimens by site-specific chemical signatures, attributed to different land use adjacent to toheroa beds. This was assumed as during this time, stream flow would be higher (austral winter) and therefore, terrestrial derived contaminants would be more readily transported to toheroa beds. Instead, more differences were found in March than September (Fig. 6.3 & 6.4). Seasonal difference in toheroa diet is a possible explanation for much of this temporal variation. Toheroa on northern, west coast beaches are said to be dependent on phytoplankton blooms associated with autumn rains as a major component of their diet (Cassie, 1955; Williams et al., 2013b). This hypothesis is supported by observations made of improved toheroa condition in July and September, associated with increased chlorophyll-*a* concentration (Chapter 3). The inter-site variation observed in March is therefore potentially due to a lack of uniform dietary trace metal exposure, where streams provide a separating environmental variable. Between June and September, large algal blooms coat Ripiro Beach (pers. obs.), potentially superseding influence from the streams by providing a uniform delivery source of bioavailable trace elements via suspended organic matter (phytoplankton). Thus,

masking the minor effect that streams might have on trace element delivery to toheroa beds in summer months (December to February). This effect is supported by the large number of diatoms detected in digestive tubules in specimens between May and September (Fig. F.3). To aid visualisation of this hypothesis, a conceptual figure showing the fluctuation of delivery source influence is shown (Fig. 6.9); dietary exposure and freshwater influence varies seasonally but aqueous exposure via marine influence remains constant. Furthermore, several elements were highly positively correlated in toheroa tissues (rho >0.7), and relationships were seasonally dependent (Fig. F.2 & Table F.3). This could indicate similar uptake rates, but more likely indicates similar delivery sources as highly correlated metal species differed between March and September. This suggests that bioavailability of highly correlated metals differed between these times.

6.5.2 Q2: Streams as a Delivery Source of Trace Metals

Despite differences in the stream catchments, there was little inter-site difference in the elemental profile of sediments either above the point where the stream enters the beach (no oceanic influence), or on the beach (oceanic influence), or in the tissues of toheroa.

When streams enter the beach, the point of entrance is narrow, so it is thought that this narrowing coupled with beach topography (manipulated by streams and wave action) creates a narrow ‘hump’ in the foreshore where deposition and thus concentration of elements occurs (Fig. 6.7 & 6.9). This is emphasised by high correlations of several elements driven by this apparent deposition zone (e.g., Co and Pb, rho = 0.94, Fig. 6.6 & Fig. 6.8). Furthermore, when streams flow towards the waterline, (a) the stream gets wider, dispersing the flow of freshwater over a greater area and likely diluting elemental concentrations in the stream over a greater area when the streams encounter toheroa beds (Cope, 2018), and (b) the ocean acts to dilute and disperse contaminants of terrestrial origin (see ‘Low’ station, Fig. 6.7). This is consistent with the relative uniformity of trace metal concentrations in tissues between study sites (Figs. 6.3 & 6.4). Hydrology (tidal and currents) and sedimentology (grain size) therefore likely interact to modulate the delivery of trace elements to toheroa beds (Belabed et al., 2013). Given previous relationships found between grain size and trace metal concentrations (Goldberg, 1954; Stoffers et al., 1977) this interaction would be unsurprising.

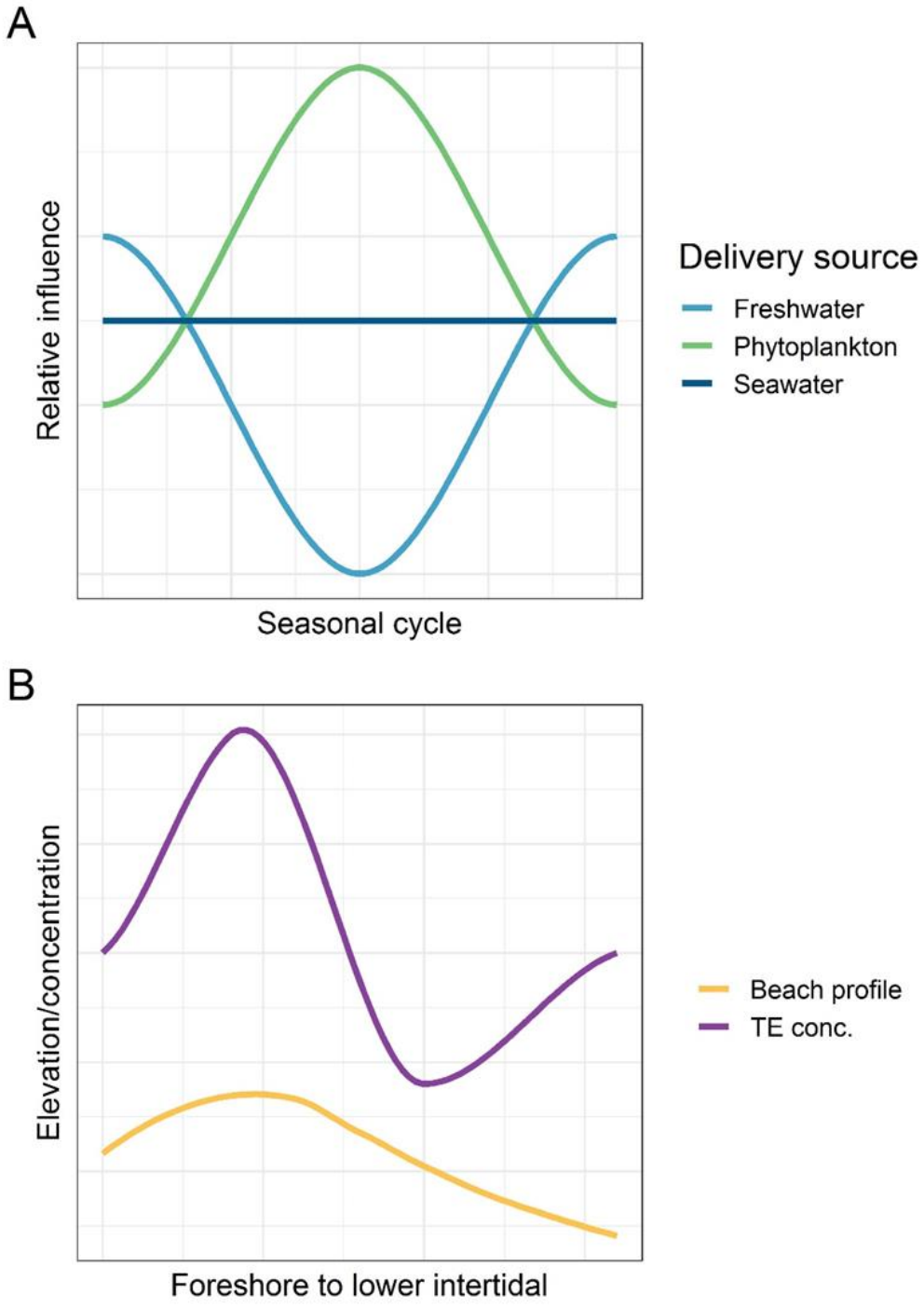

Fig. 6.9. Conceptual figures showing the relative influence of delivery sources of bioavailable trace elements to toheroa in the intertidal and concentrations in surface sediment. A: In summer, freshwater influence is more pronounced due to a lack of uniform dietary exposure. During winter and autumn diet takes precedence following phytoplankton blooms. The influence of the ocean (seawater) is constant, though likely less influential than diet and probably more influential than freshwater streams. B: Beach topography appears to influence trace element (TE) concentrations. In the foreshore, deposition likely increases trace element concentrations, moving seaward concentrations drop (dilution via the ocean and stream dispersal). Though ocean delivery increases the concentration of several elements (e.g., As and Mg). Concept (B) here summarises the data in Figs. 6.6 & 6.7.

Little variation of trace metal concentrations in sediment was observed between study sites in September 2020 (Figs. 6.5-6.7), echoing the limited site-specific variation observed in toheroa tissues the previous year (Fig. 6.4). Additionally, the increased concentration of arsenic and magnesium towards the lower intertidal zone points to the ocean (aqueous or phytoplankton) as the delivery source (Fig. 6.9). Lower on the shore, elevated concentrations could also be attributed to increased organic matter, a primary factor contributing to trace element content in sediment (Goldberg, 1954; Stoffers et al., 1977). This is plausible, given that almost all varieties of chlorophyll encompass an Mg ion. This also supports the hypothesis that diet is a major pathway for trace elements to enter toheroa tissues, with aqueous exposure likely playing a significant role too (Luoma, 1983; Wang and Rainbow, 2005).

Trace element levels here are low compared to those reported in marine surface sediments elsewhere (Table 6.5). However, reported values are not directly comparable to due differing methodologies, geographic locations, and environments. Despite being within an estuary, two interesting comparisons can be made with Bastakoti et al. (2018), a study carried out almost directly east of Ripiro Beach at Mangawhai *c.* 80 km away. Firstly, surface sediment arsenic concentrations were extremely high in Bastakoti et al. (2018) compared to that reported herein. This frames the levels reported here in an Aotearoa context i.e., mean arsenic concentration of 4.24 μg g^{-1} (±SD 0.7) is not particularly high compared to 54.74 μg g^{-1} (±SD 1.96). Secondly, a much higher iron concentration was reported here (Table 6.5). This is not surprising considering the geological history of the west coast beaches of the North Island, Aotearoa (Carter, 1980). Furthermore, this highlights the richness of iron in toheroa habitats (Fig. 6.2), within the region home to major remaining toheroa populations. Although, as Cassie (1955) noted, mineral content of sediments is likely not critical for toheroa, as populations have been historically abundant in both iron sand rich (Muriwai) and poor regions (Hokianga).

6.5.3 Q3: Human and Toheroa Health

Due to its size, relative to the entire body mass of toheroa, the foot (or 'tongue') is often the most readily consumed part of toheroa (though the whole visceral mass is often consumed too). It is important to consider that only one soft tissue was analysed in this study. Bivalve molluscs have been shown to partition metals in different soft tissues and structures (Rodney et al., 2007; Saavedra et al., 2008; Szefer et al., 2002). For example, Saavedra et al. (2008) showed that metal concentrations in the foot tissue of *Pecten maximus* contributed between 0.3% to 1% of total metal concentrations in soft body tissues. Furthermore, Stanley (2003) found that metal-containing granules in shellfish contained trace metals at relatively high concentrations, hypothesising that their formation could be related to accumulation and detoxification. Previous histological

observations of toheroa tissues identified the presence of calcareous granules in toheroa nephridia (Fig. F.3 & Chapter 3). Like other calcite ($CaCO_3$) structures, it is likely trace elements have been incorporated into these concretions and concentrated over an individual's life history. Examining a single soft tissue undoubtedly narrows the observational lens and misses concentrations of various trace elements. However, examining a soft tissue, with higher turnover rates compared to shells and muscle, was considered more appropriate to provide a snapshot of recent or acute trace metal exposure versus chronic exposure over an individual's entire life history (Bennion et al., 2019). The intention was to reduce bias of chronic exposure between several possible habitats (as toheroa are not sedentary), enabling the investigation of the influence of freshwater influx via acute exposure to trace metals at respective sites.

Only one published study could be found where trace metals were previously reported in toheroa (from Oreti Beach in Southland/Murihiku) (Table 6.3). The concentration of Zn was higher in this study, but Pb, Fe, and Cu were higher in Nielsen and Nathan (1975). All trace metals reported here were at lower concentrations than those in other studies of clam spp. shown in Table 6.3, except for arsenic, which was higher here than that reported in the surf clam *M. veneriformis* from Laizhou Bay, China (Liu et al., 2017a). This is not surprising given that high arsenic concentrations have previously been reported in wild-caught food in Aotearoa, attributed to geothermal activity (Cressey et al., 2019; Phillips et al., 2014). The relatively high As concentration in foot tissues is the driver of the low HQ scores reported here (HQ total: 2.71-3.33) (Table 6.3), though this hazard score requires framing. Firstly, HQ scores here are only valid for foot tissues and not the entire visceral mass of toheroa. Secondly, toxicity of arsenic depends on whether compounds are 'organic' or 'inorganic', as inorganic arsenic is highly toxic compared to organic arsenic (Cressey et al., 2019; Muñoz et al., 2000). In the present study, arsenic is presented as total arsenic within tissues. Putting this hazard in context, Cressey et al. (2019) reported that in a variety of shellfish in Aotearoa only *c.* 5% (conservative estimate) of total As is inorganic. Considering all the elements assessed, and the HQ scores calculated, the risk of trace metal exposure via the consumption of toheroa is likely very low (Table 6.4). The MPI score for toheroa is also low when compared to studies on other clam species (Table 6.3). This could be attributed to the remote location of the study location (Fig. 6.1 & 6.2) and the high-energy hydrology of this region, or due to a high shedding capacity and internal compartmentalising (distribution of metals to different tissues for detoxification) (Fig. F.3).

Having once been a staple food source throughout Aotearoa, there are long-held sentiments of the nutritional value of toheroa. Studies on the safety and (or) nutritional value of consuming toheroa are scarce but in the 1920s, Malcolm (1928) provided a summary of the nutritional value of canned toheroa soup, concerning Vitamin A content.

In this study, relatively high concentrations of Zn (an essential micronutrient) were recorded (mean = 13.4 μg g^{-1} ±2.0). Importantly, while Zn concentration was found to be high in toheroa, less desirable trace metals (e.g., Cr, Cu, and Pb) are low (Table 6.3), supporting the notion that toheroa are a good source of some essential nutrients.

6.6 Conclusions

Freshwater streams do seem to be delivering trace metals to the beach, but there is no evidence of elevated levels in the surface sediments of toheroa beds (based on the two sampled time-points used herein), or of site-specific accumulated trace metals in toheroa (foot tissue). It is uncertain if this is because trace elements are deposited high on the shore and do not reach the area of the beach where toheroa beds are found, or if the trace metals are transported by streams down the beach but diluted and dispersed every tidal cycle. Regardless, there were no indications of trace metal concentrations at levels that represent a risk to either toheroa, or a risk to humans through consumption during the timeframe of this study. Seasonal differences in some trace metal concentrations in toheroa tissues were large, and attributable to seasonal phytoplankton blooms that constitute a large part of the toheroa diet. Inter-site differences were minor despite differences in adjacent land use. While this study focused on trace elements, streams are potential avenues for the delivery of a range of other contaminants used on the adjacent land. Future studies should incorporate assessment of agrichemicals including the compounds found in pesticides and fertilizers (e.g., NO_{3-} and PO_4^{3-}).

6.7 References

Abdou, M., et al., 2020. Organotropism and biomarker response in oyster *Crassostrea gigas* exposed to platinum in seawater. Environmental Science and Pollution Research. 27**,** 3584-3599.

Bastakoti, U., et al., 2018. Spatial variation of heavy metals in sediments within a temperate mangrove ecosystem in northern New Zealand. Marine Pollution Bulletin. 135**,** 790-800.

Beentjes, M. P., 2010. Toheroa survey of Oreti Beach, 2009, and review of historical surveys. New Zealand Fisheries Assessment Report 2010/6. 40.

Beiras, R., Albentosa, M., 2004. Inhibition of embryo development of the commercial bivalves *Ruditapes decussatus* and *Mytilus galloprovincialis* by trace metals; implications for the implementation of seawater quality criteria. Aquaculture. 230**,** 205-213.

Belabed, B.-E., et al., 2013. Factors contributing to heavy metal accumulation in sediments and in the intertidal mussel *Perna perna* in the Gulf of Annaba (Algeria). Marine Pollution Bulletin. 74**,** 477-489.

Bennett, P. M., et al., 2001. Exposure to heavy metals and infectious disease mortality in harbour porpoises from England and Wales. Environmental Pollution. 112**,** 33-40.

Bennion, M., et al., 2019. Trace element fingerprinting of blue mussel (*Mytilus edulis*) shells and soft tissues successfully reveals harvesting locations. Science of The Total Environment. 685**,** 50-58.

Boening, D. W., 1999. An Evaluation of Bivalves as Biomonitors of Heavy Metals Pollution in Marine Waters. Environmental Monitoring and Assessment. 55**,** 459-470.

Bosch, A. C., et al., 2016. Heavy metals in marine fish meat and consumer health: a review. Journal of the Science of Food and Agriculture. 96**,** 32-48.

Calabrese, A., et al., 1973. The toxicity of heavy metals to embryos of the American oyster *Crassostrea virginica*. Marine Biology. 18**,** 162-166.

Carter, L., 1980. Ironsand in continental shelf sediments off western New Zealand—a synopsis. New Zealand Journal of Geology and Geophysics. 23**,** 455-468.

Cassie, R. M., 1955. Population Studies on the Toheroa, *Amphidesma ventricosum* Gray (Eulamellibranchiata). Marine and Freshwater Research. 6**,** 348-391.

Chien, L.-C., et al., 2002. Daily intake of TBT, Cu, Zn, Cd and As for fishermen in Taiwan. Science of The Total Environment. 285**,** 177-185.

Chora, S., et al., 2009. Effect of cadmium in the clam *Ruditapes decussatus* assessed by proteomic analysis. Aquatic Toxicology. 94**,** 300-308.

Cisneros-Montemayor, A. M., et al., 2016. A Global Estimate of Seafood Consumption by Coastal Indigenous Peoples. PLOS ONE. 11**,** e0166681.

Cope, J., The modification of toheroa habitat by streams on Ripiro Beach. MSc. University of Waikato, Hamilton, New Zealand, 2018, pp. 126.

Costello, C., et al., 2020. The future of food from the sea. Nature. 588**,** 95-100.

Cressey, P., et al., Risk Profile: Chemical Forms of Contaminant Elements (Species). Ministry of Primary Industries, Wellington, NZ, 2019, pp. 175.

de Souza, M. M., et al., 2011. Shellfish from Todos os Santos Bay, Bahia, Brazil: Treat or threat? Marine Pollution Bulletin. 62**,** 2254-2263.

Dinno, A., Dinno, M., Package 'dunn. test'. CRAN Repository, Vol. 10, 2017.

Goldberg, E. D., 1954. Marine Geochemistry 1. Chemical Scavengers of the Sea. The Journal of Geology. 62**,** 249-265.

Goldberg, E. D., et al., 1978. The Mussel Watch. Environmental Conservation. 5**,** 101-125.

Hamed, M. A., Emara, A. M., 2006. Marine molluscs as biomonitors for heavy metal levels in the Gulf of Suez, Red Sea. Journal of Marine Systems. 60**,** 220-234.

Ivanina, A. V., et al., 2011. Interactive effects of cadmium and hypoxia on metabolic responses and bacterial loads of eastern oysters *Crassostrea virginica* Gmelin. Chemosphere. 82**,** 377-389.

Jonathan, M. P., et al., 2017. Bioaccumulation of trace metals in farmed pacific oysters *Crassostrea gigas* from SW Gulf of California coast, Mexico. Chemosphere. 187**,** 311-319.

Khan, R., et al., 2017. Spatial and multi-layered assessment of heavy metals in the sand of Cox's-Bazar beach of Bangladesh. Regional Studies in Marine Science. 16**,** 171-180.

Kumar, S. B., et al., 2017. Elemental distribution and trace metal contamination in the surface sediment of south east coast of India. Marine Pollution Bulletin. 114**,** 1164-1170.

Liu, J., et al., 2017a. Bioaccumulation of heavy metals and health risk assessment in three benthic bivalves along the coast of Laizhou Bay, China. Marine Pollution Bulletin. 117**,** 98-110.

Liu, Q., et al., 2018. Concentration and potential health risk of heavy metals in seafoods collected from Sanmen Bay and its adjacent areas, China. Marine Pollution Bulletin. 131**,** 356-364.

Liu, X., et al., 2017b. Concentration, risk assessment, and source identification of heavy metals in surface sediments in Yinghai: A shellfish cultivation zone in Jiaozhou Bay, China. Marine Pollution Bulletin. 121**,** 216-221.

Luoma, S. N., 1983. Bioavailability of trace metals to aquatic organisms — A review. Science of The Total Environment. 28**,** 1-22.

Luoma, S. N., Rainbow, P. S., 2008. Metal contamination in aquatic environments: science and lateral management. Cambridge University Press, Cambridge.

Malcolm, J., 1928. Food values of New Zealand fish. Part 9: Tinned toheroa and toheroa soup. Transactions and Proceedings of the Royal Society of New Zealand. 59**,** 85-90.

Marsden, I. D., et al., 2014. Effects of environmental and physiological variables on the accumulated concentrations of trace metals in the New Zealand cockle *Austrovenus stutchburyi*. Science of The Total Environment. 470-471**,** 324-339.

Millero, F. J., et al., 2009. Effect of ocean acidification on the speciation of metals in seawater. Oceanography 22**,** 72–85.

Muñoz, O., et al., 2000. Total and inorganic arsenic in fresh and processed fish products. Journal of Agricultural and Food Chemistry. 48**,** 4369-4376.

Nielsen, S. A., Nathan, A., 1975. Heavy metal levels in New Zealand molluscs. New Zealand Journal of Marine and Freshwater Research. 9**,** 467-481.

Nobi, E. P., et al., 2010. Geochemical and geo-statistical assessment of heavy metal concentration in the sediments of different coastal ecosystems of Andaman Islands, India. Estuarine, Coastal and Shelf Science. 87**,** 253-264.

O'Mahony, M., 2018. EU Regulatory Risk Management of Marine Biotoxins in the Marine Bivalve Mollusc Food-Chain. Toxins. 10**,** 118.

Okazaki, R. K., Panietz, M. H., 1981. Depuration of twelve trace metals in tissues of the oysters *Crassostrea gigas* and *C. virginica*. Marine Biology. 63**,** 113-120.

Oksanen, J., et al., 2019. vegan: Community Ecology Package. R package version 2. 5–6. 2019.

Phillips, N. R., et al., 2014. Human Health Risks of Geothermally Derived Metals and Other Contaminants in Wild-Caught Food. Journal of Toxicology and Environmental Health, Part A. 77**,** 346-365.

Rainbow, P. S., Phillips, D. J. H., 1993. Cosmopolitan biomonitors of trace metals. Marine Pollution Bulletin. 26**,** 593-601.

Rainbow, P. S., Wang, W.-X., 2001. Comparative assimilation of Cd, Cr, Se, and Zn by the barnacle *Elminius modestus* from phytoplankton and zooplankton diets. Marine Ecology Progress Series. 218**,** 239-248.

Roberts, D. A., et al., 2013. Ocean acidification increases the toxicity of contaminated sediments. Global Change Biology. 19**,** 340-351.

Rodney, E., et al., 2007. Bioaccumulation and Tissue Distribution of Arsenic, Cadmium, Copper and Zinc in *Crassostrea virginica* Grown at Two Different Depths in Jamaica Bay, New York. In vivo. 29**,** 16-27.

Ross, P. M., et al., 2018. The biology, ecology and history of toheroa (*Paphies ventricosa*): a review of scientific, local and customary knowledge. New Zealand Journal of Marine and Freshwater Research. 52**,** 196-231.

Saavedra, Y., et al., 2008. Anatomical distribution of heavy metals in the scallop *Pecten maximus*. Food Additives & Contaminants: Part A. 25**,** 1339-1344.

Sezer, N., et al., 2020. Impacts of elevated pCO2 on Mediterranean mussel (*Mytilus galloprovincialis*): Metal bioaccumulation, physiological and cellular parameters. Marine Environmental Research. 160**,** 104987.

Squadrone, S., et al., 2016. Presence of trace metals in aquaculture marine ecosystems of the northwestern Mediterranean Sea (Italy). Environmental Pollution. 215**,** 77-83.

Stanley, F. J., Studies on the metal-containing granules in the mussels, *Mytilus galloprovincialis* and *Velesunio angasi*. PhD. Murdoch University, Perth, Australia, 2003, pp. 182.

Stewart, B. D., et al., 2021. Metal pollution as a potential threat to shell strength and survival in marine bivalves. Science of The Total Environment. 755**,** 143019.

Stewart, M., et al., 2011. Organochlorines and heavy metals in wild caught food as a potential human health risk to the indigenous Māori population of South Canterbury, New Zealand. Science of The Total Environment. 409**,** 2029-2039.

Stoffers, P., et al., 1977. Copper and other heavy metal contamination in sediments from New Bedford Harbor, Massachusetts: a preliminary note. Environmental Science & Technology. 11**,** 819-821.

Szefer, P., et al., 2002. Distribution and relationships of trace metals in soft tissue, byssus and shells of *Mytilus edulis trossulus* from the southern Baltic. Environmental Pollution. 120**,** 423-444.

Team, R. C., R: A language and environment for statistical computing. R Foundation for Statistical Computing, Vienna, Austria, 2013.

Trefry, J. H., et al., 2014. Trace metals and organic carbon in sediments of the northeastern Chukchi Sea. Deep Sea Research Part II: Topical Studies in Oceanography. 102**,** 18-31.

Usero, J., et al., 1996. Trace metals in the bivalve mollusc *Chamelea gallina* from the Atlantic coast of southern Spain. Marine Pollution Bulletin. 32**,** 305-310.

Usero, J., et al., 2005. Heavy metal concentrations in molluscs from the Atlantic coast of southern Spain. Chemosphere. 59**,** 1175-1181.

Wang, Q., et al., 2009. Toxicity of lead, cadmium and mercury on embryogenesis, survival, growth and metamorphosis of *Meretrix meretrix* larvae. Ecotoxicology. 18**,** 829-837.

Wang, S.-L., et al., 2013. Heavy metal pollution in coastal areas of South China: A review. Marine Pollution Bulletin. 76**,** 7-15.

Wang, W.-X., 2002. Interactions of trace metals and different marine food chains. Marine Ecology Progress Series. 243**,** 295-309.

Wang, W.-X., Rainbow, P. S., 2005. Influence of metal exposure history on trace metal uptake and accumulation by marine invertebrates. Ecotoxicology and Environmental Safety. 61**,** 145-159.

Wang, X.-N., et al., 2018. Biological risk assessment of heavy metals in sediments and health risk assessment in bivalve mollusks from Kaozhouyang Bay, South China. Marine Pollution Bulletin. 133**,** 312-319.

Wei, T., et al., 2017. Package 'corrplot'. Statistician. 56**,** e24.

Wickham, H., 2009. ggplot2: Elegant Graphics for Data Analysis. Springer, New York.

Willer, D. F., Aldridge, D. C., 2020. Sustainable bivalve farming can deliver food security in the tropics. Nature Food. 1**,** 384-388.

Williams, J., et al., Distribution and abundance of toheroa (*Paphies ventricosa*) and tuatua (*P. subtriangulata*) at Ninety Mile Beach in 2010 and Dargaville Beach in 2011. Ministry of Primary Industries, Wellington, 2013a, pp. 52.

Williams, J. R., et al., Review of factors affecting the abundance of toheroa (*Paphies ventricosa*). New Zealand Aquatic Environment and Biodiversity Report No. 114, 2013b, pp. 76.

Chapter 7
Investigation of Gas Bubble Manifestation on Toheroa (*Paphies ventricosa*)

Toheroa with gas bubbles
Mahuta Gap, Ripiro Beach

7.1 Abstract

Toheroa (*Paphies ventricosa*) presenting gas bubbles under the periostracum on their shells were first reported from Ripiro Beach, northern Aotearoa in 2017. It was suggested that this was gas bubble disease (GDB), but this was not certain and the mechanisms leading to gas bubble formation were not known. Therefore, a seasonal investigation was undertaken to track gas bubble prevalence and severity over time to provide a better understanding of temporal patterns of GBD. Toheroa were photographed in situ, gas bubbles were counted and extent of cover was calculated, and the toheroa microbiome was investigated (data gathered in Chapter 5). The survey revealed that the number of gas bubbles and extent of cover on the shells was both site and seasonally variable. Gas bubble intensity was most severe in September 2019 at Mahuta Gap, indicating local and seasonal environmental conditions contributed to the manifestation of gas bubbles on shells.

Gas bubbles appeared to be most prevalent where beach sediments appeared hypoxic, and when bacteria from the Desulfobacterota taxa were present in the toheroa microbiome (range: 0.05 to 1.8% relative abundance) following a period of high organic matter inundation on Ripiro Beach. Together, this led me to the hypothesis that gas bubbles are likely attributed to hydrogen sulfide (H_2S), a by-product of sulfate-reducing bacteria in the sediment and (or) on the surface of shells (under the periostracum). No pathomorphological features associated with gas bubbles or potential H_2S exposure were detected in soft tissues of even the most severely affected individuals. Given the limited evidence of negative implications for toheroa intrinsic health, it is suggested that gas bubbles are a natural phenomenon linked to the habitat toheroa favour, and not a factor preventing the recovery of toheroa.

7.2 Introduction

Gas bubble disease (GBD) is a non-infections condition of aquatic animals generally caused by supersaturation of total dissolved gases (TDG) in water. GBD has been observed in aquaculture (Malouf et al., 1972; Weitkamp and Katz, 1980), but has also been observed in wild populations associated with manmade dams in China and the United States (Beeman et al., 2003; Liu et al., 2019; Mesa et al., 2000). Though gas bubble disease is more commonly detected in fish (Beeman et al., 2003; Bouck, 1980; Weitkamp and Katz, 1980), it has also been reported in marine molluscs (Malouf et al., 1972; Ross et al., 2018b), crustaceans (Johnson, 1976; Lightner et al., 1974), and cetaceans (Danil et al., 2014). Gas bubble disease is a general term to describe gaseous related trauma in organisms. For example, in molluscs and finfish GBD generally relates to supersaturation of TDG (Beeman et al., 2003), though the aetiology has also been

associated with rapid decompression in finfish, crustaceans, and cetaceans (Beyer et al., 1976; Jepson et al., 2003; McDonough and Hemmingsen, 1984), and gas-producing bacterial infections (*Clostridium perfringens*) in long-beaked common dolphins, *Delphinus capensis* (Danil et al., 2014). In shellfish, gas bubble disease has been infrequently detected in the wild compared to cultured animals, except for Ross et al. (2018b) in toheroa (*Paphies ventricosa*) from Aotearoa. Much of the literature of gas bubble disease are *ex situ* investigations of the drivers of gas bubble formation, determining thresholds for their manifestation (Bisker and Castagna, 1987; Weitkamp and Katz, 1980) and consequences for host health. In scallops (*Argopecten irradians*) and oysters (*Crassostrea virginica*) for instance, gas bubbles manifested at 116% TDG saturation (110% oxygen and 118% nitrogen) (Bisker and Castagna, 1987). Mortality was subsequently reported in *A. irradians* after seven days at 116% TDG exposure and reduced growth was reported in juvenile *C. virginica* in the absence of mortality after 28 days (Bisker and Castagna, 1987).

Ross et al. (2018b) reported GBD in toheroa for the first time from specimens collected at Ripiro Beach (Fig. 7.1). Due to the depressed state of toheroa populations, further examination of this phenomenon was necessary to determine if this is a factor preventing recovery of toheroa. Commercial and recreational fishing of toheroa, among a series of other pressures, reduced populations significantly in the 20th century (Ross et al., 2018a; Williams et al., 2013). While the recreational and commercial harvesting of toheroa has been prohibited since the 1970s (although limited customary take is permitted), toheroa remain threatened. Information of toheroa health is scarce, but recent work has attempted to close knowledge gaps of their reproductive health (Gadomski, 2017) and collate existing information of their biology and ecology (Ross et al., 2018a; Williams et al., 2013). To compliment this growing knowledge base, here I investigate the spatio-temporal manifestation of gas bubbles on toheroa from one of the few major remaining populations. Additionally, I strive to identify pathways to gas bubble manifestation based on *in situ* observations and examination of the toheroa-associated bacterial community.

7.3 Methods

7.3.1 Study Site and Gas Bubble Disease

To examine the spatial and temporal variation of gas bubble manifestation and intensity in toheroa, repeated sampling expeditions were made to Ripiro Beach (Te Tai Tokerau) over a ten-month period, every two months (Fig. 7.1). Three sub-sites, Island, Mahuta Gap, and Kopawai (Fig. 7.1) were sampled to examine spatial variability of gas bubble manifestation. Toheroa tend to concentrate at freshwater outlets (Beentjes, 2010;

Ross et al., 2018a), and these three sub-sites, where small streams flow onto the beach, were chosen based on knowledge of consistent toheroa beds present. Specimens were examined *in situ* between March 2019 and January 2020 (*n* = 30, per sampling event), with a single larger survey repeated in September 2020 (*n* = 167). Specimen selection within a bed was spatially haphazard but adults were targeted, *c.* 70 mm (length). Further to this, a series of random quadrats were used to sample toheroa in November 2019 and September 2020. Air temperature was taken on location while sampling, and rainfall (monthly total, mm) was gathered retrospectively from (www.nrc.gov.nz) based on the closest weather station at Kai Iwi Lakes.

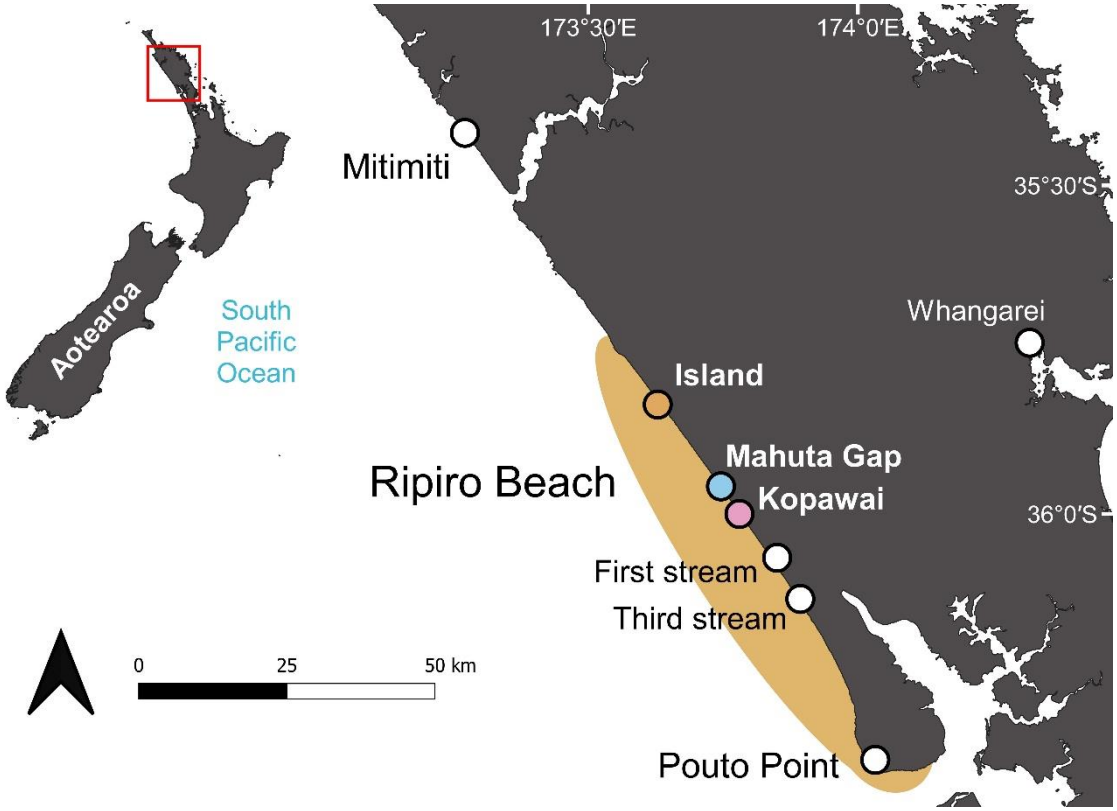

Fig. 7.1. Location of seasonal study sites at Ripiro Beach. Ripiro Beach (shaded brown) is the longest drivable beach in Aotearoa at 106 km in length. Island, Mahuta Gap, Kopawai, First stream, and Third stream icons indicate the location of the studied streams on Ripiro Beach. Spatial data obtained from DIVA-GIS. CRS: WGS 84 (EPSG: 4326).

A custom-built light box (Fig. G.1) was used to photograph toheroa shells on site using a Canon EOS 60D (both left and right valves). Photographs were analysed using ImageJ v1.44, gas bubbles were counted, and each bubble area (mm^2) was recorded. Gas bubble area as a measure of intensity was calculated as the ratio of total gas bubble area (mm^2) to total shell area (mm^2) (both valves; not accounting for curvature). Due to an observational link made between freshwater flow and gas bubble intensity, an investigation was undertaken in November 2019 to establish if sediment moisture

content, as a proxy of freshwater influx, was associated with gas bubbles. The Island site stream typically has a low volume, flowing through agricultural land (pasture) and a wetland. Mahuta Gap consistently has the highest volume stream. Land use nearby is agricultural (pasture). At Kopawai, the stream is consistently present, but typically not as great in volume as the stream present at Mahuta Gap. The stream at Kopawai comes from primarily groundwater sources (and a small lake), as opposed to the Mahuta Gap and Island streams, which could be more accurately described run-off (overland flows). Adjacent land use is also pasture farmland. A series of random quadrats (0.25 m^2) were used to sample specimens at the three sub-sites on Ripiro Beach. In total, 661 toheroa were visually assessed for gas bubbles and graded on a four-point severity scale: None, Low (1-5), Moderate (6-15) and High (>15). A sediment corer (diameter = 3 cm, depth = 10 cm) was used to take a *c.* 70 cm^3 surface sediment sample for moisture content analysis. Extracted cores were weighed (to the nearest 0.001 g), dehydrated for 12 hrs at 60 °C and reweighed post drying. Moisture content was taken to be the percentage difference between wet and dried sediment mass.

In September 2020, a survey was undertaken to sample five toheroa beds (Fig. 7.1) along Ripiro Beach (Island, Mahuta Gap, Kopawai, and First and Third Stream), a 0.25 m^2 quadrat was dug at each site. All toheroa presenting with gas bubbles were photographed and images were analysed using the same method described above. At this time, dissolved oxygen (%) was also recorded from water within toheroa beds at Island, Mahuta Gap and Kopawai using an OxyGuard™ Handy Polaris dissolved oxygen meter.

7.3.2 Histology

Gross pathology was examined on toheroa samples to determine whether gas bubbles had any consequence for toheroa soft tissue morphology. All specimens sampled during site visits (*n* = 180) were prepared for routine histology (Howard et al., 2004). Tissues were fixed in 10% formalin for a maximum of 48 hrs, trimmed and placed in tissue cassettes in 70% EtOH. Slide preparation by haematoxylin and eosin (H&E) staining was carried out at SVS Laboratories Ltd. (Hamilton, NZ). Slides were viewed using an Olympus BX53 compound light microscope.

7.3.3 Molecular Analysis

Following an investigation of the toheroa microbiome (see Chapter 5), the composite microbiome was examined for OTUs taxonomically assigned to the phylum Desulfobacterota. Due to on-site observations of organic matter decomposition and anoxic conditions in the sediment of toheroa beds, the decision was made to focus on

Desulfobacterota. This is in part due to the role members of this phylum play, in organic matter decomposition (sulfur-cycle) and production of hydrogen sulfide (H_2S). Additionally, OTUs taxonomically assigned to this phylum were identified as 'indicator taxa' for toheroa from Mahuta Gap (Chapter 5), prompting further exploration.

The top five OTUs in terms of relative abundance were compared to published sequences using the National Centre for BioTechnology Information (NCBI) nucleotide BLAST tool (Johnson et al., 2008). The top five Desulfobacterota OTUs, published sequences of other sulfate-reducing bacteria, and other common marine bacteria associated with shellfish were then used to create phylogenetic trees. OTUs and published nucleotide sequences were imported into Geneious v.9 (Kearse et al., 2012), aligned using default parameters (global alignment 70% similarity), and a neighbour-joining tree was constructed using the Jukes-Cantor substitution matrix with 100,000 bootstrapped replicates.

7.3.4 Statistical Analyses

All statistical analyses were performed in R (R Core Team 2013). Kruskal-Wallis tests were used to detect site and seasonal differences in gas bubble extent using the 'Dunn test' package (Dinno and Dinno 2017) (95% confidence). Dunn tests were carried out to establish where differences lay when statistically significant differences were detected (Dinno and Dinno 2017). Where applicable, Bonferroni's correction was used to account for multiple comparisons. To examine site-specific differences in the relative abundance of Desulfobacterota taxa in the toheroa composite microbiome, a heatmap was constructed using the relative abundance of OTUs taxonomically assigned to Desulfobacterota. Wilcoxon's rank sum test was used to compare GB intensity ratio between Sept-19 and Sept-20 at Mahuta Gap. All data visualisation was carried out using the package 'ggplot2' (Wickham, 2009). A map of sampled sites was produced using Quantum GIS (v.3.8.1).

7.4 Results

Both the prevalence and intensity of gas bubbles varied over space (locally) and time (seasonally) (Fig. 7.2 & 7.3). The highest prevalence of gas bubbles (three sub-sites combined) was in Sept-19 (50%, n = 30) and the lowest in Jan-20 (3.3%, n = 30). The mean number of gas bubbles on shells echoed this trend, with the greatest mean number of bubbles recorded on toheroa from Mahuta Gap in Sept-19 (20.4 ±SE 4.35) and the lowest in Jan-20 (Fig. 7.2). Gas bubble intensity is given as a ratio of bubble area to total shell area. Beginning in Mar-19, there was an upward trend in gas bubble intensity moving into the austral winter (X^2 = 21.25, df = 5, p = <0.001). The greatest

mean intensity was recorded in Sept-19 (0.09 ±SE 0.025), though only mean intensity in Jan-20 was significantly lower (Z = -4.16, p = 0.0002) than Sept-19. Overall, a significant spatial effect was detected. Mean gas bubble intensity was greater in specimens from Mahuta Gap (0.009 ±SE 0.014) than both Island and Kopawai (Fig. 7.3) (X^2 = 61.43, df = 2, p = <0.001). This spatial effect is clearer when site and sampling date are considered together (Fig. 7.3, A). No gas bubbles were measured from samples at Island, and no statistical difference could be detected between sampled months at Kopawai (p = 0.44). Gas bubble intensity at Mahuta Gap was different between sampling months (X^2 = 33.22, df = 5, p = <0.001), with the greatest mean gas bubble intensity ratio in Sept-19 (0.025 ±SE 0.004) and the lowest in Jan-20, where gas bubbles were only measured on one specimen (Fig. 7.3, A). See Tables G.2-G.5 for summary statistics and further details of statistical test results.

During the September 2020 survey, previously sampled toheroa beds were absent or diminished compared to previous surveys, except for Mahuta Gap. For this reason, few toheroa were found at Island and the densities at Kopawai, 'First' and 'Third Stream' were relatively low (15, 14 and 8 per 0.25 m^2, respectively), influencing available sample sizes. Prevalence in Sept-20 was 12% (n = 661), compared to a prevalence of 50% (n = 30) in Sept-19. Comparing gas bubble intensity at Mahuta Gap only between September 2019 and 2020, intensity was significantly lower in 2020 (W = 24, p = 0.0048), with mean intensity ratio recorded as 0.025 (±SE 0.004) in 2019 and 0.006 (±SE 0.001) in 2020. Dissolved oxygen in toheroa beds in September 2020 was found to be 97.6% at Island, 26.6% at Kopawai, and 13.8% at Mahuta Gap.

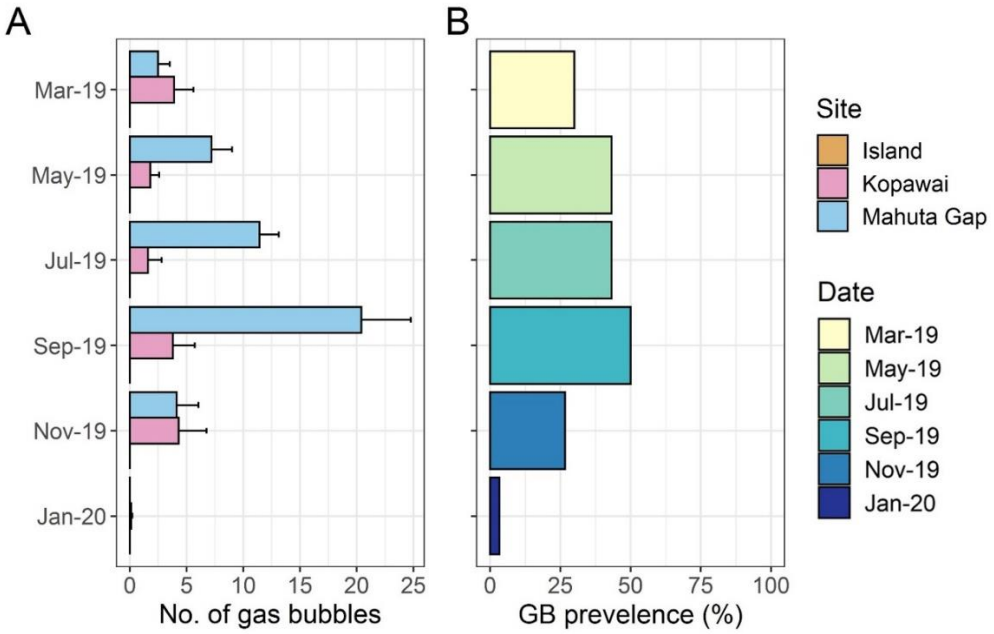

Fig. 7.2. A: Mean count of gas bubbles on shells of toheroa (left and right valves combined) from three sites on Ripiro Beach sampled between March 2019 and January 2020. Error bars show standard error of the mean. B: Gas bubble (GB) prevalence (%) in toheroa specimens examined between March 2019 and January 2020 at Ripiro Beach.

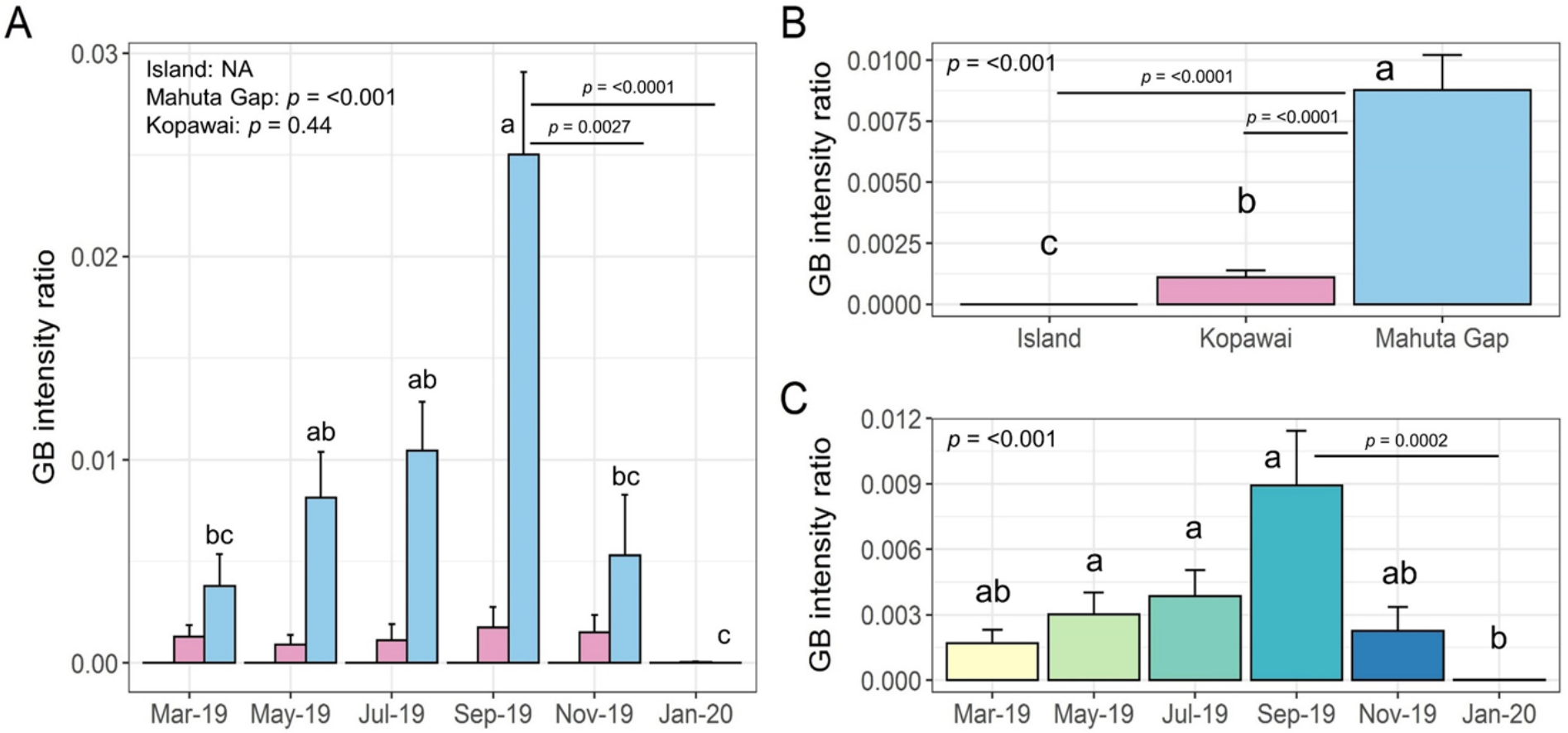

Fig. 7.3. Gas bubble (GB) intensity as a ratio of total shell area (both valves). Bars show the mean GB intensity ratio, error bars show the standard error. A: Sites on Ripiro Beach between March 2019 and January 2020. B: Site variation (Island, Kopawai, and Mahuta Gap). C: Temporal variation of gas bubble intensity on toheroa shells (sub-sites pooled). Kruskal-Wallis test *p*-values are shown (top left). Where bars do not show the same letter, the corresponding means are statistically different, Dunn tests (*p*-adj for multiple comparisons).

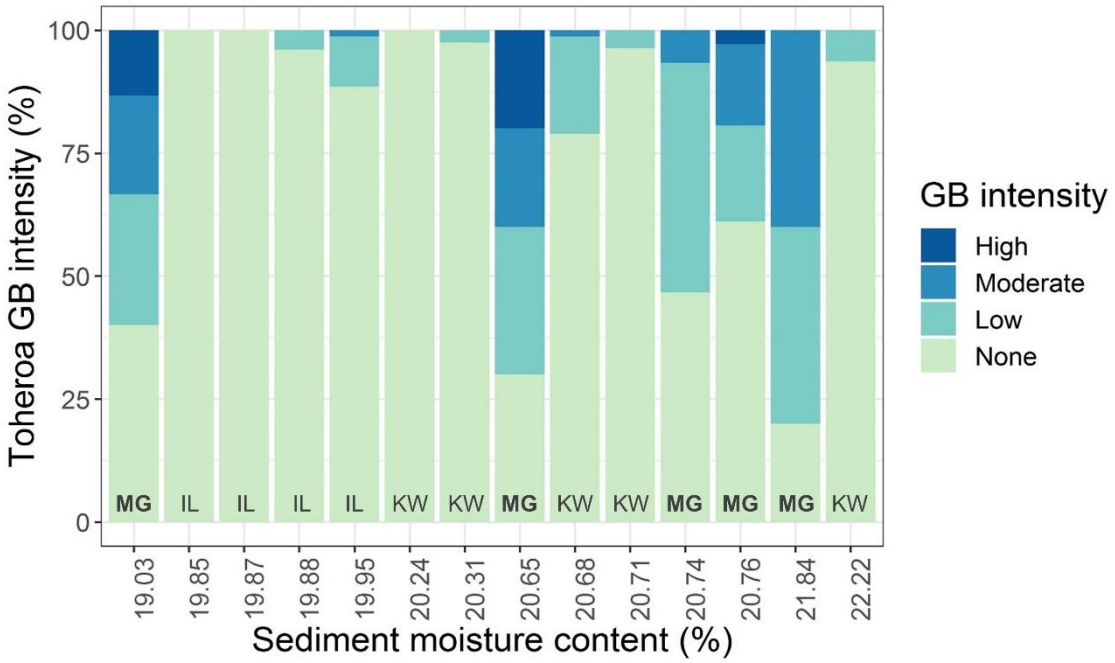

Fig. 7.4. Gas bubble (GB) intensity on toheroa shells over a gradient of sediment moisture content (%). A series of quadrats (0.25 m2) were excavated at several toheroa beds on Ripiro Beach. Moisture content at each quadrat was determined and each toheroa was hand dug and graded on a four-point scale for gas bubble intensity: None, Low, Moderate, and High. Stacked bars show proportion (%) of toheroa specimens graded at each gas bubble intensity level for each moisture content (%) level. IL: Island, MG: Mahuta Gap, KW: Kopawai. Toheroa were visually assessed/graded (*n* = 661).

The series of quadrats sampled to examine the relationship between gas bubble manifestation and sediment moisture content (as a proxy for stream flow exposure) fell across a moisture content gradient ranging from 19.03% to 22.22%. Visual assessment of *n* = 661 toheroa hand-dug at the three sub-sites indicated that moisture content of bed sediments (in *c.* 70 cm^3 of surface sediment) had little bearing on gas bubble intensity (Fig. 7.4). Instead, the highest prevalence, and intensity was again recorded in specimens sampled from Mahuta Gap (marked as MG in bold in Fig. 7.4), regardless of moisture content. The lowest moisture content recorded (19.03%) was taken at the same quadrat where the second greatest proportion of toheroa were graded as ‘high’, for gas bubble intensity (Fig. 7.4). Other than the gross pathology of gas bubbles under the periostracum (Fig. 7.5), no external or internal pathomorphological features examined (using histologically prepared tissue, *n* = 180) could be strictly associated with specimens displaying gas bubble-related trauma on shells (Fig. 7.5).

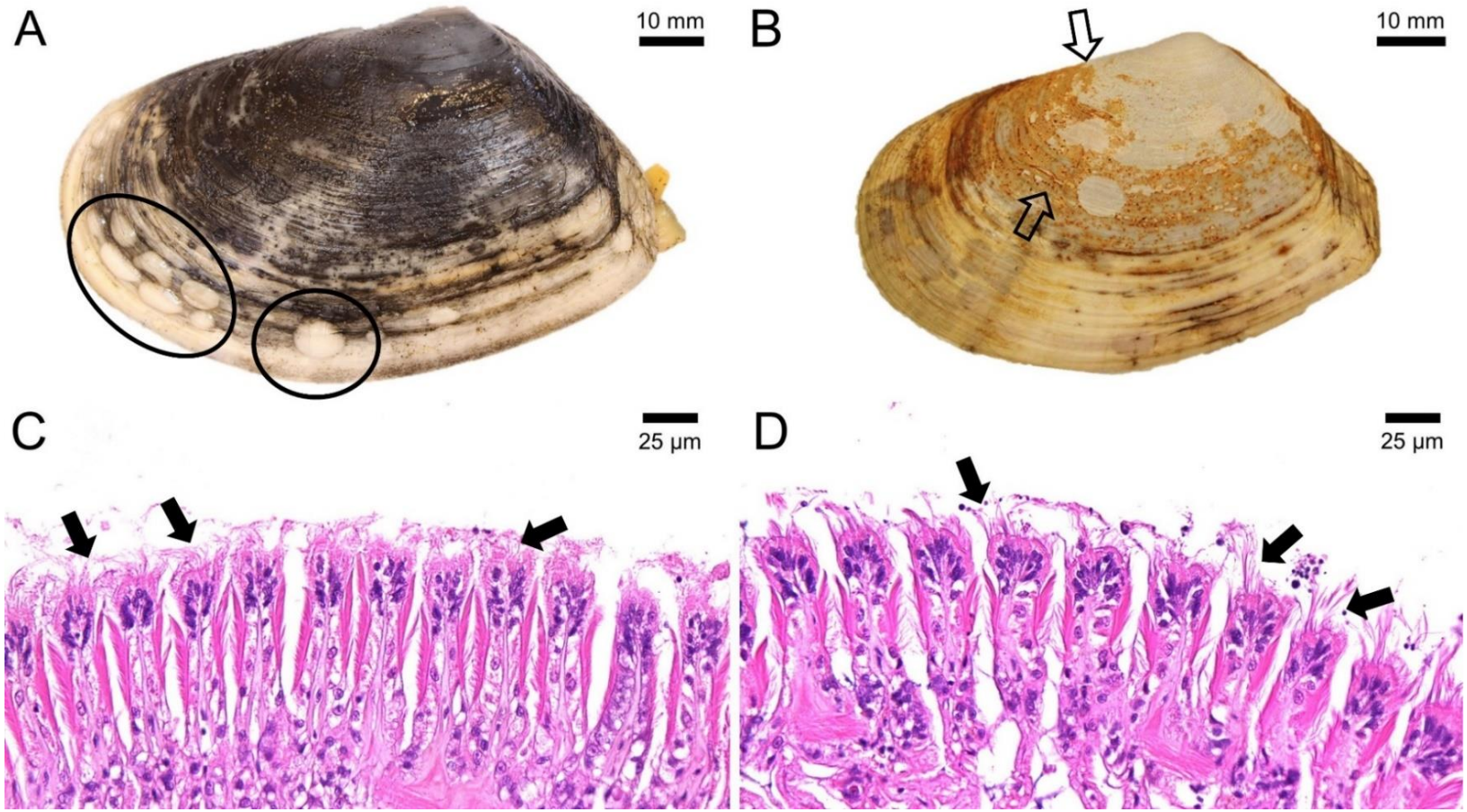

Fig. 7.5. A: Toheroa presenting gas bubbles (rings), photographed *in situ* using the custom-built light box (see Appendix G). Black deposits on the shell are presumed to be iron sulfide formed following reaction to hydrogen sulfide (H_2S). B: After dissipation of black deposits, a corroded area remains and what is presumed to be Fe(III) within the calcium carbonate structure of the shell (hollow arrows). C: Ciliary epithelium in the gills of toheroa that was negative for the presence of black deposits (FeS) and gas bubbles (arrows: cilia). D: Ciliary epithelium (arrows: cilia) in the gills of the toheroa specimen that was found to have the highest gas bubble intensity of all specimens examined (sampled from Mahuta Gap in Sept-19).

The relative abundance of OTUs assigned to Desulfobacterota was generally higher in Kopawai and Mahuta Gap specimens compared to those sampled from Island (Fig. 7.6 & Chapter 5). For instance, median relative abundance of Desulfobacterota taxa in Mahuta Gap specimens (0.8%) was close to the median for Kopawai samples (0.9%), but greater than the median for Island specimens (0.3%) (Fig. 7.6).

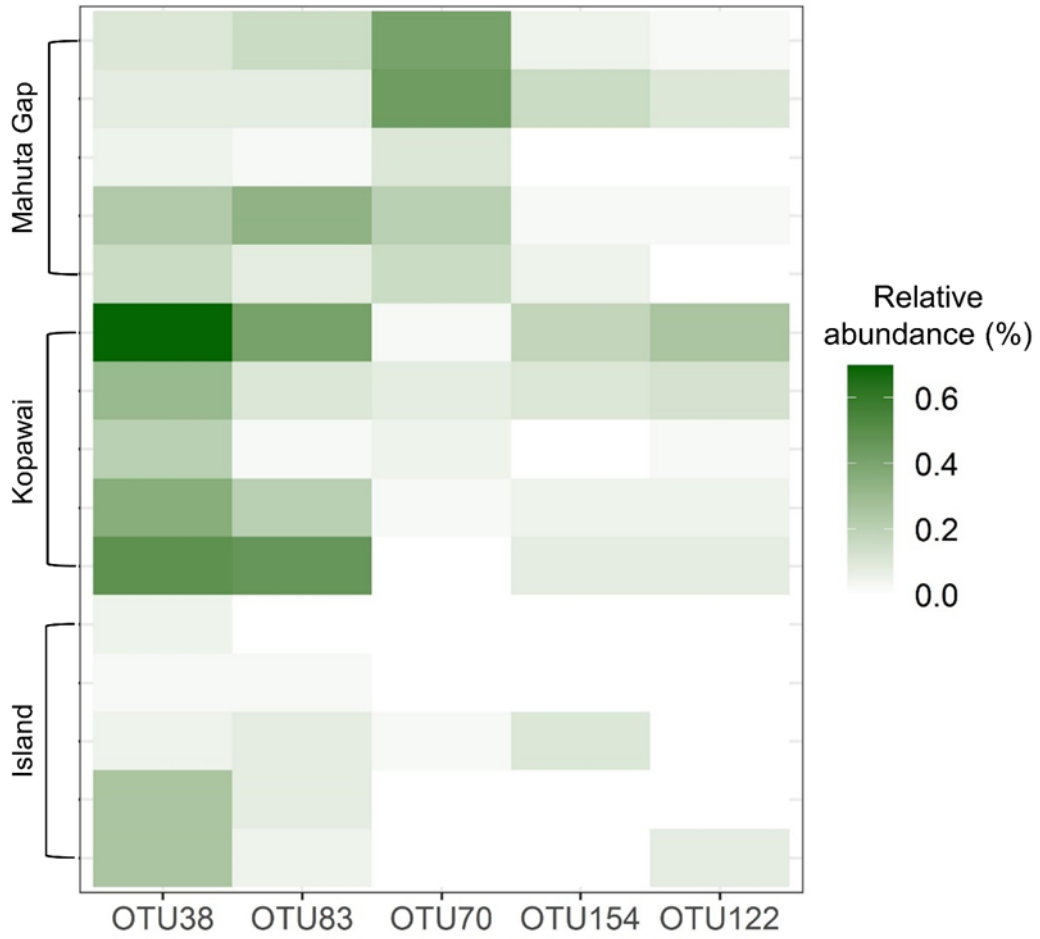

Fig. 7.6. Relative abundance of OTUs within the toheroa composite microbiome (digestive gland and gills) that were taxonomically assigned to the phylum Desulfobacterota (Fig. 7.7), across three sites: Island, Mahuta Gap, and Kopawai (*n* = 5, for each site). Specimens collected in September 2019. Data reproduced from Chapter 5.

Furthermore, when the top five Desulfobacterota OTUs were compared to published sequences in the NCBI databases, several closely related bacteria species were identified. The top five Desulfobacterota were between 81.7% and 95.4% similar. OTU83 and OTU122 the most dissimilar, while OTU38 and OTU70 were most closely related to each other (95.4%) and to *Desulfocapsa* sp. (AF228119.2) (97.9 and 94.2%, respectively). Similarly, OTU83 and OTU154 were closely related (94.9%) and both were closely related to Desulfobacteraceae (99.5 and 94.1%, respectively). OTU122 was most closely related to *Desulfarculus* sp. (100%). All Desulfobacterota OTUs were grouped with other publicly available bacteria from this phylum (see Fig. 7.7).

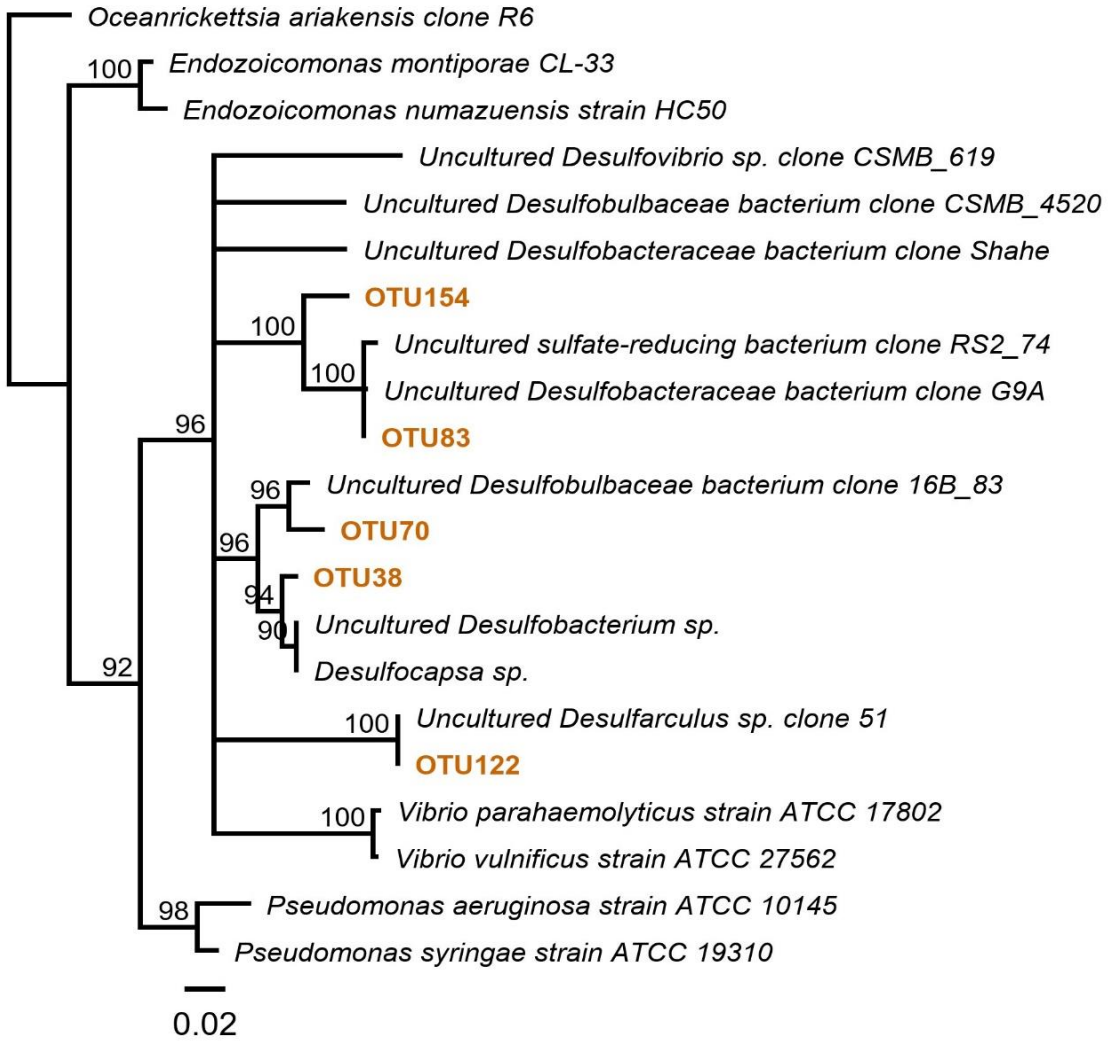

Fig. 7.7. Phylogenetic tree showing the genetic relatedness of the top five (>0.01% relative abundance) OTUs taxonomically assigned to Desulfobacterota, derived from the toheroa microbiome (composite: gill and digestive gland). Branches labelled with percentage consensus support based on 100,000 bootstrapped replicates. Mustard coloured font indicates Desulfobacterota OTUs. See Appendix G, Table G.1 for NCBI GenBank accession numbers.

7.5 Discussion

Gas bubbles were observed on shells of toheroa at Ripiro Beach at each of the sampling events between March 2019 and September 2020. While seasonality appeared to influence gas bubble prevalence and intensity, site proved the most important factor explaining the observed variation, with gas bubble intensity consistently higher at Mahuta Gap compared to the other study sites examined herein (Fig. 7.3, B). Observations made throughout this study linked gas bubbles to freshwater outflow. Mahuta Gap, where gas bubbles were consistently most intense, was also the site with the most consistent and highest volume stream. Interestingly, in Jan-20, when a historic drought occurred in the Northland region (Table 7.1), gas bubble prevalence and intensity was at its lowest, with only one specimen from Kopawai presenting gas bubbles. Similarly, gas bubble intensity varied seasonally, with larger and greater numbers of gas bubbles present in the austral winter/spring, potentially associated with increased precipitation and subsequent greater freshwater flow to the beach (Table 7.1). This link between gas bubbles and freshwater was explored by taking cores at sub-sites (Island, Mahuta Gap, and Kopawai) in Nov-19 and examining surface sediment moisture content as a proxy of stream exposure. While there does appear to be some link to a higher sediment moisture content and gas bubble severity, gas bubble prevalence of >50% was recorded in toheroa dug from the driest sediment (19.03%) at Mahuta Gap. A link to freshwater appears plausible; however, locally specific conditions appear to be more important than the physical presence of freshwater alone.

Ross et al. (2018b) postulated that gas bubbles could be attributed to supersaturation of TDG within shell cavities, caused by high temperature in the austral summer. This now seems unlikely as a reverse seasonal effect was found with greater gas bubble intensity in the austral winter/spring. Instead, I offer an alternate hypothesis, that sulfate-reducing microorganisms in the sediment and on the shells of individuals are producing H_2S gas that causes bubbles to form on the outside of the shells (see Fig. 7.8 for conceptual illustration). This hypothesis would explain why bubbles are present on the shells, but do not manifest in the tissues as is typical with previously described ‘gas bubble disease’ (Bisker and Castagna, 1987) because exposure to toheroa internally would likely be limited. No evidence of this pathology occurring in any other infaunal bivalve species could be found during a literature search. I posit that this is due to the unique conditions created at some stream-bearing sites on the northwest coast of Aotearoa, elaborated on below, that toheroa alone are subjected to. I suggest this is partly due to their deep burying capacity (typically 10 cm), their ability to withstand prolonged periods without oxygen (V. Taikato, in prep), and their location on the beach, often in the mid- and upper-intertidal (pers. obs.) permissible due to aforementioned traits.

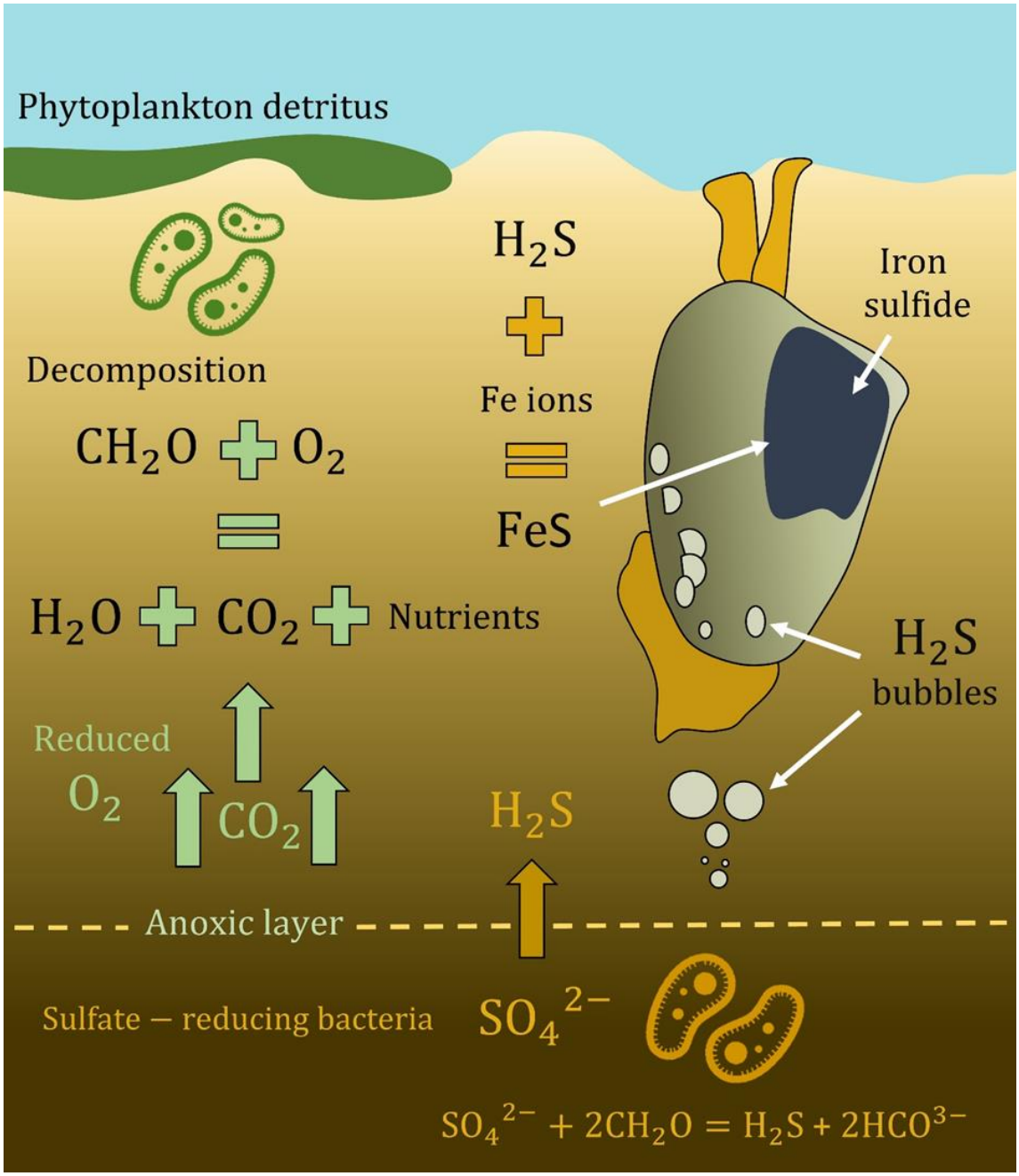

Fig. 7.8. Conceptual illustration of processes leading to the manifestation of gas bubbles and iron sulfide deposits on the shells of toheroa (*P. ventricosa*). Decomposition of phytoplankton reduces oxygen availability in the sediment. Sulfate-reducing bacteria produce hydrogen sulfide gas (H_2S) that result in bubbles under the periostracum on toheroa shells and interact with Fe ions in the calcium carbonate matrix or on the surface of shells, forming iron sulfide (FeS) deposits.

The sulfur cycle (sulfate reduction and sulfide oxidation) is a critical natural process of well-functioning aquatic environments (reviewed by Jørgensen et al., 2019). Studies of sulfur-cycling microorganisms have been conducted in Brazilian mangroves (Varon-Lopez et al., 2014), the Yangtze Estuary (Niu et al., 2018) and in northern Europe sandy beaches (van Erk et al., 2020). Bacteria that reduce sulfate (SO_4^{2-}) include the phylum Desulfobacterota (in a recently proposed reclassification of the Deltaproteobacteria) (Waite et al., 2020). Here, exploration of the toheroa microbiome revealed differential abundance of Desulfobacterota in toheroa tissues depending on collection site (Fig. 7.6). There is historical association between phytoplankton blooms, toheroa, and freshwater streams on Ripiro Beach (Ross et al., 2018a; Williams et al., 2013). Large phytoplankton blooms are commonplace on high-energy Northland west-coast beaches of Aotearoa (Cassie, 1955), which have been linked to autumn rains (pers. obs.), subsequent nutrient run-off and offshore (westerly) winds (Williams et al., 2013). After these blooms, dense mats of decaying microalgae coat the beach. These dense mats of algal detritus would increase microbial respiration and decomposition (Alongi, 2009). Furthermore, beach topography varies between study sites investigated here, with elevation steeper on either side of the Mahuta Gap stream compared to Kopawai, creating a basin or funnel-like beach profile (Fig. 7.9) (Cope, 2018), which potentially concentrates more phytoplankton detritus at Mahuta Gap (compared to other beds), increasing organic matter content in the sediment.

Desulfobacterota relative abundance varied across sampling sites and was greatest (*c.* 0.9%) in specimens at stream bearing sites (Mahuta Gap and Kopawai) compared to Island (0.3%, no stream present at time of sampling in September 2019). This pattern may be explained by greater abundance of organic matter at stream-bearing sites due to nutrient outflow from land and channelling of phytoplankton due to altered beach morphology (Fig. 7.9). For example, van Erk et al. (2020) found greater relative abundance of sulfate-reducing bacteria in sediments from a sandy beach bearing kelp detritus than a beach not bearing decaying kelp. Furthermore, the specimens used for bacterial community analysis were collected in September 2019, following recent observations of phytoplankton blooms on Ripiro Beach (pers. obs.). Sulfate-reducing bacteria and low oxygen concentrations are generally associated with fine-grain sediments and high organic matter content e.g., mangrove habitats (Lewis et al., 2011). Cope (2018) investigated the sedimentology on Ripiro Beach including Kopawai and Island (referred to therein as Kelly's), though not Mahuta Gap. Cope (2018) reported finer-grained sediment composition at Kopawai compared to Island. This could explain the difference in gas bubble prevalence and intensity observed here between Island and Kopawai. Finer grain sediments might be contributing to reduced oxygen availability for bacterial decomposition, increasing the abundance of sulfate-reducing bacteria (Fig. 7.6).

Another point to consider is toheroa bed location on the beach. Compared to Kopawai and Mahuta Gap, the bed at Island is typically higher on the beach, meaning that toheroa at Island site might simply be less exposed to algal detritus than sites where beds are situated in the low- to mid-intertidal zone. Organic matter content in the sediment is likely increased by the physical presence of toheroa too. For example, Hansen et al. (1996) showed sulfate reduction rates were 1.5 to 2 times greater in soft-shell clam *Mya arenaria* burrows compared to ambient sediment, suggesting increased organic enrichment in *M. arenaria* burrows via excreta (mucus and faeces) and by wells created by siphons (Hansen et al., 1996). Toheroa density (Asami et al., 2005) and size class structure (Zhang et al., 2020) could therefore modify the abundance of sulfate reducers in toheroa beds, contributing to site/bed and temporal variability.

Table 7.1. Collection details and environmental conditions at Ripiro Beach during specimen sampling period. Air and water (surf zone) temperature were recorded on site, total rainfall for previous 30 days/24 hours was obtained from www.nrc.gov.nz. Rainfall data was collected from the closest rainfall station at Kai Iwi Lakes *c.* 10 km from the closest sub-site on Ripiro Beach, Island. In the table, IL: Island, MG: Mahuta Gap, and KW: Kopawai.

Beach	Sub-sites	Date	*n*	Air temp. (°C)	Water temp. (°C)	Rainfall (mm) previous 30 days	Rainfall (mm) previous 24 hours
Ripiro	IL, MG, KW	Mar-19	30	25	19	31	0
	IL, MG, KW	May-19	30	18	17	53	3.5
	IL, MG, KW	Jul-19	30	9	12	184	0
	IL, MG, KW	Sep-19	30	13	14	72	3
	IL, MG, KW	Nov-19	30	17	17	60.5	0.5
	IL, MG, KW	Jan-20	30	20	19	4.5*	0
	IL, MG, KW, '1st stream', '3rd stream'	Sep-20	167	14	13	123.5	0

*A significant drought occurred in Te Tai Tokerau (Northland) in early 2020

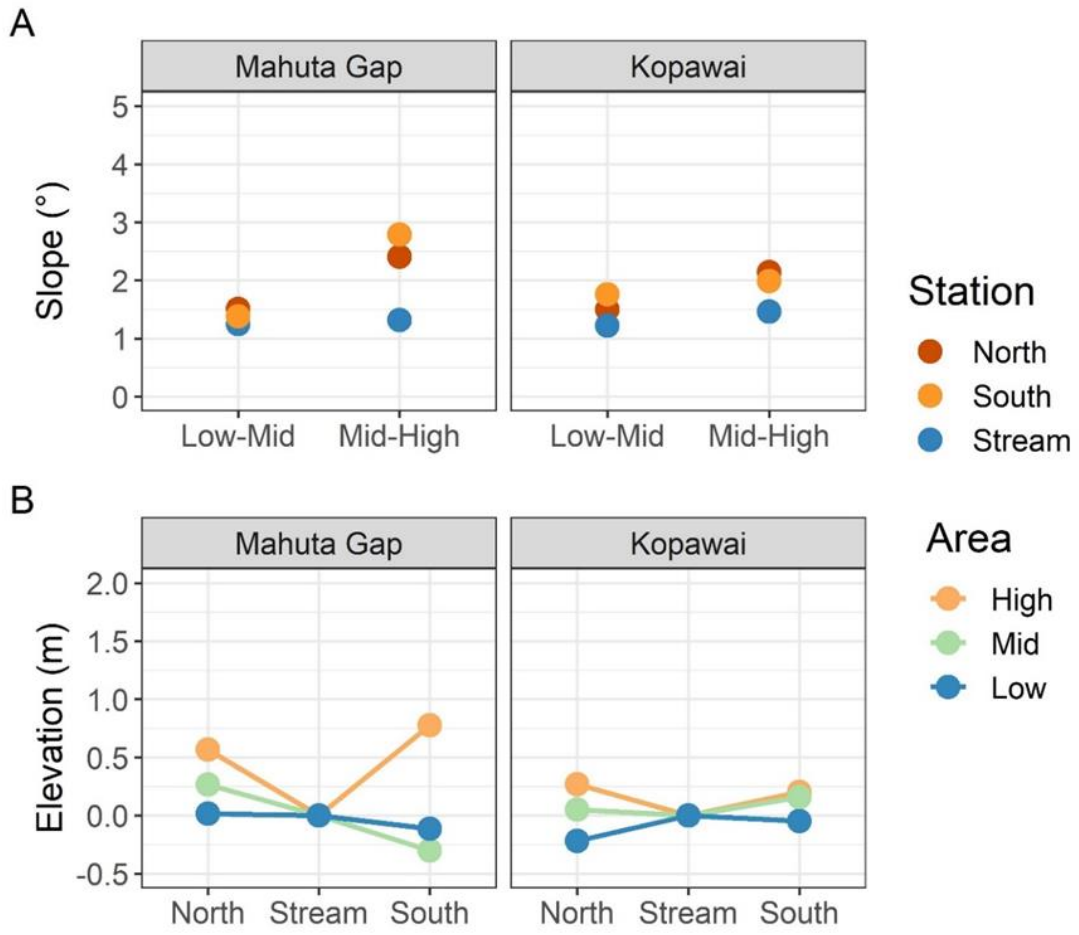

Fig. 7.9. Slope and elevation information from two stream sites on Ripiro Beach (Mahuta Gap and Kopawai). A: Shows the slope of the beach profile between two areas, low to mid shore and mid to high shore. B: Shows the elevation of the beach on the North and South sides of streams at three areas along the beach profile. Streams here are '0 m' elevation. Elevation on North and South sides are referenced from respective streams. Data obtained from Cope (2018). See Cope (2018) for methods and further details of beach modification by streams. Figure produced using 'ggplot2' package (Wickham, 2009) in RStudio.

Similarly, the occurrence of gas bubble disease found in common dolphins (*D. capensis*) was associated with anaerobic bacteria (Danil et al., 2014), though in contrast to the common dolphin case, no soft tissue pathogenesis was detected in toheroa. Following links made between H_2S and gas bubbles on toheroa, histology sections were re-examined for malformation of the ciliary epithelium in the gills, as described by Nagasoe et al. (2011), who found implications for gill health and feeding in Manila clams (*Ruditapes philippinarum*) linked to hypoxia and H_2S exposure. Similar damage to the ciliary epithelium that could be attributed to chronic H_2S exposure was not detected, even in toheroa specimens presenting a high intensity of gas bubbles (Fig. 7.5). However, lethal effects of H_2S on surf clams has been shown previously. In *Donax serra*, Laudien et al. (2002) showed that chronic exposure to hypoxia and H_2S induced mortality with an LT_{50} of 80 hrs for juveniles. Exposure levels used in this case were meant to mirror

'sulfide eruptions' off the coast of Namibia. Natural exposure of toheroa to hypoxia and H_2S is likely considerably lower, nevertheless, in light of the mortality observed in *D. serra*, the potential consequences of hypoxia and H_2S exposure for juvenile toheroa and recruitment should be considered. Furthermore, Coffin et al. (2021) showed that the presence of anaerobic bacteria (sulfate-reducing bacteria) halved oyster (*C. virginica*) survival rates under anoxic conditions. The authors go on to suggest that mass mortality events in a range of species that are linked to anoxia/hypoxia are likely mediated by bacterial processes. Given the findings presented here, future investigations of mass mortality events in toheroa and other Aotearoa shellfish, should consider the synergistic effects of anoxia and bacterial processes (H_2S production) on mortality outcome.

Shells examined at Mahuta Gap were consistently blue/black in colour (Fig. 7.5), possibly attributed to iron sulfide (FeS) formed when Fe(III) or Fe(II) ions react with H_2S. Different concentrations of Fe(III) and Fe(II) would be expected between sites with more or less organic matter and subsequent bacterial decomposition. For example, van Erk et al. (2020) measured Fe(II) and Fe(III) concentrations in sediments from a kelp-bearing beach and a reference beach (without kelp detritus). Finding considerably higher Fe(III) (mean kelp-beach: 17.44, mean reference-beach 9.25 mmol L^{-1}) and Fe(II) (mean kelp-beach: 127.02, mean reference-beach 0.62 mmol L^{-1}) concentrations in sediments from the kelp-bearing beach. This blue/black colour phenomenon on toheroa shells offers an interesting parallel to the black scaly-foot gastropod *Chrysomallon squamiferum*, a hydrothermal vent-associated snail famous for its FeS skeleton (Okada et al., 2019). Similar to the black coloration observed in toheroa shells here, the FeS coloration of C. *squamiferum* shells and scales has been shown to be site-specific, linked to Fe content in the surrounding environment (Okada et al., 2019). Nearly all toheroa specimens that were positive for gas bubbles, and photographed, exhibited blue/black deposits on shells (75/80). Taikato (in prep) also observed the manifestation of gas bubbles on toheroa shells, coinciding with blue/blackish deposits on the shells of specimens during unrelated *ex situ* experimentation. Echoing the scally-foot snail, this coloration appears to be associated with environmental conditions at certain sites (Okada et al., 2019) as not all toheroa exhibit black coloration on the shell. In this study, black deposits and gas bubbles dissipated after *c.* 12 hours when sampled specimens were exposed to oxygenated seawater (pers. obs.). Deposits of supposed FeS on shells provides another parallel, this time to 'FeS scale' a pervasive issue in the oil and gas industry where producer, injection and supply wells, contaminated with H_2S, develop an FeS scale. The scale can reduce equipment performance and reduce the structural integrity of pipes via enhanced corrosion rates (Kasnick and Engen, 1989; Mahmoud et al., 2018). Interestingly, when FeS deposits or scale dissipated from toheroa shells, shells appeared corroded (Fig. 7.5, B), often with degraded or missing periostracum in the area where the supposed FeS

scale had been present (typically umbo). This is unsurprising given the corrosive potential of H_2S (reviewed by Anandkumar et al., 2016) and potentially explains why gas bubbles were typically detected in the ventral area of the shell. As assumed FeS scale was typically less abundant and thus, the periostracum was still intact (Fig. 7.5, A) allowing bubbles to manifest.

In light of these findings, it is worth considering whether disruption to the periostracum could be affecting toheroa by reducing shell strength, integrity, growth and (or) repair rate? (Peck et al., 2016). A size frequency study carried out on toheroa populations on Ripiro Beach in September 2019 found that a significant adult size mode (>70 mm) was present at Mahuta Gap compared to other study sites (e.g., Kopawai) (Vallyon, 2020), indicating no significant growth rate reduction that could be attributed to locally specific conditions. Conversely, toheroa at this site constitute a robust and apparently healthy population on Ripiro Beach. Interestingly, mātauranga (Indigenous knowledge systems) informed restoration or enhancement practices reportedly used in southern Aotearoa involve burying kelp in toheroa beds (Futter, 2011). This practice would undoubtedly increase bacterial respiration in the sediment by sulfate-reducing bacteria (Aires et al., 2018; van Erk et al., 2020), creating conditions akin to Mahuta Gap in September 2019. Due to the perceived good health at toheroa at Mahuta Gap, and the use of this restoration technique, it is possible this practice modifies microbial communities and bacterial processes in toheroa beds in a way that is favourable for toheroa. The possible benefits of this kind of habitat modification for toheroa populations therefore presents an intriguing avenue for further exploration.

A mechanism to gas bubble formation cannot be fully resolved here, though a link to sulfate-reducing bacteria (Desulfobacterota) and organic matter presents an interesting hypothesis. I therefore postulate that, phytoplankton blooms associated with autumn/winter rains (nutrient run-off) result in large quantities of organic matter detritus. Additionally, modification of beach morphology by streams, that channels algal detritus, increases bacterial decomposition/respiration by sulfate-reducing bacteria and increases H_2S production that causes gas bubbles and FeS to appear on the shells of toheroa. It is unlikely that these mechanisms are comprehensive. Rather, several factors probably contribute synergistically to increase bacterial respiration leading to gas bubble formation on toheroa shells. However, the hypothesis given is in line with *in situ* and *ex situ* observations made thus far. Gas bubble prevalence and intensity was consistently greatest at Mahuta Gap, the site with the most consistent freshwater stream. Manifestation via supersaturated total dissolved gases (TDG) is not possible due to observations of gas bubbles on shells of toheroa even in anoxic/hypoxic conditions (i.e., September 2020). Further, histological examination did not indicate gas bubble related trauma in the tissues, inconsistent with supersaturated TDG-induced gas bubble

disease. It is therefore more likely that gas bubbles are a result of gas production in the surrounding environment and on the shells by microorganisms. Finally, the detection of Desulfobacterota taxa in the toheroa microbiome at relatively high abundance (*c.* 1%) suggests high environmental exposure, supporting this hypothesis.

7.6 Conclusion and Recommendations

This study suggests that gas bubbles on toheroa shells are not a result of supersaturation of TDG as previously proposed by Ross et al. (2018b), and therefore not an indication of 'gas bubble disease'. Instead, a mechanism for their formation seems likely to be H_2S-producing sulfate-reducing bacteria in sediment or on the surface of toheroa shells. No health-related implications were associated with gas bubbles or possible H_2S exposure. Despite this, given the potential lethal effects of hypoxia and H_2S for juvenile surf clams (Laudien et al., 2002), investigations of toheroa health and recruitment in the future should consider their impact. Though gas bubbles were intermittently observed on toheroa shells at other sites, toheroa at Mahuta Gap on Ripiro Beach were considerably more affected. Local conditions are likely contributing to this disparity. It is possible that nutrient pollution (eutrophication) introduced by freshwater outflow at this site (cattle pasture) is modulating oxygen availability within the toheroa bed via increased bacterial decomposition. Equally, gas bubble manifestation could be a natural phenomenon resulting from the toheroa typically forming beds in association with freshwater outflows onto high-energy beaches.

Keeping in mind the absence of evidence of health implications noted here, future explorations of gas bubble manifestation on toheroa should investigate the pathway to gas bubble formation via sulfate-reducing bacteria, by analysis of gases (H_2S) present in the sediment or in bubbles present on toheroa shells. Links between streams and organic matter content should be explored to determine the extent to which streams deliver nutrients and (or) modify beach chemistry through the channelling phytoplankton to toheroa beds. Finally, as severely affected individuals were from apparently healthy and robust toheroa populations, the possible health benefits of environmental conditions associated with this phenomenon should be explored (via sulfur-cycling symbionts). Subsequent outcomes from explorations like these could have profound implications for future conservation and enhancement efforts (translocations and *in situ* restoration) and toheroa aquaculture.

7.7 References

Aires, T., et al., 2018. Seaweed Loads Cause Stronger Bacterial Community Shifts in Coastal Lagoon Sediments Than Nutrient Loads. Frontiers in Microbiology. 9**,** 3283.

Alongi, D. M., Water and Sediment Dynamics. In: D. M. Alongi, (Ed.), The Energetics of Mangrove Forests. Springer Netherlands, Dordrecht, 2009, pp. 47-64.

Anandkumar, B., et al., 2016. Corrosion characteristics of sulfate-reducing bacteria (SRB) and the role of molecular biology in SRB studies: an overview. Corrosion Reviews. 34**,** 41-63.

Asami, H., et al., 2005. Accelerated sulfur cycle in coastal marine sediment beneath areas of intensive shellfish aquaculture. Applied and Environmental Microbiology. 71**,** 2925-2933.

Beeman, J. W., et al., Gas bubble disease in resident fish below Grand Coulee Dam: final report of research. USGS, Boise, ID, 2003, pp. 159.

Beentjes, M. P., 2010. Toheroa survey of Bluecliffs Beach, 2009, and review of historical surveys. New Zealand Fisheries Assessment Report 2010/7. 42.

Beyer, D. L., et al., 1976. Decompression-induced bubble formation in salmonids: comparison to gas bubble disease. Undersea Biomedical Research. 3**,** 321-38.

Bisker, R., Castagna, M., 1987. Effect Of Air-Supersaturated Sea Water On *Argopecten irradians concentricus* (Say) And *Crassostrea virginica* (Gmelin). Journal of Shellfish Research. 6**,** 79-83.

Bouck, G. R., 1980. Etiology of Gas Bubble Disease. Transactions of the American Fisheries Society. 109**,** 703-707.

Cassie, R. M., 1955. Population Studies on the Toheroa, *Amphidesma ventricosum* Gray (Eulamellibranchiata). Australian Journal of Marine and Freshwater Research. 6**,** 348-391.

Coffin, M. R. S., et al., 2021. The killer within: Endogenous bacteria accelerate oyster mortality during sustained anoxia. Limnology and Oceanography. 9999**,** 1-16.

Cope, J., The modification of toheroa habitat by streams on Ripiro Beach. MSc. University of Waikato, Hamilton, New Zealand, 2018, pp. 126.

Danil, K., et al., 2014. *Clostridium perfringens* septicemia in a long-beaked common dolphin *Delphinus capensis*: an etiology of gas bubble accumulation in cetaceans. Diseases of Aquatic Organisms. 111**,** 183-190.

Dinno, A., Dinno, M., Package 'dunn. test'. CRAN Repository, Vol. 10, 2017.

Futter, J. M., An investigation into the Murihiku toheroa (*Paphies ventricosa*): mātauranga, monitoring and management. MSc. University of Otago, Dunedin, 2011, pp. 140.

Gadomski, K., Reproduction and larval ecology of the toheroa, *Paphies ventricosa*, from Oreti Beach, Southland, New Zealand. PhD. University of Otago, 2017, pp. 155.

Hansen, K., et al., 1996. Impact of the soft-shell clam *Mya arenaria* on sulfate reduction in an intertidal sediment. Aquatic Microbial Ecology. 10**,** 181-194.

Howard, D. W., et al., Histological techniques for marine bivalve mollusks and crustaceans. NOAA Tech Memo NOS NCCOS 5. NOAA, Oxford, Maryland, 2004, pp. 218.

Jepson, P. D., et al., 2003. Gas-bubble lesions in stranded cetaceans - Was sonar responsible for a spate of whale deaths after an Atlantic military exercise? Nature. 425**,** 575-576.

Johnson, M., et al., 2008. NCBI BLAST: a better web interface. Nucleic Acids Research. 36**,** W5-9.

Johnson, P. T., 1976. Gas-bubble disease in the blue crab, *Callinectes sapidus*. Journal of Invertebrate Pathology. 27**,** 247-253.

Jørgensen, B. B., et al., 2019. The Biogeochemical Sulfur Cycle of Marine Sediments. Frontiers in Microbiology. 10**,** 849.

Kasnick, M. A., Engen, R. J., Iron Sulfide Scaling and Associated Corrosion in Saudi Arabian Khuff Gas Wells. Middle East Oil Show. OnePetro, 1989.

Kearse, M., et al., 2012. Geneious Basic: An integrated and extendable desktop software platform for the organization and analysis of sequence data. Bioinformatics. 28**,** 1647-1649.

Laudien, J., et al., 2002. Survivorship of juvenile surf clams *Donax serra* (Bivalvia, Donacidae) exposed to severe hypoxia and hydrogen sulphide. Journal of Experimental Marine Biology and Ecology. 271**,** 9-23.

Lewis, M., et al., 2011. Fate and effects of anthropogenic chemicals in mangrove ecosystems: A review. Environmental Pollution. 159**,** 2328-2346.

Lightner, D. V., et al., 1974. Gas-bubble disease in the brown shrimp (*Penaeus aztecus*). Aquaculture. 4**,** 81-84.

Liu, X., et al., 2019. Lethal Effect of Total Dissolved Gas-Supersaturated Water with Suspended Sediment on River Sturgeon (*Acipenser dabryanus*). Scientific Reports. 9**,** 13373.

Mahmoud, M., et al., 2018. Development of efficient formulation for the removal of iron sulphide scale in sour production wells. The Canadian Journal of Chemical Engineering. 96**,** 2526-2533.

Malouf, R., et al., 1972. Occurrence of Gas-Bubble Disease in Three Species of Bivalve Molluscs. Canadian Journal of Fisheries and Aquatic Sciences. 29**,** 588-589.

McDonough, P. M., Hemmingsen, E. A., 1984. Bubble formation in crustaceans following decompression from hyperbaric gas exposures. Journal of Applied Physiology. 56**,** 513-519.

Mesa, M. G., et al., 2000. Progression and Severity of Gas Bubble Trauma in Juvenile Salmonids. Transactions of the American Fisheries Society. 129**,** 174-185.

Nagasoe, S., et al., 2011. Effects of hydrogen sulfide on the feeding activity of Manila clam *Ruditapes philippinarum*. Aquatic Biology. 13**,** 293-302.

Niu, Z.-s., et al., 2018. Sulphate-reducing bacteria (SRB) in the Yangtze Estuary sediments: Abundance, distribution and implications for the bioavailibility of metals. Science of The Total Environment. 634**,** 296-304.

Okada, S., et al., 2019. The making of natural iron sulfide nanoparticles in a hot vent snail. Proceedings of the National Academy of Sciences. 116**,** 20376.

Peck, V. L., et al., 2016. Outer organic layer and internal repair mechanism protects pteropod *Limacina helicina* from ocean acidification. Deep Sea Research Part II: Topical Studies in Oceanography. 127**,** 41-52.

Ross, P. M., et al., 2018a. The biology, ecology and history of toheroa (*Paphies ventricosa*): a review of scientific, local and customary knowledge. New Zealand Journal of Marine and Freshwater Research. 52**,** 196-231.

Ross, P. M., et al., 2018b. First detection of gas bubble disease and *Rickettsia*-like organisms in *Paphies ventricosa*, a New Zealand surf clam. Journal of Fish Diseases. 41**,** 187-190.

Team, R. C., R: A language and environment for statistical computing. R Foundation for Statistical Computing, Vienna, Austria, 2013.

Vallyon, L.-M. D., Birds vs. Clams: Assessing the impacts of South Island pied oystercatcher predation on Toheroa at Ripiro Beach, New Zealand. MSc. The University of Waikato, 2020, pp. 115.

van Erk, M. R., et al., 2020. Kelp deposition changes mineralization pathways and microbial communities in a sandy beach. Limnology and Oceanography. 65**,** 3066-3084.

Varon-Lopez, M., et al., 2014. Sulphur-oxidizing and sulphate-reducing communities in Brazilian mangrove sediments. Environmental Microbiology. 16**,** 845-55.

Waite, D. W., et al., 2020. Proposal to reclassify the proteobacterial classes *Deltaproteobacteria* and *Oligoflexia*, and the phylum *Thermodesulfobacteria* into four phyla reflecting major functional capabilities. International Journal of Systematic and Evolutionary Microbiology. 70**,** 5972-6016.

Weitkamp, D. E., Katz, M., 1980. A Review of Dissolved Gas Supersaturation Literature. Transactions of the American Fisheries Society. 109**,** 659-702.

Wickham, H., 2009. ggplot2: Elegant Graphics for Data Analysis. Springer, New York.

Williams, J. R., et al., Review of factors affecting the abundance of toheroa (*Paphies ventricosa*). New Zealand Aquatic Environment and Biodiversity Report No. 114, 2013, pp. 76.

Zhang, K., et al., 2020. Fish growth enhances microbial sulfur cycling in aquaculture pond sediments. Microbial Biotechnology. 13**,** 1597-1610.

Chapter 8
Discussion

Toheroa with dark blue/black shells and gas bubbles
Mahuta Gap, Ripiro Beach

Conservation and disease are inherently linked. Disease can threaten conservation goals directly (Raymundo et al., 2020) or threatened species can be at greater risk of disease due to low genetic variability (Acevedo-Whitehouse et al., 2009). Additionally, disease can interact with factors responsible for the initial population decline of a species, with unpredictable outcomes (Altizer et al., 2013). Conservation relies on robust health data to ensure population recovery efforts are not in vain (Sas et al., 2020; West et al., 2019). In a worst-case scenario, restorative efforts can even diminish conservation goals by causing new disease outbreaks through translocation of infected conservation targets (Cunningham, 1996).

In Chapter 2, an appeal was made for increased surveillance of the health of shellfish populations in general. For toheroa (*Paphies ventricosa*), there has never been any surveillance, and consequently this thesis was an attempt fill some of the many unknowns for this species. The schematic below (Fig 8.1) summarises the findings of this research, showing the interconnectedness of different facets of toheroa health. The concepts explored in this thesis are shown under three overarching headings: toheroa health and disease, aquaculture, and conservation (Fig. 8.1). In this general discussion chapter, I highlight the main findings of this research and discuss avenues for future research.

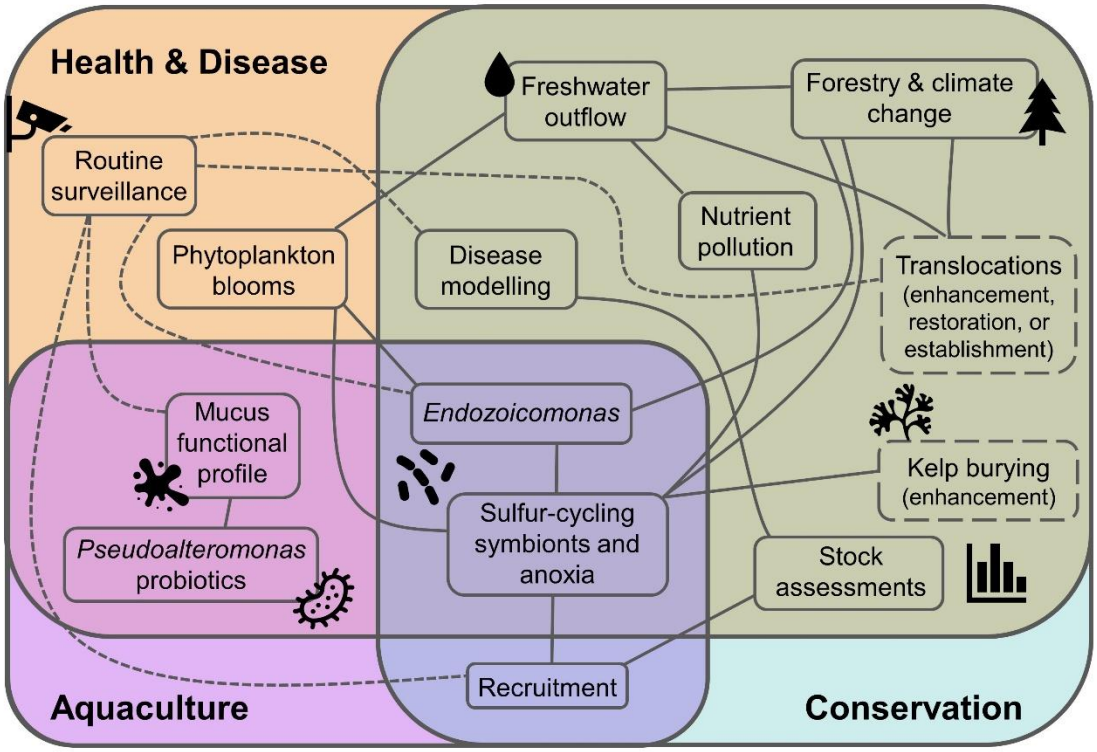

Fig. 8.1. Schematic placing facets of toheroa health within the context of aquaculture and conservation. Thin dashed lines denote actions that require routine surveillance of health to facilitate their success or provide necessary baseline data. Wide-dashed boxes denote population restoration or enhancement practices (tikanga) informed by Indigenous knowledge systems (mātauranga). Schematic should be used as a guide for future study of toheroa health for aquaculture and the conservation of wild populations.

8.1 Indirect Modulation of Toheroa Health by Freshwater Streams

My exploration of the link between toheroa populations and freshwater outflows was by no means novel to this research. What is novel about the findings of this thesis are the links between freshwater flows and the health of these shellfish populations. For example, the presence and absence of *Endozoicomonas* spp. (Chapter 4), sulfate-reducing bacteria (Chapter 5), gas bubbles (Chapter 7), and gill ciliates (Chapter 3) linked to freshwater stream presence, consistency, and volume.

Primarily, it appears that the presence of a stream results in increased amounts of organic matter in the mid to low intertidal zone where toheroa reside. This was hypothesised by Cope (2018) based on beach morphology (Chapter 7) and has been referred to time and again based on observations by researchers (Akroyd et al., 2002; Cassie, 1955; Redfearn, 1974; Smith, 2003). In Chapter 6, trace elements were analysed in surface sediments along stream paths at three sites, Island (typically no freshwater outflow), Kopawai (moderate stream), and Mahuta Gap (large stream) on Ripiro Beach. During the sampling expedition (Sept-2020), dense slicks of microalgae were present on the beach and subsequently collected with surface sediments. The key component of nearly all chlorophyll forms is a magnesium (Mg^{2+}) ion. It is reasonable to assume that where increased Mg is found in surface sediment, a higher volume of photosynthetic organisms (detritus) is present. For instance, using data from Silva et al. (2015), I calculated the average proportion of Mg in microalgae to be 10.3% (range: 5.4-26.9%) of the 21 elements analysed therein. Thus, Mg is going to be viewed as a proxy for photosynthetic organisms in surface sediments examined in Chapter 6.

Higher Mg concentrations were observed in the region of the beach where toheroa beds are present (Fig. 8.2). At Mahuta Gap, the magnesium concentration was both greater, and also present further up the beach (landwards; Fig. 8.2), supporting the notion that the beach profiles associated with streams (shallow basins) channel microalgae to the toheroa beds (see conceptual illustration, Fig. 8.3). This hypothesis is further supported by the higher relative abundance of cyanobacteria, *Synechococcus* taxa (picoplankton), in the bacterial community of toheroa from stream-bearing sites compared to those without a consistent freshwater flow (Chapter 5).

It is evident that the stream-modified beach morphology constitutes a favourable habitat for toheroa feeding success (Figs. 8.2 & 8.3). Toheroa condition was found to be higher following an increase of estimated chlorophyll-*a* concentration (Chapter 3). This increase in condition, coincident with algal blooms is something that has been previously reported across the distribution of toheroa (Cassie, 1955; Gadomski and Lamare, 2015). In contrast, it has been suggested that climate related decreases in the frequency and magnitude of algal blooms may have contributed to the decline of toheroa (O'Halloran, 1961).

In Chapter 7, the manifestation of gas bubbles on toheroa shells was investigated and links were made to sulfate-reducing bacteria. In the South Island (Te Waipounamu), Māori are known to have traditionally buried kelp (likely *Durvillaea* spp.) in select toheroa beds to enhance productivity and health (Futter, 2011) (Fig. 8.1). Macroalgae, and their derivatives, are known to benefit the health of shellfish via immunomodulation (Rudtanatip et al., 2018) and antiviral activity (Lynch et al., 2021). In the case of toheroa, the addition of organic matter in this fashion would increase bacterial decomposition, with sulfur-cycling bacteria likely to be highly represented (van Erk et al., 2020), where immunomodulation effects would also be possible. This would create conditions like those observed at Mahuta Gap in July and September 2019 (Chapter 7), which coincided with gas bubble occurrence i.e., increased H_2S production (Fig. 8.4). Large adult toheroa are generally present at Mahuta Gap (see Vallyon, 2020) indicating toheroa energy demands and niche requirements are being met at this location. Furthermore, the first toheroa cannery on Ripiro Beach was opened at Mahuta Gap (Chapter 1), suggesting that this site has historically been highly productive. It is possible that burying kelp in toheroa beds, creates conditions akin to those at Mahuta Gap (owed to high organic matter content, Fig. 8.2 & 8.3) and that subsequent biogeochemical cycling (sulfur & carbon) is beneficial for toheroa life histories. For instance, if the toheroa is chemosymbiotic and heterotrophic, increased sulfide concentration in toheroa beds could provide a source of carbon for tissue growth and repair via sulfide-oxidising endosymbionts in the gills (van der Geest et al., 2014).

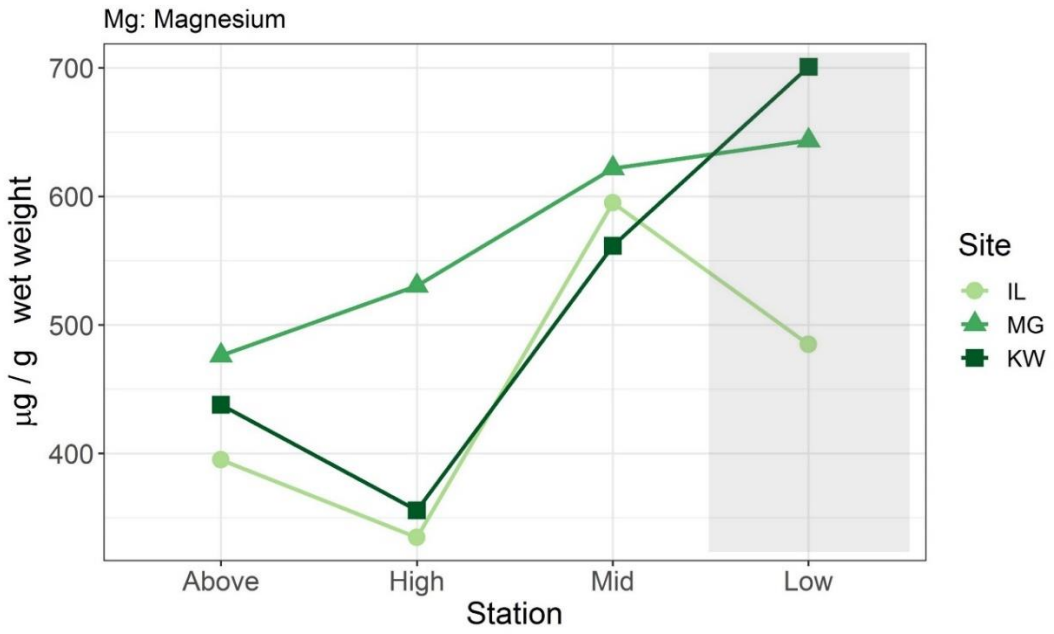

Fig. 8.2. Magnesium concentration (µg g^{-1} wet weight) of surface sediment gathered from sampling sites, IL: Island, MG: Mahuta Gap, and KW: Kopawai on Ripiro Beach in September 2020. Data reproduced from Chapter 6. Sediment samples gathered at four stations along a gradient from 'Above' stream where stream enters the beach towards the low-intertidal zone. Shaded area: approximate location of toheroa beds.

Going forward, molecular techniques could be used to gain insight into the bacterial/biogeochemical dynamics occurring in the sediment (Varon-Lopez et al., 2014) that makes up the toheroa beds and in tissues and on the shells of the toheroa themselves (Banker and Coil, 2020). Sulfate-reducing bacteria could be characterised by gene sequencing and quantified with specific real-time PCR assays. Reverse transcription PCR (RT-PCR) could similarly provide insights into sediment dynamics by analysing functional gene expression. For instance, targeting genes encoding for key enzymes of sulfate-reducing bacteria energy metabolism like sulfite reductase (dsrB) and adenosine- 5` -phosphosulfate reductase (aprA) (Varon-Lopez et al., 2014; Wagner et al., 2005). These methods could help shed light on toheroa habitat requirements and interactive effects of toheroa health and biogeochemical cycles like the sulfur cycle (Fig. 8.3). Similarly, determining where (and when) toheroa derive nutrition, whether from suspended organic matter or endosymbionts (van der Geest et al., 2014), would reveal niche requirements that could guide restoration efforts (Fig. 8.1). This could be achieved using a combination of the aforementioned tools and stable isotope analysis ($\delta^{13}C$).

Understanding the ecological drivers of this habitat selection by toheroa is important, but it is well recognised that streams are central to toheroa life histories. If streams, phytoplankton blooms, and toheroa health are intrinsically linked, as they appear to be, it makes sense that to protect toheroa emphasis must be placed on freshwater outflows being preserved (maintaining flow and quality).

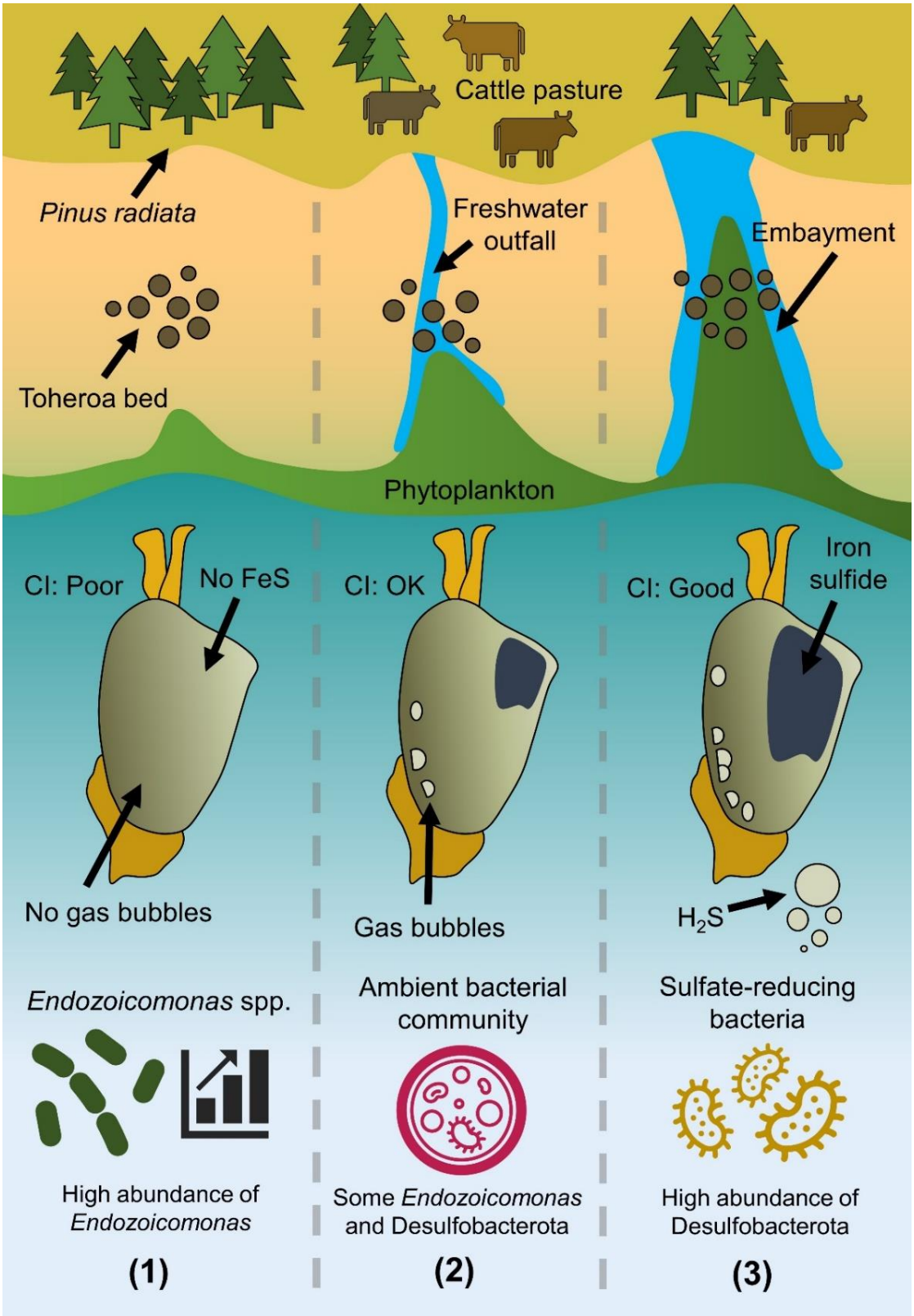

Fig. 8.3. Conceptual illustration of the habitat modification dynamics associated with freshwater outflows and toheroa. Scenario (1) shows a toheroa bed without a stream present and intensive forestry (*P. radiata*) on land. Scenario (2) shows some forestry and bovine pasture behind beach and a small stream, creating a small embayment. Scenario (3) shows intensive cattle pasture, large freshwater outflow, and a large embayment (i.e., Mahuta Gap, Fig. 8.2), channelling phytoplankton to the toheroa bed. Consequences for toheroa intrinsic and extrinsic health for each scenario are also shown. CI: condition index, FeS: Iron(II) sulfide, H_2S: hydrogen sulfide.

8.2 *Endozoicomonas* Endosymbionts: Sheep in Wolf Clothing?

"…even the most harmonious symbioses are tinged with antagonism."

- Ed Yong, I Contain Multitudes: The Microbes Within Us and a Grander View of Life

In Chapter 4, intracellular microcolonies (IMCs) were identified as bacteria within the genus *Endozoicomonas*. Howells et al. (2021) showed that IMCs implicated in mass mortality events (MMEs) of several shellfish in Aotearoa (New Zealand) were *Endozoicomonas* spp. and higher gene copy counts (qPCR) were reported in mortality cases compared to 'healthy' counterparts. Naturally, when no other apparent cause could be found, mortalities were linked to IMCs (Chapter 2). Therefore, when this research began, IMCs were hypothesised as a pathogen and important to shellfish health (Chapters 2-4).

IMCs get bad press! This is largely attributed to the devastating impacts of withering syndrome *Rickettsia*-like organism (WS-RLO) on abalone spp. (e.g., *Haliotis cracherodii*, west coast USA) (Crosson et al., 2014). For IMCs and *Endozoicomonas* spp., many studies report no host inflammatory response and mild 'infection' (Cano et al., 2020, and references therin). The findings of this thesis are in line with those of many previous accounts (Appendix A, Table A.1). In apparently healthy toheroa, no inflammation could be linked to IMCs and, for the most part, 'infection' was mild (Chapters 3 and 4). Furthermore, when mortalities of shellfish (i.e., various clam and scallop species) have been reported in association with IMCs (Cano et al., 2018; Howells et al., 2021; Zhu et al., 2012), links have been tentative. Breaking from the mould somewhat, Lohrmann et al. (2019) suggested IMCs were symbionts of the Chilean mussel *Mytilus chilensis* and were not pathogenic.

Following the lead of Lohrmann et al. (2019), for the purposes of an informed thought experiment, I am going to view IMCs/*Endozoicomonas* spp. as important endosymbionts in Aotearoa shellfish. The evidence that *Endozoicomonas* spp. are endosymbionts rather than emerging pathogens is tangible. No link was made between *Endozoicomonas* spp. (IMCs) and ill health in this thesis. Instead, associations were made to nutrition and freshwater exposure. IMCs were associated with condition in Chapter 3, which could indicate IMCs were behaving opportunistically, with intensity increasing when host condition is reduced. Alternatively, it could indicate increased activity when nutrient availability is poor, like for maxima clams *Tridacna maxima*

(Rossbach et al., 2019) and lucinid clams *Loripes lucinalis* (van der Geest et al., 2014). In Chapter 4, when qPCR assays were used to examine abundance patterns, a key finding was that the abundance of *Endozoicomonas* spp. dropped sharply in autumn/winter at stream-bearing sites (Chapter 4). Additionally, when the bacterial community of toheroa was examined, *Endozoicomonas* spp. abundance was 'swapped' for sulfate-reducing bacteria in the toheroa microbiome between stream-bearing sites and sites without streams (Chapter 5).

Interestingly, Tandon et al. (2020) provided evidence of the role *Endozoicomonas acroporae* plays in the coral sulfur cycle. The authors identified genes encoding for the metabolism of dimethylsulfoniopropionate (DMSP) into dimethylsulfide (DMS), a key process within the marine sulfur cycle (Tandon et al., 2020; Yoch, 2002). This could explain a relative 'swapping' of sulfate-reducers for *Endozoicomonas* species (see Chapter 5). For example, if a sulfur-cycling niche (e.g., oxidation) were being filled by *Endozoicomonas* spp., then they would be highly abundant in the absence of environmentally available nutrients, like suspended organic material (Fig. 8.3 & 8.4), and the reverse would be true for sulfate-reducers (Fig. 8.3). Furthermore, a high percentage of oxidative stress-responsive genes have been identified in multiple *Endozoicomonas* strain genomes (Tandon et al., 2020, see supplementary material therein). It is possible that *Endozoicomonas* strains in Aotearoa shellfish are increasingly abundant at times of increased thermal (oxidative) stress (Fig. 8.4), which could explain their elevated abundance in toheroa tissues in austral-summer months (Chapter 4).

Increased abundance of sulfate-reducing bacteria is an indication of organic matter enrichment (Hansen et al., 1996; van Erk et al., 2020), so this relative difference is probably attributed to differences in the amount of microalgae detritus present at different sites (Fig. 8.2 & 8.3). This paints the picture that *Endozoicomonas* spp. are potentially fulfilling an important role like that reported by Rossbach et al. (2019) in nutrient cycling, when nutrient availability is poor. This again suggests a heterotrophic and chemosymbiotic life history, where chemosynthetic endosymbionts may be crucial for toheroa nutrition and growth (van der Geest et al., 2014) under certain conditions (or times). Reinforcing this concept, Biessy et al. (2020) reported high relative abundance of *Endozoicomonadaceae* in the bacterial community of pipi (*P. australis*) gills from northwest coast beaches in Aotearoa compared to all other study sites. Pipi were collected in summer months (Biessy et al., 2020, see supplementary material therein) when nutrient availability was likely lowest (chlorophyll-*a* conc., Chapter 3). Remarkably, this is not the first time *Endozoicomonas* spp., the sulfur cycle and nutrition in toheroa have been mentioned. Cano et al. (2020) drew a connection between sulfur-oxidising endosymbionts, nutrition, and toheroa while reviewing *Endozoicomonas* spp. (and IMCs)

in shellfish globally. The authors linked a sulfide-oxidising endosymbiont found in the toheroa microbiome (gill & mantle) to one found in *Ridgeia piscesae* (a hydrothermal vent tubeworm), which provide their hosts with nutrients through chemosymbiosis (Feldman et al., 1997). Furthermore, one of the most abundant OTUs identified in Chapter 5 was taxonomically assigned to the phylum Spirochaetes. When the sequence was compared to sequences in the NCBI database, 88% identity was found to a symbiont of a gut-less worm (*Olavius crassitunicatus*), with links to both sulfide-oxidising and sulfate-reducing bacteria (Blazejak et al., 2005). Additionally, the *Endozoicomonas* spp. reported in Chapter 4 were found to be modestly related (*c*. 94-97%) to sulfide-oxidising endosymbionts taxonomically assigned to the genus *Endozoicomonas* in other marine molluscs (Kurahashi and Yokota, 2007; Zielinski et al., 2009).

Due to the severe impacts of WS-RLOs on abalone spp., IMCs in shellfish tend to be viewed as harmful. While, in reality, apart from WS-RLO, there is little evidence that IMCs are responsible for many of the shellfish mortalities with which they have been associated (Appendix A, Table A.1). This link is understandable, because if many strains are endosymbionts, fulfilling roles in nutrient cycling, they would naturally be prominent when host condition is low (Chapter 3, model output). For example, when food (microalgae) is deficient (van der Geest et al., 2014) or hosts are stressed (Li et al., 2019). In fact, Li et al. (2019) showed that *Endozoicomonas* spp. dominated the gut microbiome of thermally stressed *Mytilus galloprovincialis*, leading the authors to suggest that it fulfils a role in maintaining host health or homeostasis. Thus, it is difficult to discern whether they are the cause of mortality, opportunistic pathogens, symbionts, or a combination of these functions depending on host (symbiome) and environmental conditions (see epidemiological triad, Chapter 1). If this is the case, no inflammatory response being observed could simply be because IMCs are important symbionts, rather than immune-by-passing pathogens.

Following recent shellfish MMEs in Aotearoa, mortalities were linked to IMCs, but data was skewed toward MME-related specimens. Howells et al. (2021) rectified this issue by sampling apparently healthy populations. It is possible that links to IMCs would never have been made if surveillance had been ongoing prior to MMEs, as undoubtedly, a high ambient intensity of IMCs would have been observed in healthy specimens and their effect in Aotearoa shellfish would have been considered benign. For example, in Chapter 4, many of the toheroa specimens (considered to be healthy) were positive for *Endozoicomonas* spp. with 16S rRNA gene copies at a higher abundance than the median number reported by Howells et al. (2021) for mortality specimens (Chapter 4). However, this does not resolve whether *Endozoicomonas* spp. have the capacity to cause mortality or not. Considering the extremely high gene copy count in apparently

healthy specimens, the lack of an inflammatory response associated with 'infection' (Chapter 3 & 4), and the links made to nutrition (Chapter 3 & 5), I suggest that *Endozoicomonas* spp. (IMCs) should be treated as important endosymbionts (probably fulfilling a sulfide-oxidising role) in toheroa and other Aotearoa shellfish until their niche is properly resolved.

Genomics of some *Endozoicomonas* strains suggest a niche shift from symbiont to pathogen through the loss of metabolic capacity and the expansion of virulence genes (e.g., nucleomodulins, Qi et al., 2018). Similarly, Cano et al. (2018) reported a small draft genome (4.83 Mb) compared to other published strains (>5.6 Mb, Neave et al., 2014), suggesting that a loss of regulatory genes may have contributed to mass mortalities of king scallops *Pecten maximus* in Lyme Bay, UK. Moreover, Ding et al. (2016) showed that *E. montiporae* can produce *N*-deglycosylation, enzymes that might help penetrate coral mucus layers, by reducing mucus viscosity. If this trait is shared with Aotearoa strains, their ability to by-pass innate defences could explain their wide host range (Howells et al., 2021). However, this does not speak to their position as symbionts (sheep) or pathogens (wolves), as both might require means to evade host defences. Culturing *Endozoicomonas* strains to fulfil Koch's postulates and conducting whole-genome sequencing should be a priority (Katharios et al., 2015) to determine their niche in Aotearoa shellfish hosts.

8.3 Toheroa Health and a Changing Environment

Under current trends (1986-2005), the annual precipitation in Te Tai Tokerau, (Northland), where majority toheroa occur, is predicted to decrease by 2-5% (RCP2.6-8.5) in spring (MfE, 2018) between 2031 and 2050. The same models (CMIP5) predict some increase in other seasons (1-3%), but overall a large decrease annually in the next century. Additionally, increased drought (MfE, 2018) and marine heatwave (Oliver et al., 2019) frequency is predicted for Aotearoa, with severity dependent on the representative concentration pathway (RCP). As mentioned, freshwater outflow has a considerable effect on toheroa health and habitat suitability. It is reasonable to suggest that decreased precipitation and increased drought frequency would have profound negative implications for toheroa in northern Aotearoa (Berkenbusch, 2015; Cope, 2018; Ross et al., 2018a, Chapters 3, 4, 5 & 7; Williams et al., 2013b).

Species range shifts are being reported globally (Pinsky et al., 2020); specifically, many species have been reported to be moving poleward in response to oceanic warming (Crustacea: Pinsky et al., 2013; Algae: Wernberg et al., 2016). Pathogens are not exempt, and geographic range shifts are being observed (Burge et al., 2014; Burge and Hershberger, 2020), for example, the northward range extension of the oyster

parasite *Perkinsus marinus* along the Atlantic coast USA (Pecher et al., 2008). Pathogen range shifts in shellfish can have implications for human health too. Baker-Austin et al. (2018) noted an increase of *Vibrio vulnificus* infections and new geographic reports, linking infection occurrence to areas undergoing rapid water warming (Baker-Austin et al., 2013). At the same time, recent epidemics have been attributed to marine heatwaves. For example, the sunflower star (*Pycnopodia helianthoides*) and the subsequent collapse of populations (decline: 80-100%) on a continental scale *c*. 3000 km (Harvell et al., 2019). It is difficult to determine the impacts pathogen range expansion could have on toheroa as biosecurity risks are intertwined with environmental change (Didham et al., 2007; Occhipinti-Ambrogi, 2007). However, several parasites that are not yet present in Aotearoa (e.g., *Marteilia* spp.) pose a risk to toheroa and other shellfish if they are introduced and are able to become established.

8.4 Notes on Safety for Consumers of Toheroa

A relatively high abundance of cyanobacteria, *Synechococcus* CC9902, was found in the toheroa microbiome (Chapter 5). Biessy et al. (2020) pointed to *Synechococcus* CC9902 as a potential producer of the toxin tetrodotoxin (TTX) in pipi. Bioactive compounds extracted from *Synechococcus* spp. have produced neurotoxic effects in mice (Martins et al., 2005). If *Synechococcus* CC9902 is found to be a source of TTX in *Paphies* clams, then examining TTX levels in toheroa should be prioritised. The relative abundance of these cyanobacteria was higher in toheroa from stream bearing sites (Chapter 5), which may be due to increased nutrients or beach topography (Fig. 8.3). Regardless, the presence of *Synechococcus* CC9902 in toheroa, and its potential link to TTX, highlights the regulatory blind spot of customary fisheries (Chapter 2) and underscores repercussions of an absence of routine biosecurity and contaminant surveillance, despite their inclusion in definitions of seafood safety (see Bank et al., 2020).

A potential consequence of ocean acidification for Aotearoa is the increased abundance of picoplankton in coastal waters, which includes cyanobacteria and *Synechococcus* spp. (Hoffmann et al., 2013). Hoffmann et al. (2013) reported an increase in the abundance of *Synechococcus,* a non-calcifier, and a decrease of larger phytoplankton in the Tasman Sea under elevated CO_2 incubation trials (although this response was not replicated by Law et al. (2018); Law et al. (2014) in a study conducted further south near the Chatham Rise). In a high CO_2 future, elevated abundances of *Synechococcus* spp. could lead to consumer safety issues around consumption of filter feeding shellfish species.

8.5 Wild Population Management & Health

The case for increased surveillance of wild shellfish has been made in this thesis (Chapter 2, 3, 4, 5, & 7). Bayesian models like the one used in Chapter 3 showcase the unwavering value of traditional histology for health screening of aquatic animals. Categorical data (with ordered levels) can be difficult to work with and is often not used effectively, and even erroneously (Liddell and Kruschke, 2018). Histologically gathered data is typically of this nature, for example IMC intensity graded 'None' to 'Severe' herein. Ordinal logistic regression models that make use of Bayes theorem are complex and can be challenging to construct and interpret. They can, however, substantially increase the utility of histopathology data (Chapter 3), providing insights that would probably not be apparent without robust data exploration. Packages in R, such as 'brms' (Bürkner, 2017) and tutorials by the authors (Bürkner and Vuorre, 2019) make their implementation more accessible to novice users. Considering this, see Appendix H for a histology-based tutorial for a model similar to the one used in Chapter 3. The effectiveness of models like these for disease investigations and diagnostics depends on robust baseline data, strengthening the call for increased surveillance of 'healthy' populations.

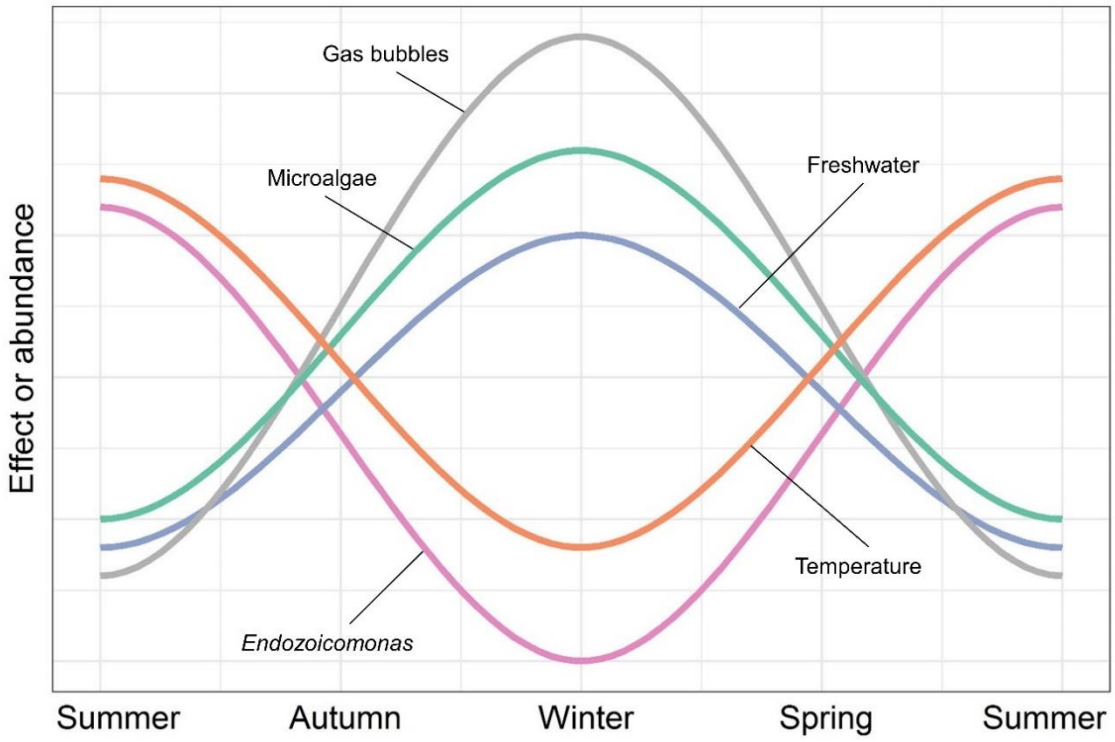

Fig. 8.4. Conceptual figure showing the effects of freshwater exposure (salinity & nutrient runoff), temperature and microalgae (nutrient availability) on the abundance of *Endozoicomonas* spp. in the bacterial community of Aotearoa shellfish across a gradient of time (seasonal cycle). Gas bubble abundance on toheroa shells over the same gradient is also shown.

The status quo of toheroa management (fishery closure) has not resulted in population recovery despite being in place for more than 45 years. In a future with increased temperature, increased CO_2 (lower pH), and increased drought frequency (in many of the regions where the remaining major toheroa populations occur), unassisted toheroa recovery would seem unlikely. The importance of maintaining freshwater outflows for toheroa health has been discussed above, as has the potential for the addition of macroalgae (kelp) to toheroa beds to increase productivity and health. Exploring how this practice modifies the bacterial community composition and function in the sediment, and within toheroa tissues, would contribute to the growing knowledge base of toheroa health and habitat requirements. Prior to the arrival of Europeans in Aotearoa, it appears that translocations of toheroa (Ross et al., 2018b), pāua and other kai moana (Taikato, in prep) were routinely conducted by Māori to create or bolster populations. If translocations are employed as restorative action for toheroa and other kai moana (Bennett et al., 2018), precautionary measures should be undertaken to avoid unintentionally transporting pathogens (or other non-endemic biota) to unaffected populations/regions (Costello et al., 2021; Ross et al., 2018c). This will be contingent on surveillance.

Surveys of the remaining populations of toheroa are intermittently carried out by government-funded research institutes. To-date disease has been absent from these assessments (Berkenbusch and Neubauer, 2018; Williams et al., 2013a), despite some mention in associated reviews (Williams et al., 2013b). Additionally, surveys thus far have not attempted to predict stocks and instead attempted to quantify populations. This is due to a lack of recruitment data from ongoing monitoring and a lack of knowledge of spat survival rates, among other facets of toheroa life histories. Lane et al. (2020) points out that the inclusion of disease data in stock assessments can have profound effects on their outcome. For example, the Bluff oyster fishery is the only fishery in Aotearoa that considers disease-related mortality in stock assessments. Furthermore, Hoenig et al. (2017) shows the importance of including disease-related mortality in stock assessments while also highlighting the effectiveness of mark-recapture methods for disease monitoring. Modelling toheroa populations is possible, but will depend on systematic monitoring, and an understanding of recruitment/survival and disease dynamics (i.e., disease-related mortality). Much of this information is still currently unavailable, though research is being conducted in these areas (Gadomski, 2017; P. Ross, personal communication) which could eventually be used to construct models. The inclusion of disease will depend on research of disease dynamics and survival in toheroa at every life-stage.

8.6 Conservation Potential of Toheroa Aquaculture

Aquaculture for conservation rather than for human consumption has been highlighted as an undervalued and underutilised tool (Froehlich et al., 2017). Twenty years ago, Sidwell (2001) concluded that toheroa were a *"suitable candidate"* for aquaculture. Momentum is building in this space once again, with research currently being conducted to explore the viability of toheroa aquaculture (P. Ross, pers. comm.). Whether for commercial enterprise or conservation, knowledge of toheroa health will shape its success. A consideration that has restricted the farming of many burrowing shellfish is the inclusion of sediment in tanks. For example, successful geoduck (*Panopea generosa*) farming requires an outplanting phase e.g., Puget Sound, WA (VanBlaricom et al., 2015). From a streamlining perspective, the inclusion of sediment in *ex situ* rearing is cumbersome and introduces recirculation and sanitation issues. The detection of Desulfobacterota in the toheroa microbiome highlights how the bacterial community in the surrounding environment has significant influence on the toheroa microbiome. This is not surprising, given that *"no microbiome is an island"* (Pennisi, 2019). The inclusion of natural substrates as microbial reservoirs has been shown to support more diverse bacterial communities in captive animals (Loudon et al., 2014). Though this also brings risks in the form of potential contaminants and pathogens, being introduced (Trevelline et al., 2019). Careful consideration should therefore be placed on the exclusion of sediment from toheroa aquaculture trials. In fact, side-by-side trials with and without sediment (microbial reservoirs) could be used to determine effects of its inclusion/exclusion for toheroa health and survival.

Whether they are important endosymbionts or opportunistic pathogens, *Endozoicomonas* spp. will play some part in the health of farmed toheroa. Determining their functional niche in toheroa will be imperative. Similarly, mucus is the first line of defence for many marine organisms (Allam and Pales Espinosa, 2016; Tiralongo et al., 2020). Mucus production in toheroa could be harnessed to increase farming success, and potentially efficiency. Analysing the antimicrobial potential of extracted compounds from mucus and characterising associated microbial taxa and functional traits could lead to the development of toheroa-specific probiotics (Fig. 8.1 & Chapter 5). For example, probiotics produced in a similar fashion have been found to increase survival rates of abalone i.e., *Haliotis tuberculata* (Offret et al., 2019). In this sense, their development for toheroa aquaculture could be used to enhance yield and therefore conservation goals.

8.7 Closing Remarks

Before this work began, there was little information of toheroa health available to either guide research or inform monitoring and management. Likewise, due to a complete lack of surveillance of healthy populations (Chapter 2), there was no benchmark for what a 'healthy' toheroa population is supposed to look like (Chapters 3-7). For example, extremely high numbers of protozoan gill ciliates were observed in apparently healthy specimens. If these had been observed in visibly 'sick' specimens they might have been attributed to ill health, when in fact, toheroa seem to be able to withstand extremely high intensities of these potentially commensal organisms (Chapters 3 & 5). The same goes for gas bubbles and *Endozoicomonas* spp. (Chapters 4 & 7). If surveillance of healthy, wild populations had been underway, these conditions might not have been associated with ill health in the first instance. The tools used in this thesis were not overly complex, and many were not very expensive to use relative to the important data they have yielded (Chapter 3). A benchmark of toheroa intrinsic health now exists. Similar baselines should be attained for many other Aotearoa shellfish to inform sustainable management of wild populations and ensure food security and safety.

8.8 References

Acevedo-Whitehouse, K., et al., 2009. Hookworm infection, anaemia and genetic variability of the New Zealand sea lion. Proceedings of the Royal Society B: Biological Sciences. 276**,** 3523-3529.

Akroyd, J. A. M., et al., 2002. Abundance, distribution, and size structure of toheroa (*Paphies ventricosa*) at Ripiro Beach, Dargaville, Northland, New Zealand. New Zealand Journal of Marine and Freshwater Research. 36**,** 547-553.

Allam, B., Pales Espinosa, E., 2016. Bivalve immunity and response to infections: Are we looking at the right place? Fish & Shellfish Immunology. 53**,** 4-12.

Altizer, S., et al., 2013. Climate Change and Infectious Diseases: From Evidence to a Predictive Framework. Science. 341**,** 514-519.

Baker-Austin, C., et al., 2018. *Vibrio* spp. infections. Nature Reviews Disease Primers. 4**,** 1-9.

Baker-Austin, C., et al., 2013. Emerging *Vibrio* risk at high latitudes in response to ocean warming. Nature Climate Change. 3**,** 73-77.

Bank, M. S., et al., 2020. Seafood Safety Revisited: Response to Comment on "Defining Seafood Safety in the Anthropocene". Environmental Science & Technology. 54**,** 12805-12806.

Banker, R. M. W., Coil, D., 2020. Inoculation With *Desulfovibrio* sp. Does Not Enhance Chalk Formation in the Pacific Oyster. Frontiers in Marine Science. 7**,** 407.

Bennett, N. J., et al., 2018. Coastal and Indigenous community access to marine resources and the ocean: A policy imperative for Canada. Marine Policy. 87**,** 186-193.

Berkenbusch, K., Distribution and abundance of toheroa in Southland, 2013–14. New Zealand Fisheries Assessment Report 2015/17, 2015, pp. 41.

Berkenbusch, K., Neubauer, P., Distribution and abundance of toheroa at Oreti Beach, Murihiku/Southland, 2016–17. Fisheries New Zealand, Wellington, 2018, pp. 1-18.

Biessy, L., et al., 2020. Seasonal and Spatial Variations in Bacterial Communities From Tetrodotoxin-Bearing and Non-tetrodotoxin-Bearing Clams. Frontiers in Microbiology. 11**,** 1860.

Blazejak, A., et al., 2005. Coexistence of bacterial sulfide oxidizers, sulfate reducers, and spirochetes in a gutless worm (Oligochaeta) from the Peru margin. Applied and Environmental Microbiology. 71**,** 1553-1561.

Burge, C. A., et al., Climate Change Influences on Marine Infectious Diseases: Implications for Management and Society. In: C. A. Carlson, S. J. Giovannoni, Eds., Annual Review of Marine Science, Vol 6, 2014, pp. 249-277.

Burge, C. A., Hershberger, P. K., Climate change can drive marine diseases. In: D. Behringer, et al., Eds., Marine Disease Ecology. Oxford University Press, Oxford, 2020.

Bürkner, P.-C., 2017. brms: An R Package for Bayesian Multilevel Models Using Stan. Journal of Statistical Software. 80**,** 1-28.

Bürkner, P.-C., Vuorre, M., 2019. Ordinal Regression Models in Psychology: A Tutorial. Advances in Methods and Practices in Psychological Science. 2**,** 77-101.

Cano, I., et al., 2020. Cosmopolitan Distribution of *Endozoicomonas*-Like Organisms and Other Intracellular Microcolonies of Bacteria Causing Infection in Marine Mollusks. Frontiers in Microbiology. 11**,** 2778.

Cano, I., et al., 2018. Molecular Characterization of an *Endozoicomonas*-Like Organism Causing Infection in the King Scallop (*Pecten maximus* L.). Applied and Environmental Microbiology. 84**,** e00952-17.

Cassie, R. M., 1955. Population Studies on the Toheroa, *Amphidesma ventricosum* Gray (Eulamellibranchiata). Australian Journal of Marine and Freshwater Research. 6**,** 348-391.

Cope, J., The modification of toheroa habitat by streams on Ripiro Beach. MSc. University of Waikato, Hamilton, New Zealand, 2018, pp. 126.

Costello, K. E., et al., 2021. The Importance of Marine Bivalves in Invasive Host–Parasite Introductions. Frontiers in Marine Science. 8**,** 147.

Crosson, L. M., et al., 2014. Abalone withering syndrome: distribution, impacts, current diagnostic methods and new findings. Diseases of Aquatic Organisms. 108**,** 261-270.

Cunningham, A. A., 1996. Disease Risks of Wildlife Translocations. Conservation Biology. 10**,** 349-353.

Didham, R. K., et al., 2007. Interactive effects of habitat modification and species invasion on native species decline. Trends in Ecology & Evolution. 22**,** 489-496.

Ding, J.-Y., et al., 2016. Genomic Insight into the Host–Endosymbiont Relationship of *Endozoicomonas montiporae* CL-33T with its Coral Host. Frontiers in Microbiology. 7**,** 251.

Feldman, R. A., et al., 1997. Molecular phylogenetics of bacterial endosymbionts and their vestimentiferan hosts. Molecular Marine Biology and Biotechnology. 6**,** 268-77.

Froehlich, H. E., et al., 2017. Conservation aquaculture: Shifting the narrative and paradigm of aquaculture's role in resource management. Biological Conservation. 215**,** 162-168.

Futter, J. M., An investigation into the Murihiku toheroa (*Paphies ventricosa*): mātauranga, monitoring and management. MSc. University of Otago, Dunedin, 2011, pp. 140.

Gadomski, K., Reproduction and larval ecology of the toheroa, *Paphies ventricosa*, from Oreti Beach, Southland, New Zealand. PhD. University of Otago, 2017, pp. 155.

Gadomski, K., Lamare, M., 2015. Spatial variation in reproduction in southern populations of the New Zealand bivalve *Paphies ventricosa* (Veneroida: Mesodesmatidae). Invertebrate Reproduction & Development. 59**,** 81-95.

Hansen, K., et al., 1996. Impact of the soft-shell clam *Mya arenaria* on sulfate reduction in an intertidal sediment. Aquatic Microbial Ecology. 10**,** 181-194.

Harvell, C. D., et al., 2019. Disease epidemic and a marine heat wave are associated with the continental-scale collapse of a pivotal predator (*Pycnopodia helianthoides*). Science Advances. 5**,** eaau7042.

Hoenig, J. M., et al., 2017. Impact of disease on the survival of three commercially fished species. Ecological Applications. 27**,** 2116-2127.

Hoffmann, L. J., et al., 2013. A trace-metal clean, pH-controlled incubator system for ocean acidification incubation studies. Limnology and Oceanography: Methods. 11**,** 53-61.

Howells, J., et al., 2021. Intracellular bacteria in New Zealand shellfish are identified as *Endozoicomonas* species. Diseases of Aquatic Organisms. 143**,** 27-37.

Katharios, P., et al., 2015. Environmental marine pathogen isolation using mesocosm culture of sharpsnout seabream: striking genomic and morphological features of novel *Endozoicomonas* sp. Scientific Reports. 5**,** 17609.

Kurahashi, M., Yokota, A., 2007. *Endozoicomonas elysicola* gen. nov., sp. nov., a γ-proteobacterium isolated from the sea slug *Elysia ornata*. Systematic and Applied Microbiology. 30**,** 202-206.

Lane, H. S., et al., 2020. Aquatic disease in New Zealand: synthesis and future directions. New Zealand Journal of Marine and Freshwater Research. 1-42.

Law, C. S., et al., 2018. Ocean acidification in New Zealand waters: trends and impacts. New Zealand Journal of Marine and Freshwater Research. 52**,** 155-195.

Law, C. S., et al., Predicting changes in plankton biodiversity and productivity of the EEZ in response to climate change induced ocean acidification. Final research report for the NZ Ministry of Primary Industries on project ZBD200811. 2014.

Li, Y.-F., et al., 2019. Characterization of Gut Microbiome in the Mussel *Mytilus galloprovincialis* in Response to Thermal Stress. Frontiers in Physiology. 10**,** 1086.

Liddell, T. M., Kruschke, J. K., 2018. Analyzing ordinal data with metric models: What could possibly go wrong? Journal of Experimental Social Psychology. 79**,** 328-348.

Lohrmann, K. B., et al., 2019. Histopathological assessment of the health status of *Mytilus chilensis* (Hupé 1854) in southern Chile. Aquaculture. 503**,** 40-50.

Loudon, A. H., et al., 2014. Microbial community dynamics and effect of environmental microbial reservoirs on red-backed salamanders (*Plethodon cinereus*). The ISME Journal. 8**,** 830-840.

Lynch, S. A., et al., 2021. Immunomodulatory and Antiviral Effects of Macroalgae Sulphated Polysaccharides: Case Studies Extend Knowledge on Their Importance in Enhancing Shellfish Health, and the Control of a Global Viral Pathogen Ostreid Herpesvirus-1 microVar. Polysaccharides. 2**,** 202-217.

Martins, R., et al., 2005. Toxicity of culturable cyanobacteria strains isolated from the Portuguese coast. Toxicon. 46**,** 454-464.

MfE, Climate Change Projections for New Zealand: Atmosphere Projections Based on Simulations from the IPCC Fifth Assessment. Ministry for the Environment, Wellington, 2018, pp. 131.

Neave, M. J., et al., 2014. Whole-genome sequences of three symbiotic *endozoicomonas* strains. Genome Announcements. 2**,** e00802-14.

O'Halloran, G. L., Report of the Marine Department for the year ended 31 March 1961. Fisheries Report. New Zealand Marine Department, Wellington, 1961, pp. 32-59.

Occhipinti-Ambrogi, A., 2007. Global change and marine communities: Alien species and climate change. Marine Pollution Bulletin. 55**,** 342-352.

Offret, C., et al., 2019. Protective Efficacy of a *Pseudoalteromonas* Strain in European Abalone, *Haliotis tuberculata*, Infected with *Vibrio harveyi* ORM4. Probiotics and Antimicrobial Proteins. 11**,** 239-247.

Oliver, E. C. J., et al., 2019. Projected Marine Heatwaves in the 21st Century and the Potential for Ecological Impact. Frontiers in Marine Science. 6**,** 734.

Pecher, W. T., et al., 2008. Assessment of the northern distribution range of selected *Perkinsus species* in eastern oysters (*Crassostrea virginica*) and hard clams (*Mercenaria mercenaria*) with the use of PCR-based detection assays. Journal of Parasitology. 94**,** 410-22.

Pennisi, E., 2019. No microbiome is an island, survey reveals. Science. 365**,** 851.

Pinsky, M. L., et al., 2020. Climate-Driven Shifts in Marine Species Ranges: Scaling from Organisms to Communities. Annual Review of Marine Science. 12**,** 153-179.

Pinsky, M. L., et al., 2013. Marine Taxa Track Local Climate Velocities. Science. 341**,** 1239-1242.

Qi, W., et al., 2018. Ca. *Endozoicomonas cretensis*: A Novel Fish Pathogen Characterized by Genome Plasticity. Genome Biology and Evolution. 10**,** 1363-1374.

Raymundo, L. J., et al., Disease ecology in marine conservation and management. In: D. Behringer, et al., Eds., Marine Disease Ecology. Oxford University Press, Oxford, 2020.

Redfearn, P., 1974. Biology and distribution of the toheroa, *Paphies* (Mesodesma) *ventricosa* (Gray). Fisheries Research Bulletin No. 11. New Zealand Ministry of Agriculture and Fisheries. 51.

Ross, P. M., et al., 2018a. The biology, ecology and history of toheroa (*Paphies ventricosa*): a review of scientific, local and customary knowledge. New Zealand Journal of Marine and Freshwater Research. 52**,** 196-231.

Ross, P. M., et al., 2018b. Historical translocations by Māori may explain the distribution and genetic structure of a threatened surf clam in Aotearoa (New Zealand). Scientific Reports. 8**,** 17241.

Ross, P. M., et al., 2018c. First detection of gas bubble disease and *Rickettsia*-like organisms in *Paphies ventricosa*, a New Zealand surf clam. Journal of Fish Diseases. 41**,** 187-190.

Rossbach, S., et al., 2019. Tissue-Specific Microbiomes of the Red Sea Giant Clam *Tridacna maxima* Highlight Differential Abundance of *Endozoicomonadaceae*. Frontiers in Microbiology. 10**,** 2661.

Rudtanatip, T., et al., 2018. Assessment of the effects of sulfated polysaccharides extracted from the red seaweed Irish moss *Chondrus crispus* on the immune-stimulant activity in mussels *Mytilus* spp. Fish & Shellfish Immunology. 75**,** 284-290.

Sas, H., et al., 2020. *Bonamia* infection in native oysters (*Ostrea edulis*) in relation to European restoration projects. Aquatic Conservation: Marine and Freshwater Ecosystems. 30**,** 2150-2162.

Sidwell, N., The toheroa, *Paphies ventricosa*, the feeding and diet of, with morphology notes. Vol. MSc. University of Otago, Dunedin, New Zealand, 2001, pp. 83.

Silva, B. F., et al., 2015. Analysis of some chemical elements in marine microalgae for biodiesel production and other uses. Algal Research. 9**,** 312-321.

Smith, S., The reproduction and recruitment of toheroa (*Paphies ventricosa*). MSc. University of Auckland, Auckland, 2003.

Tandon, K., et al., 2020. Comparative genomics: Dominant coral-bacterium *Endozoicomonas acroporae* metabolizes dimethylsulfoniopropionate (DMSP). The ISME Journal. 14**,** 1290-1303.

Tiralongo, F., et al., 2020. Skin Mucus of Marine Fish as a Source for the Development of Antimicrobial Agents. Frontiers in Marine Science. 7**,** 760.

Trevelline, B. K., et al., 2019. Conservation biology needs a microbial renaissance: a call for the consideration of host-associated microbiota in wildlife management practices. Proceedings of the Royal Society B: Biological Sciences. 286**,** 20182448.

Vallyon, L.-M. D., Birds vs. Clams: Assessing the impacts of South Island pied oystercatcher predation on Toheroa at Ripiro Beach, New Zealand. MSc. The University of Waikato, 2020, pp. 115.

van der Geest, M., et al., 2014. Nutritional and reproductive strategies in a chemosymbiotic bivalve living in a tropical intertidal seagrass bed. Marine Ecology Progress Series. 501**,** 113-126.

van Erk, M. R., et al., 2020. Kelp deposition changes mineralization pathways and microbial communities in a sandy beach. Limnology and Oceanography. 65**,** 3066-3084.

VanBlaricom, G. R., et al., 2015. Ecological effects of the harvest phase of geoduck clam (*Panopea generosa* Gould, 1850) aquaculture on infaunal communities in southern Puget Sound, Washington USA. Journal of Shellfish Research. 34**,** 171-187.

Varon-Lopez, M., et al., 2014. Sulphur-oxidizing and sulphate-reducing communities in Brazilian mangrove sediments. Environmental Microbiology. 16**,** 845-55.

Wagner, M., et al., 2005. Functional marker genes for identification of sulfate-reducing prokaryotes. Methods in Enzymology. 397**,** 469-89.

Wernberg, T., et al., 2016. Climate-driven regime shift of a temperate marine ecosystem. Science. 353**,** 169.

West, A. G., et al., 2019. The microbiome in threatened species conservation. Biological Conservation. 229**,** 85-98.

Williams, J., et al., Distribution and abundance of toheroa (*Paphies ventricosa*) and tuatua (*P. subtriangulata*) at Ninety Mile Beach in 2010 and Dargaville Beach in 2011. Ministry of Primary Industries, Wellington, 2013a, pp. 52.

Williams, J. R., et al., Review of factors affecting the abundance of toheroa (*Paphies ventricosa*). New Zealand Aquatic Environment and Biodiversity Report No. 114, 2013b, pp. 76.

Yoch, D. C., 2002. Dimethylsulfoniopropionate: Its Sources, Role in the Marine Food Web, and Biological Degradation to Dimethylsulfide. Applied and Environmental Microbiology. 68**,** 5804-5815.

Zhu, Z. W., et al., 2012. *Rickettsia*-like organism infection associated with mass mortalities of blood clam, *Tegillarca granosa*, in the Yueqing Bay in China. Acta Oceanologica Sinica. 31**,** 106-115.

Zielinski, F. U., et al., 2009. Widespread occurrence of an intranuclear bacterial parasite in vent and seep bathymodiolin mussels. Environmental Microbiology. 11**,** 1150-1167.

Appendix A: Introduction

Table. A.1. Summary of information related to intracellular microcolonies of bacteria (IMCs) in marine molluscs from 40 studies. A brief description of clinical symptoms and physiological implications of infections is given as well as additional illnesses/parasitic organisms detected.

ID	Common name	Species	Location	Tissue(s)	Gross signs of illness/ clinical symptoms	Physiological implications	Additional illness, parasites and (or) viruses	Mortality? Yes (Y) or no (N)	Wild (W) or farmed (F)	H & E staining	Measured IMCs or related bodies (µm)	Reason for investigation	Reference study
1	Mangrove oyster	*Crassostrea rhizophorae*	NE Atlantic Coast, Brazil	Gills	-	Disappearance of the apical cilia; cell lysis in the gills	-	N	W	-	**[a]1.8 to 2.3 long, 0.4 to 0.7 wide; [b]4.1 to 4.5 long	Routine survey	Azevedo et al. (2005)
2	Green mussel	*Perna viridis*	Western Johor Straits, Malaysia	Gonads	-	Inflammatory lesions	*Nematopsis;* coccidians; protozoan	N	W	-	-	General pathology survey	Azmi et al. (2018)
3	-	*Tellina tenuis*	Scotland	Intestines	-	Normally pyramidal cells becoming hypertrophied and spherical; evidence of cell lysis	-	N	W	Eosinophilic	**0.3 to 0.5 diameter	Bespoke study	Buchanan (1978)
4	Common cockle	*Cerastoderma edule*	Galicia, NW Spain	Gills; digestive gland	-	No inflammatory responses	Various	N	W	Basophilic	***[a]14 to 20 long; [b]13 to 22 long	General pathology survey	Carballal et al. (2001)
5	Yellow clam	*Mesodesma mactroides*	Rio Grande do Sul State, Brazil	Gills; intestines	Moribund	-	-	N	W	Basophilic	*1.6 long, 0.2 to 0.6 wide	Following observation of moribund clams	Carvalho et al. (2013)
6	Pacific oysters	*Crassostrea gigas*	Baja California Sur, Mexico	Gills; mantle; labial palps; intestines; male and female gametes	Mantle blisters; gill damage	Damage to mantle epithelium, gills, labial palps, digestive tract, digestive gland and possible gametes (male + female)	-	N	F	Eosinophilic	***1.4 to 2.9 diameter	First report	Carvalho-Saucedo et al. (2018)
7	Mangrove mussel	*Mytella guyanensis*	Camamu Bay, Bahia, Brazil	Digestive gland; gills	-	Hypertrophy & cell lysis	*Nematopsis;* turbellaria; *Bucephalus;* various others	N	W	-	***[a]7 to 21 diameter; [b]16 to 49 diameter	General pathology survey	Ceuta and Boehs (2012)

ID	Common name	Species	Location	Tissue(s)	Gross signs of illness/ clinical symptoms	Physiological implications	Additional illness, parasites and (or) viruses	Mortality? Yes (Y) or no (N)	Wild (W) or farmed (F)	H & E staining	Measured IMCs or related bodies (µm)	Reason for investigation	Reference study
8	Several spp.	-	San Jose´ Gulf, Argentina	Gills; digestive gland; gonads	Mud blisters on shell; calcareous blisters on the inner shell surface; pearls in the mantle; calcarean ridges below the umbo; pits and brown spots on inner shell	-	Various parasites	N	W	-	-	General pathology survey	Cremonte et al. (2005)
9	Several abalone spp.	*Haliotis* spp.	Seattle, USA	Posterior esophagus; digestive gland	Reduced condition index score; pedal atrophy	Digestive gland metaplasia	-	Y	F	-	-	Experiment	Crosson and Friedman (2018)
10	Mangrove oyster	*Crassostrea gasar*	Sergipe, Brazil	Gills; digestive gland	*maladie du pied* (shell disease)	-	Various parasites	N	F & W	Basophilic	***20 to 25 diameter	General pathology survey	da Silva et al. (2015)
11	Banded carpet shell	*Polititapes virgineus*	Galicia, NW Spain	Gills	-	-	-	N - maybe cause of declines	W	Basophilic	***[a]14.87 ± 4.34 long; [b]15.53 ± 4.04 long (mean ± SD)	Bespoke study	Darriba et al. (2012)
12	Various coloured abalone	*Haliotis diversicolor*	Fujian Province, China	Muscle; foot; digestive gland	Atrophied pedal musculature; mantle retraction; epipodial discolorations; diminished response to stimuli	Muscle fibres disorderly arranged; fibre arrangement loose; muscle fibres focal necrosis; myofibers appear hollow & reduced; morphology of mitochondria abnormal	-	N	F	-	-	Bespoke study	Di et al. (2016)
13	Pacific geoduck	*Panopea generosa*	Washington state, USA	Gills	Asymptomatic	-	Metazoan parasite; microsporidia-like species	N	W	Basophilic	*13.22 ± 0.85 (mean ± SD)	General survey to gather baseline data	Dorfmeier et al. (2015)
14	Red abalone	*Haliotis rufescens*	Cayucos, California	Digestive gland; posterior esophagus	-	-	-	N	F	[a]Basophilic, violet; [b]basophilic, navy blue	***[a]0.5 ± 0.15 x 0.12 ± 0.09; [b]2.28 ± 1.53 x 1.04 ± 0.43 (mean ± SD)	General pathology survey	Friedman and Crosson (2012)

ID	Common name	Species	Location	Tissue(s)	Gross signs of illness/ clinical symptoms	Physiological implications	Additional illness, parasites and (or) viruses	Mortality? Yes (Y) or no (N)	Wild (W) or farmed (F)	H & E staining	Measured IMCs or related bodies (µm)	Reason for investigation	Reference study
15	Black abalone	*Haliotis cracherodii*	California, USA	Posterior esophagus; transport ducts; digestive gland; intestines	-	-	-	N	W	Basophilic	**[a]0.3 x 1.5 (rod); [b]1.4 (spherical); [c]0.62 diameter, 1.27 long (coccobacillus)	Bespoke study	Friedman et al. (2000)
16	Soft shell clam	*Mya arenaria*	Delaware, USA	Gills	-	-	-	N	W	-	**1.09 ± 0.10 x 3.56 ± 0.44 (mean ± SD)	First report	Fries et al. (1991)
17	Boring clam	*Tridacna crocea*	Heron Island, Great Barrier Reef	Gills	Spherical, cream-colored cysts in gills	Cysts likely compromise gill function	-	N	W	Basophilic	**0.61 ± 0.01 diameter (mean ± SD), up to 1.6 long	First report	Goggin and Lester (1990)
18	Grooved carpet shell clam	*Ruditapes decussatus*	Galicia, NW Spain	Intestines; gills	-	-	Brown ring disease; various parasites	N	F	Basophilic	-	General pathology survey	Gomez-Leon et al. (2007)
19	Blue mussel	*Mytilus edulis*	Matunuck, Rhode Island, USA	Plicate membrane; gills	-	-	-	N	W	Basophilic	**3.4 to 4.6 long	Bespoke study	Gulka and Chang (1985a)
20	Atlantic deep-sea scallop	*Placopecten magellanicus*	NE Atlantic Coast, USA	Gills	-	Little indication of tissue degradation	-	N - indirectly	W	Basophilic	**1.9 to 2.9 long	Bespoke study	Gulka and Chang (1985b)
21	Several spp.	-	California, USA	Digestive gland	-	-	Chlamydiae-like organisms; mycoplasmas	N	W	Basophilic	**2.5 x 0.3	General pathology survey	Harshbarger et al. (1977)
22	New Zealand scallop	*Pecten novaezelandiae*	Aotearoa	Gills; mantle	-	Hypertrophy	Virus-like particles; other prokaryotes	N	W	Basophilic	***[a]2.0 x 0.5, [b]0.5 x 0.2 (diameter)	General pathology survey	Hine and Diggles (2002)
23	Pāua	*Haliotis iris*	Aotearoa	-	Sluggish could not right themselves; could not adhere well to the surface; pale lesions on foot	-	*Haplosporidium*	N	F	-	-	Following observation of clinical symptoms	Hine et al. (2002)
24	South African abalone	*Haliotis midae*	South Africa	Digestive gland	Asymptomatic	No morphological abnormalities	-	N	F	Slightly eosinophilic and basophilic	*8.5 (major axis), 6.7 (minor axis) (average)	Routine survey	Horwitz et al. (2016)
25	Japanese black abalone	*Haliotis discus discus*	Tottori, Japan	Intestines; posterior esophagus	Moribund; anorexia; excess mucus production	Little degeneration of digestive gland	-	N	F	Basophilic	*up to 40	First report	Kiryu et al. (2013)

ID	Common name	Species	Location	Tissue(s)	Gross signs of illness/ clinical symptoms	Physiological implications	Additional illness, parasites and (or) viruses	Mortality? Yes (Y) or no (N)	Wild (W) or farmed (F)	H & E staining	Measured IMCs or related bodies (µm)	Reason for investigation	Reference study
26	Saint-Jacques scallop	*Pecten maximus* L.	Brittany, France	Gills	-	-	-	Y	W	Basophilic	***[a]Up to 1.5 long, 1 diameter; [b]1 to 2.5 long, 0.5 diameter	Histopathology following mass mortality	Le Gall et al. (1988)
27	Purple mussel	*Perumytilus purpuratus*	Antofagasta, Chile	Digestive gland	-	Only moderate infection	Ciliates; virus-like particles; digeneans	N	W	-	-	General pathology survey	Montenegro et al. (2012)
28	Red abalone	*Haliotis rufescens*	California, USA	Posterior esophagus; digestive gland	-	Digestive gland degeneration	*Pseudoklossia haliotis* (coccidian)	N	F	-	-	Experiment	Moore et al. (2000)
29	Bear paw clam	*Hippopus hippopus*	Philippines; Federated States of Micronesia	Gills	Syphonal mantle brown and sagged inward away from shell valves	Near total loss of normal gill structure, replaced with inflammatory cells	-	Y	F	Basophilic	***[a]0.5 diameter, 1.3 long; [b]0.6 diameter, 0.9 to 2.4 long (average)	First report	Norton et al. (1993)
30	Toheroa	*Paphies ventricosa*	Ripiro Beach, Aotearoa	Gills	-	Damaged gill architecture	Gas bubble disease	N	W	Basophilic	-	Following observation of blisters under periostracum	Ross et al. (2018)
31	Pod razor clam	*Ensis siliqua*	Galicia, NW Spain	Digestive gland; gills; labial palps; pericardial	-	-	Various parasites	N	W	Basophilic	**0.20 to 0.80 long	General pathology survey	Ruiz et al. (2013)
32	Suminoe oyster	*Crassostrea ariakensis* Gould	Guangdong Province, China	Gills; mantle; digestive gland	Moribund	Hypertrophy and disintegration of host cells; severe damage to various tissues	-	N	F	Acidophilic	**0.58 to 1.20	General pathology survey	Sun and Wu (2004)
33	Puelche oyster; False oyster	*Ostrea puelchana; Pododesmus rudis*	San Jose´ Gulf, Argentina	Digestive gland	-	Hypertrophy; cell lysis	*Urastoma*-like turbellarian; *Nematopsis*-like oocysts; *Perkinsus*-like protozoan; various others	N	W	Basophilic	***15.74 ± 1.6 (mean ± SD) (*P. rudis*)	General pathology survey	Vázquez et al. (2018)
34	-	*Venerupis rhomboides*	Galicia, NW Spain	Gills; digestive gland	-	Extreme hypertrophy; lysis of host epithelial cells	Various parasites	Y	W	Basophilic	**1 to 3 long, 0.5 to 0.8 diameter	Histopathology following mass mortality	Villalba et al. (1999)

ID	Common name	Species	Location	Tissue(s)	Gross signs of illness/ clinical symptoms	Physiological implications	Additional illness, parasites and (or) viruses	Mortality? Yes (Y) or no (N)	Wild (W) or farmed (F)	H & E staining	Measured IMCs or related bodies (µm)	Reason for investigation	Reference study
35	Mussel spp.	*Bathymodiolus* spp.	Various sites, USA	Gills; mantle	-	-	Various parasites	N	W	Basophilic	***[a]**20; **[b]**37 (average diameter)	General pathology survey	Ward et al. (2004)
36	-	*Haliotis diversicolor supertexta*	Thailand; Taiwan; China	Posterior esophagus; intestines	Asymptomatic	-	-	N	F	Basophilic	****0.4 ± 0.14 to 1.7 ± 0.32 (mean ± SD)	Routine survey	Wetchateng et al. (2010)
37	Pearl oyster	*Pinctada maxima*	Xinying Bay, China	Mantle; gills; intestines; digestive gland	Moribund	Hypertrophy, cell lysis and disintegration; destruction in many tissues	-	N	F	Eosinophilic	****0.967 x 0.551 (average)	First report	Wu and Pan (1999)
38	Suminoe oyster	*Crassostrea ariakensis*	Kaozhou Bay, China	Gills; intestines; digestive gland; mantle	Moribund	Lesions in epithelial cells of gills, digestive tube and gland and mantle; parasitized cells and hypertrophy; extensive cell lysis	-	N	F	Eosinophilic	*****[a]**1.23 x 0.772; **[b]**1.45 x 0.732 (average)	General pathology survey	Wu and Pan (2000)
39	Blood clam	*Tegillarca granosa*	Yueqing Bay, China	Mantle; gills; digestive gland	Moribund; anorexic; lethargic; gill atrophy	Infected organs presented serious and extensive necrosis	-	Y	F	Eosinophilic	****0.28 to 0.71	Histopathology following mass mortality	Zhu et al. (2012)
40	European flat oyster	*Ostrea edulis* L.	Apulian region, Italy	Dgiestive gland	Asymptomatic	Hypertrophy, necrosis, cell lysis	-	N	W	Basophilic	**c*. 20-µm long and 0.5-µm wide; *c*. 30/40-µm diameter, ***2.5-µm long and 1.5-µm long, *****c*. 8-µm long and 6-µm wide	Routine survey	Tinelli et al. (2020)

[a,b,c] Measurements of different IMCs and IMC-related bodies in different organs/tissues, host species and in hosts from different sites/locations within the same study

***** Measurement of inclusions

****** Measurement of individual intracellular bacteria

******* Measurement of 'microcolonies'

References

Azevedo, C., et al., 2005. Ultrastructural analysis of *Rickettsia*-like organisms in the oyster *Crassostrea rizophorae* from the northeastern Atlantic coast of Brazil. Brazilian Journal of Morphological Sciences. 22**,** 5-8.

Azmi, N. F., et al., Parasites and Pathological Condition in Green Mussel *Perna viridis* Linnaeus, 1758 From Western Johor Straits, Malaysia. In: K. Ibrahim, et al., Eds., 2017 Ukm Fst Postgraduate Colloquium, 2018.

Buchanan, J. S., 1978. Cytological studies on a new species of *rickettsia* found in association with a phage in the digestive gland of the marine bivalve mollusc, *Tellina tenuis* (da Costa). Journal of Fish Diseases. 1**,** 27-43.

Carballal, M. J., et al., 2001. Parasites and pathologic conditions of the cockle *Cerastoderma edule* populations of the coast of Galicia (NW Spain). Journal of Invertebrate Pathology. 78**,** 87-97.

Carvalho-Saucedo, L., et al., 2018. First Report of an Eosinophilic *Rickettsia*-like Organism in Diseased Oysters *Crassostrea gigas*. Journal of Shellfish Research. 37**,** 507-513.

Carvalho, Y. B. M., et al., 2013. *Rickettsia*-Associated Mortality of the Yellow Clam *Mesodesma mactroides* (Bivalvia: Mesodesmatidae) in Southern Brazil. Malacologia. 56**,** 301-307.

Ceuta, L. O., Boehs, G., 2012. Parasites of the mangrove mussel *Mytella guyanensis* (Bivalvia: Mytilidae) in Camamu Bay, Bahia, Brazil. Brazilian Journal of Biology. 72**,** 421-427.

Cremonte, F., et al., 2005. A histopathological survey of some commercially exploited bivalve molluscs in northern Patagonia, Argentina. Aquaculture. 249**,** 23-33.

Crosson, L. M., Friedman, C. S., 2018. Withering syndrome susceptibility of northeastern Pacific abalones: A complex relationship with phylogeny and thermal experience. Journal of Invertebrate Pathology. 151**,** 91-101.

da Silva, P. M., et al., 2015. Survey of Pathologies in *Crassostrea gasar* (Adanson, 1757) Oysters from Cultured and Wild Populations in the São Francisco Estuary, Sergipe, Northeast Brazil. Journal of Shellfish Research. 34**,** 289-296.

Darriba, S., et al., 2012. Phage particles infecting branchial Rickettsiales-like organisms in banded carpet shell *Polititapes virgineus* (Bivalvia) from Galicia (NW Spain). Diseases of Aquatic Organisms. 100**,** 269-272.

Di, G. L., et al., 2016. Pathology and physiology of *Haliotis diversicolor* with withering syndrome. Aquaculture. 453**,** 1-9.

Dorfmeier, E. M., et al., 2015. Temporal and Spatial Variability of Native Geoduck (*Panopea generosa*) Endosymbionts in the Pacific Northwest. Journal of Shellfish Research. 34**,** 81-90.

Friedman, C. S., et al., 2000. '*Candidatus* Xenohaliotis californiensis', a newly described pathogen of abalone, *Haliotis* spp., along the west coast of North America. International Journal of Systematic and Evolutionary Microbiology. 50**,** 847-855.

Friedman, C. S., Crosson, L. M., 2012. Putative Phage Hyperparasite in the Rickettsial Pathogen of Abalone, "*Candidatus* Xenohaliotis californiensis". Microbial Ecology. 64**,** 1064-1072.

Fries, C. R., et al., 1991. Rickettsiae in the cytoplasm of gill epithelial cells of the soft-shelled clam, *Mya arenaria*. Journal of Invertebrate Pathology. 57**,** 443-445.

Goggin, C. L., Lester, R. J. G., 1990. Rickettsiales-like Infection in the Gills of *Tridacna crocea* from the Great Barrier Reef Journal of Invertebrate Pathology. 56**,** 135-138.

Gomez-Leon, J., et al., 2007. Temporal distribution of potentially pathogenic agents detected on carpet-shell clam, *Ruditapes decussatus* cultured in Galicia (NW Spain). Aquatic Living Resources. 20**,** 185-189.

Gulka, G., Chang, P. W., 1985a. Host response to rickettsial infection in blue mussel, *Mytilus edulis* L. Journal of Fish Diseases. 8**,** 319-323.

Gulka, G., Chang, P. W., 1985b. Pathogenicity and infectivity of a *Rickettsia*-like organism in the sea scallop, *Placopecten magellanicus*. Journal of Fish Diseases. 8**,** 309-318.

Harshbarger, J. C., et al., 1977. Chlamydiae (with Phages), Mycoplasmas, and Rickettsiae in Chesapeake Bay Bivalves. Science. 196**,** 666-668.

Hine, P. M., Diggles, B. K., 2002. Prokaryote infections in the New Zealand scallops *Pecten novaezelandiae* and *Chlamys delicatula*. Diseases of Aquatic Organisms. 50**,** 137-144.

Hine, P. M., et al., 2002. Ultrastructure of a haplosporidian containing Rickettsiae, associated with mortalities among cultured paua *Haliotis iris*. Diseases of Aquatic Organisms. 49**,** 207-219.

Horwitz, R., et al., 2016. Characterization of an intracellular bacterium infecting the digestive gland of the South African abalone *Haliotis midae*. Aquaculture. 451**,** 24-32.

Kiryu, I., et al., 2013. First Detection of *Candidatus* Xenohaliotis Californiensis, the Causative Agent of Withering Syndrome, in Japanese Black Abalone *Haliotis discus discus* in Japan. Fish Pathology. 48**,** 35-41.

Le Gall, G., et al., 1988. Branchial Rickettsiales-like infection associated with a mass mortality of sea scallop *Pecten maximus*. Diseases of Aquatic Organisms. 4**,** 229-232.

Montenegro, D., et al., 2012. Report of pathogens and parasites in *Perumytilus purpuratus* from San Jorge Bay, Antofagasta, Chile. Revista De Biologia Marina Y Oceanografia. 47**,** 345-350.

Moore, J. D., et al., 2000. Withering syndrome in farmed red abalone *Haliotis rufescens*: Thermal induction and association with a gastrointestinal *Rickettsiales*-like prokaryote. Journal of Aquatic Animal Health. 12**,** 26-34.

Norton, J. H., et al., 1993. Mortalities in the Giant Clam *Hippopus hippopus* Associated with Rickettsiales-like Organisms. Journal of Invertebrate Pathology. 62**,** 207-209.

Ross, P. M., et al., 2018. First detection of gas bubble disease and *Rickettsia*-like organisms in *Paphies ventricosa*, a New Zealand surf clam. Journal of Fish Diseases. 41**,** 187-190.

Ruiz, M., et al., 2013. Histological survey of symbionts and other conditions of pod razor clam *Ensis siliqua* (Linnaeus, 1758) in Galicia (NW Spain). Journal of Invertebrate Pathology. 112**,** 74-82.

Sun, J. F., Wu, X. Z., 2004. Histology, ultrastructure, and morphogenesis of a *rickettsia*-like organism causing disease in the oyster, *Crassostrea ariakensis* gould. Journal of Invertebrate Pathology. 86**,** 77-86.

Tinelli, A., et al., 2020. Histological features of *Rickettsia*-like organisms in the European flat oyster (*Ostrea edulis* L.). Environmental Science and Pollution Research. 27**,** 882-889.

Vázquez, N., et al., 2018. Parasites in two coexisting bivalves of the Patagonia coast, southwestern Atlantic Ocean: The Puelche oyster (*Ostrea puelchana*) and false oyster (*Pododesmus rudis*). Journal of Invertebrate Pathology. 158**,** 6-15.

Villalba, A., et al., 1999. Branchial *rickettsia*-like infection associated with clam *Venerupis rhomboides* mortality. Diseases of Aquatic Organisms. 36**,** 53-60.

Ward, M. E., et al., 2004. Parasitism in species of *Bathymodiolus* (Bivalvia : Mytilidae) mussels from deep-sea seep and hydrothermal vents. Diseases of Aquatic Organisms. 62**,** 1-16.

Wetchateng, T., et al., 2010. Withering syndrome in the abalone *Haliotis diversicolor supertexta*. Diseases of Aquatic Organisms. 90**,** 69-76.

Wu, X. Z., Pan, J. P., 1999. Studies on *rickettsia*-like organism disease of the tropical marine pearl oyster I: The fine structure and morphogenesis of *Pinctada maxima* pathogen *Rickettsia*-like organism. Journal of Invertebrate Pathology. 73**,** 162-172.

Wu, X. Z., Pan, J. P., 2000. An intracellular prokaryotic microorganism associated with lesions in the oyster, *Crassostrea ariakensis* Gould. Journal of Fish Diseases. 23**,** 409-414.

Zhu, Z. W., et al., 2012. *Rickettsia*-like organism infection associated with mass mortalities of blood clam, *Tegillarca granosa*, in the Yueqing Bay in China. Acta Oceanologica Sinica. 31**,** 106-115.

Appendix B: Wild Shellfish Health in Aotearoa (New Zealand): A Case for Increased Surveillance

Table B.1. Potential function of the bacterial genus *Endozoicomonas* in marine taxa. Information used to construct alluvial plot in Chapter 2.

Host	Function	Reference
Corals	Host health	Gignoux-Wolfsohn et al. (2017); Glasl et al. (2016); Meyer et al. (2014); Ransome et al. (2014); Roder et al. (2015); Vezzulli et al. (2013); Webster et al. (2016); Ziegler et al. (2016)
	Microbiome structure	Jessen et al. (2013)
	Antimicrobial activity	Morrow et al. (2015)
	Disease	Ziegler et al. (2016)
	Bleaching protection	Pantos et al. (2015)
	Biogeochemical cycle	Bourne et al. (2013); Correa et al. (2013); Morrow et al. (2015); Raina et al. (2009); Tandon et al. (2020)
Molluscs	Disease	Cano et al. (2018); Hooper et al. (2019); Howells et al. (2021)
	Host health	Dubé et al. (2019); Nguyen et al. (2020)
	Biogeochemical cycle	Beinart et al. (2014); Rossbach et al. (2019)
Fish	Disease	Katharios et al. (2015); Mendoza et al. (2013); Qi et al. (2018)
Porifera	Host health	Gardères et al. (2015)
	Defence	Haber and Ilan (2014)
	Biogeochemical cycle	Nishijima et al. (2013)
	Antibiotic production	Rua et al. (2014)
Ascidians	Biogeochemical cycle	Dishaw et al. (2014)
	Commensals	Schreiber et al. (2016)
Annelida	Biogeochemical cycle	Forget and Kim Juniper (2013)

References

Beinart, R. A., et al., 2014. Intracellular Oceanospirillales inhabit the gills of the hydrothermal vent snail *Alviniconcha* with chemosynthetic, *γ*-Proteobacterial symbionts. Environmental Microbiology Reports. 6**,** 656-64.

Bourne, D. G., et al., 2013. Coral reef invertebrate microbiomes correlate with the presence of photosymbionts. The ISME Journal. 7**,** 1452-1458.

Cano, I., et al., 2018. Molecular Characterization of an *Endozoicomonas*-Like Organism Causing Infection in the King Scallop (*Pecten maximus* L.). Applied and Environmental Microbiology. 84**,** e00952-17.

Correa, H., et al., 2013. Bacterial Communities of the Gorgonian Octocoral *Pseudopterogorgia elisabethae*. Microbial Ecology. 66**,** 972-985.

Dishaw, L. J., et al., 2014. The Gut of Geographically Disparate *Ciona intestinalis* Harbors a Core Microbiota. PLOS ONE. 9**,** e93386.

Dubé, C. E., et al., 2019. Microbiome of the Black-Lipped Pearl Oyster *Pinctada margaritifera*, a Multi-Tissue Description With Functional Profiling. Frontiers in Microbiology. 10, 1548.

Forget, N. L., Kim Juniper, S., 2013. Free-living bacterial communities associated with tubeworm (*Ridgeia piscesae*) aggregations in contrasting diffuse flow hydrothermal vent habitats at the Main Endeavour Field, Juan de Fuca Ridge. Microbiologyopen. 2**,** 259-275.

Gardères, J., et al., 2015. Lipopolysaccharides from Commensal and Opportunistic Bacteria: Characterization and Response of the Immune System of the Host Sponge *Suberites domuncula*. Marine drugs. 13**,** 4985-5006.

Gignoux-Wolfsohn, S. A., et al., 2017. Complex interactions between potentially pathogenic, opportunistic, and resident bacteria emerge during infection on a reef-building coral. FEMS Microbiology Ecology. 93, fix080.

Glasl, B., et al., 2016. The microbiome of coral surface mucus has a key role in mediating holobiont health and survival upon disturbance. The ISME Journal. 10**,** 2280-2292.

Haber, M., Ilan, M., 2014. Diversity and antibacterial activity of bacteria cultured from Mediterranean *Axinella* spp. sponges. Journal of Applied Microbiology. 116**,** 519-532.

Hooper, P. M., et al., 2019. Shedding and survival of an intracellular pathogenic *Endozoicomonas*-like organism infecting king scallop *Pecten maximus*. Diseases of Aquatic Organisms. 134**,** 167-173.

Howells, J., et al., 2021. Intracellular bacteria in New Zealand shellfish are identified as *Endozoicomonas* species. Diseases of Aquatic Organisms. 143**,** 27-37.

Jessen, C., et al., 2013. In-situ Effects of Eutrophication and Overfishing on Physiology and Bacterial Diversity of the Red Sea Coral *Acropora hemprichii*. PLOS ONE. 8**,** e62091.

Katharios, P., et al., 2015. Environmental marine pathogen isolation using mesocosm culture of sharpsnout seabream: striking genomic and morphological features of novel *Endozoicomonas* sp. Scientific Reports. 5**,** 17609.

Mendoza, M., et al., 2013. A novel agent (*Endozoicomonas elysicola*) responsible for epitheliocystis in cobia *Rachycentrum canadum* larvae. Diseases of Aquatic Organisms. 106**,** 31-37.

Meyer, J. L., et al., 2014. Community Shifts in the Surface Microbiomes of the Coral *Porites astreoides* with Unusual Lesions. PLOS ONE. 9**,** e100316.

Morrow, K. M., et al., 2015. Natural volcanic CO_2 seeps reveal future trajectories for host–microbial associations in corals and sponges. The ISME Journal. 9**,** 894-908.

Nguyen, V. K., et al., 2020. The Sydney rock oyster microbiota is influenced by location, season and genetics. Aquaculture. 527**,** 735472.

Nishijima, M., et al., 2013. *Endozoicomonas numazuensis* sp. nov., a gammaproteobacterium isolated from marine sponges, and emended description of the genus *Endozoicomonas* Kurahashi and Yokota 2007. International Journal of Systematic and Evolutionary Microbiology. 63**,** 709-714.

Pantos, O., et al., 2015. Habitat-specific environmental conditions primarily control the microbiomes of the coral *Seriatopora hystrix*. The ISME Journal. 9**,** 1916-1927.

Qi, W., et al., 2018. Ca. *Endozoicomonas cretensis*: A Novel Fish Pathogen Characterized by Genome Plasticity. Genome Biology and Evolution. 10**,** 1363-1374.

Raina, J.-B., et al., 2009. Coral-Associated Bacteria and Their Role in the Biogeochemical Cycling of Sulfur. Applied and Environmental Microbiology. 75**,** 3492-3501.

Ransome, E., et al., 2014. Disturbance to conserved bacterial communities in the cold-water gorgonian coral *Eunicella verrucosa*. FEMS Microbiology Ecology. 90**,** 404-416.

Roder, C., et al., 2015. Microbiome structure of the fungid coral *Ctenactis echinata* aligns with environmental differences. Molecular ecology. 24**,** 3501-3511.

Rossbach, S., et al., 2019. Tissue-Specific Microbiomes of the Red Sea Giant Clam *Tridacna maxima* Highlight Differential Abundance of *Endozoicomonadaceae*. Frontiers in Microbiology. 10**,** 2661.

Rua, C. P., et al., 2014. Diversity and antimicrobial potential of culturable heterotrophic bacteria associated with the endemic marine sponge *Arenosclera brasiliensis*. PeerJ. 2**,** e419.

Schreiber, L., et al., 2016. *Endozoicomonas* Are Specific, Facultative Symbionts of Sea Squirts. Frontiers in Microbiology. 7, 1042.

Tandon, K., et al., 2020. Comparative genomics: Dominant coral-bacterium *Endozoicomonas acroporae* metabolizes dimethylsulfoniopropionate (DMSP). The ISME Journal. 14**,** 1290-1303.

Vezzulli, L., et al., 2013. 16SrDNA Pyrosequencing of the Mediterranean Gorgonian *Paramuricea clavata* Reveals a Link among Alterations in Bacterial Holobiont Members, Anthropogenic Influence and Disease Outbreaks. PLOS ONE. 8**,** e67745.

Webster, N. S., et al., 2016. Host-associated coral reef microbes respond to the cumulative pressures of ocean warming and ocean acidification. Scientific Reports. 6**,** 19324.

Ziegler, M., et al., 2016. Coral microbial community dynamics in response to anthropogenic impacts near a major city in the central Red Sea. Marine Pollution Bulletin. 105**,** 629-40.

Appendix C: Histopathology Survey of a Threatened Endemic Surf Clam, Toheroa (*Paphies ventricosa*), from Aotearoa (New Zealand)

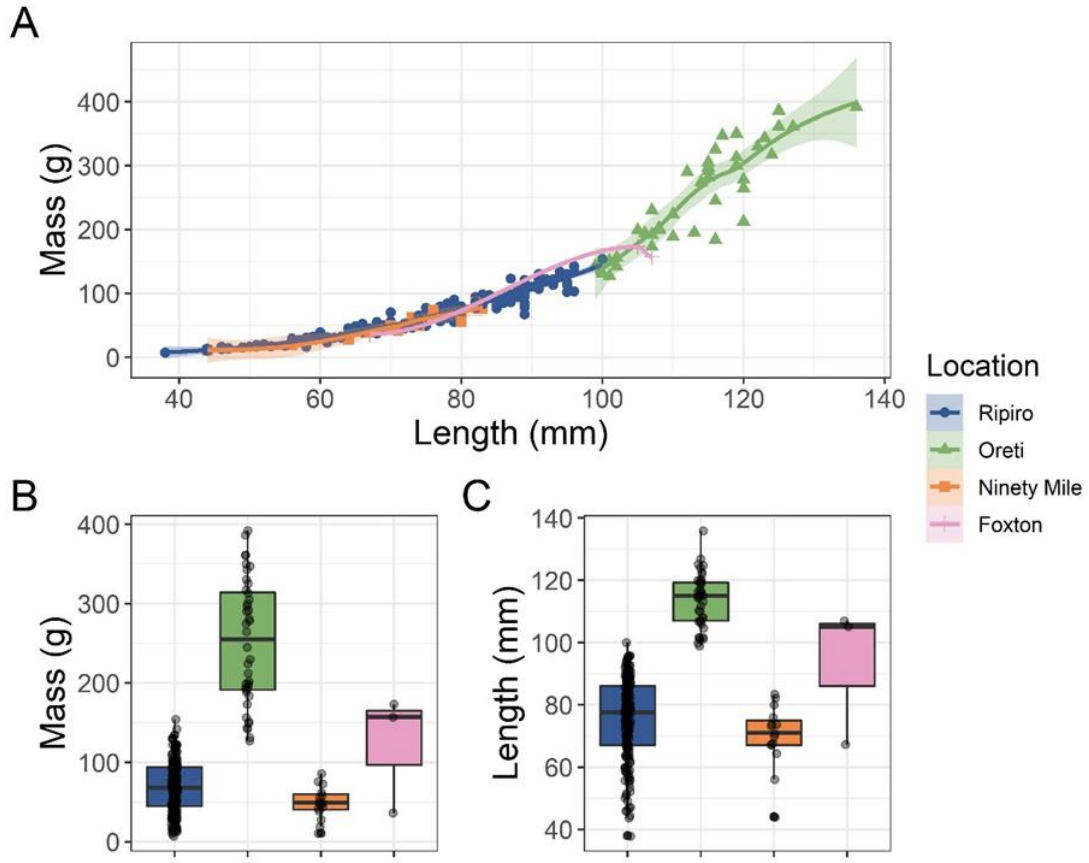

Fig. C.1. Size and mass of specimens gathered from four toheroa populations around Aotearoa (New Zealand), Ripiro Beach (*n* = 180), Oreti Beach (*n* = 40), Ninety Mile Beach (Te-Oneroa-a-Tōhē) (*n* = 15), and Foxton Beach (*n* = 3). A: loess smoothing showing mass (g) versus length (mm) for each specimen at each site. Line: loess, shaded area: 95% confidence interval. B & C: Box plots showing mass and length respectively for each site (all seasonal samples pooled). Lateral line: median, box: interquartile range, line: min/max.

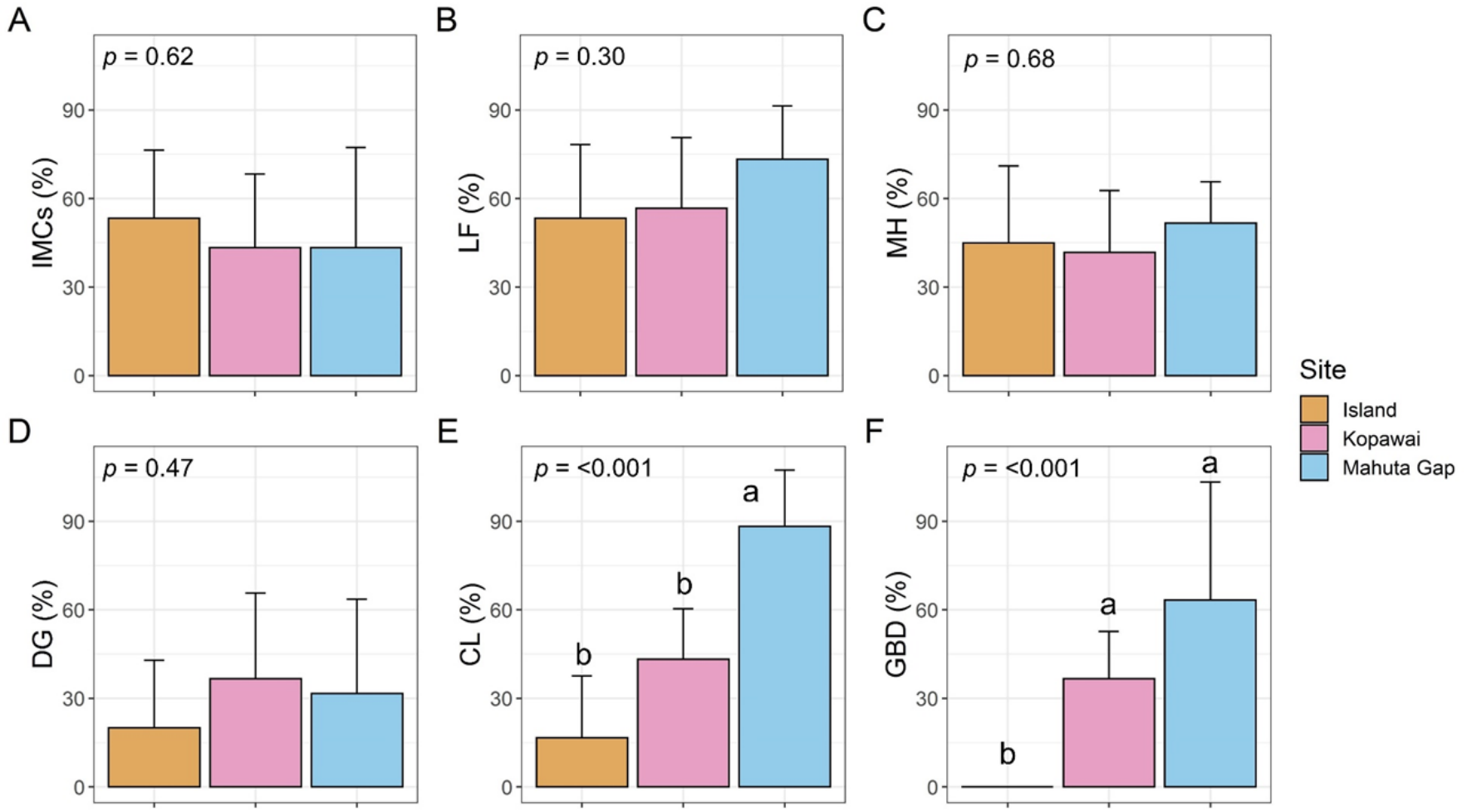

Fig. C.2. Barplots show the mean prevalence (%) and 95% confidence of several histological and pathomorphological observations between three sites: Island, Mahuta Gap, and Kopawai on Ripiro Beach. Data are pooled based on observations made between March 2019 and January 2020, *n* = 60 for each site. A: intracellular microcolonies (IMCs), B: lipofuscin pigmented cells (LF), C: mucous hyperplasia (MH), D: digestive gland atrophy (DG), E: gill ciliates (CL), F: gas bubble disease (GBD). Kruskal-Wallis test *p*-values are shown. Bars that do not share letters are statistically different (Dunn test).

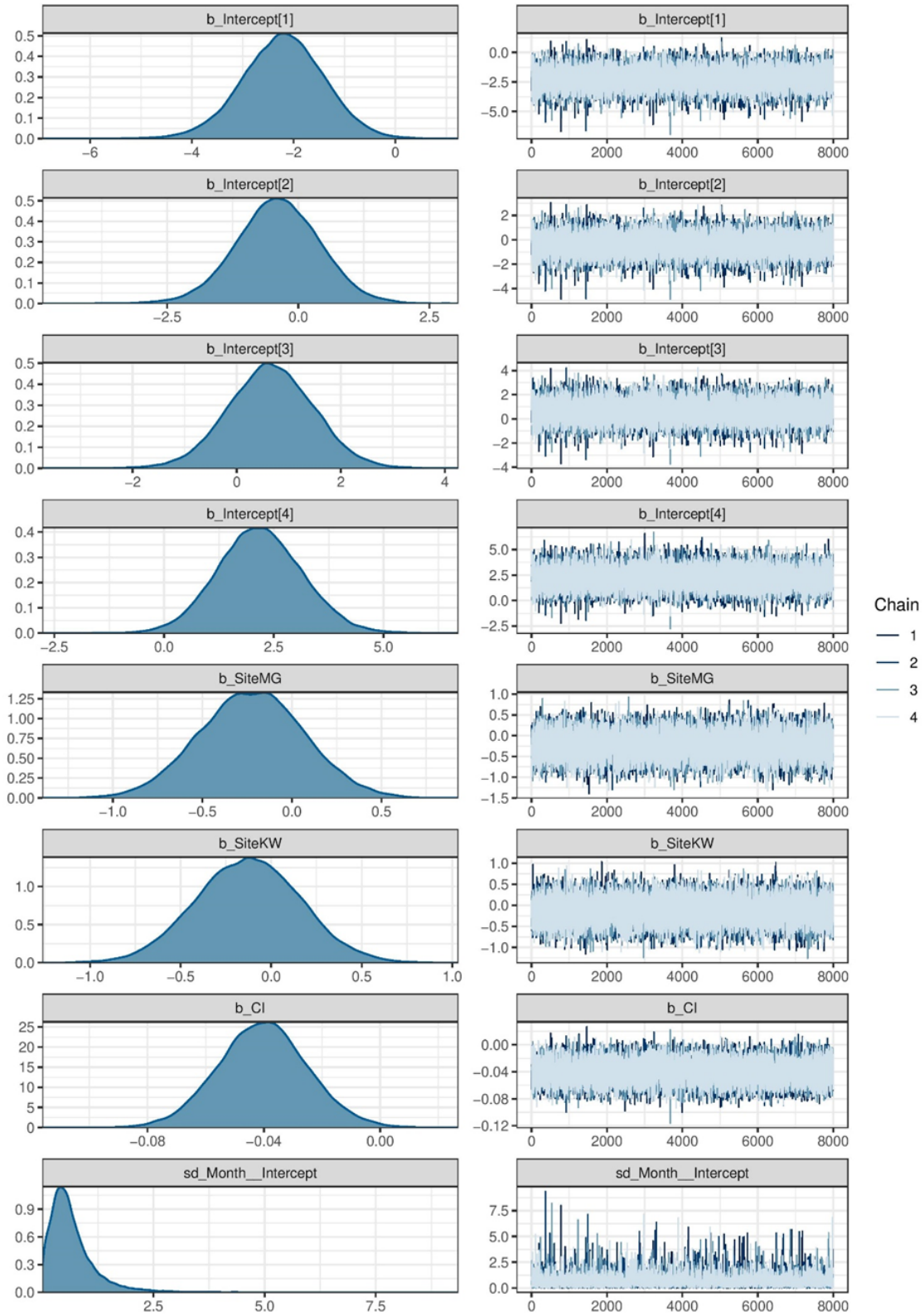

Fig. C.3. Diagnostics from the best fitting model 'Model 3'. Density and corresponding trace plots are shown for each intercept and fixed (Site and condition) and random (Month) factors.

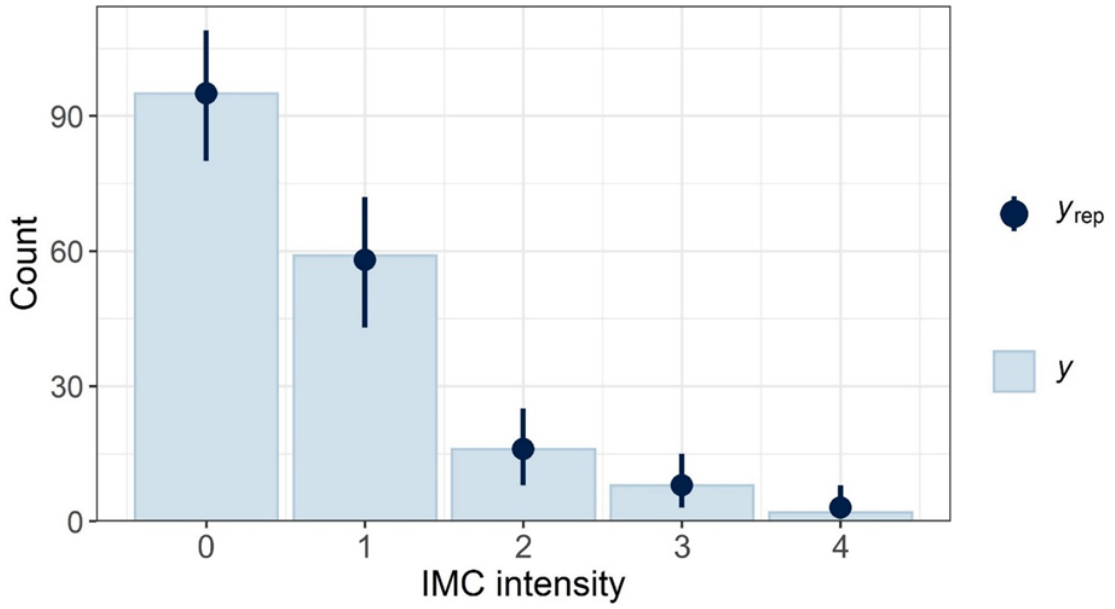

Fig. C.4. Posterior predictive checks (pp_check) for the best performing model (Model 3). Bars (*y*) show the observed data of toheroa infection intensity (five levels). Dots (*Y*rep) show the mean posterior estimates of toheroa infection intensity, whiskers show 95% CI based on 1500 draws. IMC intensity levels: [0] = None, [1] = Low, [2] = Medium, [3] = High, [4] = Severe.

Table C.1. Mean oocyte diameter and oocyte density estimated using ImageJ v1.44 image analysis software. Mean oocyte diameter/density is presented for toheroa sampled at Ripiro Beach between March 2019 and January 2020. Diameter is in µm, *n* = 30 for each sampling date.

Date	Mean oocyte diameter (±SE)	Mean oocyte density (±SE) per mm^2
Mar-19	40.84 (0.4)	476.79 (20.3)
May-19	36.88 (0.6)	547.92 (21.2)
Jul-19	33.74 (0.5)	498.33 (28.1)
Sep-19	35.32 (0.6)	437.50 (17.1)
Nov-19	36.38 (0.4)	376.67 (17.0)
Jan-20	39.71 (0.4)	400.00 (13.4)

Table C.2. The proportion (%) of toheroa specimens in each scoring level for several histological observations. Scoring levels: 0 = None, 1 = Low, 2 = Medium, 3 = High, 4 = Severe. Results are based on six sampling dates at Ripiro Beach between March 2019 and January 2020, *n* = 30 for each sampling occasion.

	Score	**Mar-19**	**May-19**	**Jul-19**	**Sep-19**	**Nov-19**	**Jan-20**
Intracellular microcolonies (IMC)	None	23.3	30.0	63.3	63.3	60.0	76.7
	Low	56.7	43.3	26.7	26.7	26.7	16.7
	Medium	13.3	16.7	0.0	0.0	13.3	3.3
	High	6.7	6.7	10.0	6.7	0.0	3.3
	Severe	0.0	3.3	0.0	3.3	0.0	0.0
Lipofuscin pigmented cells (LF)	None	56.7	30.0	26.7	40.0	46.7	30.0
	Low	26.7	43.3	56.7	33.3	36.7	60.0
	Medium	0.0	23.3	10.0	23.3	10.0	10.0
	High	13.3	3.3	0.0	3.3	3.3	0.0
	Severe	3.3	0.0	6.7	0.0	3.3	0.0
Mucous cell hyperplasia (MH)	None	30.0	53.3	50.0	73.3	60.0	53.3
	Low	40.0	26.7	13.3	13.3	16.7	26.7
	Medium	16.7	10.0	20.0	6.7	10.0	10.0
	High	13.3	3.3	3.3	3.3	10.0	6.7
	Severe	0.0	6.7	13.3	3.3	3.3	3.3
Digestive gland atrophy (DG)	None	86.7	56.7	30.0	86.7	80.0	83.3
	Low	10.0	20.0	33.3	13.3	20.0	13.3
	Medium	3.3	23.3	30.0	0.0	0.0	3.3
	High	0.0	0.0	6.7	0.0	0.0	0.0
	Severe	0.0	0.0	0.0	0.0	0.0	0.0
Gill ciliates (CL)	None	63.3	40.0	56.7	43.3	36.7	66.7
	Low	6.7	10.0	6.7	16.7	6.7	10.0
	Medium	0.0	10.0	23.3	20.0	13.3	16.7
	High	6.7	13.3	3.3	20.0	23.3	0.0
	Severe	23.3	26.7	10.0	0.0	20.0	6.7

Appendix D: Characterisation and Distribution of the Bacterial Genus *Endozoicomonas* in a Threatened Surf Clam

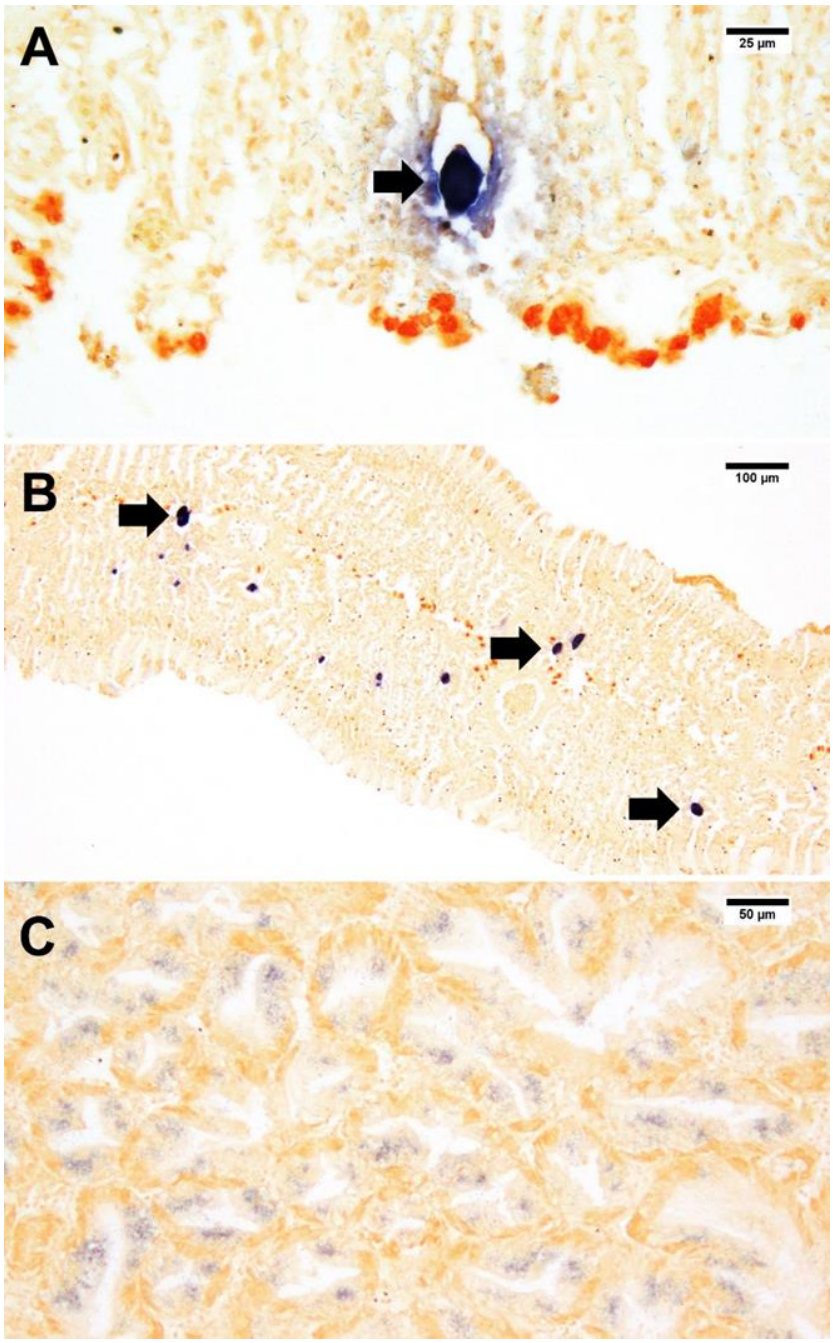

Fig. D.1. Photomicrographs of toheroa (*P. ventricosa*) tissues. A and B: *In situ* hybridization using *Endozoicomonas* specific probe in the gills of toheroa (x 10 and x100 under oil). Dark blue staining indicates a positive reaction with *Endozoicomonas* genetic material. C: *In situ* hybridization in the digestive gland with dark blue patches in the digestive tubules indicating the presence of *Endozoicomonas* genetic material (x20, under oil). ISH stained tissue sections viewed using light microscopy on an Olympus BX53. Filled arrows indicate ISH labelled inclusions.

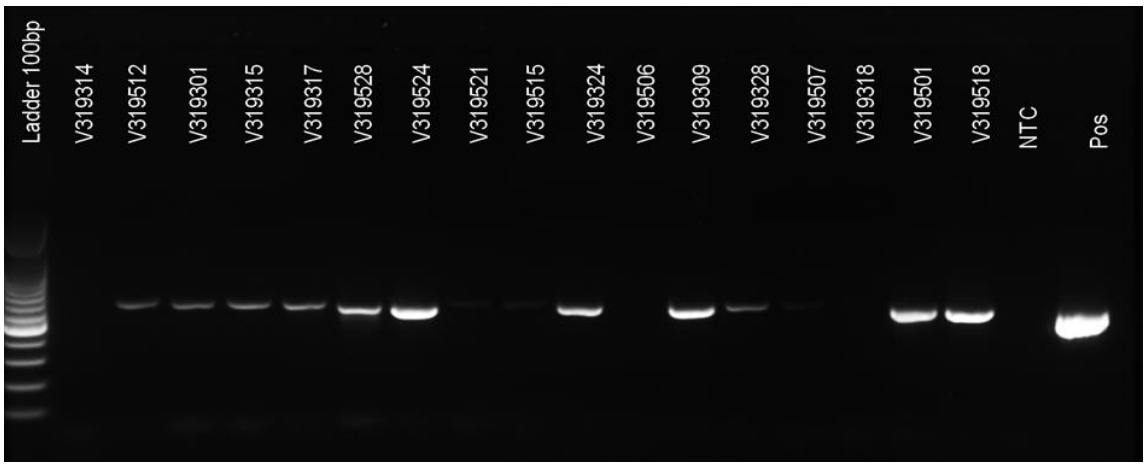

Fig. D.2. Detection of the *Endozoicomonas* spp. 16S rRNA gene in toheroa tissues. Agarose gel showing an amplified PCR band of 528 bp corresponding to a fragment of the *Endozoicomonas* spp. 16S rRNA gene in toheroa sampled from Ripiro Beach in March and May 2019. Pos: positive control, NTC: negative control (ultrapure H_20).

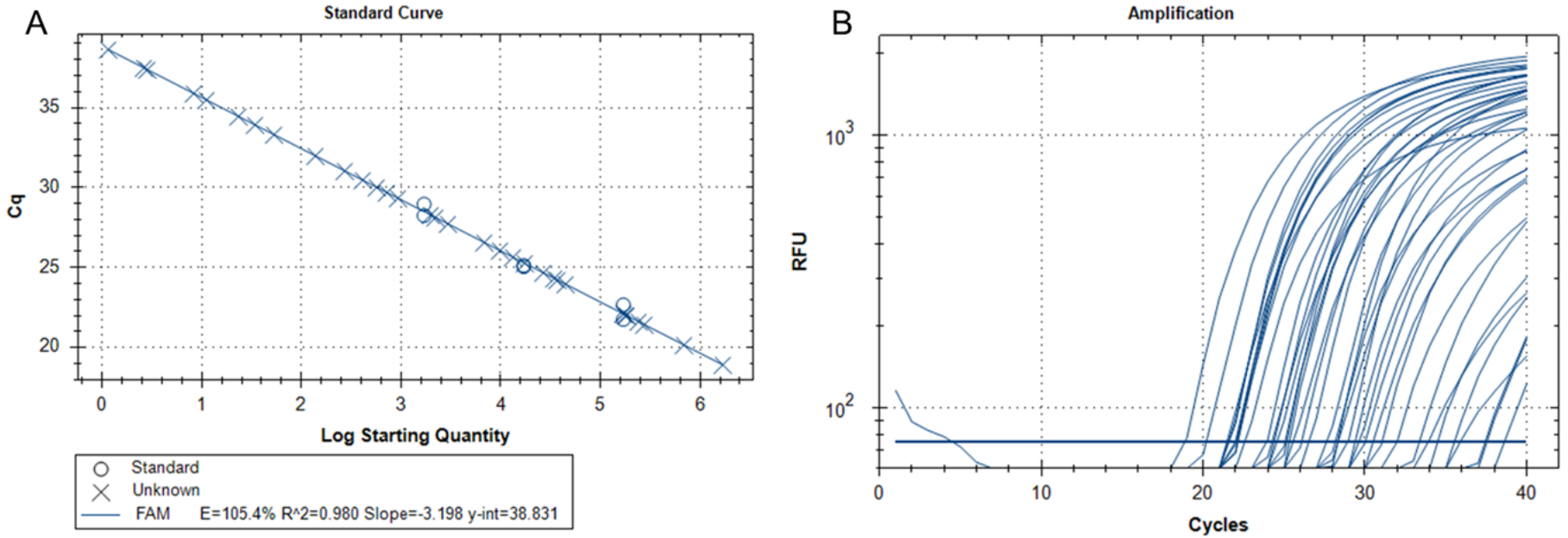

Fig. D.3. A: Example of a standard curve used to calculate transcribed gene copy numbers of *Endozoicomonas* spp. in toheroa tissues, and B: amplification of amplicons. Positive controls used to calibrate the standard curve were at the following concentrations, $1x10^{-4}$, $1x10^{-5}$, and $1x10^{-6}$ ng μl^{-1}.

Table D.1. Descriptive statistics of *Endozoicomonas* spp. 16S rRNA gene copy data. Results of non-parametric Kruskal-Wallis tests are shown. Summarised results from Dunn comparisons tests are also shown. Distributions that do not share the same letter are statistically significantly different (*p*-adj).

Date	**Median**	***n***	**Mean**	**SD**	**SE**	**Dunn's test**
Mar-19	34490.8	29	175703.7	354118.4	65758.1	a
May-19	26198.5	30	98301.9	176208.5	32171.1	a
Jul-19	2543.4	30	17081.5	39693.1	7246.9	ab
Sep-19	369.3	30	8485.1	15356.2	2803.6	b
Nov-19	698.8	30	1908.7	3831.3	699.5	b
Jan-19	665.6	30	6137.3	12749.4	2327.7	b
Kruskal-Wallis $X^2 = 34.84$, df = 5, *p*-value = <0.001						
Ripiro Beach						
Site	**Median**	***n***	**Mean**	**SD**	**SE**	**Dunn's test**
Island	690.3	60	44340.1	138326.7	17857.9	b
Kopawai	10641.4	60	91044.8	10641.4	1373.8	a
Mahuta Gap	1333.1	59	15758.4	39036.7	5082.1	b
Kruskal-Wallis $X^2 = 7.84$, df = 2, *p*-value = 0.02						
Beaches						
Location/Date	**Median**	***n***	**Mean**	**SD**	**SE**	**Dunn's test**
Foxton-Mar	0.0	3	986.5	1708.6	986.5	ab
Ninety Mile-Nov	7395.9	15	10529.2	11292.2	2915.6	a
Oreti-Feb	741.2	40	1511.9	1927.2	304.7	b
Ripiro-Mar	34490.8	29	175703.7	354118.4	65758.1	a
Ripiro-Nov	698.8	30	1908.7	3831.3	699.5	b
Kruskal-Wallis $X^2 = 37.46$, df = 4, *p*-value = <0.001						

Table D.2. Results from Dunn's test, comparisons following Kruskal-Wallis test. Comparisons are based on *Endozoicomonas* spp. 16S rRNA gene copies from toheroa from Ripiro Beach, sampled between March 2019 and January 2020. For each comparison, Dunn's Z statistic is shown as well as *p*-values adjusted using Bonferroni's correction for multiple comparisons. Statistically significant differences are indicated in bold with an asterisk.

Months		**Jan-20**	**Jul-19**	**Mar-19**	**May-19**	**Nov-19**
Jul-19	Z	-1.06				
	p	1.000				
Mar-19	Z	-3.97	-2.91			
	p	**0.001***	0.027			
May-19	Z	-3.48	-2.41	0.52		
	p	**0.004***	0.118	1.000		
Nov-19	Z	0.18	1.24	4.14	3.65	
	p	1.000	1.000	**0.000***	**0.002***	
Sep-19	Z	0.02	1.08	3.99	3.50	-0.16
	p	1.000	1.000	**0.001***	**0.004***	1.000

Table D.3. Results from Dunn's test, comparisons following Kruskal-Wallis test. Comparisons are based on *Endozoicomonas* spp. 16S rRNA gene copies from toheroa from Ripiro Beach, sampled at three sites: Island, Mahuta Gap, and Kopawai. For each comparison, Dunn's Z statistic is shown as well as *p*-values adjusted (Bonferroni). Statistically significant differences are indicated in bold with an asterisk.

Ripiro Beach		**Island**	**Kopawai**
Kopawai	Z	-2.44	
	p	**0.022***	
Mahuta Gap	Z	-0.02	2.41
	p	1.000	**0.024***

Table D.4. Results from Dunn's test, comparisons following Kruskal-Wallis tests. Comparisons are based on *Endozoicomonas* spp. 16S rRNA gene copies from toheroa from Ripiro Beach, Ninety Mile Beach, Foxton Beach, and Oreti Beach. For each comparison, Dunn's *Z* statistic is shown as well as *p*-values adjusted using Bonferroni's correction for multiple comparisons. Statistically significant differences are indicated in bold with an asterisk.

		Foxton-Mar	**Ninety Mile-Nov**	**Oreti-Feb**	**Ripiro-Mar**
Ninety Mile-Nov	*Z*	-2.31			
	p	0.105			
Oreti-Feb	*Z*	-0.77	3.30		
	p	1.000	**0.005***		
Ripiro-Mar	*Z*	-2.77	-0.68	-4.99	
	p	0.028	1.000	**0.000***	
Ripiro-Nov	*Z*	-0.80	3.08	-0.11	4.57
	p	1.000	**0.011***	1.000	**0.000***

Table D.5. Descriptive statistics of *Endozoicomonas* spp. 16S rRNA gene copy data. Results of non-parametric Kruskal-Wallis tests are shown based on comparisons between sampling months at sites: Island, Mahuta Gap, and Kopawai. Summarised results from Dunn comparisons tests are also shown. Distributions that do not share the same letter are statistically significantly different (*p*-adj, Bonferroni correction).

Island						
Date	**Median**	***n***	**Mean**	**SD**	**SE**	**Dunn's test**
Mar-19	30960.8	10	190976.8	296706.4	93826.8	-
May-19	420.4	10	25678.5	57612.2	18218.6	-
Jul-19	9664.9	10	34275.8	65329.1	20658.9	-
Sep-19	9246.7	10	10928.4	13020.9	4117.6	-
Nov-19	638.6	10	3759.2	6324.4	2000.0	-
Jan-20	151.6	10	423.4	595.6	188.3	-
Kruskal-Wallis X^2 = 8.45, df = 5, p-value = 0.13						
Mahuta Gap						
Date	**Median**	***n***	**Mean**	**SD**	**SE**	**Dunn's test**
Mar-19	16761.5	9	29980.0	33168.8	11056.3	ab
May-19	29884.9	10	56010.4	77084.6	24376.3	a
Jul-19	166.1	10	4751.0	8642.8	2733.1	c
Sep-19	4.7	10	1474.2	4384.6	1386.5	c
Nov-19	597.2	10	839.3	854.3	270.2	bc
Jan-20	1731.7	10	2918.8	3390.7	1072.2	abc
Kruskal-Wallis X^2 = 27.12, df = 5, p-value = <0.001						
Kopawai						
Date	**Median**	***n***	**Mean**	**SD**	**SE**	**Dunn's test**
Mar-19	93453.2	10	291582.3	514495.6	162697.8	a
May-19	114536.4	10	213216.9	261279.0	82623.7	ab
Jul-19	7259.9	10	12218.3	14505.9	4587.2	abc
Sep-19	672.8	10	13053.5	22059.4	6975.8	bc
Nov-19	977.2	10	1127.8	902.5	285.4	c
Jan-20	1141.2	10	15070.5	19376.5	6127.4	abc
Kruskal-Wallis X^2 = 23.57, df = 5, p-value = <0.001						

Table D.6. Results from Dunn's test, comparisons following Kruskal-Wallis test. Comparisons are based on *Endozoicomonas* spp. 16S rRNA gene copies from toheroa from Ripiro Beach, sampled at sites: Mahuta Gap, and Kopawai. For each comparison, Dunn's *Z* statistic is shown as well as *p*-values adjusted (Bonferroni). Statistically significant differences are indicated in bold with an asterisk.

Mahuta Gap						
		Jan-20	Jul-19	Mar-19	May-19	Nov-19
Jul-19	Z	1.04				
	p	1.000				
Mar-19	Z	-1.53	-2.54			
	p	0.936	0.082			
May-19	Z	-2.33	-3.37	-0.73		
	p	0.149	**0.006***	1.000		
Nov-19	Z	0.90	-0.14	2.41	3.23	
	p	1.000	1.000	0.119	**0.009***	
Sep-19	Z	2.00	0.97	3.48	4.33	1.10
	p	0.339	1.000	**0.004***	**0.000***	1.000
Kopawai						
		Jan-20	Jul-19	Mar-19	May-19	Nov-19
Jul-19	Z	-0.19				
	p	1.000				
Mar-19	Z	-2.77	-2.57			
	p	0.042	0.075			
May-19	Z	-2.27	-2.08	0.50		
	p	0.175	0.285	1.000		
Nov-19	Z	0.90	1.10	3.67	3.17	
	p	1.000	1.000	**0.002***	**0.011***	
Sep-19	Z	0.63	0.83	3.40	2.90	-0.27
	p	1.000	1.000	**0.005***	0.028	1.000

Appendix E: The Bacterial Community in a Threatened Beach Clam Endemic to Aotearoa (New Zealand)

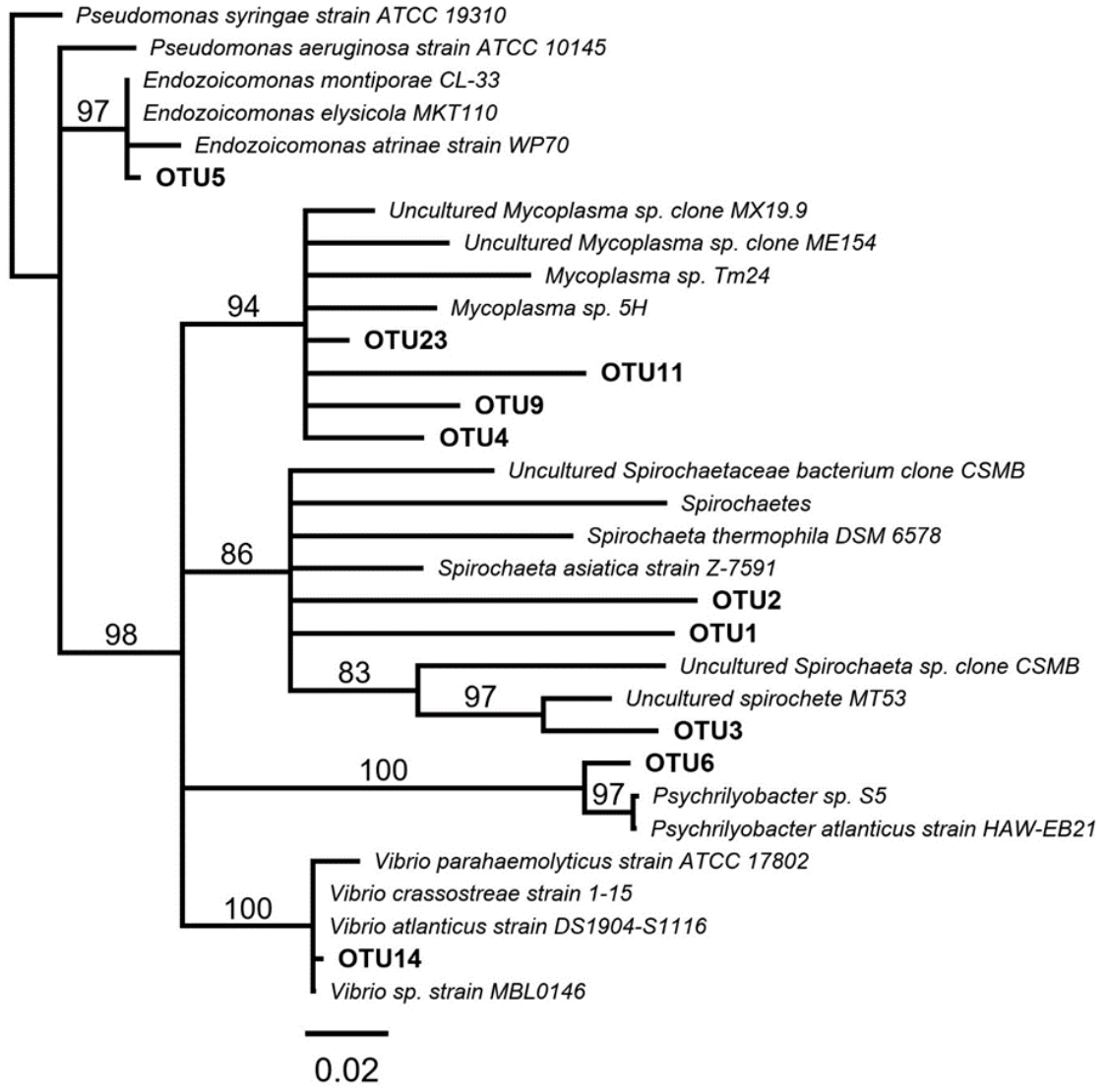

Fig. E.1. Phylogenetic tree showing genetic relatedness of ten OTU 16S rRNA sequences isolated from toheroa (*Paphies ventricosa*) gills and digestive gland (composite microbiome), with other closely related marine bacteria. Branches labelled with consensus support (%) based on 100,000 bootstrapped replicates. Top 10 OTUs (average relative abundance) present in >70% of specimens are in bold. Accession numbers are in Table E.3.

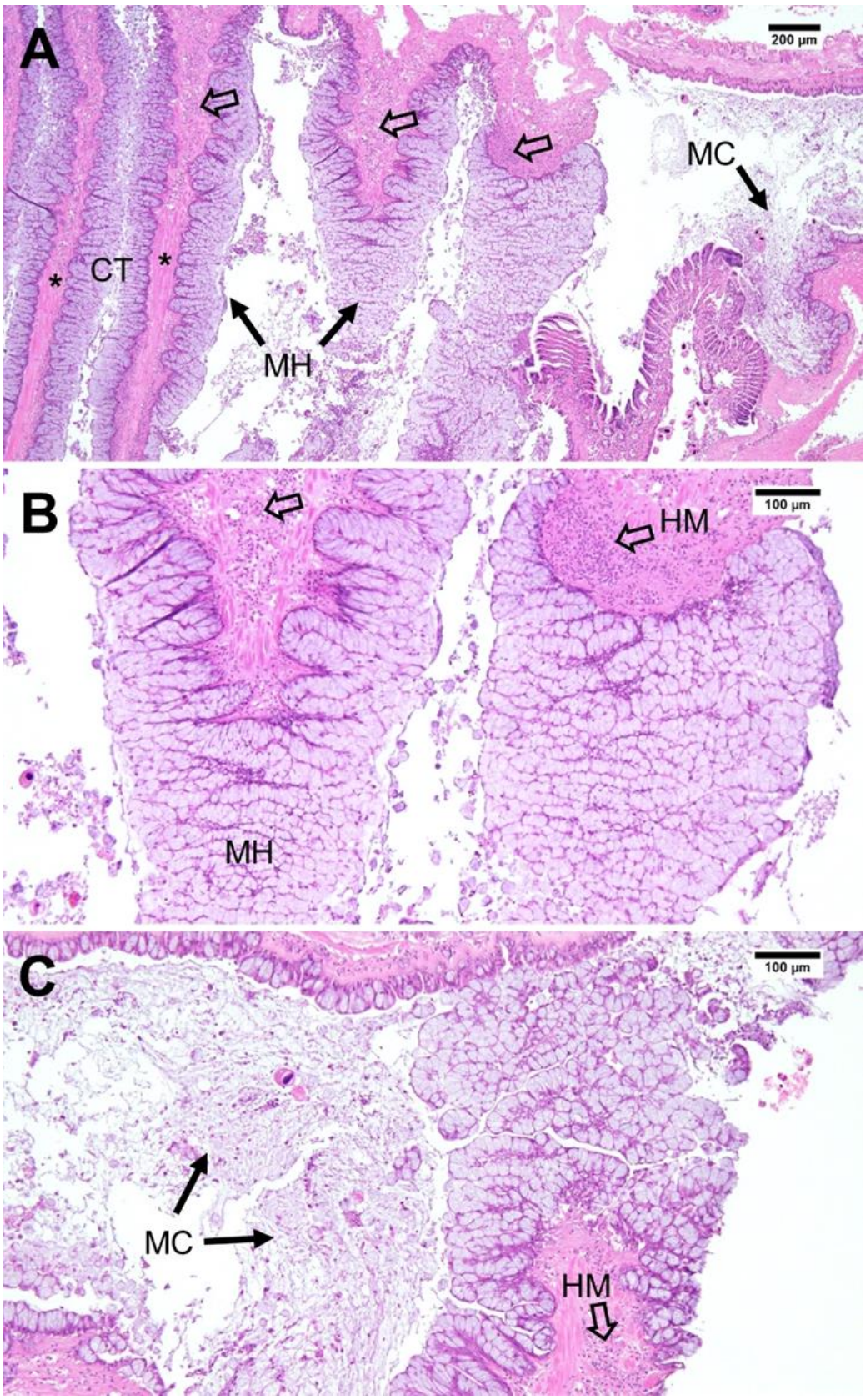

Fig. E.2. Histological tissue sections (H&E stained) of toheroa (Olympus BX51 at x4 and x10 magnification). Photomicrographs show the superbranchial chamber at the posterior of the gills. A: Mucous cell hyperplasia (MH) surrounding siphon connective tissues (CT) indicated with an asterisk. MH: mucus in the superbranchial chamber. Hollow arrows: haemocyte infiltration at the base of mucous cells. B: Mucous cell hyperplasia (MH) and haemocytes (HM and hollow arrows). C: Large quantities mucus (MC) and more hyperplastic mucous cells and haemocyte infiltration (HM).

Table E.1. OTUs and corresponding sequences of the core toheroa composite microbiome. Here, core is defined as the top 10 OTUs (according average to relative abundance) present in 70% of samples. OTUs that were detected in 90% of toheroa at a relative abundance >1% per sample are in bold. BLAST results are given too, based on genetic relatedness to sequences in the NCBI database. Identity match is provided as well as corresponding accession number.

OTU	Average relative abundance	Taxa	Identity (accession number)	Sequence
OTU6	1.4%	*Psychrilyobacter*	97.6% (LR606286.1)	TACGTATGTCGCAAGCGTTATCCGG AATTATTGGGCGTAAAGCGAGTCTA GGCGGTTTGTTAAGTCAGATGTGAA AATGCGGGGCTCAACTCCGTATGGC CTTTGATACTGGCAAACTAGAGTACT GGAGAGGTGGGCGGAACTACAAGT GTAGAGGTGAAATTCGTAGATATTTG TAGGAATGCCGATAGTGAAGACAGC TCACTGGACAGATACTGACGCTAAA GCTCGAAAGCGTGGGGAGCGAACA
OTU2	19.8%	Uncultured *Spirochaetes*	94.8% (EU857763.1)	TACGTAGGGGATGAACGTTGTTCGG AATCACTGGGCGTAAAGAGTACGTA GGCGGTTTGGTAAGTCAATAGTGAA ATCTCAGGGCTCAACTTTGAGACTA CTATTGAAACTACCAAACTAGAGTTA ATGATAGAGGTAGCAGGAATTCCTG GTGGAAGGGTGAAATCTGTAGATAT CAGGAAGAACACCAAGGGCGAAGG CAAGCTACTGGGTATTAACTGACGC TGAGGTACGAAAGCTAGGGGAGCG A
OTU1	33.2%	Uncultured *Spirochaetes*	89.64% (KY687499.1)	TACGTAAGGGGCAAGCGTTGTTCGG AATTATTGGGCGTAAAGGGCATGTA GGTGGTACAATAAGCCTAGAGTAAA AGCCCACAGCTTAACTGTGGGAAGC GTTAGGAACTGTAGTACTGGAGTCT AGGAGGGGAAACTGGAATTCTTGGT GGAGGGGTGAAATCTGTAGATCCCA AGGAGAACACCGGAGGCGAAGGCG AGTTTCTGGCCATAGACTGACACTG AGATGCGAAAGCGTGGGGAGCGAA CA
OTU3	20.2%	Uncultured *Spirochaetes*	94.4% (MH999891.1)	CACGTAAGGTGCAAGCGTTGTTCGG AATTATTGGGCGTAAAGGGCTTGTA GGCGGCTAGCCAAGTCTTTCGTGAA ATTTCAGGGCTCAACCCTGGAACTG CGAGGGAAACTGGTTGGCTTGAATC TTGGAGGGGGTACTGGAATTCCTAG TGTAGGGGTGAAATCTGTTGATATTA GGAAGAACACCGGAGGCGAAGGCG AGTACCTGGCCAAAGATTGACGCTG ATAAGCGAAAGCGTAGGGAGCGAAC
OTU9	1.3%	Uncultured *Mycoplasma*	90.8% (HE648941.1)	TACATAGGGTGCAAGCGTTATCCGG ATTTATTGGGCGTAAAGCGTTCGTA GGTGGTTTATTAAGTCTGAAGTCAAA GACCGGAGCTCAACTCCGGCTCGCT TTGGATACTGGTAGACTAGAGTTAC GGAGAGGTTAGTGGAATTTCATGTG AAGCGGTGGAATGCGTAGATATATG

				AAGGAACACCAATGGCGAAGGCAAC TAACTGGCCGTATACTGACACTCAG GAACGAAAGCGTGGGTAGCAAACA
OTU4	2.3%	Uncultured *Mycoplasma*	92.03% (KP174127.1)	TACATAGGGTGCAAGCGTTATCCGG ATTTATTGGGCGTAAAGCGTTCGTA GGCGGTTTGTTAAGTCTAAAATTAAA GCCTGGTGCTCAACGCCAGCCCGTT TTAGATACTGATAGACTAGAGTTATA GAGAGGTTAGTGGAACTCCATGTGA AGCGGTGGAATGCGTAGATATATGG AAGAACACCAATGGCGAAGGCAACT AACTGGCTATATACTGACGCTGAGG GACGAAAGCGTGGGGAGCAAACA
OTU14	1.6%	*Vibrio*	100% (MT510175.1)	TACGGAGGGTGCGAGCGTTAATCGG AATTACTGGGCGTAAAGCGCATGCA GGTGGTTCATTAAGTCAGATGTGAA AGCCCGGGGCTCAACCTCGGAACT GCATTTGAAACTGGTGAACTAGAGT ACTGTAGAGGGGGGTAGAATTTCAG GTGTAGCGGTGAAATGCGTAGAGAT CTGAAGGAATACCAGTGGCGAAGGC GGCCCCCTGGACAGATACTGACACT CAGATGCGAAAGCGTGGGGAGCAA AC
OTU11	1.2%	Uncultured *Mycoplasma*	86.69% (MG813923.1)	TACATAGGTGGCAAGCGTTATCCGG AATTATTGGGCGTAAAGAGTTCGTA GGTGGTTTATTAAGTTCAGAGTTAAA GACTAAAGCTTAACTTTAGCATGCTT TGAATACTGATAAACTAGAGTTATAT AGAGGTTAGTGGAACTTCAAGTGGA GCGGTGGAATGCGTAGATATTTGAA AGAACACCAGTGGCGAAGGCGACT GACTGGATATATACTGACACTCAAGA ACGAAAGCGTGGGGAGCAAATA
OTU23	0.9%	Uncultured *Mycoplasma*	94.42% (KP174127.1)	TACATAGGGTGCAAGCGTTATCCGG AATTATTGGGCGTAAAGCGTTCGTA GGCGGTTTATTAAGTCTGAAGTTAAA GCCCGGGGCTCAACCCCGGCCCGC TTTGGATACTGATAGACTAGAGTTAT AGAGAGATTAGCGGAACTCCATGTG AAGCGGTGGAATGCGTAGATATATG GAAGAACACCAATGGCGAAGGCAGC TAATTGGCTATACACTGACGCTGAG GAACGAAAGCGTGGGGAGCAAACA
OTU5	2.1%	*Endozoicomonas*	98.8% (KX611231.1)	TACGGAGGGTGCAAGCGTTAATCGG AATTACTGGGCGTAAAGCGTGCGTA GGCGGCCTTTTAAGTTGGATGTGAA AGCCCCGGGCTCAACCTGGGAACG GCATCCAAAACTGAGAGGCTAGAGT GCGGAAGAGGAGTGTGGAATTTCCT GTGTAGCGGTGAAATGCGTAGATAT AGGAAGGAACACCAGTGGCGAAGG CGACACTCTGGTCTGACACTGACGC TGAGGTACGAAAGCGTGGGGAGCA AAC

Table E.2. Mean and standard error of alpha diversity indices (evenness, richness, and diversity), given for each site or beach. Kruskal-Wallis test statistics are also shown. Foxton and Oreti were not included in statistical testing (low replication). Diversity indices estimated using the 'phyloseq' and 'microbiome' packages (Lahti, 2017; (McMurdie and Holmes, 2013).

Location/site	*n*	Chao1 (Richness)	±SE	Simpson (Evenness)	±SE	Shannon (Diversity)	±SE
Ninety-Mile	6	99.11	24.27	0.319	0.04	1.56	0.14
Island	5	124.68	32.98	0.322	0.07	1.80	0.30
Mahuta Gap	5	212.23	22.44	0.239	0.03	2.28	0.18
Kopawai	5	242.95	44.09	0.275	0.05	2.21	0.24
Foxton	1	114.60	-	0.294	-	2.02	-
Oreti	2	135.38	13.33	0.201	0.00	2.51	0.10
X^2		9.4		2.4		6.4	
df		3		3		3	
p		0.02		0.49		0.09	

References

Lahti, L., et al., 2017. Tools for microbiome analysis in R. Version. 1**,** 504.

McMurdie, P. J., Holmes, S., 2013. phyloseq: An R Package for Reproducible Interactive Analysis and Graphics of Microbiome Census Data. PLOS ONE. 8**,** e61217.

Table E.3. Bacteria sequences downloaded from the NCBI database that were used to construct phylogenetic trees. Corresponding accession numbers are provided.

Bacteria strain	**NCBI accession no.**
Endozoicomonas montiporae CL-33	FJ347758.1
Endozoicomonas elysicola MKT110	NR_041264.1
Endozoicomonas atrinae strain WP70	KC878324.1
Vibrio sp. strain MBL0146	MT187918.1
Vibrio parahaemolyticus strain ATCC 17802	NR_118928.1
Vibrio crassostreae strain 1-15	MT510175.1
Vibrio atlanticus strain DS1904-S1116	MT269622.1
Uncultured spirochete MT53	AF211322.1
Uncultured *Spirochaeta* sp. clone CSMB	MF896037.1
Uncultured *Spirochaetaceae* bacterium clone CSMB	MF898324.1
Spirochaetes bacterium	MT095074.1
Spirochaeta thermophila DSM 6578	NR_074795.1
Spirochaeta asiatica strain Z-7591	NR_026300.1
Uncultured *Mycoplasma* sp. clone MX19.9	JF521606.1
Uncultured *Mycoplasma* sp. clone ME154	DQ917898.1
Mycoplasma sp. Tm24	HQ326170.1
Mycoplasma sp. 5H	LT716015.1
Psychrilyobacter sp. S5	LR606284.1
Psychrilyobacter atlanticus strain HAW-EB21	AY579753.1
Pseudomonas syringae strain ATCC 19310	AF094749.1
Pseudomonas aeruginosa strain ATCC 10145	AF094713.1

Appendix F: Do Freshwater Streams Deliver Trace Metal Pollution to a Threatened Intertidal Beach Clam?

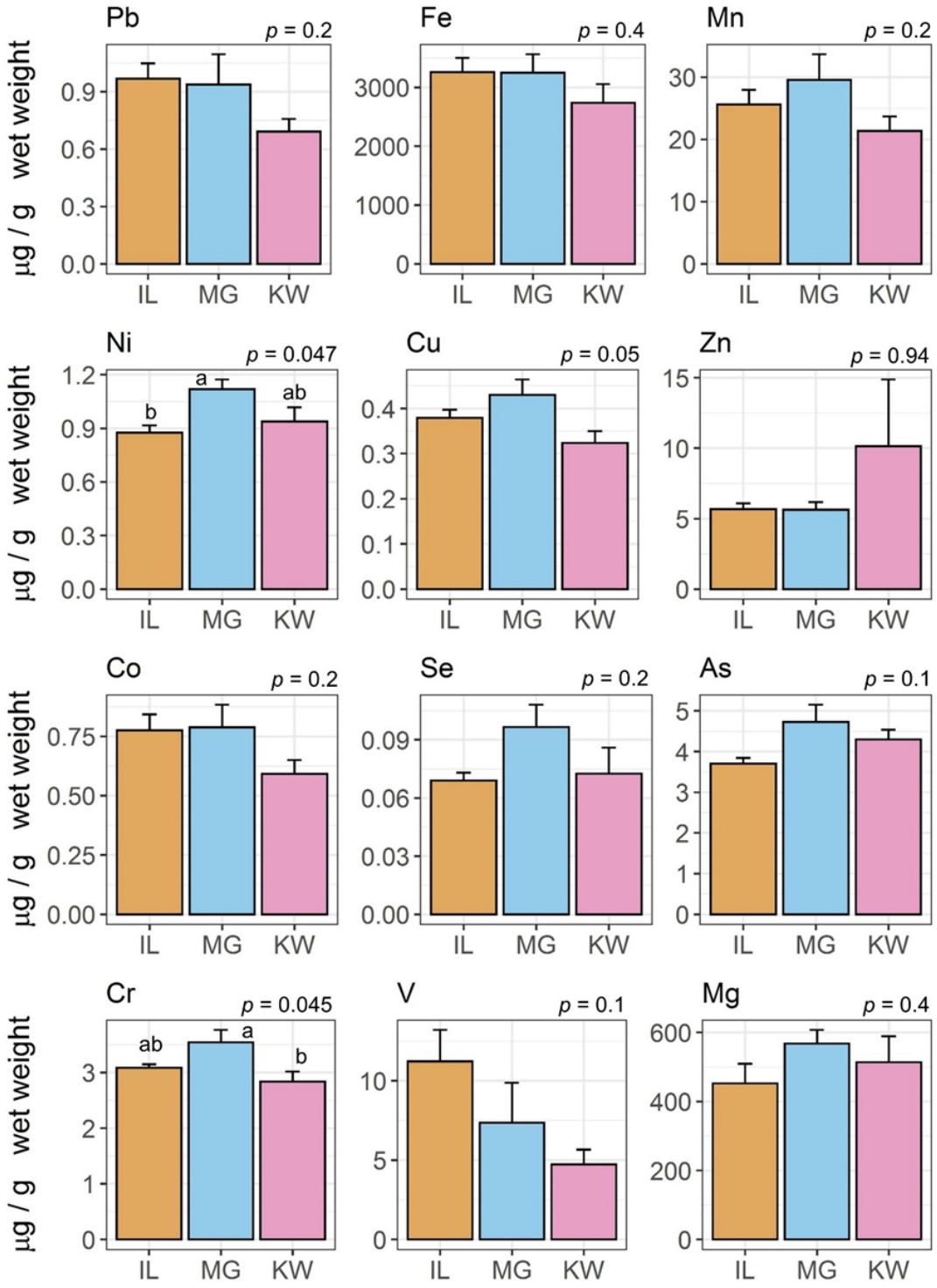

Fig. F.1. Trace element concentrations (µg g^{-1} wet weight) in sediment samples from three streams sampled on Ripiro Beach in September 2020. IL: Island, MG: Mahuta Gap, KW: Kopawai. Bars show the mean and standard error for the mean based on *n* = 4 for each bar. Bars that do not share the same letter denote statistically significant differences based on One-way ANOVA tests and Tukey's post-hoc tests (95% significance level). Kruskal-Wallis tests were used for Zn and Se (p = >0.05).

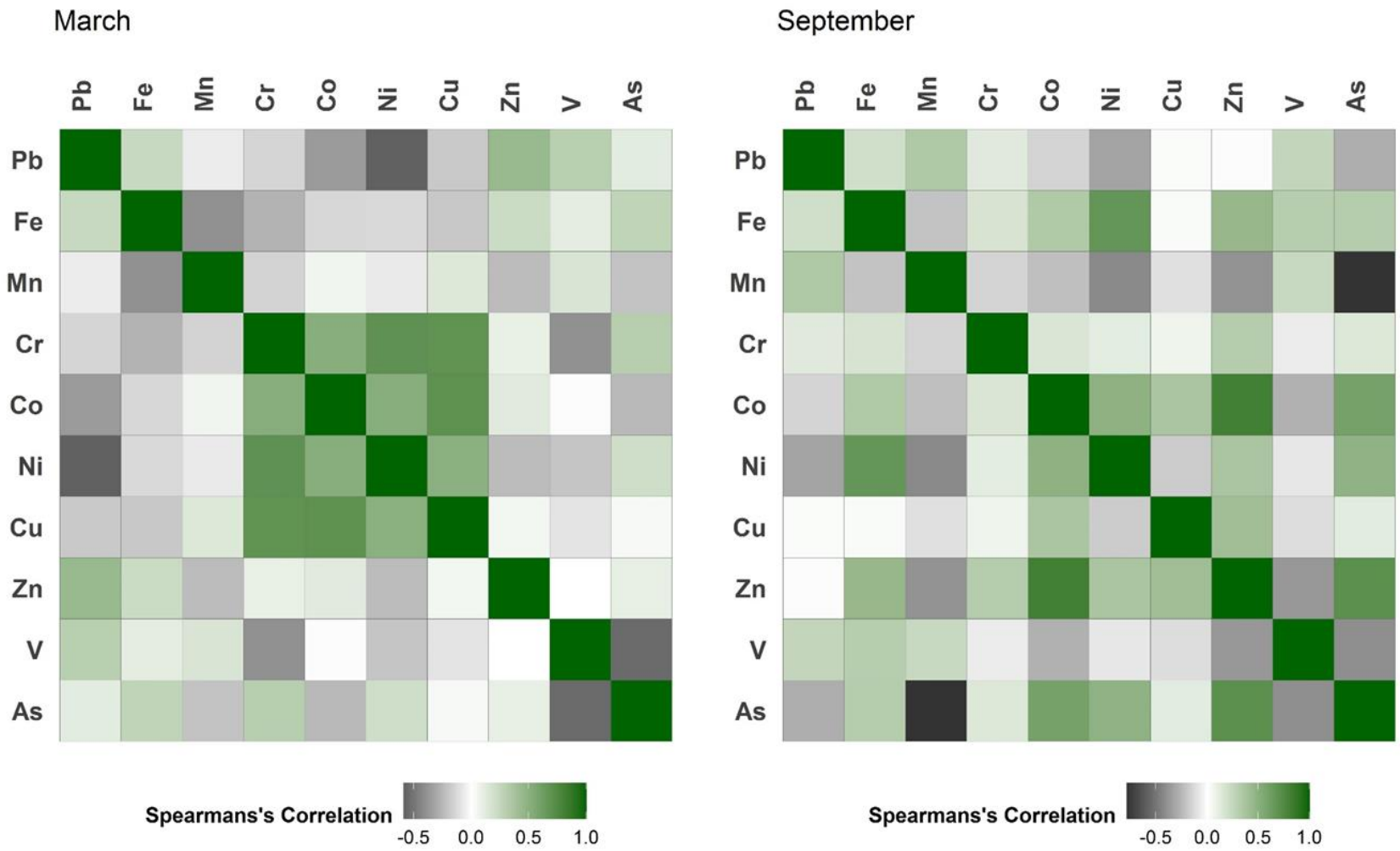

Fig. F.2. Correlation matrix constructed using Spearman's correlation, showing the relationship between detected trace metals in toheroa (Paphies ventricosa) foot tissue collected from Ripiro Beach in March and September 2019. Heatmap shows positive and negative correlations between respective TEs.

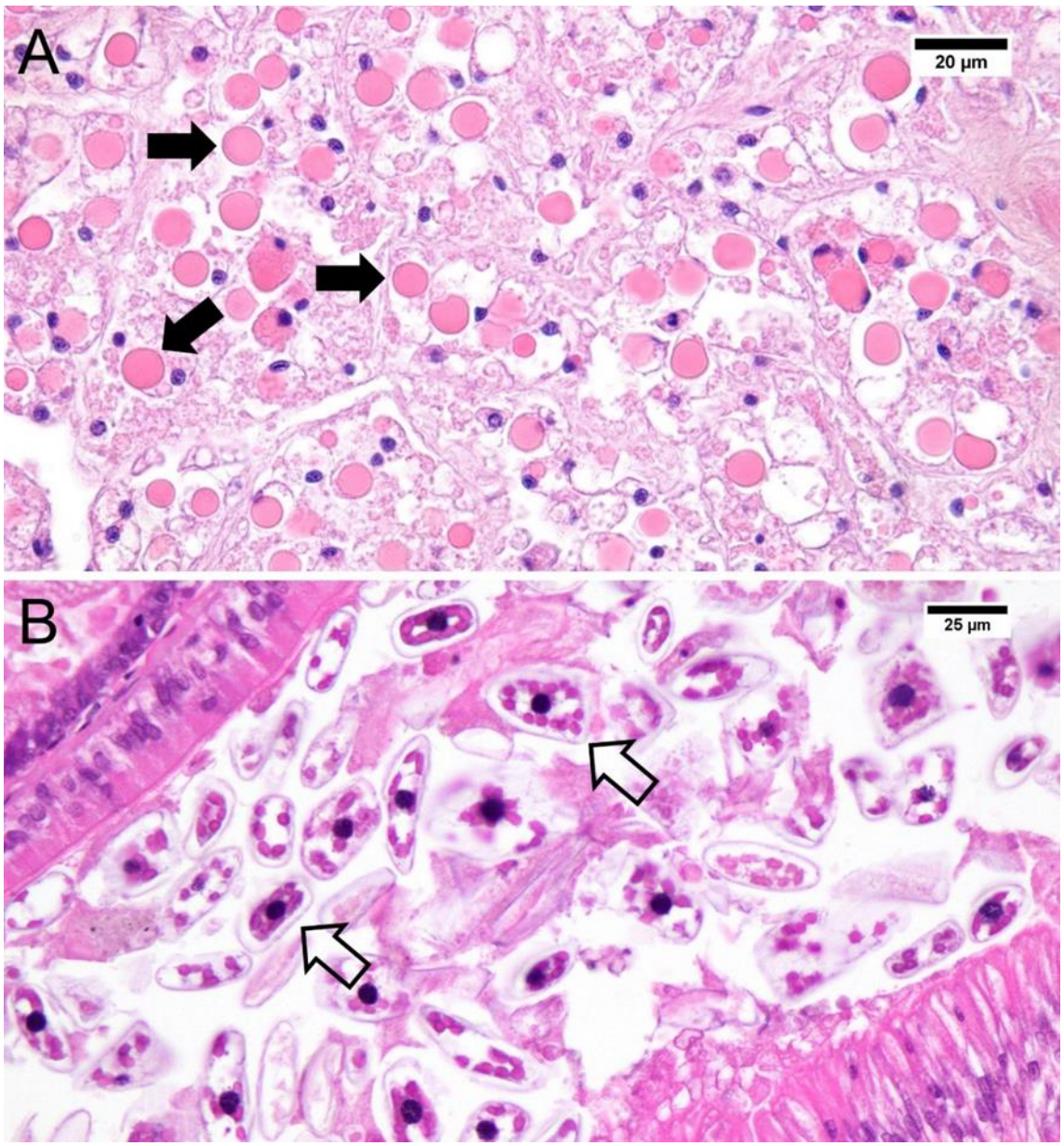

Fig. F.3. Histological tissue sections (H&E stained) of toheroa (Olympus BX53 at x100 magnification, under oil). A: Calcareous concretions/intracellular granules (filled arrows) in the nephridium of toheroa, potentially metal containing like other $CaCO_3$ structures. B: Diatoms (hollow arrows) in the digestive glands of toheroa. Specimens gathered from Ripiro Beach, Northland.

Table F.1. Mean and standard error (SE) trace metal concentrations (µg g^{-1} wet weight) derived from toheroa foot tissue. Results from Unpaired T-tests and Mann-Whitney U-tests based on trace metal concentrations derived from toheroa foot tissues in March and September 2019 are also shown. Tests conducted on pooled sample concentrations for three sites (*n* = 15 for each month), *p* significant at <0.05.

Element	March		September				
	Mean	SE	Mean	SE	*t*	*df*	*p*
Fe	19.66	1.64	15.03	1.1	2.34	28	**0.027**
Co	0.03	0.002	0.03	0.002	1.44	28	0.161
Ni	0.03	0.002	0.07	0.01	-4.82	28	**<0.001**
Cu	0.64	0.02	0.45	0.02	5.79	28	**<0.001**
Zn	12.32	0.4	11.32	0.47	1.63	28	0.115
As	1.99	0.06	1.76	0.09	2.14	28	**0.041**
					W	*df*	*p*
V	0.0054	0.0004	0.0064	0.0009	92	28	0.412
Pb	0.02	0.001	0.01	0.003	210	28	**<0.001**
Mn	0.39	0.03	0.36	0.02	130	28	0.486
Cr	0.03	0.01	0.01	0.001	180	28	**0.004**

Table F.2. Metal pollution index (MPI) scores (mean and standard error). Calculated from trace metal concentrations derived from toheroa foot tissues and sediment samples gathered at three sites on Ripiro Beach.

	Date	Statistic	Island	Mahuta Gap	Kopawai
Toheroa	Mar-19	Mean	0.22	0.19	0.19
		SE	0.009	0.010	0.017
	Sept-19	Mean	0.16	0.15	0.16
		SE	0.003	0.009	0.024
Sediment	Sept-20	Mean	2.12	2.34	2.01
		SE	0.107	0.156	0.205

Table F.3. Spearman's correlation showing the relationship between trace elements in toheroa foot tissues. Spearman's *rho* is shown; values in bold and marked with an asterisk are statistically significant ($p \leq 0.05$).

Mar-19									
	Pb	Fe	Mn	Cr	Co	Ni	Cu	Zn	V
Fe	0.24								
Mn	-0.06	-0.4							
Cr	-0.15	-0.27	-0.15						
Co	-0.36	-0.14	0.06	0.51					
Ni	**-0.59***	-0.13	-0.07	**0.69***	0.51				
Cu	-0.19	-0.19	0.15	**0.69***	**0.70***	0.5			
Zn	0.44	0.22	-0.24	0.09	0.13	-0.24	0.05		
V	0.3	0.11	0.16	-0.4	-0.01	-0.2	-0.09	0	
As	0.12	0.27	-0.21	0.31	-0.25	0.21	0.04	0.1	**-0.55***
Sept-19									
Fe	0.2								
Mn	0.34	-0.21							
Cr	0.13	0.17	-0.15						
Co	-0.15	0.34	-0.22	0.16					
Ni	-0.33	**0.67***	-0.42	0.11	0.49				
Cu	0.02	0.03	-0.11	0.07	0.37	-0.18			
Zn	-0.01	0.45	-0.39	0.31	**0.81***	0.37	0.41		
V	0.26	0.31	0.24	-0.06	-0.28	-0.08	-0.12	-0.37	
As	-0.29	0.31	**-0.79***	0.14	0.59	0.48	0.12	**0.71***	-0.41

Table F.4. Spearman's correlation showing the relationship between trace elements in sediment samples gathered at Ripiro Beach in Sep-20. Spearman's *rho* is shown; values in bold and marked with an asterisk are statistically significant ($p \leq 0.05$).

	Mg	**V**	**Cr**	**Mn**	**Fe**	**Co**	**Ni**	**Cu**	**Zn**	**Se**	**As**
V	-0.31										
Cr	0.45	0.39									
Mn	-0.22	0.53	0.54								
Fe	-0.12	**0.87***	0.56	**0.62***							
Co	-0.13	0.90	**0.65***	**0.72***	**0.86***						
Ni	**0.61***	-0.05	**0.79***	0.50	0.20	0.27					
Cu	0.21	0.55	**0.83***	0.57	**0.64***	**0.73***	**0.59***				
Zn	-0.31	0.31	0.29	0.46	0.36	0.5	0.14	0.36			
Se	0.33	0.14	0.58	0.36	0.39	0.16	**0.66***	0.34	0		
As	0.56	-0.46	0.13	-0.03	-0.12	-0.31	0.39	0.09	-0.38	0.16	
Pb	-0.17	0.94	0.55	0.55	**0.82***	**0.94***	0.16	**0.66***	0.48	0.18	-0.48

Appendix G: Investigation of Gas Bubble Manifestation on Toheroa (*Paphies ventricosa*)

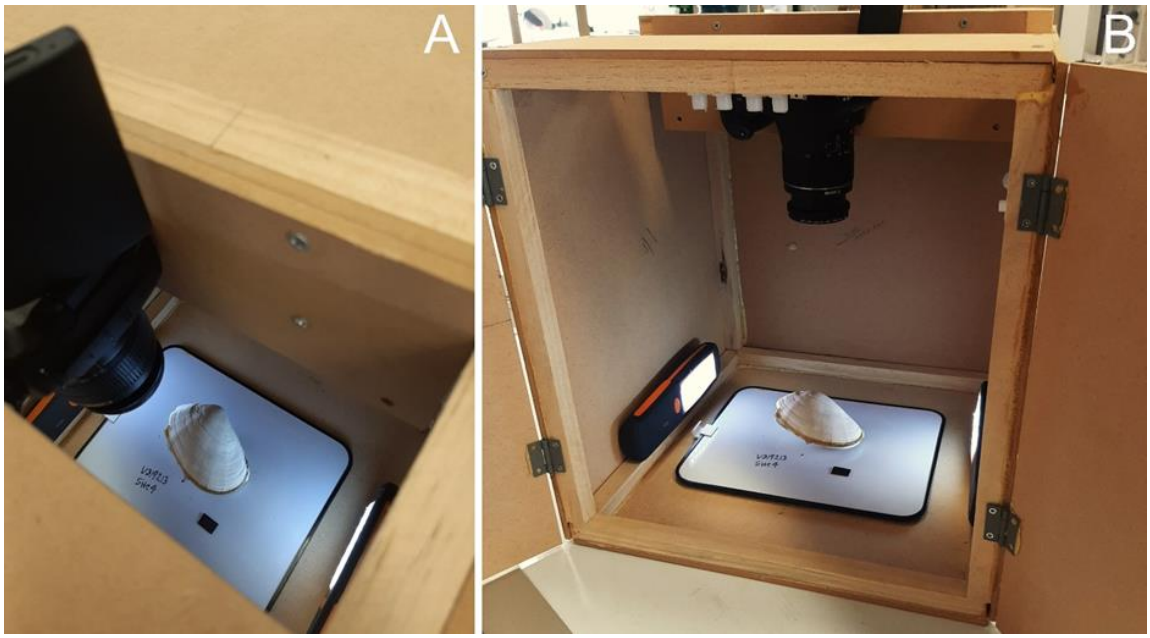

Fig. G.1. A & B: show the custom-built ‘gas bubble light box’ for photographing gross pathology of specimens *in situ*. LEDs light the box from the top (strip lights) and sides, controlling the light balance and allowing for clearer images for assessment of gas bubble intensity and extent on the shells of toheroa.

Table G.1. Bacteria sequences downloaded from the NCBI database that were used to construct phylogenetic trees. Corresponding accession numbers are provided.

Bacteria strain	**NCBI accession no.**
Uncultured sulfate-reducing bacterium clone RS2_74	KT424471.1
Desulfocapsa sp.	AF228119.2
Uncultured *Desulfobulbaceae* bacterium clone 16B_83	AM501699.1
Uncultured *Desulfobulbaceae* bacterium clone CSMB_4520	MF897677.1
Uncultured *Desulfobacterium* sp.	AY274445.1
Uncultured *Desulfobacteraceae* bacterium clone Shahe	MH356751.1
Uncultured *Desulfobacteraceae* bacterium clone G9A	HQ847964.1
Uncultured *Desulfarculus* sp. clone 51	MF042413.1
Oceanrickettsia ariakensis clone R6	DQ118733.1
Pseudomonas syringae strain ATCC 19310	AF094749.1
Pseudomonas aeruginosa strain ATCC 10145	AF094713.1
Endozoicomonas numazuensis strain HC50	NR_114318.1
Endozoicomonas montiporae CL-33	FJ347758.1
Vibrio vulnificus strain ATCC 27562	NR_118930.1
Vibrio parahaemolyticus strain ATCC 17802	NR_118928.1
Uncultured *Desulfovibri*o sp. clone CSMB_619	MF894076.1

Table G.2. Descriptive statistics of gas bubble intensity (ratio) data. Results of non-parametric Kruskal-Wallis tests are shown. Summarised results from Dunn comparisons tests are shown. Distributions that do not share the same letter are significantly different (*p*-adj).

Date	***n***	**Mean**	**SD**	**SE**	**Dunn's test**
Mar-19	30	0.0017	0.0033	0.0006	ab
May-19	30	0.0030	0.0055	0.0010	a
Jul-19	30	0.0039	0.0065	0.0012	a
Sep-19	30	0.0089	0.0137	0.0025	a
Nov-19	30	0.0023	0.0059	0.0011	ab
Jan-20	30	0.0000	0.0001	0.0000	b
Kruskal-Wallis X^2 = 21.25, df = 5, *p*-value = <0.001					
Site	***n***	**Mean**	**SD**	**SE**	**Dunn's test**
Island	60	0.0000	0.0000	0.0000	c
Kopawai	60	0.0011	0.0022	0.0003	b
Mahuta Gap	60	0.0088	0.0111	0.0014	a
Kruskal-Wallis X^2 = 61.43, df = 2, *p*-value = <0.001					

Table G.3. Results from Dunn's test, comparisons following Kruskal-Wallis test. Comparisons are based on gas bubble intensity (ratio) derived from toheroa shells from Ripiro Beach, sampled at three sites: Island, Mahuta Gap, and Kopawai. For each comparison, Dunn's Z statistic is shown as well as *p*-values adjusted (Bonferroni). Statistically significant differences are indicated in bold with an asterisk.

Ripiro Beach		**Island**	**Kopawai**
Kopawai	*Z*	-3.34	
	p	**0.001***	
Mahuta Gap	*Z*	-7.81	-4.47
	p	**0.000***	**0.000***

Table G.4. Descriptive statistics of gas bubble intensity (ratio) data. Results of non-parametric Kruskal-Wallis tests are shown for monthly comparisons of gas bubble intensity within sites: Island, Mahuta Gap, and Kopawai. Summarised results from Dunn comparisons tests are shown. Distributions that do not share the same letter are significantly different (*p*-adj).

Island					
Date	***n***	**Mean**	**SD**	**SE**	**Dunn's test**
Mar-19	10	0	0	0	-
May-19	10	0	0	0	-
Jul-19	10	0	0	0	-
Sep-19	10	0	0	0	-
Nov-19	10	0	0	0	-
Jan-20	10	0	0	0	-
Mahuta Gap					
Date	***n***	**Mean**	**SD**	**SE**	**Dunn's test**
Mar-19	10	0.0038	0.0050	0.0016	bc
May-19	10	0.0081	0.0071	0.0023	ab
Jul-19	10	0.0105	0.0076	0.0024	ab
Sep-19	10	0.0250	0.0128	0.0041	a
Nov-19	10	0.0053	0.0094	0.0030	bc
Jan-20	10	0	0	0	c
Kruskal-Wallis	$X^2 = 33.22$, df = 5, *p*-value = <0.001				
Kopawai					
Date	***n***	**Mean**	**SD**	**SE**	**Dunn's test**
Mar-19	10	0.0013	0.0018	0.0006	-
May-19	10	0.0009	0.0015	0.0005	-
Jul-19	10	0.0011	0.0025	0.0008	-
Sep-19	10	0.0017	0.0032	0.0010	-
Nov-19	10	0.0015	0.0027	0.0009	-
Jan-20	10	0.0000	0.0001	0.0000	-
Kruskal-Wallis	$X^2 = 4.78$, df = 5, *p*-value = 0.44				

Table G.5. Differences in mean gas bubble intensity ratio between March 2019 and January 2020 at Mahuta Gap. Multiple comparisons not carried out for Kopawai (p = 0.44) or Island (no bubbles measured). Output of Dunn's test showing Z and adjusted p-value (Bonferroni) for multiple comparisons.

Mahuta Gap		**Jan-20**	**Jul-19**	**Mar-19**	**May-19**	**Nov-19**
Jul-19	Z	-3.62				
	p	**0.002***				
Mar-19	Z	-1.57	2.05			
	p	0.875	0.299			
May-19	Z	-2.94	0.68	-1.37		
	p	**0.025***	1.000	1.000		
Nov-19	Z	-1.63	1.99	-0.07	1.31	
	p	0.766	0.350	1.000	1.000	
Sep-19	Z	-5.20	-1.58	-3.63	-2.26	-3.57
	p	**0.000***	0.863	**0.002***	0.179	**0.003***

Appendix H: Bayesian Ordinal Logistic Regression for Histopathology: A Tutorial using R and the 'brms' Package

Load relevant packages

```
library(brms)
library(ggplot2)
```

Load data

```
data <- read.csv("G:/Histology/Data/R/bayes/brms_example.csv")
```

Assign levels to ordinal variable(s)

```
data$infection <- factor(data$infection, levels=c("Low", "Medium", "High", ordered=TRUE)
```

Set seed (for reproducibility)

```
set.seed(12345678)
```

Construct initial model. NB: sample priors = TRUE. Set priors for your data.

```
modeltest <- brm(formula = infection ~ temperature + (1|gr(Site)),          Group level effect
data = data,
family = cumulative("logit"),
control = list(adapt_delta = 0.999),                                        If divergence encountered
sample_priors = TRUE,                                                       Sample priors
warmup = 200,
iter = 800,
chains = 4,
cores = 4,
prior = c(set_prior(prior = "normal(0, 10)", class = "Intercept"),          Intercept prior
      set_prior(prior = "normal(0, 10)", class = "b"),                      Fixed effects prior
      set_prior(prior = "student_t(10, 0, 3)", class = "sd")))              Group-level (random) effects
```

Visualise priors

```
plot(hypothesis(modeltest, "temperature > 0"))
```

Update model, increase iterations, change priors etc.

```
Histologymodel <- brm(
formula = infection ~ temperature + (1|gr(Site)),
data = data,
family = cumulative("logit"),
warmup = 2000,
iter = 10000,
chains = 4,
cores = 4,
prior = c(set_prior(prior = "normal(0, 2)", class = "Intercept"),
          set_prior(prior = "normal(0.5, 0.5)", class = "b"),          Weakly informative priors
          set_prior(prior = "cauchy(0, 5)", class = "sd")))
```

Model summary

```
summary(Histologymodel)
```

Fixed effects

```
fixef(Histologymodel)
```

Random/group level effects: (1|gr(Site))

```
ranef(Histologymodel)
```

Compare models using LOO (looic & epld)

```
loo(model_1, model_2, Histologymodel)
```

Diagnostics

```
plot(Histologymodel, pars = c(“temperature))                    Trace plots for chain mixing
pp_check(Histologymodel, nsamples = 500, type = "bars")  Posterior predictive checks (fit)
```

Marginal effects plot (visualise probability)

```
conditional_effects(Histologymodel, "temperature",categorical = TRUE)
```